PERMEABILITY OF CONCRETE IN A MARINE ENVIRONMENT

by

Nicholas Robert Buenfeld MSc, DIC, CEng, MICE

November, 1984

A Thesis submitted for the degree of Doctor of Philosophy
of the University of London.

Department of Civil Engineering
Imperial College
London, S.W.7

Title of Thesis : PERMEABILITY OF CONCRETE IN A MARINE ENVIRONMENT

Author : Nicholas Robert Buenfeld

ABSTRACT

Permeability is a fundamental property governing the durability of concrete in the marine environment and it has only recently been appreciated that some concretes exhibit a very significant reduction in permeability on immersion in sea-water. To investigate this phenomenon further, chloride ion diffusion and electrical resistivity techniques have been developed and used to monitor the changes in permeability of five mortars and one concrete on exposure to sea-water. All mixes studied showed a reduction in permeability on immersion in sea-water. Indeed, 25 mm thick specimens of the two most permeable mortars showed a fall equivalent to over 20 mm of additional thickness after only 10 weeks. This reduction was due to the formation of a discrete layer on the surface of the cement paste, together with a more widespread bulk effect associated with a modification of the pore structure. The surface layer generally consisted of a brucite (magnesium hydroxide) layer, which was in evidence after only 1 day, overlain by a more slowly developing layer of aragonite (calcium carbonate). After 3 months of sea-water exposure the layers were typically 30 μm and 100 μm thick respectively. Layer development appeared to be more dependent upon environmental factors than on mix parameters.

Initial surface absorption testing showed that the mechanisms producing the permeability-reducing phenomenon also have a considerable effect upon the absorption capacity of concrete after a period of drying, which is important in the tidal and splash zones.

A limited number of naturally exposed submerged zone specimens were tested and all exhibited substantial surface resistances.

It is important that the existence of the permeability-reducing phenomenon is appreciated when planning tests, or interpreting data from tests, on sea-water exposed concrete.

The next phase of this research will be concerned with developing methods of deliberately enhancing the permeability-reducing phenomenon which could, in due course, allow the specification of ultimately impermeable, and hence far more durable, concrete.

To Mum, Dad and Sara

ACKNOWLEDGEMENTS

This work was undertaken in the Concrete Section, Department of Civil Engineering, Imperial College, under the general direction of the Head of Section, Professor J.W. Dougill. I wish to express my gratitude for financial support from The Science and Engineering Research Council Marine Technology Directorate through grants awarded to The London Centre.

I am particularly indebted to Dr. John Newman for his continued support and supervision.

I also wish to acknowledge the help received from the following:
Mr. Roy Baxter for technical assistance throughout the experimentation;
Professor P.L. Pratt of the Department of Metallurgy and Materials Science, Imperial College, who made facilities and assistance available for SEM studies of the surface formation;
Dr. Chris Page, Materials Research Group, Department of Construction, The University of Aston, who supervised the extraction and analysis of pore solution from the "pore press" specimens;
Dr. Dave Hughes and Mr. Trevor Grounds of Hatfield Polytechnic, who undertook the mercury intrusion porosimetry;
Dr. Peter Bush of the Department of Geology, Imperial College, who advised on aspects of carbonate equilibria;
Dr. Harry Shaw of the Department of Geology, Imperial College, who undertook a large proportion of the X-ray diffraction analysis;
Mr. Barry Foster of the Department of Geology, Imperial College, who prepared the polished sections; and
Mr. Mike Leeming, Technical Manager of the *Concrete in the Oceans* research programme for providing a number of specimens.

CONTENTS

Chapter I : INTRODUCTION

Most good quality concrete performs rather better in sea-water than might be expected from a study of the reactions between cement paste and the individual chemical constituents of sea-water in isolation (2.2.2). One reason for this is that the formation of the expansive reaction products normally associated with sulphate attack is inhibited due to their increased solubility in a chloride solution (2.2.2.2). Virtually all mechanisms causing deterioration of concrete in a marine environment are dependent upon concrete permeability (2.4.1) and it has only recently been recognised that certain concretes exhibit a reduction in permeability when exposed to sea-water (2.4.2). This *permeability-reducing phenomenon* may also contribute to the durability of concrete in a marine environment. There are, however, numerous cases of concrete deterioration in a marine environment (2.3) where the permeabilty-reducing mechanism was clearly unable to counter the aggressive environment, or was not initiated at all.

A greater understanding of the permeability-reducing phenomenon could eventually facilitate its deliberate enhancement, with the possibility of allowing the specification of *ultimately* impermeable, and hence far more durable, concrete.

The primary aims of this research were therefore to:

(1) develop techniques to monitor changes in the permeability of laboratory specimens during sea-water immersion, preferably with the capability of isolating the contribution due to further hydration;

(2) compare the relative reduction in permeability of a range of mixes, corresponding to typical offshore concretes, during immersion in sea-water;

(3) investigate the mechanism producing the permeability-reducing phenomenon;

(4) assess the likely effect of the phenomenon in the splash and tidal zones (Figure 2.1).

Permeability is that property of a porous medium which characterises the ease with which fluid will pass through it. Permeability is conventionally determined by subjecting one face of a specimen of the material under test to a relatively high water pressure, measuring the steady state volumetric flow rate and then calculating a coefficient of permeability from D'Arcy's law (3.2.3). However,

a coefficient of permeability determined in this way bears little *direct* relation to the performance of concrete in a marine environment (except perhaps for concrete at ocean depths). There are other parameters which correlate more closely with the transport processes participating in deterioration mechanisms. For example, if sulphate attack in submerged concrete is a problem, the sulphate ion diffusion coefficient would be a more appropriate parameter to monitor. Since the basis of this research is the monitoring of changes in the aspects of permeability most relevant to the performance of concrete in a marine environment the term permeability is therefore used throughout this thesis, and indeed in the title of the thesis, to mean the susceptibility of concrete to the ingress (or egress) of ions or molecules. Hence, a reduction in chloride ion diffusion coefficient is regarded as a reduction in permeability, as is a decrease in initial surface absorption.

This thesis is divided into chapters as outlined below:

Chapter 2 reviews the performance of concrete in the marine environment with particular emphasis on the mechanisms that cause deterioration. The importance of permeability is emphasised and all references in published documents to experimental results suggesting the presence of a permeability-reducing phenomenon are discussed.

In Chapter 3 test methods that might be used to monitor changes in the permeability of concrete exposed to sea-water are compared and ion diffusion, electrical resistivity and initial surface absorption techniques are selected.

Chapter 4 reports on experimentation in which the ion diffusion cell technique is applied to monitor changes in the chloride ion diffusion coefficient of a range of mortars exposed to sea-water (and other chloride solutions).

Chapter 5 reports on the development and subsequent use of an electrical resistivity technique for monitoring changes in permeability. Results are presented showing the changes in permeability of mortars and a concrete over several months of exposure to sea-water.

Chapter 6 presents the results of examination and analyses of the surface layers formed on various concretes and mortars exposed to sea-water. Theoretical aspects relating to the development and stability of such layers are

also discussed.

Chapter 7 shows the effect of sea-water exposure on the pore size distribution (determined by mercury intrusion porosimetry) of various mortars.

Chapter 8 reports on the effect of sea-water exposure on the absorptive properties of concrete, through use of the initial surface absorption test.

A discussion of the practical implications of this research is presented in Chapter 9. The conclusions are drawn in Chapter 10 and suggestions for future work are made in Chapter 11.

Chapter 2: DURABILITY OF CONCRETE IN THE MARINE ENVIRONMENT

2.1 Use of concrete in the sea

Concrete has been widely used for many years in the construction of harbours, docks, piers, breakwaters and many other structures exposed to sea-water. The Romans were building sea-structures using lime-pozzolan mortar almost 2000 years ago and a few of these structures are still in service. The durability of concrete in sea-water has attracted much attention and a very extensive literature relating to it exists. Recognition of mechanisms producing chemical deterioration of concrete in sea-water is due to Vicat (1857), who began his experiments in 1812. Le Chatelier, Candlot and Michaelis (Atwood & Johnson 1924) also carried out important research during the nineteenth century. Many laboratory and natural exposure studies have been undertaken over the last 80 years and durable structures have generally been built as a result of lessons learnt from past experience.

The 1970's witnessed a major advance in the utilisation of concrete in the marine environment; the most spectacular example must be offshore concrete gravity platforms in the North Sea, subjected to 30m waves and founded at depths approaching 150m. Oceans make up 80 percent of the surface of the earth and the ever increasing demand for resources is rapidly extending the sphere of a wide variety of human activities to the continental shelves. Many new and exciting concepts are currently under development, including offshore windmills, concrete LNG carriers and floating airports and extensive planning and design has been carried out for concrete structures to serve in the Arctic Ocean (UEG 1982). This trend towards more and larger concrete structures exposed to deeper and more severe sea-waters, while assuming minimal maintenance, justifies a fresh look at the subject of concrete durability in the marine environment. This is particularly true in the light of the recent use of less conventional concretes and the current doubt as to the durability of modern cements (Parkinson 1983).

2.2 Mechanisms of concrete deterioration

2.2.1 Introduction

Concrete may deteriorate in sea-water due to chemical reaction between components of hydrated cement and dissolved sea-water salts, leaching, crystallisation of salts within the cement paste accelerated by alternate wetting and drying, frost action, marine growth, abrasion and corrosion of embedded reinforcement. This section (2.2) outlines the most important features of these mechanisms.

The durability of a structural concrete element in a marine environment is likely to depend upon the following:

(1) Environmental factors:
- (a) exposure zone: a structure in an offshore (marine) environment may be conveniently divided into a number of exposure zones (see Figure 2.1)
- (b) coastal or offshore: a structure in a coastal (maritime) environment is more likely to be subjected to frost action and abrasion from sand and gravel than an offshore structure.
- (c) climate: temperature, relative humidity etc.
- (d) sea-water properties: temperature, salts concentration, CO_2 concentration etc.

(2) Structural factors: shape and orientation of element, cover to reinforcement, crack widths etc.

(3) Material factors: concrete type, mix constituents and their proportions, curing history, workmanship etc.

The only influence that the Engineer has over the factors in (1) is in the choice of location for the structure. It is generally only through consideration of the factors in (2) and (3) that the Engineer can control the long-term durability of a marine or maritime structure and the influence of these on the performance of concrete is discussed in 2.3.

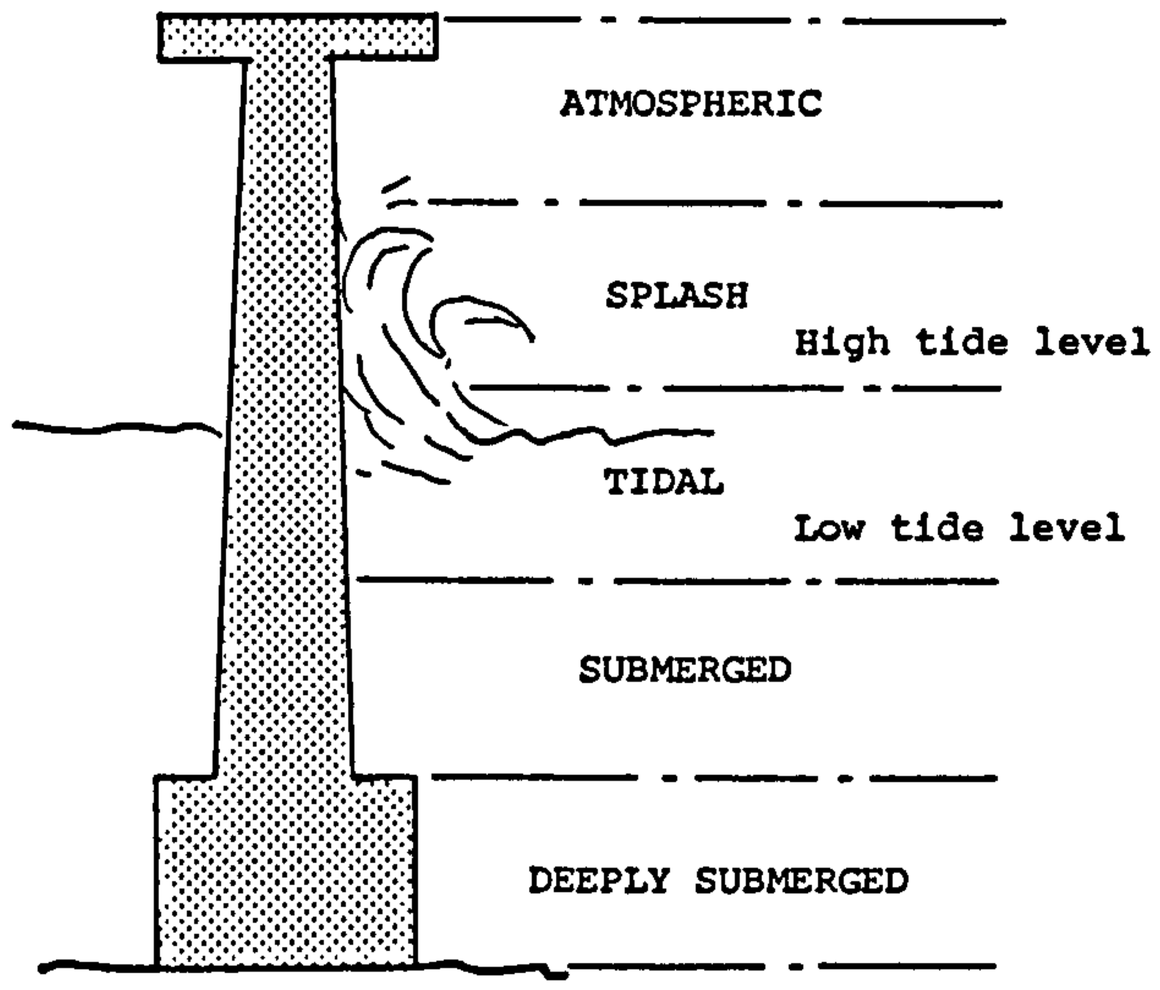

Figure 2.1: Exposure zones for offshore structures.

2.2.2 Chemical mechanisms

2.2.2.1 Introduction

Although the total salt content (salinity, Appendix 9) of sea-water can be variable, the ratios of the major constituents remain nearly constant (Marcet's principle; Horne 1969). Table 2.1 shows the salinity of various seas. Extremes of salinity occur in coastal regions and in certain partially enclosed seas. The surface waters of the Dead Sea have a salinity of 332 g/kg; however, the Dead Sea is a land-locked lake rather than a true sea and consequently Marcet's principle is violated. The salinity in the open ocean is normally between 33.0 and 37.0 g/kg and a value of 35 g/kg is therefore generally assumed as the average ocean salinity.

Sea	Salinity (g/kg)
Arctic Ocean	35
Atlantic Ocean	35
Baltic Sea	7 (0-15)
Black Sea	18
Indian Ocean	36
Mediterranean Sea	38
North Sea	33 (29-35)
Pacific Ocean	35
Persian Gulf	37-60
Red Sea	41

Table 2.1: Salinity of various seas (based on King 1975 and Fairbridge 1966).

Table 2.2 shows the ionic and salts concentration of typical 35 g/kg salinity sea-water. Although Na, K and even Ca are present as simple hydrated (i.e. free) cations, in the case of Mg and nonhalide anions more complex species account for appreciable fractions of their total quantities; the percentage free ion is indicated in Table 2.2. Further properties of sea-water are presented in Appendix 2.

Salt	Concentration (g/kg)
$NaCl$	27.0
$MgCl_2$	3.2
$MgSO_4$	2.2
$CaSO_4$	1.3
$CaCl_2$	0.6

Ion		% free ion
Cl^-	19.35	100
Na^+	10.76	99
SO_4^{2-}	2.71	54
Mg^{2+}	1.29	87
Ca^{2+}	0.41	91
K^+	0.39	99
HCO_3^-	0.14	69

Table 2.2: Chemical composition of typical 35 g/kg salinity sea-water (based on Horne 1969 and Biczok 1967).

The chemical action of sea-water on concrete is primarily due to the presence of magnesium sulphate. Carbon dioxide dissolved in sea-water can also be instrumental in decomposing cement paste. The chemical effect of chloride ions on concrete is relatively mild; however, the interaction of chloride ions with cement paste is of extreme importance to the reinforcement corrosion mechanism and hence is also covered in this section.

2.2.2.2. Effects of sulphates

2.2.2.2.1. Introduction

The action of sulphate ions on concrete is conveniently divided into three distinct, though interrelated, mechanisms according to the hydrated cement compound under attack:

(1) attack of C_3A-hydrates to form calcium sulphoaluminate hydrate (ettringite), resulting in disruptive expansion (2.2.2.2.2);

(2) conversion of $Ca(OH)_2$ to gypsum producing surface softening

(2.2.2.2.3); and

(3) decomposition of hydrated calcium silicates (2.2.2.2.4).

Hydrated C_4AF is considerably less resistant to sulphate attack than calcium silicate hydrates and is capable of producing expansion, but being more resistant than C_3A, has received only sparse coverage in the literature (Bogue & Lerch 1934, Thorvaldson & Wolochow 1938).

Sea-water contains appreciable concentrations of calcium and potassium sulphates, but their influence is insignificant relative to the effect of magnesium sulphate which is both more aggressive and present in greater concentration. Hence, most studies of sulphate attack of cement paste in sea-water are based exclusively upon the properties of magnesium sulphate.

2.2.2.2.2. Sulphate attack of C_3A-hydrates

Attack of C_3A-hydrates, known as *sulphoaluminate* sulphate attack, is generally the predominant sulphate attack mechanism; it is represented by the equation:

$$MgSO_4 + [Ca(OH)_2 + C_3A.CaSO_4.18H_3O] \longrightarrow \underset{\text{brucite}}{Mg(OH)_2} + \underset{\text{ettringite}}{C_3A.3CaSO_4.32H_2O}$$

Ettringite cystallises from a saturated solution, in the form of needle-shaped crystals, to over twice the original volume. The actual mechanism of expansion is still uncertain (Mehta 1973, 1983). The pressure induced by this expansion causes the cracking that is associated with sulphate attack of land-based structures. However, although ettringite has been detected in minor quantities, it has seldom been conclusively demonstrated to be the sole cause of cracking of an offshore concrete structure exposed to sea-water. Ettringite is more soluble in solutions containing chloride than in pure sulphate solutions and consequently expansion phenomena associated with reactions involving the formation of ettringite are inhibited in chloride solutions such as sea-water (Lea 1970).

Ettringite, though one of the initial products of the reaction of hardened cement paste with magnesium sulphate, is unstable in the resulting solution and eventually decomposes to form hydrated alumina, gypsum and brucite:

$$C_3A.3CaSO_4.32H_2O \longrightarrow Al_2O_3.aq. + CaSO_4.2H_2O + Mg(OH)_2$$

The effect of different crystalline forms of C_3A on the sulphate resistance of cement pastes in sea-water is currently a subject of contention. An implication of the work of Regourd (1975) is that the presence of cubic instead of orthorhombic or tetragonal C_3A will make a Portland cement more vulnerable. Work by Mehta (1980) does not confirm this. Regourd (1975) also reports that less magnesium silicate hydrate was formed when the cement contained cubic C_3A; ie. the attack of C_3A was enhanced, but decomposition of hydrated calcium silicates was reduced.

2.2.2.2.3. Sulphate attack of $Ca(OH)_2$

Conversion of $Ca(OH)_2$ to gypsum with the precipitation of $Mg(OH)_2$ (brucite) is known as *acid* sulphate attack:

$$MgSO_4 + Ca(OH)_2 \longrightarrow \underset{\text{brucite}}{Mg(OH)_2} + \underset{\text{gypsum}}{CaSO_4.2H_2O}$$

This conversion more than doubles the solid volume and hence if sufficient gypsum were to crystallise, concrete cracking would be inevitable. However, the solubility of gypsum in the presence of sodium chloride is so high that crystallisation is unlikely. Thus, deterioration due to disruptive expansion from this reaction is very unlikely in a marine environment. However, the increased solubilities of gypsum and $Ca(OH)_2$, together with conditions produced by wave motion, are reported to result in increased leaching and surface softening (2.2.3).

2.2.2.2.4. Sulphate attack of calcium silicate hydrates

Magnesium sulphate is more aggressive than other sulphates and decomposes the hydrated calcium silicates in addition to attacking hydrated C_3A and $Ca(OH)_2$. The calcium silicates react in the following general manner:

$$3CaO.2SiO_2.aq. + 3MgSO_4.7H_2O \longrightarrow CaSO_4.2H_2O + 3Mg(OH)_2 + 2SiO_2.aq$$

Steopoe (Lea 1970) found that this was not the end of the reaction and that the brucite and silica gel can react very slowly to form a hydrated magnesium

silicate. This was confirmed by the discovery of a compound having an approximate composition of $4MgO.SiO_2.8.5H_2O$ in a deteriorated concrete sea-wall (Cole 1953).

$$4Mg(OH)_2 + SiO_2.aq. \longrightarrow 4MgO.SiO_2.8.5H_2O$$

This silicate has no binding capacity, in contrast to silica gel, and its formation represents the final stage of sulphate attack of concrete.

2.2.2.3. Effects of chlorides

In addition to their influence on sulphate attack (2.2.2.2), the chlorides which abound in sea-water can interact chemically with concrete in two other main ways. Firstly, by participating in the mechanism of embedded steel corrosion (2.2.8) and secondly via chemical reactions similar to those between sulphates and hydrated cement compounds.

Chloride ions may react with hydrated aluminate and ferrite phases to form compounds which are analagous to ettringite. Friedel's salt, $C_3A.CaCl_2.10H_2O$, is normally the reaction product, although $C_3A.CaCl_2.30H_2O$ has been identified in the USSR, where exceptionally large amounts of calcium chloride have ben used for placing concrete in sub-zero temperatures (Figg 1983). A fall in the pH of the cement paste pore solution due to, say, carbonation, can cause the decomposition of chloroaluminate hydrates (Page & Treadaway 1982). Similarly chloroaluminate hydrates are unstable in a sulphate environment where ettringite is formed preferentially and chloride ions are released. Kalousek and Benton (1970) suggest this to be the explanation for the increasing concentration of ettringite in the deep interior of paste specimens with simultaneous presence of chloride. This explanation also accounts for the absence of chloroaluminate in the outer zone of the specimens, even when high-C_3A Portland cements were subjected to prolonged sea-water exposure (Mehta 1980). Hence, concrete deterioration in the marine environment due to the formation of chloroaluminate hydrates is very unlikely. The main interest in the capacity of a cement to bind chloride ions relates to the mechanism of reinforcement corrosion protection in concrete (2.2.8).

Chlorides, and particularly magnesium chloride, react with $Ca(OH)_2$ to form

calcium chloride which is readily soluble in sea-water and can be leached from concrete:

$$MgCl_2 + Ca(OH)_2 \longrightarrow Mg(OH)_2 + CaCl_2$$

Brucite precipitated in the cement paste pores as a result of the reactions detailed above, as well as the three sulphate attack reactions (2.2.2.2), hinders ingress of ions and hence can inhibit further reaction.

2.2.2.4. Carbonation

Carbon dioxide, present in the atmosphere at a concentration of approximately 300 ppm, diffuses into the cement paste pores and reacts, primarily with $Ca(OH)_2$, to form calcium carbonate. The consequent removal of OH^- ions from the cement paste pore solution results in reduced alkalinity, which is of fundamental importance to the reinforcement corrosion mechanism (2.2.8).

The complete carbonation of hydrated Portland cement paste, to $CaCO_3$, hydrated silica, alumina and ferric oxide is chemically possible; sulpho-aluminates carbonate to gypsum, vaterite and hydrous alumina (Lawrence 1981).

The kinetics of carbonation for various types of concrete in different environments have been widely investigated and it has generally been observed that the relationship between carbonation layer thickness (x) and exposure time (t) is approximately parabolic in form (Page & Treadaway 1982):

$$\frac{dx}{dt} = kt^{-\frac{1}{2}}$$

The magnitude of the proportionality constant (k) depends on variables related to the quality of the concrete and to the environment. The rate of advance of carbonation, (dx/dt), is particularly sensitive to environmental humidity, reaching a maximum at a relative humidity of around 50%; at this humidity, carbonation is accompanied by considerable shrinkage (Lawrence 1981). However, for "good quality" concrete, the carbonation rate soon declines to less than 1mm yr^{-1} (Page & Treadaway 1982).

Generally only small quantities of dissolved CO_2, derived mainly from absorption of atmospheric CO_2, are present in sea-water and since diffusion of

CO_2 is 10^4 to 10^5 times as slow in solution as in the gas phase (Lawrence 1981), carbonation depths in submerged concrete are normally negligible. However, decaying vegetable matter can lead to substantially larger concentrations of dissolved CO_2 (Mehta 1980) and hence the following reactions can be important:

$$CO_2 + Ca(OH)_2 \longrightarrow \underset{\text{aragonite}}{CaCO_3} + H_2O \overset{+\,CO_2}{\longrightarrow} \underset{\text{calcium bicarbonate}}{Ca(HCO_3)_2}$$

$$CO_2 + [Ca(OH)_2 + C_3A.CaSO_4.18H_2O] \longrightarrow C_3A.CaCO_3.xH_2O + \underset{\text{gypsum}}{CaSO_4.2H_2O}$$

$$3CO_2 + 3CaO.2SiO_2.3H_2O \longrightarrow \underset{\text{aragonite}}{3CaCO_3} + 2SiO_2.H_2O$$

It should be noted that in a Mg^{2+} ion environment, such as sea-water, aragonite is the stable polymorph of calcium carbonate (6.4.2.2). Both calcium bicarbonate and gypsum are soluble in sea-water and their formation can therefore lead to leaching and surface softening (2.2.3).

2.2.2.5. Alkali-aggregate reaction

The alkali ions present in cement paste pore solution may participate in any of several reactions with reactive silica or reactive carbonate constituents of the aggregate. The most common reaction, alkali-silica reaction, results in the formation of an alkali-silicate gel which imbibes water and expands; this results in diffusion of gel through the cement paste pore system away from the reaction site, and may result in cracking and eventual disruption of the cement paste. The reactive forms of silica are opal (amorphous), chalcedony (cryptocrystalline fibrous), and tridymite (crystalline) which may occur in rocks such as opaline or chalcedonic cherts and siliceous limestones. The generally accepted minimum alkali content of cement at which expansive reaction may take place is 0.6 percent of the soda equivalent (Neville 1978). Other factors influencing the progress of the reaction include moisture availability, aggregate grading and porosity and cement paste permeability. Alkali-silica reaction is likely to be accelerated in the marine environment due to the high cement contents generally specified for offshore construction, the external source (sea-water) of alkali metal salts and the presence of wetting and drying in the tidal and splash zones.

Another type of deleterious aggregate reaction is that between some dolomitic limestone aggregates and alkalis in the cement, producing expansion of

concrete similar to that occurring as a result of alkali-silica reaction. However, as far as is known, there have as yet been no documented cases of alkali-carbonate reaction which have caused deterioration of concrete structures exposed to sea-water (Mather 1982).

2.2.3. Leaching

Strictly speaking, leaching is the removal of soluble matter by the action of *percolating* fluid. The term is used more generally in the present context to mean the loss of solid matrix or pore solution ions from concrete as a result of immersion in an aqueous solution.

In the submerged zone, sea-water ions diffuse into concrete and likewise cement paste pore solution ions counter-diffuse into the sea-water. This does not, however, result in an immediate rapid reduction in pH of the cement paste; completely hydrated pastes of pure Portland cement contain about 24 percent $Ca(OH)_2$ by weight (Mehta 1980) and this acts as a reservoir, keeping the pore solution saturated with respect to $Ca(OH)_2$ and hence maintaining a minimum pH of around 12.6. However, the process results in the gradual loss of solid matrix (lime leaching), weakening the concrete and increasing its permeability, thereby exacerbating other mechanisms of deterioration. $Ca(OH)_2$ is also the most vulnerable constituent of cement paste to attack by the aggressive components of sea-water such as $MgSO_4$, $MgCl_2$ and CO_2 and since many of the reaction products are soluble in sea-water, the removal of $Ca(OH)_2$ is consequently accelerated. A reduction in the lime content of concrete also leads to decomposition of the other cement paste phases (Biczok 1967). Leaching action is likely to be particularly rapid around the low tide level, where the swirling action of the sea-water will further accelerate the removal of soluble material.

2.2.4. Wetting and drying

Those parts of a structure situated in the tidal or splash zones (2.2.1) are subject to alternate wetting and drying. There are three main effects due to such cycling:

(1) volume changes: shrinkage, swelling and thermal movements;

(2) crystallisation of salts in the pores of the concrete; and

(3) exacerbation of frost action.

When concrete is exposed to air at a humidity of less than 100% the drying that occurs is accompanied by a volume change (drying shrinkage). When subsequently placed in water concrete swells, although not all of the initial drying shrinkage is recovered, even after prolonged storage in water. For the usual range of concretes the irreversible part of shrinkage represents between 30 and 60 percent of the initial drying shrinkage, the lower value being more common. The absence of fully reversible behaviour is probably due to the introduction of additional links within the gel during the period of drying, when closer contact between gel particles is established (Neville 1978). Drying shrinkage results in an increase in the permeable porosity of the cement paste and a consequent increase in permeability (Powers *et al.* 1954).

Concrete just above the water line is subject to capillary rise with evaporation continually drawing more sea-water through the pore system and resulting in deposition of sea-water salts at the point of evaporation. Under these circumstances the sea-water may slowly attack the cement chemically (2.2.2), while the pressures exerted as a result of crystallisation of salts in the concrete can also have a disruptive action; alternate wetting and drying of the surface accelerates this effect.

Air temperature variation, in a true offshore marine environment, is rarely sufficient to produce significant freeze-thaw cycling and hence concrete in the atmospheric zone is unlikely to deteriorate due to frost action (2.2.5). However, at sub-zero air temperatures concrete in the tidal zone is subject to as severe frost action as concrete in any natural exposure.

2.2.5. Frost action

As the temperature of saturated concrete is lowered, the water held in the pore system starts to freeze, initially in the largest capillaries and gradually extending to the smaller pores; gel pores are too small to permit the formation of ice above -78°C, so that in practice no ice is formed in them. Helmuth (1962) showed that nucleation of ice does not occur automatically within the structure of hydrated cement pastes, even at temperatures as low as -15°C; external ice seeds are necessary to initiate freezing.

Freezing may produce a dilating pressure within concrete, by two main

mechanisms. Firstly, freezing of water results in an increase in volume of approximately 9 percent, so that the excess water is forced to permeate away from the pore. The second mechanism is the diffusion of water to locations of ice formation, driven by osmotic pressure brought about by local increases in pore solution concentration due to the separation of frozen (pure) water from the solution. This mechanism can be particularly important in situations where there is an external source of water, since the total moisture content of the concrete can then become greater than before freezing.

When the dilating pressure in the concrete exceeds its tensile strength, damage occurs. On re-freezing, further expansion takes place so that repeated cycles of freezing and thawing have a cumulative effect. The extent of the damage varies from surface scaling to complete disintegration as layers of ice are formed, starting at the exposed surface of the concrete and progressing through its depth.

The main factors influencing the frost resistance of concrete are the degree of saturation and the pore structure of the cement paste. There is no unique value of critical saturation, since it depends on the size of the body, on its homogeneity and on the rate of freezing. The space available to accommodate expelled water must be close enough to the pore in which the ice is being formed; this is the basis of air entrainment; if the paste is subdivided into sufficiently thin layers by air voids, the paste has no critical saturation.

The effect of freezing and thawing of concrete in sea-water is much more severe than in fresh-water (Lyse 1961). This is probably due to penetration of sea-water ions causing a high osmotic pressure with a consequent movement of water toward the freezing surface zone of the concrete. However, air entrained voids may also be more easily filled when salt is present and hence critical saturation is reached more quickly.

2.2.6. Effects of marine organisms

Living organisms that may be found in the vicinity of offshore structures are essentially the same as those colonising natural habitats. They range in size from microscopic bacteria through to seaweeds several metres in length. In the context of this research it is convenient to consider marine life in three distinct categories: bacteria and hard and soft marine growth.

The part played by bacteria in the corrosion of concrete sewers is well recognised, sulphur compounds being reduced by anaerobic bacteria to hydrogen sulphide which dissolves and undergoes oxidation by aerobic bacteria, finally producing sulphuric acid. It has been suggested (Ruberichik 1942) that bacteria play a part in the deterioration of concrete in the Black Sea. However, conditions under which hydrogen sulphide can occur in sea-water are similar to those for abnormal levels of carbon dioxide (2.2.2.4), ie. sheltered waters containing decaying vegetation, and it is not clear whether any significant effect of bacteria, in comparison with direct chemical action, has been proved (Lea 1970).

The second category (hard growth) consists of animals with calcareous shells or plates, for example mussels and barnacles; attachment is usually by a cement as in barnacles and tubeworms or by strong anchoring threads as in the case of mussels. It has been suggested (Friese 1938) that molluscs can damage concrete by the liberation of ammonium carbonate. Molluscs may also cause deterioration by boring into concrete; concrete structures on the Panama Canal were severely damaged by boring shells which formed ducts and passages in the concrete (Biczok 1967). Haynes and Zubiate (1973), however, reported that concrete that had been exposed in a location known to contain borers for 67 years showed excellent resistance.

The third category (soft growth) includes plants such as seaweeds and animals such as anemones, sponges and hydroids. Plants of the lowest order, the algae, require continuous moisture, or at least a vapour-saturated atmosphere, to exist, and hence assume greatest significance in the submerged zone. The presence of algae is generally likely to result in a beneficial self-sealing effect (2.4.2) rather than deterioration. Plants of higher order, such as seaweeds, have a lower water demand, but only settle on concrete once leaching (2.2.3) and carbonation (2.2.2.4) have significantly reduced the pH at the concrete surface. Seaweed does not have proper roots, but clings to concrete by means of a holdfast; consequently the damage associated with the growth of the fine hair roots of many land-based plants is not a problem. However, decomposition of marine growth results in the production of carbon dioxide, thereby accelerating concrete carbonation (2.2.2.4). Unlike plants, animals such as hydroids, anemones and corals show no sign of "die-back" during winter months and may rapidly form a "turf" over large areas of an offshore structure (Forteath *et al.* 1984). Large accumulations of silt and debris may become trapped in the root-like attachments of such species

resulting in an environment in which sulphate-reducing bacteria may thrive.

The growth of marine organisms is dependent upon the complex interaction of a wide range of environmental factors; for example, exposure zone, distance from shore, temperature, season, salinity, water current, food availability, other species present, etc. In the North Sea marine growth is most dense in the tidal zone and this may accelerate chemical degradation (2.2.2) by retaining sea-water during the drying phase which, due to evaporation, becomes more concentrated and hence, more aggressive. However, the few reported cases of marine life directly causing concrete degradation are insignificant in comparison with cases of deterioration due to mechanisms such as chemical attack or frost action.

2.2.7. Abrasion and cavitation

Concrete in the marine environment may be subject to abrasion from sand and gravel, floating ice and wave action, leading to surface erosion.

Surface erosion may also be caused by cavitation: when water flows past irregularities in a concrete surface at a sufficiently high velocity, the reduced local pressure can fall to the vapour pressure of water, causing surface pitting of the concrete. The necessary flow rate is unlikely to occur in the vicinity of normal marine structures, although instances of this type of damage have occurred in turbine chutes and dam spillways associated with hydroelectric power construction (Browne & Baker 1980).

2.2.8. Reinforcement corrosion

Although corrosion of steel in concrete due to stress corrosion, hydrogen embrittlement or electrolysis due to "stray" electrical currents has been reported, virtually all corrosion distress is due to electrochemical corrosion. Electrochemical corrosion in concrete results because of the existence of non-uniformities of the steel or in the chemical or physical environment afforded by the surrounding concrete; under certain specific conditions these non-uniformities can produce significant electrical potential differences and hence corrosion.

Concrete generally provides excellent corrosion resistance to embedded steel. This resistance to corrosion is primarily attributed to passivation of the steel surface in the alkaline concrete environment, ie. to the formation of a stable film of corrosion product (gamma Fe_2O_3) on the steel surface which severely limits the anodic current density (Wilkins & Lawrence 1980). Reinforcement corrosion results from the failure of this passivating film which is generally attributable to two possible processes:

(a) reduction in alkalinity of concrete surrounding the steel;
(b) electrochemical action involving chloride ions.

The normal alkalinity of OPC concrete is around 12.8, but a reduction may be effected by leaching (2.2.3), carbonation (2.2.2.4) or the ingress of other acidic substances. At a pH of less than 11.5, corrosion may occur without the presence of chloride ions; at a pH of greater than 11.5 a measurable amount of chloride is required, and that amount increases as the pH at the steel-liquid interface increases (Popovics *et al.* 1983).

Chloride ions are able to destroy the passivating film and this generally results in a very small anodic surface facing a large cathodic surface still coated with the passivating film. These conditions cause a highly accelerated, deeply penetrating, corrosion (pitting corrosion) and the chloride ion is not consumed but simply acts as a catalyst. A threshold value of Cl^-/OH^- at the steel-paste interface, of 0.63, has been suggested (Mehta 1980) as representing the minimum Cl^-/OH^- ratio needed to initiate corrosion. However, in high C_3A Portland cements, a higher value may be tolerated because of the capacity of C_3A to remove some of the free chloride ion by formation of chloroaluminate (2.2.2.3). Experience from corrosion problems in the field (2.3) suggests that under U.K. conditions, the risk of corrosion in OPC concrete is small when chloride ion contents (by weight of cement) are $< 0.4\%$ and high for contents $> 1.0\%$ (Everett & Treadaway 1980).

The time to initiation of corrosion (breakdown of passivating film) is therefore dependent upon the effectiveness of the concrete cover as a barrier against ingress of chloride ions and loss of alkalinity. Particularly important in this respect are the thickness of cover and the permeability and degree of saturation (3.1) of the concrete, although the presence of cracking can obviously negate all other factors. (Factors controlling ionic diffusion through concrete are studied in detail in Chapter 4).

Once the passivating film has failed, corrosion can proceed. The following reactions represent a highly simplified model of the corrosion process; in practice the reactions take place in several intermediate stages (Wilkins & Lawrence 1980).

ANODE: $Fe \rightleftharpoons 2e^- + Fe^{2+}$

CATHODE: $\frac{1}{2}O_2 + H_2O + 2e^- \rightleftharpoons 2OH^-$

$Fe^{2+} + 2OH^- \longrightarrow Fe(OH)_2$

$4Fe(OH)_2 + 2H_2O + O_2 \longrightarrow Fe(OH)_3$ (red rust)

$3Fe + 8OH^- \longrightarrow Fe_3O_4 + 8e^- + 4H_2O$ (black rust)

The positively charged ferrous ions pass into solution at the anode; the remaining free electrons combine with water and oxygen at the cathode to produce hydroxyl ions. The hydroxyl and ferrous ions combine, precipitating iron hydroxide ($Fe(OH)_2$) which is then oxidised to haematite (red rust) or magnetite (black rust) according to oxygen availability. The volume of the corrosion products is several times greater than that of the original steel, so that tensile forces are set up around the steel, leading to the eventual cracking and spalling of the cover.

Once initiated, the rate of corrosion will depend upon:

(1) low concrete *resistivity*
(2) *water* availability; and
(3) *oxygen* in the pore water directly surrounding the reinforcement.

(1) Resistivity

In order for an electrochemical reaction to occur, a potential difference must exist along the bar to drive the corrosion current through the concrete from the anode site to the cathode site. The anode and cathode sites on the rebar can be adjacent (micro corrosion cell) or separated by a significant distance (macro corrosion cell); micro corrosion cells usually result in general corrosion whereas macro corrosion cells produce localised corrosion. The magnitude of the corrosion current is controlled by the resistivity of the concrete. If the resistivity is high, the corrosion current will be so small that no corrosion results. Factors affecting concrete resistivity are examined in detail in Chapter 5. An empirical scale of measured resistivity against likely rate of corrosion is given in Table 2.3.

Resistivity (Ωm)	Rate of Corrosion
over 200	Negligible
100-200	Low
50-100	High
under 50	Very high

Table 2.3: Likely rate of corrosion for various resistivity levels (Browne & Baker 1980).

(2) Water

Electrical conduction in concrete is effected by ionic diffusion (driven by an electrical potential) through the pore solution, and hence is very dependent upon degree of saturation (5.3). If concrete resistivity is sufficiently low for a significant corrosion current to flow there will necessarily be sufficient water present to allow corrosion to proceed unhindered.

(3) Oxygen

It has often been suggested that the virtual absence of corrosion in sea-water-immersed concrete (2.3) is due to its low permeability to dissolved oxygen. Hoever, a sufficiently high oxygen flux can generally be sustained, even through specimens that are fully submerged for long periods in water (Gjorv *et al.* 1976), to allow significant corrosion; this is particularly true in the case of pitting corrosion (Arup 1983) and in fully immersed conditions (Wilkins & Lawrence 1980), due to the large cathode/anode area ratio. Page (1975) therefore suggests that such corrosion suppression is not due to lack of oxygen, but due to retention of anodic passivity (even in the presence of chloride ion) by an interfacial lime-rich layer separating concrete and embedded steel, which stabilises the pH at the surface. However, once the passivating film is destroyed, oxygen diffusion is often the rate-determining factor (Fidjestol & Nilsen 1980, Arup 1983). Oxygen flux through the cover to the steel will clearly depend upon cover thickness, the presence of cracking and some parameter indicative of the permeability of the concrete to oxygen diffusion; this parameter will be highly dependent upon the moisture condition of the concrete since, theoretically, oxygen diffusion is 3.36×10^5 times less in water than in air (Tuutti 1980). However, Gjorv *et al.* (1976) found that for water-saturated uncracked concrete, quality and thickness had only minimal influence compared with the surface finish of the specimens.

Figure 2.2 shows the factors that are likely to determine the time to initiation (passivating film breakdown) and the rate of corrosion, once initiated, for the various zones of an offshore structure; no single factor stands out as determining the corrosion rate in the splash or tidal zones.

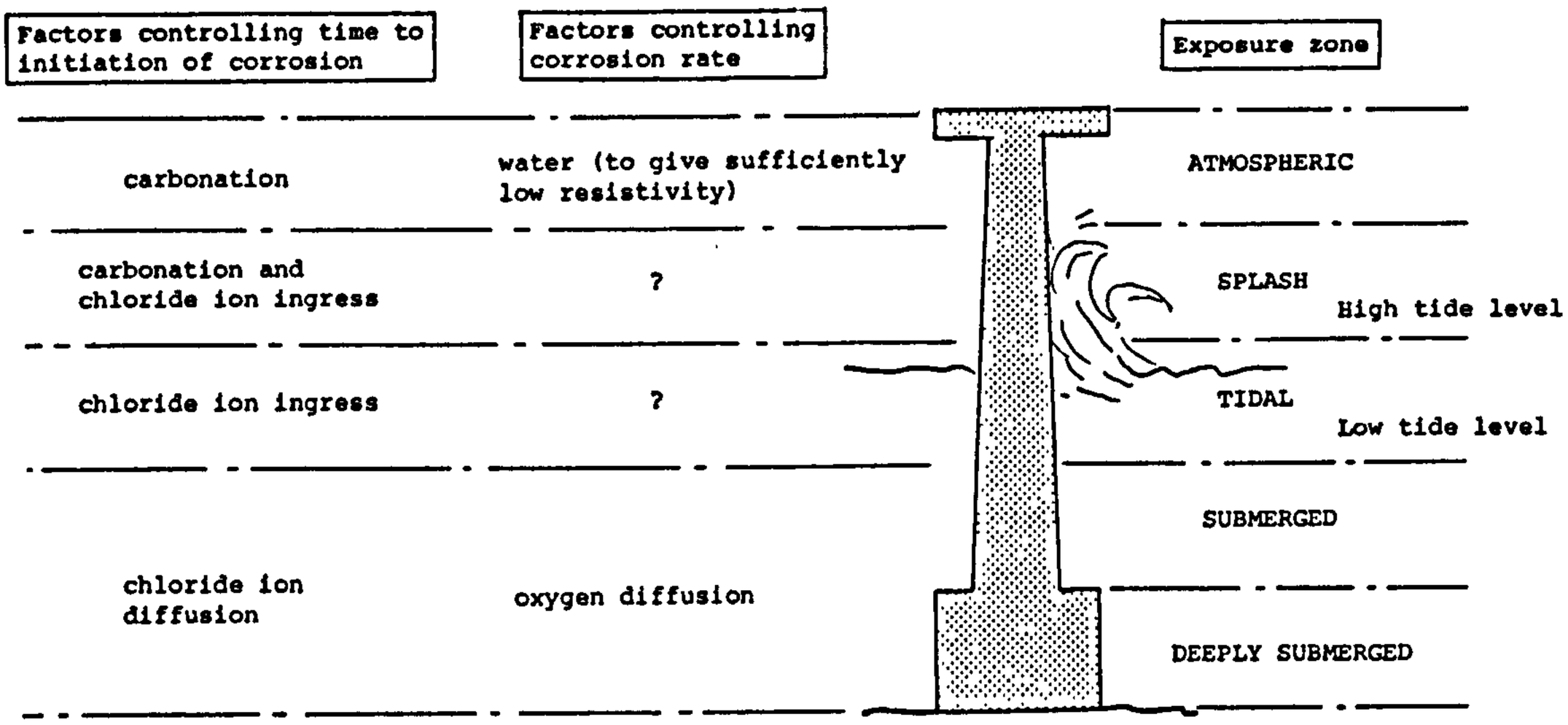

Figure 2.2: Factors likely to control time to initiation of corrosion and corrosion rate, in a concrete offshore structure.

2.3 Performance of offshore structural concrete

2.3.1 Introduction

Many marine concrete structures of over eighty years old are still in use today, indicating that long-term durability is often achieved using common and readily available construction materials. However, there have also been a large number of reported cases of deterioration, particularly to piling and soffits to decks of jetties and wharves, and instances of very severe attack due to virtually all of the mechanisms described in the previous section (2.2) have been observed. The relative contribution produced by each of these mechanisms, as well as the total deterioration, is dependent upon the environmental, structural and material factors outlined in 2.2.1. Of these factors, climate, and more specifically, the regularity of freeze-thaw cycling, is particularly important, deterioration due to frost action often far outweighing degradation due to other mechanisms. It therefore proves convenient to study the performance of sea-structures in mild climates (2.3.2) and cold climates (2.3.3) separately. The ambient air temperature offshore over the North Sea rarely falls below zero and hence, with the exception of part of the Scandinavian coastline, the North Sea represents mild marine exposure. Cold marine exposure conditions are prevalent in parts of Canada, Scandinavia and the Arctic. Within these categories of mild and cold marine exposure, the effects of the other factors are assessed, largely based on the results of natural exposure studies reported in the literature.

2.3.2 Mild marine exposure

2.3.2.1 Effect of environmental factors

Case histories of concrete deterioration show that individual mechanisms of deterioration tend to be limited to particular exposure zones (Figure 2.1). The most frequently reported mode of degradation occurring in offshore concrete structures is steel corrosion (2.2.8) in the tidal zone and particularly in the splash zone; this is not unexpected since, in these zones, concrete is exposed to intermittent wetting and drying, abrasion, carbonation, differential chloride penetration and has an ample supply of oxygen. In the submerged zone concrete is vulnerable to strength retrogression and loss of

material as a result of chemical mechanisms (2.2.2), but corrosion of reinforcing steel is seldom a problem.

Coastal structures such as sea-walls are generally subjected to greater abrasion from sand and gravel than ofshore structures and significant erosion is often observed in such locations.

The chemical aggressiveness of sea-water increases with both salinity and temperature.

2.3.2.2 Effect of structural factors

Member shape is significant in so far as sharp edges allow biaxial penetration of the environment, thereby causing more rapid deterioration.

The concrete cover acts as a physical barrier between embedded reinforcement and the external environment, limiting the access of substances which may play a part in corrosion. A sufficiently thick cover is therefore vital. Furthermore, increasing cover facilitates more effective compaction and increases the expansive corrosion pressures that can be contained. Table 2.4 shows the minimum permissible thickness of concrete cover recommended by various codes of practice for structures in a marine environment. These figures are largely based on past experience; there are literally hundreds of cases of reinforcement corrosion due to insufficient cover reported in the literature.

Integrity of cover is also of fundamental importance. Cracks allow the carbonation front to reach the reinforcing steel, causing local depassivation, and also allow rapid ingress of chlorides and oxygen, thereby increasing the rate of corrosion. Cracking also increases the surface area of concrete exposed to chemical attack. It would seem logical to suppose that the wider the crack, the more corrosion it will cause. Indeed, many codes of practice and design regulations stipulate maximum permissible crack widths (Table 2.4). However, Schiessel (1975) found that the extent of corrosion of the reinforcement in concrete exposed on a sea-shore was not related to crack width. A possible explanation of this observation is that the meaningful factor is the width of the crack where it reaches the steel bar and not the width on the ouside surface of the concrete; although it is usually the latter that is

		PIP (1977)	DNV (1977)	ACI 357 (1978)	BS 6235 (1982)
MINIMUM COVER to reinforcing bars (cover to prestressing tendons in brackets) mm	Atmospheric zone	--	40 (80)	50 (75)	75 (100)
	Splash/tidal zone	75 (100)	50 (100)	65 (90)	75 (100)
	Submerged zone	60 (75)	50 (100)	50 (75)	60 (75)
CEMENT C_3A CONTENT		< 12%	> 5% < 10%	> 4% < 10%	< 12%
MAXIMUM WATER/CEMENT RATIO		0.45 & preferably 0.40	0.45 & preferably 0.40	submerged zone: 0.45 other zones 0.40	0.40
MINIMUM CEMENT CONTENT kg/m³	Atmospheric	320 (40mm aggregate) 360 (20mm aggregate)		356	400
	Splash/tidal zone	400	400		400
	Submerged zone	as atmospheric zone			320 (40mm aggregate) 360 (20mm aggregate)
MINIMUM characteristic cube STRENGTH N/mm²	Normal exposure	40		35*	40
	Subjected to severe scouring action	45		42*	50
AIR ENTRAINMENT		4 - 7% in fresh concrete	3 - 5% in fresh concrete. Calculated spacing factor < 0.25 mm		

* 28-day cylinder compressive strength

Table 2.4: Code recommendations for durable offshore concrete.

measured, the crack width narrows with depth (Popovics *et al.* 1983).

2.3.2.3 Effect of material factors

2.3.2.3.1 Cement type and replacement materials

Low C_3A cements are generally specified for offshore concrete (see Table 2.4) in view of the susceptibility of the hydrated cement paste to sulphoaluminate sulphate attack. A considerable number of trials have shown a good correlation between C_3A content and durability. However, as mentioned earlier (2.2.2.2.2), disruption due to the formation of expansive ettringite is extremely rare in offshore structures and several investigators, including Regourd (1975), Mehta and Haynes (1975) and Fluss and Gorman (1958) have observed excellent long-term durability of relatively rich and impermeable concretes made with Portland cements of 12-17 percent C_3A content. Furthermore, C_3A can have a beneficial effect by delaying the time to corrosion initiation; Verbeck (1968) investigated the effect of long-term sea-water exposure on reinforced concrete piles made with 22 Portland cements of different composition. He found that an 8-11 percent C_3A cement gave a threefold reduction in cracking (caused by reinforcement corrosion) over a 2-5 percent C_3A cement. This reduction was attributed to the removal of much of the chloride from the pore solution by reaction with C_3A, thereby reducing steel corrosion.

A large number of investigations have demonstrated that cements which contain little or no $Ca(OH)_2$ on hydration are more durable to chemical attack and leaching than ordinary Portland cement. As a result of experiments initiated in 1886, Feret (1922) concluded that in general the behaviour of Portland cements was relatively poor, but that durability was enhanced by the addition of suitable pozzolana or granulated slag; both replacement materials react with $Ca(OH)_2$ to produce more chemically resistant hydrates. In a study involving 30 years of immersion in sea-water of 2500 concrete specimens, made with 18 different kinds of cements and mixtures having 0.55 to 0.65 water/cement ratio, Gjorv (1971) established that concretes made with calcium aluminate cement, supersulphated cement and blastfurnace slag cements resisted the action of sea-water fairly well, even when the specimens were not cured prior to immersion in sea-water. However, even the low C_3A Portland cements were affected. Addition of trass, a pozzolan, greatly improved the durability

of the concrete. Most of the investigations quoted above were based on the exposure of *plain* concrete specimens. It should be realised that in *reinforced* concrete, some free time in the hydrated cement paste is desirable to prevent rapid loss of alkalinity and hence early corrosion (2.2.8). The optimum mix for offshore construction is therefore a compromise, with sufficient free lime to prevent premature corrosion, but not so much that chemical degradation is significant.

2.3.2.3.2 Water/cement ratio and cement content

Virtually all studies which include water/cement ratio as a variable have shown that for a particular cement, durability decreases as water/cement ratio increases. This is due to the dependence of permeability on water/cement ratio (Figure 2.3). Other factors being equal, an increase in cement content also generally results in greater durability by promoting improved compaction and hence lower permeability (Mehta & Haynes 1975, Regourd 1975). The fundamental importance of permeability to most of the mechanisms of deterioration in a marine environment is discussed in 2.4.1. Table 2.4 shows the maximum water/cement ratio and minimum cement content as recommended by various codes of practice for structures in a marine environment.

2.3.2.3.3 Concreting practice

Case histories show that permeability is the most important property determining long-term durability, (discussed in 2.4.1). The following causes of lack of watertightness, associated with concreting practice, have been identified:

(1) dilution of mix with additional water;
(2) careless placement, leading to segregation etc.;
(3) poor compaction;
(4) poorly constructed joints (laitence not removed etc.);
(5) poor curing;
(6) cracking of concrete, as a result of thermal stresses due to temperature gradients in thick concrete members and carelessness in transporting precast members and driving precast piles.

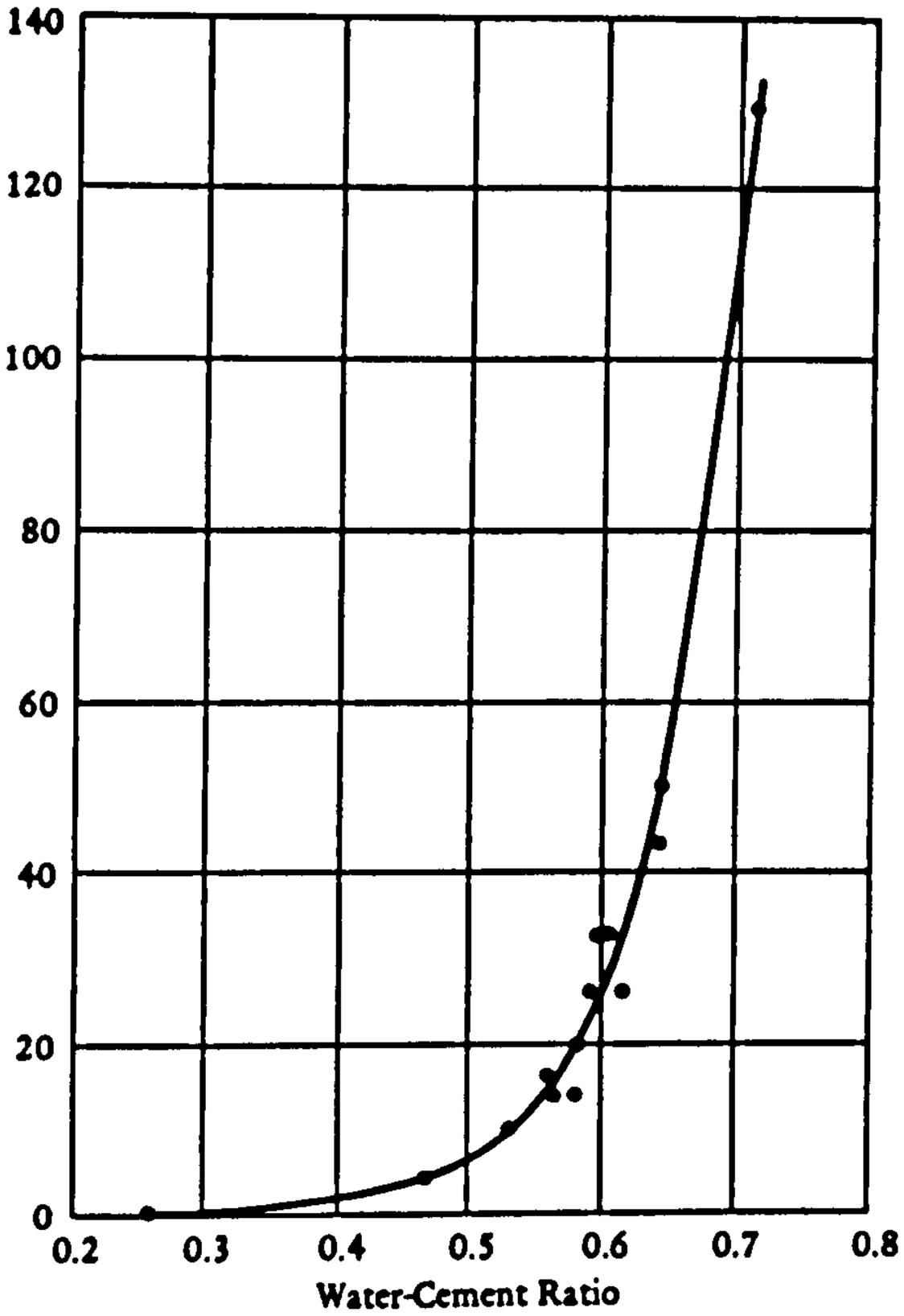

Figure 2.3: The effect of water/cement ratio on the permeability of mature cement paste (Powers *et al*. 1954).

2.3.2.3.4 Additional protection

A number of techniques are available to give increased protection to concrete, especially to the reinforcing system; for example, coatings, cathodic protection and corrosion inhibitors.

Coatings can be used, either to provide additional protection directly to the steel, for example by galvanising, or as sealants applied to the concrete surface, to prevent the ingress of chloride, oxygen etc., necessary for corrosion to continue at a significant rate. Coated reinforcement must be handled very carefully to prevent damage prior to concreting and there is evidence to suggest that hot dip galvanised reinforcment can produce cracking

and loss of bond to concrete due to corrosion of the zinc coating (Corrosion Institute Denmark 1978) and that its performance is poor in the splash zone (Makita *et al.* 1980). The most simple and economic method of reducing corrosion would seem to be the application of a coating to the concrete surface. However, there is always the possibility of local defects in such a coating and hence the danger of local steel corrosion (Gjorv 1972) and little protection is offered if the concrete is subject to cracking. Clearly the most direct way of reducing corrosion would be to develop new types of reinforcing steel that are more chloride resistant.

Experience gained from the use of cathodic protection of structural steel in soil or sea-water has been extended, by some companies, to steel in concrete. Cathodic protection has been applied successfully to freshwater tanks, to reinforced and prestressed concrete pipelines in the soil (King *et al.* 1979) and more recently to bridge decks (Stratfull 1983). Very little work has been done, as yet, to establish what risks are inherent in the application of cathodic protection to reinforced concrete. For offshore platforms it is almost certain that the underwater sections of concrete will be under the influence of cathodic protection systems, due to accidental (or otherwise) connection of cathodically protected external steelwork to the reinforcing grid (Browne & Baker 1980).

Incorporation of chemical corrosion inhibitors into concrete has often been successful, although they have not experienced widespread usage due largely to uncertainties regarding long-term effectiveness and possible detrimental effects of the inhibitor upon the concrete. Various organics, chromate and nitrite have been used, of which nitrite appears to be the most thoroughly investigated.

2.3.3 Cold marine exposure

In northern regions where the ambient temperature is regularly sub-zero, frost action is the predominant mechanism causing deterioration. Concrete in the tidal zone of an offshore structure is subjected to cycles of freezing and thawing as it is alternately immersed in the sea and then exposed to air at low temperatures, and it is indeed concrete in the tidal zone which, case histories show (e.g. Gjorv 1968), suffers most damage in such climates. Frost action may also contribute to concrete degradation in relatively mild marine climates,

but only if the structure in question is sited near to the coast and in a location where the ambient temperature regularly fluctuates between above and below zero; such diurnal variations can only occur in the vicinity of large land masses.

Extensive field and laboratory studies have shown that air entrainment and water/cement ratio are of prime importance in providing resistance to frost action. A higher amount of entrained air in concrete is necesary to obtain the same degree of frost resistance in sea-water as in freshwater. Under Norwegian conditions Lyse (1961) found that up to 10-12 percent entrained air was necessary for maximum durability (about twice as much as for freshwater). Table 2.4 shows the air entrainment levels recommended by various codes of practice. Water/cement ratio proves vital since it governs capillary porosity, and hence the volume of water available to be frozen and it also controls permeability (Figure 2.2) and hence movement of water to the freezing surface zone of the concrete (2.2.5). Table 2.4 presents code recommendations for the water/cement ratio of concrete exposed to a marine environment. The influence of cement replacement materials, cement content and concreting practice in limiting permeabilty and watertightness, as discussed in relation to mild marine exposure (2.3.2), is equally important in the context of concrete exposed to freeze-thaw cycling.

Under cold marine exposure conditions chemical reactions between sea-water and cement paste components are more slow, as is reinforcement corrosion. However, it would be a mistake to assume that the chemical action of sea-water does not represent a problem in such an environment. Gjorv (1968) observed extensive chemical degradation to a large number of concrete structures in Norwegian harbours, associated with local rises in permeability due to tremie placing of concrete.

2.4 Permeability of concrete in the marine environment

2.4.1 Influence of permeability on durability

The previous section (2.3) highlights the importance of permeability to durability in the marine environment. This relationship is clarified by considering the theoretical effect of a change in permeability on each of the mechanisms which may lead to the deterioration of concrete; Table 2.5 presents the effects of a reduction in permeability from which it can be seen that a reduction in permeability has a beneficial effect on all mechanisms. Only in the case of a mechanism in which fluid is forced away from a zone of expansion may a reduction in permeability theoretically have a deleterious effect. Such a process occurs in both the frost action and alkali-aggregate reaction mechanisms and is marked by an asterisk. Both frost action and alkali-aggregate reaction are exceptionally unlikely to occur under North Sea offshore exposure conditions using conventional U.K. materials.

2.4.2 Permeability variation of sea-water exposed concrete

Despite the vast number of laboratory and natural exposure studies on many aspects of the performance of concrete in the marine environment, it has only recently been appreciated that some concretes exhibit a very significant reduction in permeability on sea-water immersion.

Taylor Woodrow Research Laboratories (1980) undertook an extensive survey of the 34-year old Tongue Sands Tower to establish the long-term performance of an offshore concrete structure. As part of the investigation 100mm diameter cores were taken from the various exposure zones (2.2.1) within the structure. Ten D'Arcy-type water permeability tests (3.2.3) were carried out on sections from seven cores and the results are presented in Table 2.6. Unfortunately, most of the samples were taken from a considerable depth into the structure, thereby neglecting surface effects; only two of the specimens included the sea-water-exposed face and even these had been scraped to remove marine growth. However, it is quite clear that the permanently submerged specimens were several orders of magnitude less permeable than splash and tidal zone specimens. This reduction was believed to be due to:

"(a) the continued hydration of cement in the underwater environment, and

Deterioration mechanism		Influence of a REDUCTION in concrete permeability	
		Transport process reduced	Effect on mechanism
CHEMICAL MECHANISMS	Sulphate attack (2.2.2.2)	SO_4^{2-} ingress	Reduces the depth of sulphate attack, reducing the formation of expansive and soluble compounds
	Chloride ingress (2.2.2.3)	Cl^- ingress	(a) Increases the time to initiation of reinforcement corrosion (b) Reduces the reaction with $Ca(OH)_2$ and resulting formation of soluble $CaCl_2$
	Carbonation (2.2.2.4)	CO_2 ingress	Reduces the rate of carbonation and hence: (a) increases the time to initiation of reinforcement corrosion (b) reduces the formation of soluble compounds that could eventually lead to weakening of cement paste
	Alkali-aggregate reaction (2.2.2.5)	(a) water movement (b) alkali-silica gel	(a) Reduces the rate of uptake of water by alkali-silica gel thereby reducing the rate of deterioration; but (b) reduces the rate of diffusion of gel out of the confined area, possibly resulting in increased expansive pressures *
Leaching (2.2.3)		cement paste pore solution ion diffusion	Reduces leaching
Wetting and drying (2.2.4)		water absorption and evaporation	(a) Reduces volume changes; and (b) reduces the rate of crystallisation of salts in pores
Frost action (2.2.5)		(a) water absorption (b) water diffusion (c) sea-water ion ingress (d) water permeation	(a) Increases the time taken to achieve the critical degree of saturation of the concrete (b) Reduces osmotic diffusion of water to locations of ice formation (c) Enhances (a) & (b) (d) Reduces the rate of permeation of water away from the location of ice formation, possibly resulting in increased expansive pressures *
Marine growth (2.2.6)		cement paste pore solution ion diffusion and CO_2 ingress	Reduces the rate of leaching and carbonation thereby maintaining a high pH at the concrete surface for longer and hence delaying the settlement of plants.
Abrasion & cavitation (2.2.7)		—	—
Reinforcement corrosion (2.2.8)		(a) cement paste pore solution ion diffusion, CO_2 ingress and Cl^- ingress (b) O_2 ingress, water movement and ion diffusion	(a) Increases the time to initiation of reinforcement corrosion (b) Reduces the rate of corrosion

Table 2.5: Influence of a reduction in concrete permeability on mechanisms of deterioration which may occur in a marine environment.

Core Reference	Exposure location	Mix type	Position of sample tested relative to exposed face	Permeability ($ms^{-1} \times 10^{-12}$)
S6	Splash zone: 2.7m above high tide level	mortar	150-210mm	980
S5	" " 2.5m " " " "	mortar	125-175mm	720
S4*	" " 2.3m " " " "	concrete	125-175mm	2400
S2	" " 1.7m " " " "	concrete	0-50 mm	310
			280-330mm	29
T1	Tidal zone: 1.0m below high tide level	concrete	0-140mm	130
U2*	Submerged zone: 3.4m below lowest tidal level	mortar	100-150mm	1.2
U3	" " 3.8m " " " "	concrete	20-70 mm	0.56
			100-150mm	0.28
			150-200mm	0.86

* Core taken at a construction joint

Table 2.6: Permeability of cores taken from the various exposure zones of Tongue Sands Tower (based on Taylor Woodrow Research Laboratories 1980).

(b) the internal pore blocking caused by the crystallisaton of ettringite, chloroaluminate, etc., as a result of salt attack on the cement."

However, the increased permeability of the splash and tidal zone specimens could have been, at least partly, due to the increase in permeable porosity of the cement paste associated with drying shrinkage (2.2.4). Additionally, accelerated leaching due to wetting and drying and cracking due to thermal movements, or expansive salt crystallisation within cement paste pores, could also have contributed to this increase.

Stillwell (1983) describes work carried out by Wimpey Laboratories, as part of the *Concrete in the Oceans* programme, investigating factors affecting the time to initiation of reinforcement corrosion and subsequent time until unacceptable damage has occurred. A limited number of permeability tests were carried out on cores cut from beams that had been exposed to either deep sea-water submersion (in Loch Linnhe, Scotland, at a depth of 140m) or the splash zone (Portland Harbour, Dorset), for 2½ years. Table 2.7 shows the results.

A triaxial cell apparatus under constant head conditions was used and the permeability values quoted correspond to the initial readings once steady state flow had been achieved. For the standard grade concrete, splash zone specimens were around 15 times more permeable than the equivalent submerged zone specimens. However, the low grade concrete showed a reversal of this trend, submerged specimens being over 3 times more permeable than their splash zone counterparts. Stillwell suggests that the slightly lower values of permeability at the surface than at the centre of the cores may be due to "clogging of the pores at the surface due to absorption of solid matter as a result of being submerged at depth under pressure". However, it is possible that this discrepancy was due to the thin dense cement paste layer present on the surface of concrete when cast against a non-absorbent form.

Stillwell (1983) also reports the results of chloride penetration analyses on unreinforced concrete prisms exposed to atmospheric, splash and tidal zones at Portland Harbour and submerged at depths of 10m and 140m in Loch Linnhe. Typical results are shown in Figure 2.4. As can be seen, with the exception of the deeply submerged low grade concrete, there was no significant increase of chloride level after the first set of readings which were taken at 6 months. Stillwell does not suggest an explanation for this phenomenon.

Core Reference	Exposure location	Grade of concrete*	Position of sample tested relative to exposed face	Permeability ($ms^{-1} \times 10^{-12}$)
43	Splash zone	standard	0- 50 mm	14.6
			60-110 mm	13.5
40	Splash zone	low	0- 50 mm	7.69
			60-110 mm	13.2
50	Submerged at a depth of 140 m.	standard	0- 50 mm	0.74
			60-110 mm	1.13
47	Submerged at a depth of 140 m.	low	0- 50 mm	27.0
			60-110 mm	42.6

*Standard grade: 65N/mm² w/c: 0.4 cement content: 435 kg/m³
Low grade: 35N/mm w/c: 0.7 cement content: 305 kg/m³

Table 2.7: Permeability of cores taken from concrete beams exposed to either deep sea-water submersion or the splash zone for 2½ years.

STANDARD grade concrete

LOW grade concrete

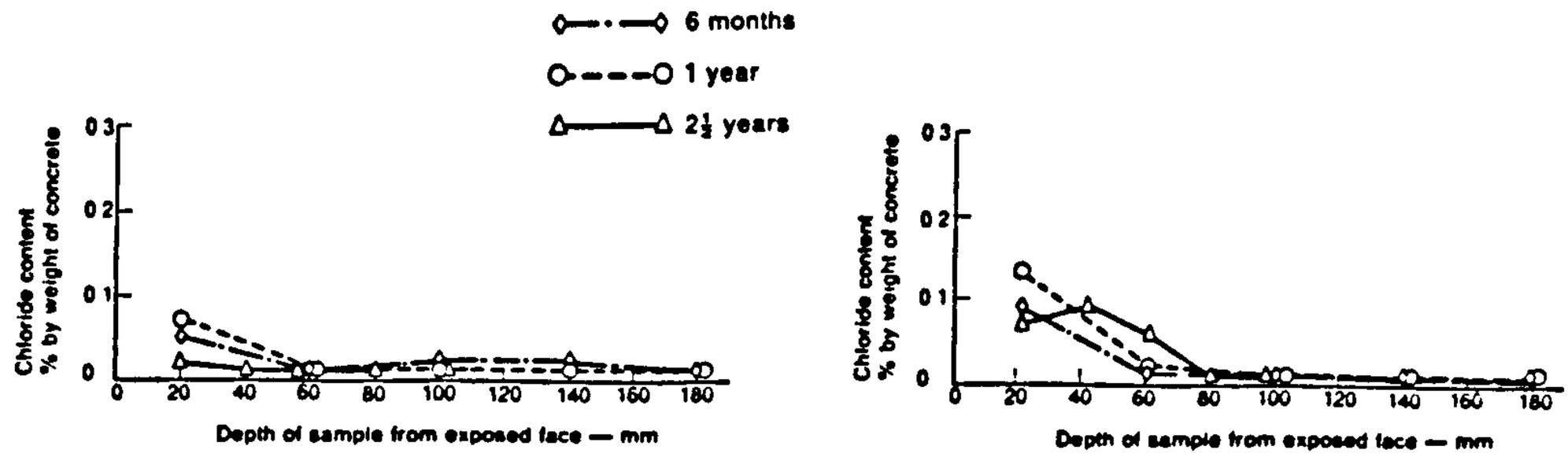

atmospheric zone

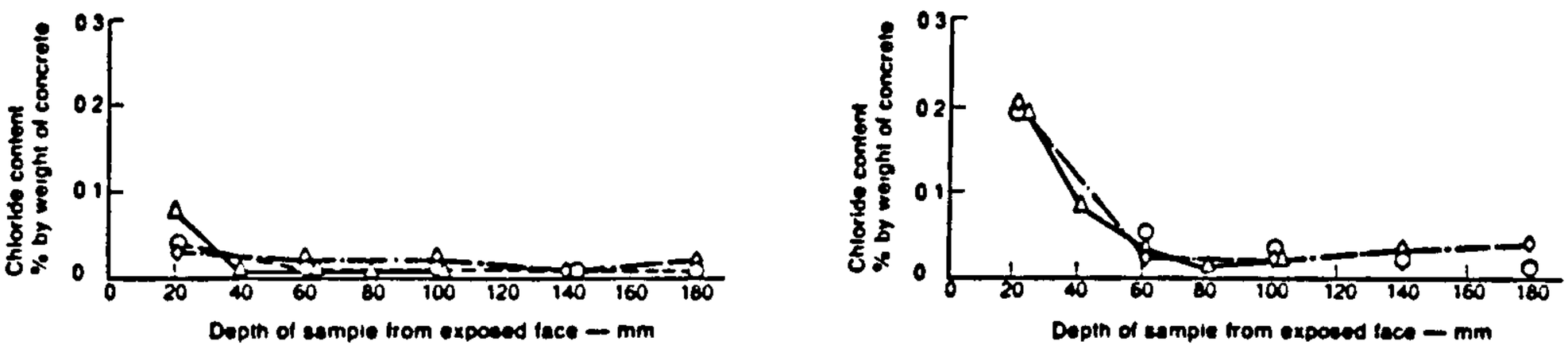

splash zone

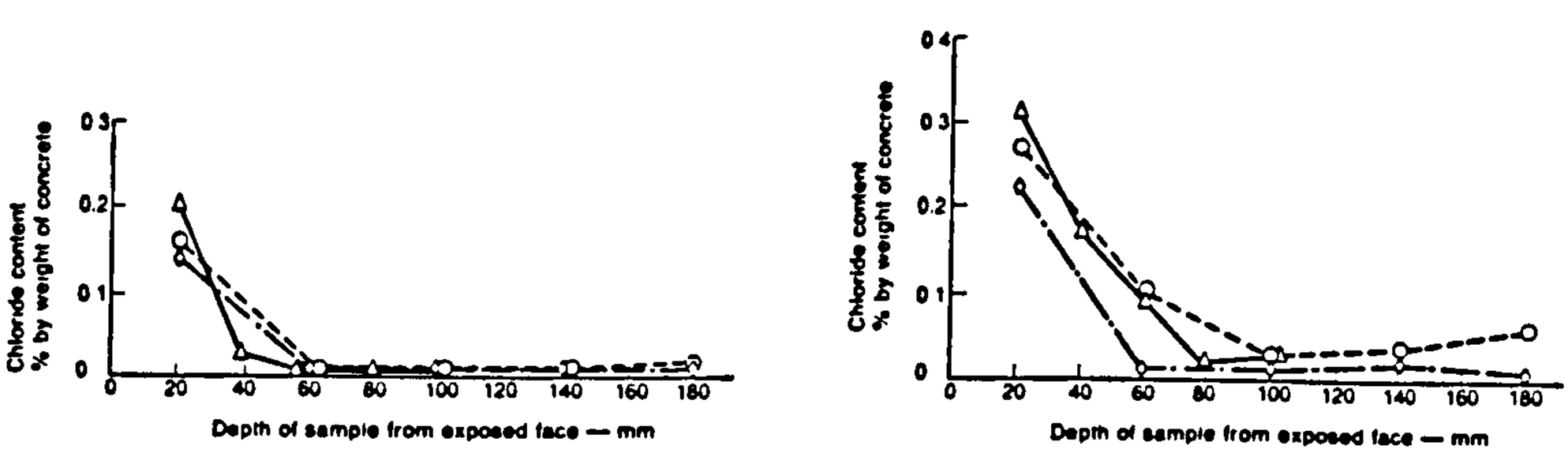

submerged zone

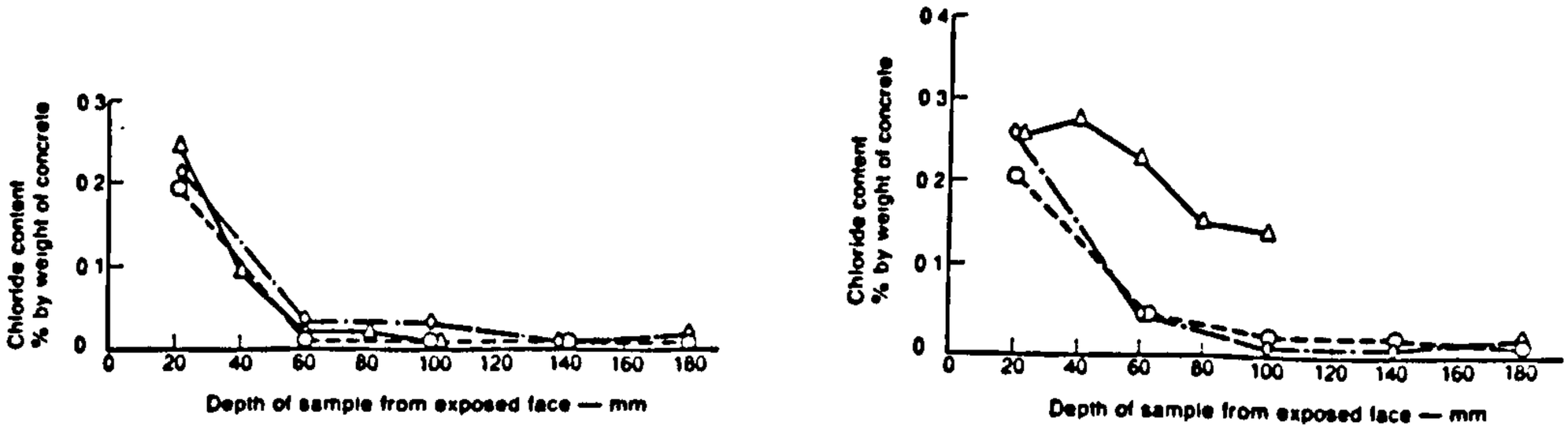

deeply submerged zone

Figure 2.4: Chloride concentration profiles for 2 grades of concrete after various periods of exposure in the atmospheric, splash and deeply submerged exposure zones (Stillwell 1983).

Haynes (1974, 1979, 1980) studied the long term performance of hollow concrete spheres exposed to ocean depths of 650 to 1500 meters. Each sphere was tethered by a chain and permeability data was obtained by monitoring the reducing number of links held off the sea floor as a result of lost buoyancy due to water absorption and permeation to the interior. The first reading was generally taken after 12 months, by which time the spheres had absorbed enough sea-water to saturate the concrete and subsequently permeate to the interior. However, later inspections showed only marginal additional permeation (Figure 2.5), some undefined mechanism having made the concrete "virtually watertight" within the first 12 months of exposure.

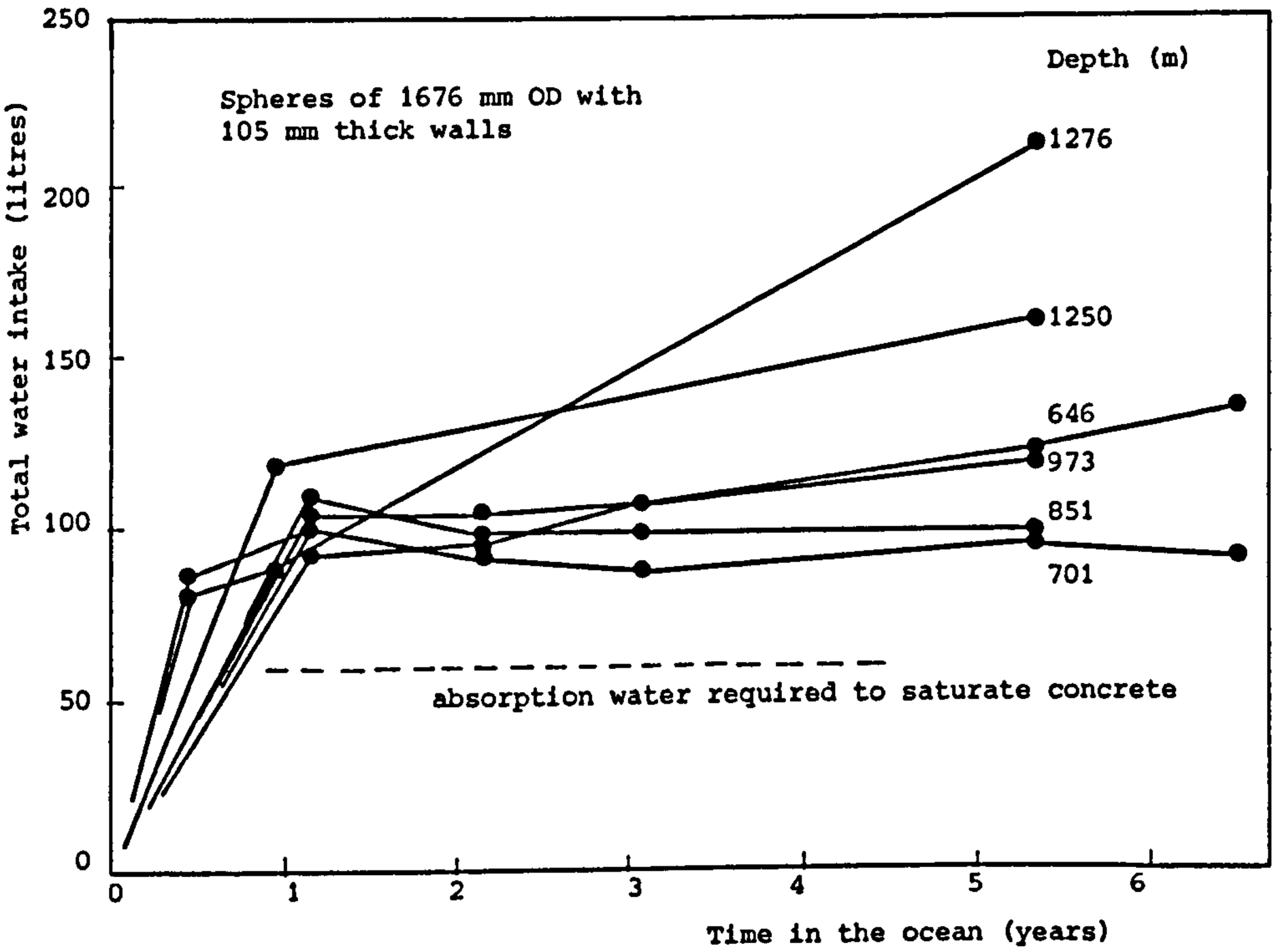

Figure 2.5: Progressive water intake of hollow concrete spheres at ocean depths (Haynes 1979).

Haynes (1972) also carried out shorter term tests on two hollow concrete spheres exposed to a head of sea-water, though in a pressure vessel rather than in the ocean. The spheres were initially subjected to water pressure on both the exterior and the interior in order to accelerate water absorption by the concrete; a pressure head of 340m was maintained for 7 days. The test set-up was then arranged so that the internal volume of a sphere, which was filled with water, was vented to the atmosphere and the water flowing out of the sphere was collected. During pressurization the water outflow represented instantaneous deformation of the sphere. When the pressure was held constant

the water outflow was a measure of creep deformation and permeated sea-water. After about 10 days the water outflow was principally a measure of permeability. Figure 2.6 shows the cumulative quantity of permeated water as a function of time, for the two spheres. One sphere was subjected to a pressure head of 768m for 21 days and the other sphere 1,145m for 42 days. The decrease in permeability with time is quite evident from the reducing gradient of the curves.

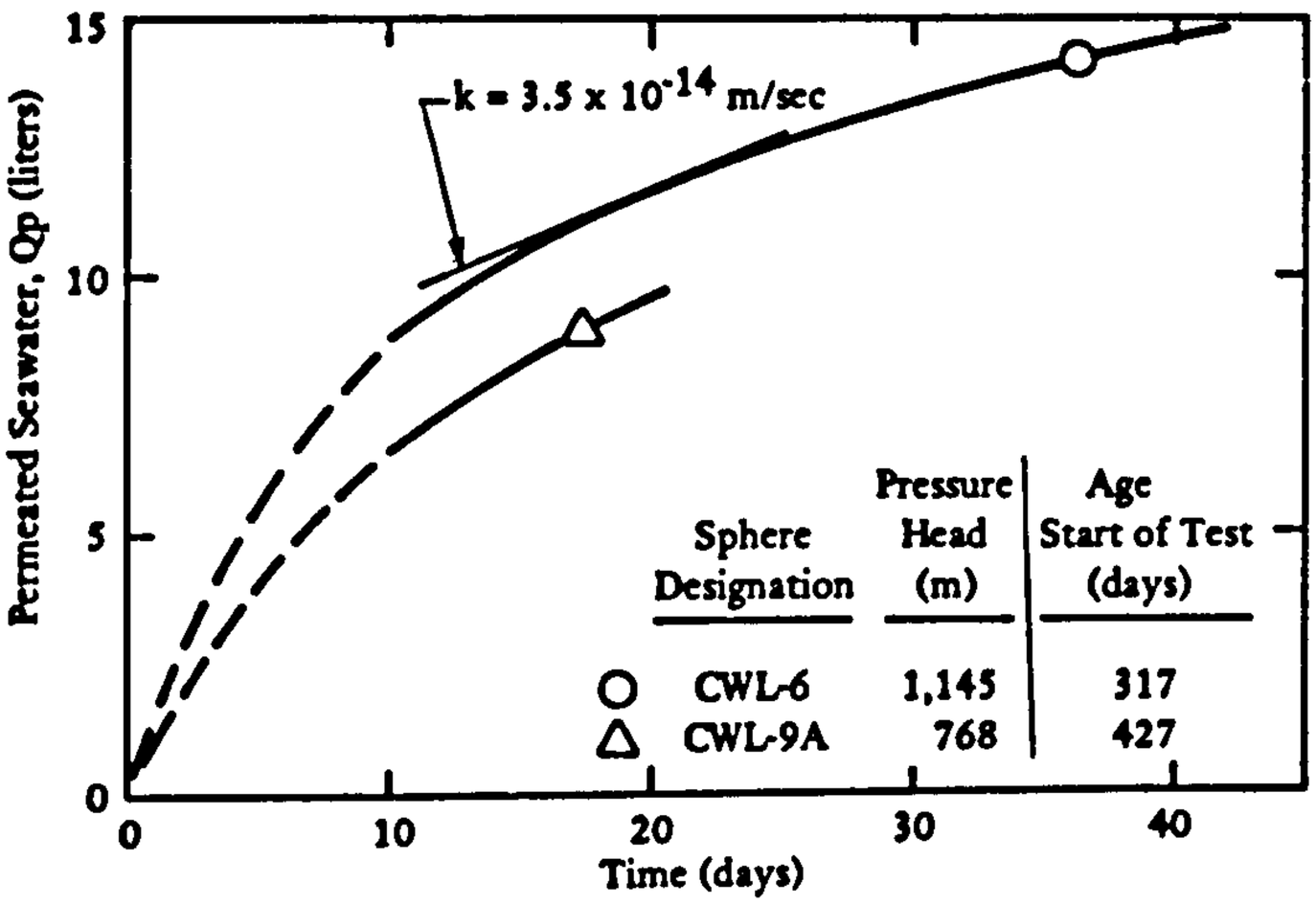

Figure 2.6: Permeability of hollow concrete spheres to sea-water during early exposure (Haynes 1980).

It should, however, be noted that a fall in permeability during the duration of a D'Arcy-type water permeability test (3.2.3) is frequently observed, even when *distilled* water is used as the permeating medium. Glanville (1931) suggests that this phenomenon is due to the combined effects of silting up, due to particles carried from one part of the specimen and deposited in the pores lower down, and further hydration and swelling of the cement. Another complicating factor is the effect of changes in the cement paste pore solution on permeability. Powers (1979) noted that permeability tests using freshwater were very sensitive to small changes in the alkali content of the pore solution, sodium and potassium ions reducing the mobility of water in small pores; sodium and potassium represent about 32% of the total ionic content of sea-water (Table 2.2).

Several workers have noted a marked increase in the electrical resistivity of concrete, generally indicating a reduction in permeability (5.5), after

immersion in sea-water. Bernhardt and Sopler (1974) measured changes in resistance over 40 months sea-water immersion between a stainless steel plate, placed 40mm from the surface of the test prism, and the central reinforcement. The slow asymptotic increase in resistance (Figure 2.7) was supposedly due to "progress in the hydration process". A similar trend was observed by

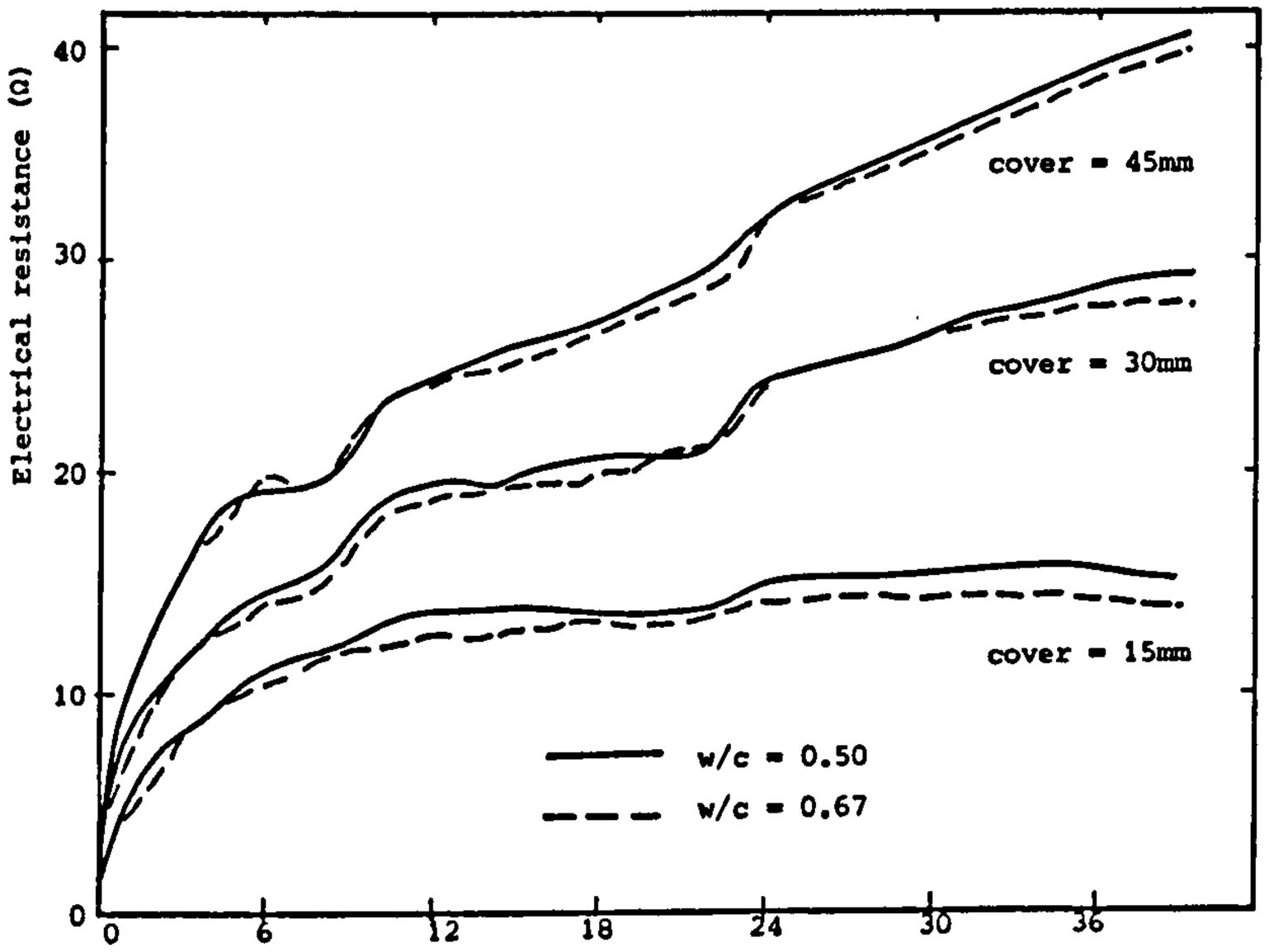

Figure 2.7: Development of electrical resistance of concrete specimens on exposure to sea-water (Bernhardt & Sopler 1974).

Askheim and Roland (1983). Gjorv *et al.* (1977) tested concrete specimens, made with rapid hardening Portland cement and cured in tap-water at 40°C for 2 months prior to testing. Once again, a similar pattern in resistance changes was observed (Figure 2.8). After 22 weeks of exposure 1mm of the sea-water exposed face was cut from the 70mm thick specimen and the resistance remeasured. The resistance had returned to the original value before exposure. Gjorv *et al.* proposed that, due to chemical action between concrete and sea-water, reaction products such as $Mg(OH)_2$ had precipitated, thereby blocking up the pores in a thin surface layer.

Conjeaud (1980) exposed 28 day old water cured 2 x 2 x 10cm OPC mortar bars to artificial sea-water for periods of up to 3 years. Figure 2.9 shows the variation of total chloride and sulphate (additional to that present in the original cement) with length of exposure, for a typical mix. It appears that

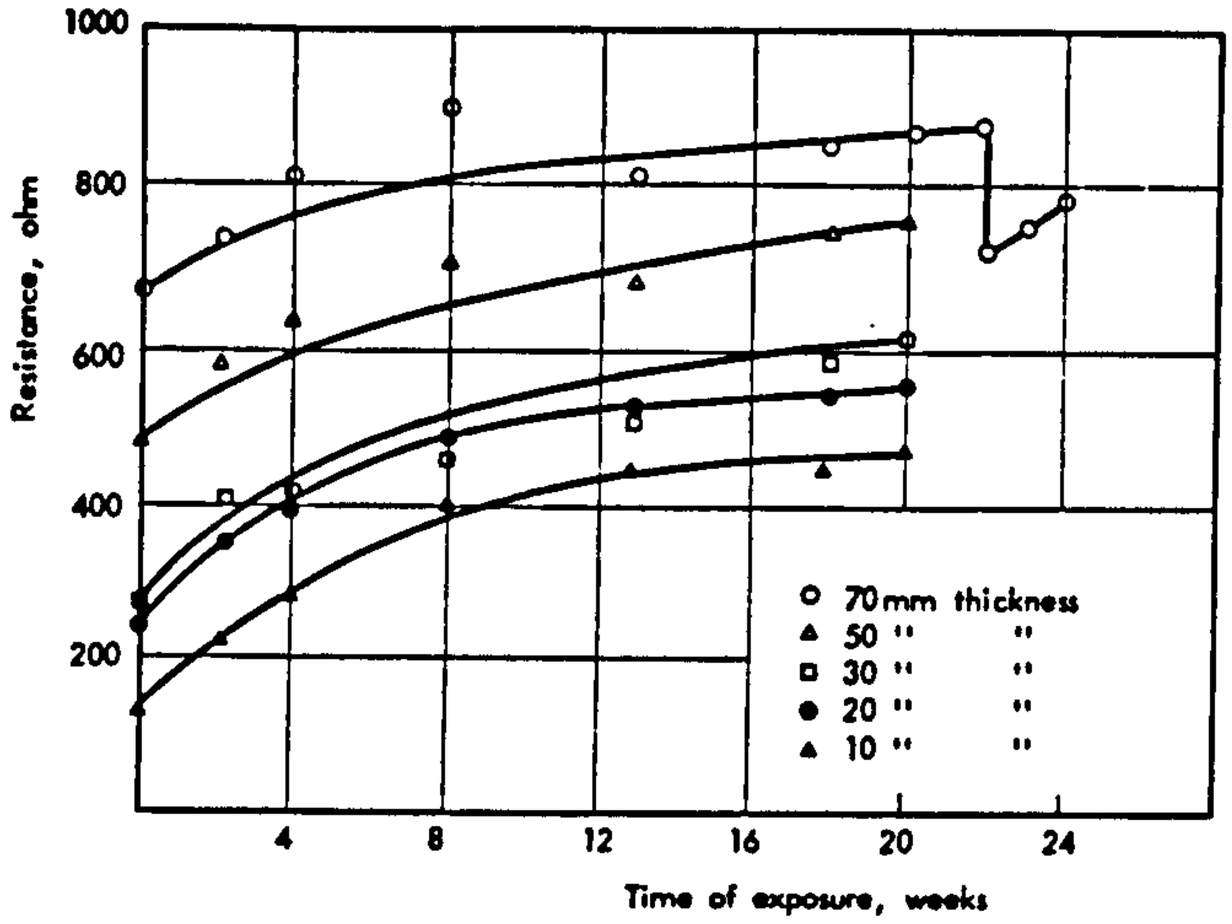

Figure 2.8: Development of electrical resistance of concrete specimens on exposure to sea-water (Gjorv *et al.* 1977).

little further sulphate penetration occurred after 2 days, while chloride penetration was reduced to a very low rate after 3 months, but continued for the full 3 years. Conjeaud does not state whether the specimens were allowed to partially dry prior to sea-water immersion, but this would result in sea-water absorption (rather than ionic diffusion) and would therefore explain the rapid early penetration of sulphate ion. The chloride penetration results should be interpreted with considerable caution. If all the C_3A present (13.55% by weight of cement) were to react with chloride to produce chloroaluminate and if the total porosity of the mortar (conservatively assumed to be 25%) was saturated with sea-water, the total chloride present (by weight of cement) would be around 5.5%. Furthermore, ettringite is formed preferentially to chloroaluminate (2.2.2.3) and hence significantly less than the total C_3A content would be available to react with the chloride ion. Clearly, therefore, the chloride levels observed after several months exposure were approaching the total capacity of the system and hence the permeability reduction might not be as significant as the shape of the curve in Figure 2.9 suggests; this issue was not discussed by Conjeaud.

Figure 2.10 shows the chloride and sulphate concentration profiles after various periods of exposure. It should be noted that because the mortar bars were of small cross-section, with the exception of relatively shallow short-term values, the measured concentration resulted from penetration through at least four faces of the mortar bar. Conjeaud does not suggest an explanation as to why the chloride concentration at all sections analysed was

lower after 6 months than at 3 months; this could be a discrepancy resulting from variation between supposedly similar specimens.

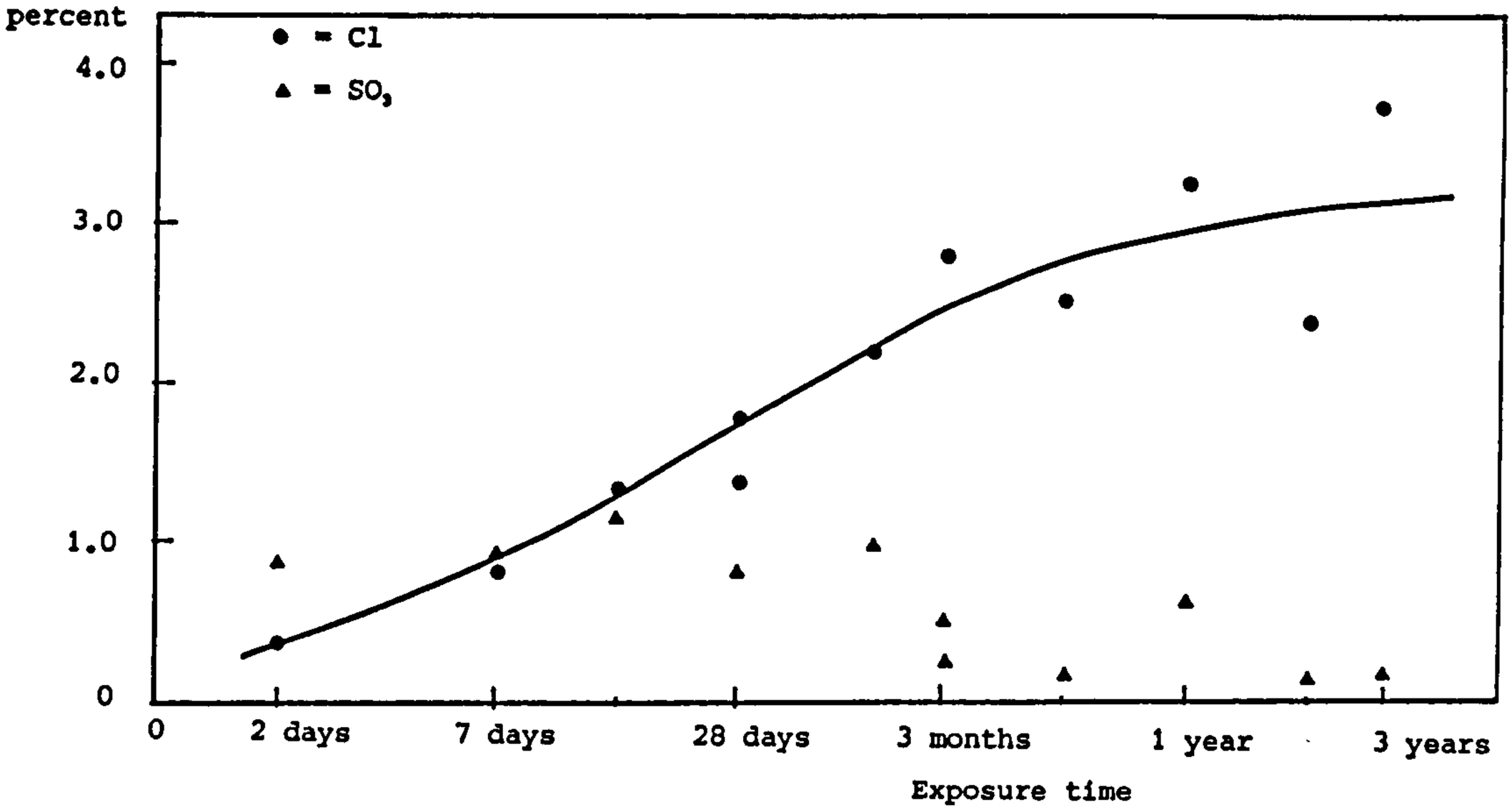

Figure 2.9: Total chloride and sulphate penetration into sea-water immersed mortar bars (based on Conjeaud 1980).

Conjeaud associated the decrease in ionic diffusion into sea-water-immersed mortar with the formation of layers of aragonite ($CaCO_3$) and brucite ($Mg(OH)_2$) on the surface of the specimens.

Midgley and Illston (1980) exposed hardened cement paste specimens to sodium chloride solutions for 6 months and then measured the pore size distribution using mercury intrusion porosimetry. Chloride ion penetration caused little changes in porosity but had effected a shift in the pore size distribution, the greater the chloride present the smaller the pores remaining. Such a shift could well produce a reduction in permeability.

Biczok (1967) notes that algae (which are generally present in offshore sea-waters) "tend to form a fibrous, tough, slimy, brown or green cover, which tends to seal the pores of concrete. Concrete in baths, spring heads, reservoirs, groundwater drainage works (shafts, chutes, pits), when overgrown with algae, becomes usually completely watertight".

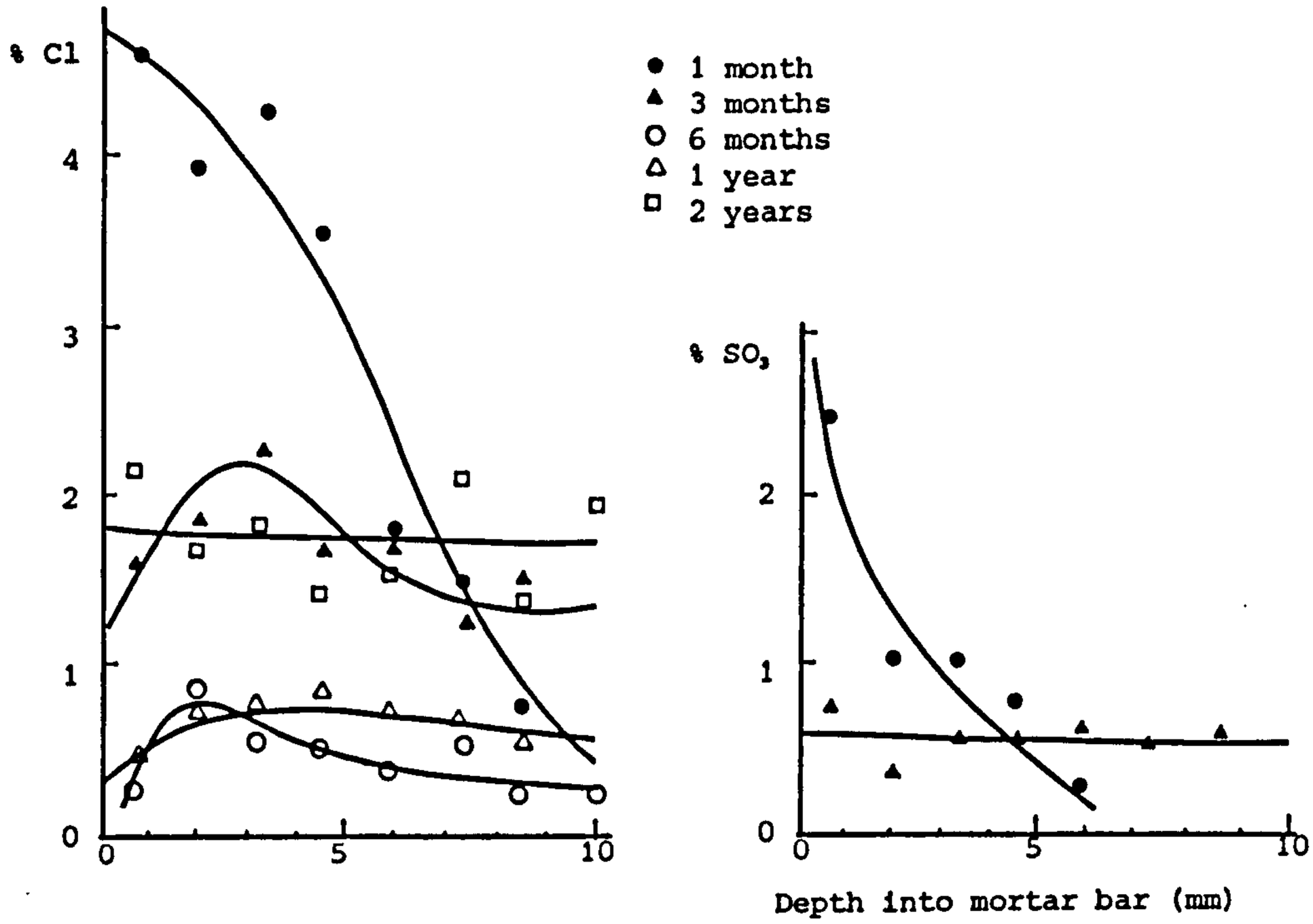

Figure 2.10: Chloride and sulphate concentration profiles for sea-water immersed mortar bars after various exposure periods (Conjeaud 1980).

Chapter 3: TEST METHODS TO MONITOR CHANGES IN PERMEABILITY OF CONCRETE EXPOSED TO SEA-WATER

3.1 Movement of fluids and ions through concrete

A water molecule or a solute ion may move in space in two different ways. It may move in the company of its neighbours in a macroscopic water mass, generally as a result of a pressure differential, or it may move microscopically and individually relative to its neighbours by *diffusion*.

The mechanism by which fluids and ions migrate through concrete is primarily dependent upon the moisture condition of the concrete. Hence, in a marine environment, the predominant mechanism will depend upon the environmental zone in which the concrete under consideration is located (Figure 3.1).

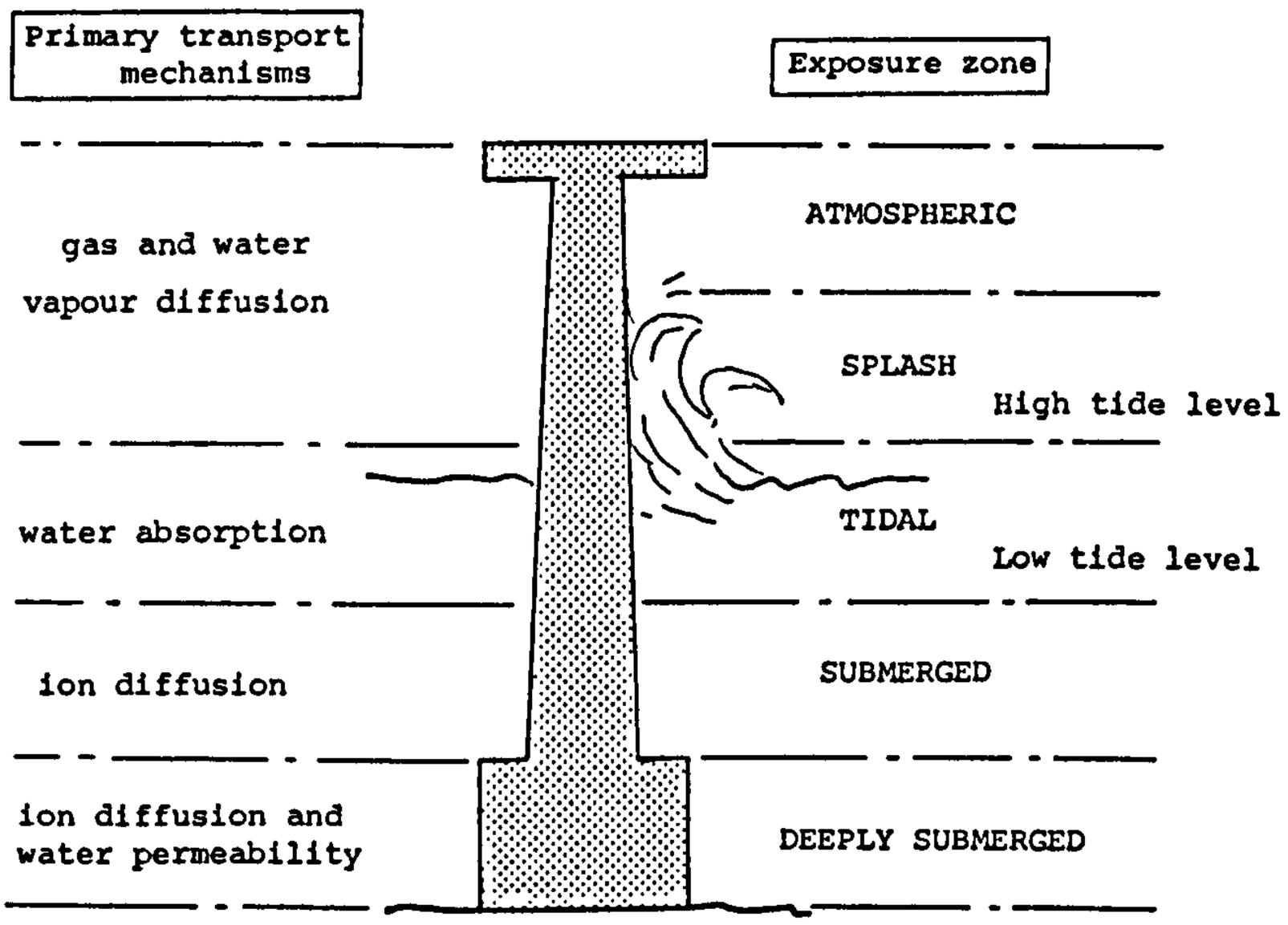

Figure 3.1: Primary transport mechanisms in the various exposure zones of a concrete offshore structure.

Figure 3.2 shows the various stages of water movement within concrete, (idealised as a single pore with a neck at each end; see 7.1.2 for a detailed description of the pore structure of concrete), as relative humidity increases. After initial surface adsorption (see Appendix 9 for definition of adsorption), movement of water vapour is via diffusion. As relative humidity increases, water condenses within the pore necks. In stage (c) the necks act as short circuits for vapour movement by shortening the effective path length for vapour diffusion (Philip & de Vries 1957). In stage (d) flow occurs in

thin liquid films and there is "vapour-assisted" liquid transfer (Rose 1965). Stages (b)-(d) correspond to concrete in the atmospheric and splash zones.

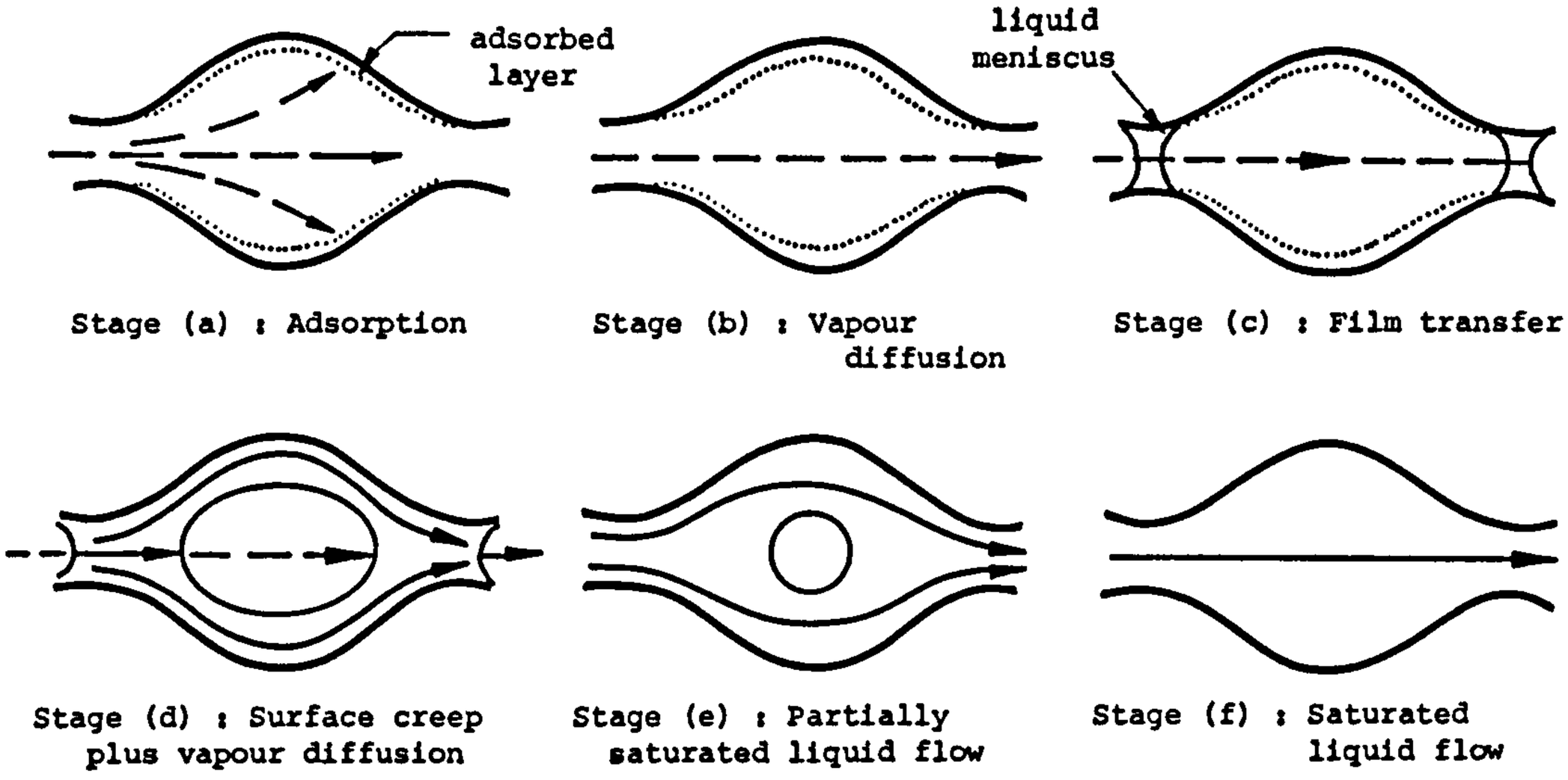

Figure 3.2: Movement of water within concrete.

Once a meniscus forms within a capillary, due to either increasing relative humidity or an external source of water, forces arise as a result of the pressure differential across the meriscus and induce flow through the capillary. This mechanism is of great significance in the tidal zone where concrete is subjected to regular cycles of wetting and drying.

When the pore system is completely saturated, water may flow as a fluid if a sufficiently high pressure head exists. It is possible that this mechanism causes sea-water penetration into concrete exposed to ocean depths.

Superimposed upon bulk fluid movement, ionic species, such as chlorides, can diffuse through free water within the concrete pore structure. This mechanism may occur in stages (c) and (d), but will be most effective in the fully saturated state. This is almost certainly the predominant process by which sea-water ions enter concrete submerged at normal depths.

A special case of diffusion occurs when an electrical potential is applied across an electrolytic solution. The ions are driven towards the electrode of opposing sign.

3.2 Conventional permeability test methods

3.2.1 Introduction

There are many test methods based on the transport processes described in 3.1 and most of these could be used directly, or else adapted, to monitor changes in the permeability of concrete exposed to sea-water. It is convenient to refer to all such techniques as "permeability" tests although many are more accurately termed absorption, diffusion or resistivity tests. These test methods are briefly outlined and are then assessed (3.3) in the context of the present investigation.

3.2.2 Water absorption

Water absorption tests generally comprise of two stages. The specimen is first equilibrated to a standard moisture condition and is subsequently exposed to a small head of water and water uptake monitored.

The basic water absorption test simply consists of oven-drying the specimen to constant weight and then immersing it in water to constant weight, results being expressed as per cent water absorbed by weight of concrete (BS 1881 : Part 122: 1983).

Slightly more sophisticated is the initial surface absorption test (ISAT). In this method the specimen is subjected to a 200mm hydraulic head via a cap fixed to the concrete surface. The rate at which water is absorbed by the concrete is monitored, generally over a two hour period, by following water movement along a capillary tube attached to the cap.

In the Figg hypodermic method (Figg 1973) a hole, typically 5.5mm diameter and 30mm deep, is drilled into the concrete, cleaned out, and the surface of the hole plugged by polyester foam and sealed with silicone sealant. A hypodermic needle supplied with 100mm head of water is then pushed through the plug and the time for the meniscus to travel 50mm is recorded. Results are expressed in seconds. A modified version of this technique (Richards 1982) requires a rather larger hole, typically 16mm diameter and 40mm deep. Two needles are inserted into the plug and water is allowed to flow through the system. After 30 minutes the inlet tap is switched off and the time for

the water to travel 25mm along a capillary tube is recorded.

3.2.3 Water permeability

This is conventionally regarded as the standard permeability test although, largely due to experimental difficulties associated with its execution (Glanville 1931), it is not a British Standard test. Generally a cylindrical specimen is fixed in a test rig with its curved face sealed and with one flat face exposed to water under a pressure of several bars. Then either the flow into the specimen or the flow out from the opposite face of the specimen is monitored. D'Arcy's empirical law relates the hydraulic gradient to the steady state rate of flow of fluids in a saturated porous material:

$$V = KA\frac{dh}{dx}$$

where K = coefficient of permeability (ms^{-1});
V = steady state volumetric flow rate (m^3s^{-1});
A = cross-sectional area of specimen (m^2);
$\frac{dh}{dx}$ = hydraulic gradient across specimen in the direction of flow (dimensionless).

For concrete specimens to be representative a thickness of at least 50mm is required and hence for good quality concretes a test duration of at least 20 days is generally necessary to achieve constant flow conditions. It is therefore often more practical to subject specimens to the hydraulic pressure for a shorter specified period and then to split the specimens open, determine the depth of water penetration and hence assess the permeability of the mix (Murata 1965). However, this method is not a true D'Arcy's law permeability test since the rate of flow results from a combined pressure and capillary action.

3.2.4 Gas permeability

The principles described in relation to water permeability (3.2.3) also apply where gas is used as the permeating medium. Permeameters have been devised to cover large ranges of pressure using air or common gases such as oxygen, nitrogen and helium.

For Darcy's law to be valid, the flow must be laminar with the resistance to

flow being caused solely by viscous drag. When highly permeabile samples or high pressures are utilised D'Arcy's law may be invalid due to the presence of turbulent flow conditions. Similarly, at very low pressures, flow will deviate from D'Arcy's conditions, due to the so-called "Klinkenberg Effect". This is most apparent for materials of fine pore structure and low permeability, where the layer of gas nearest to the surface moves relatively freely, especially if inert gases such as helium are used, yet liquids such as water are immobilised at the surface layer by dispersion forces. This slip-effect is an inverse function of the mean pressure and can be corrected for by measuring at a number of pressures and extrapolating to infinite mean pressure (Whiting 1981a).

3.2.5 Gas diffusion

Gas diffusion techniques are conveniently considered in two categories according to whether the specimens are water-saturated or not.

The testing of pre-dried samples generally involves sweeping opposite faces of a cylindrical concrete specimen (curved faces sealed) with the diffusing gas and nitrogen respectively and measuring the small percentage of the diffusing gas which is incorporated in the nitrogen stream after it has passed over the specimen. Diamon *et al.* (1971) used hydrogen as the diffusing gas, though oxygen has generally been preferred (Darr & Ludwig 1973, Lawrence 1982) due to the significance of oxygen diffusion to the corrosion of embedded reinforcement (2.2.8).

Gjorv *et al.* (1976) developed a test method whereby one flat face of a thin cylindrical concrete specimen formed one side of an otherwise sealed test cell containing lime-water. The cell was then submerged in a tank of aerated water and oxygen diffusion through the specimen and into the limewater was monitored using an electrochemical technique. This type of test, where the specimen is water-saturated, is more akin to ion diffusion tests (3.2.7).

3.2.6 Water vapour diffusion

The test specimen, in the form of a flat plate, is brought to a constant moisture state and is then sealed into a wide shallow pan containing either a desiccant or water. The rate of change of weight of the specimen is taken as

a measure of the water vapour transmission (ASTM C355-64).

$$WVT = \frac{G}{tA}$$

where WVT = water vapour transmission ($kgs^{-1}m^{-2}$);

$\frac{G}{t}$ = rate of water gain or loss (kgs^{-1});

A = area of test specimen exposed to desiccant or water (m^2).

Results may also be expressed in terms of *water vapour permeance*, defined as the ratio of WVT to the vapour pressure differential. The *average permeability* (for homogeneous specimens) is the product of water vapour permeance and the thickness of the specimen.

Morrison *et al.* (1979) developed an interesting variation on this method, exposing one face of the specimen to water and the other to a desiccant-controlled environment.

3.2.7 Ion diffusion

Ion diffusion can be monitored directly by analysing the concrete under consideration at various depths after exposure to a source of the ion in question, thereby producing a *concentration profile*. Analysis after various periods of exposure gives further insight into the diffusion process.

The diffusion of chloride ion has received most attention in the literature, primarily due to the significance of chloride ion to the corrosion process (2.2.8). However, a large proportion of the diffusing chloride ion is bound by reacting with C_3A, and furthermore can later be released if the pH of the pore solution falls (2.2.2.3). Consequently precise interpretation of chloride ion concentration profiles is very difficult (A 6.2).

An alternative type of diffusion test (*diffusion cell test*) allowing more straightforward interpretation requires that a thin slice of the mortar or concrete under test is placed to form a barrier between one section of a tank and another. One side of the tank is filled with a solution of an appropriate chloride salt and the rate of diffusion is monitored by analysing the water in the other side of the tank for chloride ion (4.3).

If the ion under consideration is already present at a significant level in the pore solution, more sophisticated techniques must be employed. Spinks *et al.* (1952) monitored sulphate ion diffusion using radioactive sulphate solutions.

A portable instrument has recently been developed (Whiting 1981a, 1981b) for measuring the *chloride permeability* of concrete both in situ and in the laboratory. The instrument relies on the accelerated migration of chloride ions toward a positive electrode. In the field the reinforcement nearest the surface is used as the positive electrode while in the laboratory, a cylindrical specimen is held in a specially designed test cell. A 60 V or 80 V direct current is applied for 6 hours using a 3% sodium chloride solution as the permeant. Data which can then be generated include total electrical charge (in coulombs), loss of chloride from the test solution and, if drilled samples are taken, chloride concentration profile into the concrete. The test is best utilised to rank concretes in terms of their relative expected permeability.

3.2.8 Electrical resistivity

Past studies of the electrical resistivity of concrete (5.1) have been associated with changes in resistivity during setting, the effect of moisture content on resistivity, the insulating properties of concrete and the influence of resistivity on the corrosion process. However, the similarity between the mechanisms of ion diffusion under a concentration gradient and electroytic conduction due to ion diffusion under an electrical potential suggests that a permeability test might be devised based on the measurement of resistivity. Electrical conduction through concrete is almost entirely due to electrolytic conduction through the pore water and is therefore dependent on degree of saturation, temperature and pore solution resistivity. Hence, in the submerged zone, at constant temperature and pore solution resistivity, an increase in specimen resistance represents a reduction in permeability (5.5).

The conventional in situ resistivity technique (Vassie 1980) involves drilling four holes, in a straight line, into the surface of the concrete, to take metal rod electrodes. An alternating current is made to flow between the outer contacts and the resulting difference in potential between the inner contacts is measured. The resistivity of the concrete can then be evaluated in terms of the spacing of the electrodes, providing the depth to which the electrodes are

inserted into the concrete is small compared with their spacing.

Most methods used in research involve either embedding electrodes or casting specimens in moulds incorporating a pair of opposite faces that may be retained as electrodes. Several workers have monitored the resistance of concrete specimens, submerged in an electrolyte solution, between embedded reinforcing bars and an electrode remote from the surface of the concrete (Bernhardt & Sopler 1974, Askheim & Roland 1983). Gjorv *et al.* (1977) measured the resistance of concrete specimens placed between half cells containing an electrolyte solution and a remote plate electrode.

3.3 Selection of test methods

3.3.1 Introduction

The main priority was to develop an experimental technique to monitor changes in the permeability of concrete *submerged* in sea-water. Most of the conventional test methods performed on saturated specimens are directly applicable for this purpose. Criteria for the ideal test method are presented in 3.3.2 and conventional permeability tests are compared and a number selected in 3.3.3.

The relatively poor performance of offshore concrete above the low tide level (2.3) necessitated consideration of changes in permeability associated with *tidal* zone exposure as well. However, the complexity of the tidal zone environment ruled out continuous monitoring of specimens using conventional permeability techniques. Three alternative approaches were considered:

(1) subjecting specimens to wetting and drying cycles in sea-water and continuously monitoring some aspect of permeability;
(2) subjecting specimens to wetting and drying cycles in sea-water and regularly stopping cycling and performing a permeability test;
(3) submerging specimens in sea-water and regularly removing them in order to carry out a permeability test appropriate to behaviour in the tidal zone.

(1) was seriously considered, but a sufficiently sensitive in situ method of monitoring any permeability-related property could not be devised. (2) initially appeared to be the most practical approach. However, although no relevant data could be found in the literature, Conjeaud (1981) found that wet/dry cycling performed in the laboratory, resulted in chloride and sulphate concentration profiles almost identical to those obtained for similar specimens submerged for the same period. This observation was not in agreement with measurements made on cores from the various zones of offshore structures (Taylor Woodrow Research Laboratories 1980) and hence the validity of simple wetting and drying tests to simulate tidal zone conditions had to be questioned. Certainly other factors such as wave abrasion and accelerated drying due to strong air currents result in a true tidal zone environment being far more complex than a simple laboratory wetting and drying test. A preliminary series of tests subjecting similar concrete specimens to a range of simulated tidal zone environments was considered; variables such as forced drying and rapid water circulation would be incorporated into the basic wetting

and drying test. The resulting chloride concentration profiles could then be compared with the profile of a submerged specimen. A test regime producing roughly the same relationship between wet-dry and submerged concrete concentration profiles as the relationship observed for offshore structures, could then be isolated and adopted as the standard laboratory tidal zone exposure. Unfortunately however, there was insufficient data in the literature on chloride concentration profiles of concrete offshore structures and virtually all the data that was available related to very long periods of exposure. Furthermore, it would have been hard to justify such a time-consuming and expensive study. Consequently approach (3) was pursued.

The same general criteria, as proposed for testing in the submerged zone, apply to permeability tests correlating with behaviour in the tidal zone; these criteria are presented in 3.3.2. Conventional permeabilty test methods are compared and a method is selected in 3.3.4.

3.3.2 Criteria for test methods

Ideally the following criteria should be satisfied:

1. Good correlation with natural exposure conditions and hence:

(a) there should be good correlation of the transport processes as monitored during the test with the transport processes predominating in the respective zone of an offshore concrete structure;

(b) the condition of the sea-water to which the concrete specimens are exposed throughout testing, should not depart significantly from that of ocean sea-water; ie. the facility should be available to regulate sea-water temperature, pH etc.;

(c) specimens should be tested in such a way that they perform as though they were part of a large structure;

(d) specimens should not be prepared or tested in a manner that could result in microstructural damage which would not occur in naturally exposed marine concrete.

2. Sensitive to small changes in permeability, therefore:

(a) testing should be non-destructive with the same specimen being retested after various periods of sea-water exposure, thereby eliminating errors due to the inherent variation between supposedly identical specimens;

(b) specimens should be permanently housed in test rigs, thereby eliminating inaccuracies associated with refitting specimens into test cells when readings are required;

(c) it should be feasible to test control specimens; e.g. specimens stored in limewater then tested similarly to those stored in sea-water.

3. Results should be informative and easily interpreted.

(a) It should be possible to distinguish between changes in permeability associated with surface effects and those due to a modification throughout the whole of the specimen.

(b) Readings should reflect the current condition of the specimen; i.e. there should not be a phase difference between the cement paste pore structure being modified and the measured permeability.

4. Relatively cheap to manufacture and operate, rapid and reproducible.

3.3.3 Submerged zone

Table 3.1 assesses potential test methods, listing advantages and disadvantages based on the criteria presented in 3.3.2. Most of the criteria are adequately satisfied and hence are not mentioned; comments are only made where a test method fails to meet a particular criterion, or where the method is unusually effective.

The D'Arcy's law permeability test would have been appropriate in the context of very deep ocean conditions and is by far the most documented permeability technique, but has too many drawbacks to be used in this research.

Both chloride ion diffusion and oxygen diffusion are very important mechanisms with respect to the reinforcement corrosion process (2.2.8) and hence, techniques based on these mechanisms are of direct quantitative value. The main feature of the chloride permeability test is that it is short in duration; However, such acceleration is not required in this context and the method was therefore rejected. The concentration profile method is a very simple means of observing the progress of ion diffusion, but the difficulty of interpreting the results to expose any variation in permeability resulted in it being adopted only as a supplementary test (Appendix 6). The principal attraction of the oxygen diffusion and diffusion cell techniques is that any change in

	TEST METHOD	ADVANTAGES	DISADVANTAGES	SECTIONS REPORTING USE OF SELECTED TEST METHODS
	Water permeability (D'Arcy's law)	1(a) Correlates with very deep submersion	1(a) See advantages 2(a) High hydraulic pressure possibly causes micro-structural damage 4 Long test duration and not very reproducible 1(b)or 2(b) Depending on whether permanently housed or not	—
	Oxygen diffusion through water saturated specimens (Gjorv *et al. (1976)*	3 Interpretation of results is straightforward	3(b) Specimens cannot be permanently housed since the limewater in the test cell rapidly approaches oxygen saturation	—
ION DIFFUSION	Concentration profile	1(a) Minimal specimen pre paration required prior to sea-water exposure or testing 4 No test rigs necessary therefore very cheap	2(a) There are practical problems associated with retesting the same specimen at different ages 3 Quantitiative inter-pretation of results is difficult (A 6.2)	Appendix 6
ION DIFFUSION	Diffusion cell	3 Interpretation of results is straightforward	1(b) It is difficult to regulate the pH of the sea-water 1(c) Thin specimens are required 3(b) There is a phase difference between permeability changes and chloride ion accumulation	Chapter 4
ION DIFFUSION	Chloride permeabil-ity (Whiting 1981a, 1981b)	—	1(a),2(a) The accelerated/ partially destructive nature of the test prohibits repeated testing at the same concrete surface 3 Quantitative interpretation of results is very difficult	—
RESISTIVITY	Embedded rod electrodes	3(b) An instantaneous indication of concrete permeability is afforded	1(a) The combined migration of all ions present is monitored; i.e. not specific to, say, chloride ion. 3(a) Surface effects neglected due to electrodes being embedded	—
RESISTIVITY	Remote plate electrodes	3(a) Simple to distinguish between surface and bulk effects 3(b) An instantaneous indi-cation of concrete permeability is afforded	1(a) The combined migration of all ions present is monitored; ie. not specific to, say, chloride ion	Chapter 5

Note: Numbers refer to criteria listed in 3.3.2.

Table 3.1: Test methods to monitor changes in permeability of concrete submerged in sea-water.

permeability is indicated by a change in the measured flux. The limited literature on oxygen diffusion through saturated concrete suggests, rather surprisingly, that unlike chloride ion diffusion, oxygen diffusion is insensitive to certain parameters that are known to affect the long term performance of offshore concrete structures. For example, Gjorv *et al.* (1976) observed that increasing specimen thickness from 10mm to 70mm only decreased oxygen flux through the specimen by a factor of 2.6 and that increasing water/cement ratio from 0.4 to 0.5 had only a very slight effect on the flux. Chloride diffusion will almost certainly determine the time to initiation of corrosion, while oxygen diffusion only influences the rate of corrosion once initiated. Consequently a chloride ion diffusion cell test method was adopted (4.3).

The diffusion cell technique has a number of disadvantages (Table 3.1) that could be overcome, it was felt, if a remote electrode resistivity method were developed to be used in conjunction with it. In particular, a resistivity technique would allow:

(1) distinction between surface and bulk effects;

(2) instantaneous indication of changes in concrete permeability;

(3) testing of representatively thick specimens; and

(4) regulation of sea-water pH, ionic composition etc..

Hence a remote electrode resistivity technique was developed and successfully utilised (Chapter 5).

3.3.4 Tidal zone

Specimens would be submerged in sea-water and then, at regular intervals, removed and tested, using a permeability technique correlating with behaviour in the tidal zone, before being resubmerged. The predominant transport processes, and hence appropriate test methods in the tidal zone are quite different from those in the submerged zone. Techniques involving water-saturated specimens relate to the submerged zone, while absorption and gas permeability methods correlate more closely with tidal zone conditions.

Table 3.2 assesses potential test methods, listing advantages and disadvantages based on the criteria presented in 3.3.2. The ISAT (Chapter 8) was found to be the most suitable technique.

	TEST METHOD	ADVANTAGES	DISADVANTAGES	SECTIONS REPORTING USE OF SELECTED TEST METHODS
WATER ABSORPTION	BASIC water absorption BS 1881: Part 122: 1983)	2 (b) No test rig required therefore 4 Cheap and simple	1(c) Water ingress through all faces of specimen therefore air trapped at the middle of the specimen opposes further ingress of water 2(a) Destructive: oven-drying causes microstructural damage. 3 Little indication of rate of absorption	—
	ISAT	1(a),3 Measures rate of surface absorption	2(b) Not practical to have specimens permanently housed in test rigs	Chapter 8
	FIGG (Figg 1973)	—	1(c),3(a) Surface effects not detected 3 Little indication of rate of absorption	—
	GAS PERMEABILITY (D'Arcy's law using oxygen or air)	—	Prior to testing (say 50mm thick specimens) either 2(a) accelerated drying results in microstructural damage or 4 Very long periods of drying 30 days + at 20°C) are necessary	—
	GAS DIFFUSION (oxygen through pre-dried specimens)	4 Steady state is achieved within a few minutes of starting test		—
	WATER VAPOUR DIFFUSION (ASTM C 355-64)	—	1(a) Water vapour diffusion is not directly responsible for the transport of sea-water ions into concrete 2(a) Possible damage of paste structure if low humidities used. Otherwise 4 Very slow.	—

Note: Numbers refer to criteria listed in 3.3.2.

Table 3.2: Test methods to monitor changes in permeability associated with the behaviour of concrete in the tidal zone.

The permeability-reducing phenomenon must result from some form of microstructural modification, whether it be a surface or a bulk effect, produced by pore blocking, salts crystallisation etc.. This chosen approach quantifies the effect of the microstructural modification produced by submersion on the predominant transport process in the tidal zone, (i.e. water absorption). However, the question of whether microstructural modification occurs in the tidal zone to a similar extent to that in the submerged zone remains unanswered. As suggested earlier (3.3.1), it was felt that this question could only be satisfactorily answered by analysis of samples taken from the various exposure zones of offshore structures. However, samples tested using apparatus devised to subject one face of up to four cylindrical concrete specimens to wetting and drying in sea-water (Fig. 6.15), were used to supplement the limited natural exposure data (6.7).

Chapter 4: ION DIFFUSION TESTING

4.1 Introduction

The diffusion cell test was outlined (3.2.7) and assessed in Chapter 3 in terms of its usefulness in the present context (Table 3.1), and Figure 4.1 shows the test arrangement. A thin slice of the mortar or concrete under test is placed to form a barrier between one section of a tank and another. One side of the tank is filled with a solution (solution A) of an appropriate salt and the rate of diffusion is monitored by analysing the water on the other side of the tank (solution B) for the ion under consideration. This method has been used as a research tool, primarily to study the kinetics of chloride ion diffusion in hardened cement pastes (Kondo *et al.* 1974, Page *et al.* 1981, Preece *et al.* 1981, Goto & Roy 1981); most workers have been interested in the effect of cement type and mix proportions on the diffusion coefficient of chloride ion. The technique is used here to monitor *changes* in diffusion coefficient over relatively long periods of sea-water exposure, an application not peviously encountered by the author.

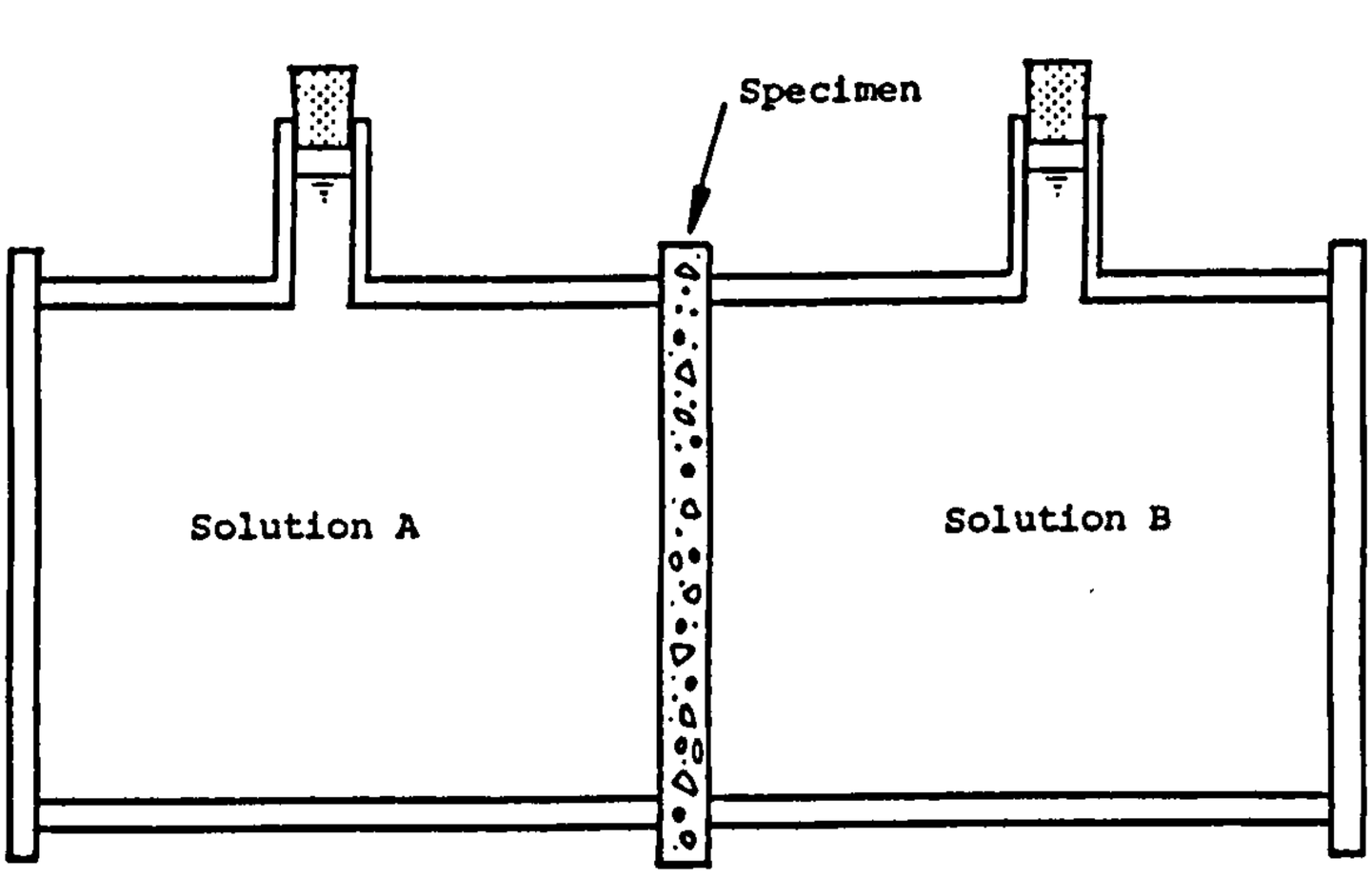

Figure 4.1: Section through diffusion cell.

For the purpose of this research, the diffusion of sulphate and particularly chloride ions were felt to be of relevance in the light of their influence on degradation processes (2.2.2.2 & 2.2.2.3). However, major practical problems were faced in attempting to apply a diffusion cell technique to sulphate ion diffusion (4.2). Consequently, chloride ion diffusion (4.3), which is certainly of more fundamental significance, was selected as the process to be monitored.

4.2 Sulphate ion diffusion

The possibility of testing for sulphate ion diffusion using a diffusion cell experimental set up was carefully considered. The idea was eventually rejected because of the following practical difficulties:

(1) if typical ocean-salinity sea-water were used as solution A, the sulphate levels attained in solution B would be extremely low, even after 3 or 4 months of exposure. This is due to two main factors. Firstly, sulphate is present in sea-water at a concentraton of around one tenth (by weight) of that of chloride and only around half of the sulphate is present in the form of simple hydrated anions (Table 2.2), the remainder forming more complex species. Secondly, the diffusion coefficient of sulphate ion in hardened cement paste is very low. The diffusion coefficients of sulphate and chloride ions in dilute solutions are about 10^{-5} $cm^2 sec^{-1}$ (Lawrence 1981). There is virtually no data in the literature on sulphate ion diffusion through cement paste. This is almost certainly due to the problems outlined here. The only work found was that of Spinks *et al.* (1952) who used radioactive isotopes and a Geiger counter to study diffusion processes in hardened cement pastes. The water/cement ratios used are not stated, but for 28 days old OPC and SRPC pastes, the sulphate ion diffusion coefficient was found to be approximately 2×10^{-10} cm^2 sec^{-1}, which is less than one-hundredth of the value one would expect for the *chloride* ion diffusion coefficient in a similar paste (Table 4.3). Even if the permeability-reducing mechanism were to have no effect, the sulphate level in solution B, after 3 months of sea-water exposure of a cement paste specimen of just 2mm thickness, would be less than 1 part per million ($D = 2 \times 10^{-10}$ cm^2 sec^{-1}, see 4.3.2 for theory).

(2) an appreciable level of sulphate is present in cement paste pore solution. The sulphate concentration of cement paste pore solution is typically of the order of 2000-4000 ppm (e.g. Page & Vennesland 1984). Clearly sulphate ion, leached into solution B from the specimen, would mask the very low levels of sulphate that had diffused through the specimen from solution A.

(3) chloride ions (inevitably present in solution B if solution A is sea-water) interfere with virtually all low-level sulphate determination techniques.

4.3 Chloride ion diffusion

4.3.1 Experimental details

44 pairs of diffusion cells of the type shown in Figure 4.2 were manufactured. Sections of 75mm ID PVC tubing were clamped between perspex end-plates by means of threaded studding, a seal being made at both ends of each tube with an "O"-ring. Each cell has a capacity of 0.5ℓ, with 12mm ID perspex access tubes allowing the cells to be topped up, samples to be withdrawn etc..

This technique requires relatively thin specimens in order to reduce the phase difference between any change in permeability at the sea-water-exposed face and chloride ion accumulation in solution B, and also to eliminate edge effects (4.3.2). Consequently mortars, rather than concretes, were tested. The mortars tested are shown in Table 4.1 and more comprehensive mix details are given in A1.1.

Mix reference	Free water/cement ratio	Cement type	Cement replacement materials
Mortar B	0.4	OPC	--
" C	0.6	"	--
" D	0.4	"	35% pfa
" F	"	SRPC	--

Table 4.1: Mixes tested.

It was generally intended that a mortar containing blast-furnace slag (A1.1: mortar E) would be tested. Unfortunately problems were encountered in analysing the resulting solutions for chloride ion; this is discussed later in this section.

A study of the limited literature on the permeability-reducing phenomenon (2.4.2) suggested that significant changes generally occur within the first 3 months of sea-water exposure; a test duration of at least 3 months was therefore necessary. Careful selection of specimen thickness was required,

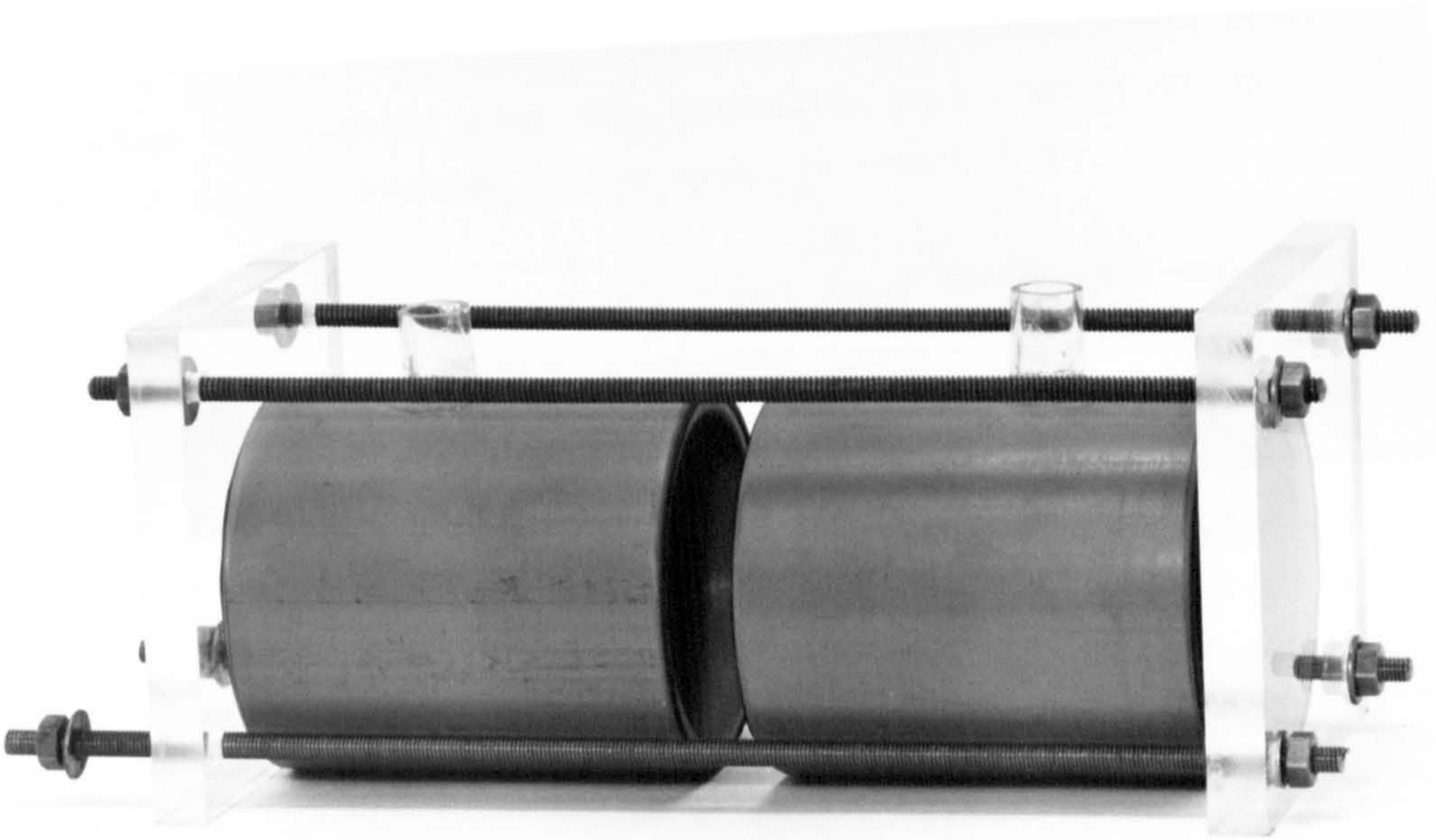

Figure 4.2 : Diffusion cell.

permitting sufficient chloride ion accumulation in solution B to allow changes in permeability to be identified without the chloride concentration becoming so high during the test that assumptions inherent in the method of analysing the results (4.3.2) were contravened. Preliminary experiments based on chloride ion diffusion coefficients from the literature (e.g. Page *et al.* 1981) demonstrated that a thicknesss of 7mm would be appropriate.

Previous studies (e.g. Page *et al.* 1981) have shown that there can be appreciable differences between supposedly identical specimens; this has generally led to 5 or 6 replicates being tested for each result. In this application, the object is to monitor trends in the variation of the diffusion coefficient of a particular *specimen* over a period of time, rather than to determine a single value for a particular *material*. Consequently at least 2 and generally 3 or 4 replicates of each test were thought to be sufficient.

The test variables are presented in Table 4.2. 55mm high 100mm diameter mortar cylinders were cast in steel moulds (A1.2); the flat face of the cylinder that was at the bottom of the mould is referred to as the *cast* face. The cylinders were demoulded after either 24 hours (mortars B and F) or 48 hours (mortar C and D) in the mould, and were stored in saturated calcium hydroxide solution (limewater) at around 20°C. At 28 days, the test specimens were cut from the cast face end of the mortar cylinders using a diamond saw, the blade of which was cooled and lubricated with limewater. Specimens were cut to within 0.2mm of the nominal thicknesses stated in Table 4.2; the *actual* thicknesses were recorded and used in subsequent calculations. Excess lime was washed from the specimens with distilled water. The specimens were then installed between diffusion cells (Figure 4.1) and solutions A and B (Table 4.2) were added before significant drying of the specimen had occurred. The solutions were added simultaneously to prevent permeation due to a pressure differential and the access tubes were then sealed with rubber bungs to prevent carbonation and water evaporation.

The sea-water used was North Sea sea-water acquired from Regent's Park Zoo (with a salinity of 32.7 g/kg and a pH of 8.15), having been collected several miles out from Scarborough. Self-healing due to the growth of algae (2.2.6) could well contribute to the permeability-reducing phenomenon. However, the growth of algae is extremely sensitive to environmental conditions which, it was felt, could not be sufficiently accurately simulated in the laboratory; particular difficulty would have been experienced in allowing

photosynthesis to proceed, at a natural rate, within closed diffusion cells. The sea-water was therefore filtered to remove algae and other suspended matter.

The role of solution B is twofold. It acts as a sink for diffusing chloride ions, but it should also provide a reservoir of cement paste pore solution ions thereby limiting any loss of solid matrix due to leaching (2.2.3); in this latter role solution B is a *simulated pore solution*. Ideally the simulated pore solution would be of identical composition to the pore solution within the specimen. Unfortunately however, the cement paste pore solution composition varies as hydration proceeds (5.5) and also varies with cement type, water/cement ratio etc., and it is therefore impractical to truly simulate it. The most important effect that the pore solution has on the cement matrix is to prevent dissolution of solid calcium hydroxide (portlandite), due to its lime saturation. It therefore proves convenient to adopt limewater as the simulated pore solution; an excess of lime was added to ensure that the solution was always saturated. It was, however, considered conceivable that the loss of sodium, potassium and hydroxyl ions from the cement paste pore solution throughout the duration of the test could distort the phenomenon under investigation. A more realistic simulated pore solution than limewater was therefore required, to provide a reservoir of all the major cement paste pore solution ions, rather than just calcium and a limited concentration of hydroxyl ions. The simulated pore solution used (test reference D8) was based on an analysis of the pore solution expressed from a 28 days old limewater cured mortar B specimen (Appendix 5).

Most of the diffusion cells were stored in a limewater-filled tank at 20 ± 1°C; the dissolved lime had the dual purpose of preventing lime leaching from the exposed portions of the specimens and also inhibiting corrosion of the metallic components of the diffusion cells. One set of replicates (test reference D9) were stored in a refrigerator at 3 ± 1°C, a temperature at the low end of the range of North Sea surface temperatures (A2.3).

It was felt that a study of the individual effects of sea-water chloride salts might elucidate the overall behaviour; solutions of sodium and magnesium chloride were therefore used. 0.5 molar sodium chloride solution was used since this is the approximate concentration of ocean sea-water. Solutions with the same chloride concentration were used in order to facilitate comparison of the effect of different cations on chloride diffusion and hence 0.25 molar

magnesium chloride solution was adopted. For one set of replicates (test reference D6) the sodium chloride solution was saturated with lime; this was to allow comparison with the work of other researchers who have almost exclusively used lime-saturated solutions. Obviously sea-water (and magnesium chloride solution) could not be saturated with lime since most of the magnesium ion would immediately be precipitated as brucite, thereby drastically altering its composition.

Another set of replicates (test reference D4) were installed with their sawn faces exposed to sea-water and their cast faces adjacent to the limewater.

Several "dummy" cells were set up with pure limewater on both sides of the specimen. Regular analyses for chloride were made to ensure that there was no significant extraneous source of chloride ions, from within the specimens, from the materials of the test cells or from the storage tank.

Test ref.	Mix reference	Nominal thickness (mm)	Solution A	Solution B	Specimen face in contact with Sol.A	Temperature °C
D1	Mortar B	9.8	sea-water	limewater	cast	20
D2	"	4.3	"	"	"	"
D3	"	7.0	"	"	"	"
D4	"	"	"	"	sawn	"
D5	"	"	0.5M NaCℓ	"	cast	"
D6	"	"	lime-saturated 0.5M NaCℓ	"	"	"
D7	"	"	0.25M $MgCℓ_2$	"	"	"
D8	"	"	sea-water	simulated pore-solution*	"	"
D9	"	"	"	limewater	"	3
D10	Mortar C	"	"	"	"	20
D11	Mortar D	"	"	"	"	"
D12	Mortar F	"	"	"	"	"

* simulated pore solution = 0.091M NaOH + 0.115M KOH + 0.017M $Ca(OH)_2$

Table 4.2: Diffusion test variables.

When a reading was required, the diffusion cells were removed from the tank (or refrigerator), solution B was stirred (via the access tube) and a pipette was used to remove 10 mℓ of solution, which was immediately replaced with fresh limewater. It was considered important to remove as little of solution B as possible (although compensated for in calculations) and hence to take as few readings as possible. Consequently a supplementary series of cells were set up and tested regularly in order to determine when the test cells should be sampled.

A chloride electrode and pH/mV meter (Kent Industrial Measurements models 8004-2 and 7045 respectively) were used to analyse the extracted samples.

The principal objective was to identify changes in diffusion coefficient with time and hence, to reduce calibration errors, all the samples were tested together at the end of the exposure period. Prior to testing the samples were stored in sealed glass bottles to prevent evaporation. The extracted solutions were lime-saturated and hence had a high pH. The pH was reduced to a value within the working limits of the chloride electrode by adding 3 mℓ of a buffer consisting of 2.0M ammonium acetate plus 2.0M acetic acid (to 10mℓ of solution). The standard sodium chloride solutions, used to calibrate the electrode, were lime-saturated and then buffered in the same way as the test solutions. The electrode was recalibrated every 2 hours during testing.

Difficulty was experienced with certain samples in obtaining a steady reading; after vigorous stirring of the solution an increase of 5 or 6 mV (e.g. from -250 to -245 mV) over a five minute period was often observed. This was almost certainly due to the development of a redox potential due to the presence of both sulphite and sulphate ions in solution. All cements tested contained significant levels of sulphite (Table A1.3) and sulphate ions may also have diffused through the specimen from the sea-water. Experiments attempting to stabilise the oxidation state of sulphur, while keeping within the required pH limits of the electrode, proved unsuccessful. However, experiments monitoring the effect of additions of sulphite and sulphate on standard chloride solutions showed that the steady reading that the electrode eventually settled to corresponded to the true chloride level.

As mentioned earlier, a further problem arose in testing solutions exposed to mortar containing blast-furnace slag due to interference caused by the presence of sulphide ion. Even a S^{2-}/Cl^{-} (moles per litre) ratio of 10^{-6} causes the deposition of a silver sulphide layer on the electrode membrane sufficiently dense to produce significant interference. The blast-furnace slag used contained 1.66 per cent sulphide ion (Table A 1.3) and hence leaching caused the sulphide level in the lime solution to be critical. Dosing samples with nickel sulphate solution removed excess sulphide ion by precipitating nickel sulphide. However, nickel sulphide is still sufficiently soluble to leave enough sulphide ion in solution to cause interference. Unfortunately the full extent of the problem was only appreciated after samples had been extracted and buffered. An ion-exchange resin method of removing sulphide might have been feasible if a larger volume of solution had been available. The size of the sample and/or the presence of acetate ion prevented the use of titrimetric, gravimetric or spectrophotometric methods. Consequently results

for mortar E are not available.

At the end of the 23 week exposure period the pH of solutions A and B was measured for selected cells (immediately to prevent carbonation). Specimens were removed from their cells, rinsed with distilled water, wrapped in polythene film and stored for later examination and analysis (6.2, 7.4).

4.3.2 Theory

Under certain circumstances the diffusion cell test may be considered to be a case of diffusion through a plane sheet of thickness ℓ and diffusion coefficient D, whose surfaces, x = 0 and x = ℓ are maintained at concentrations C_A and C_B respectively. The chloride ion flux (J) entering solution B is then given by:

$$J = \frac{V}{a}\frac{dC_B}{dt} = \frac{D}{\ell}(C_A - C_B) \qquad (4.1)$$

where V is the volume of solution B, and a is the cross-sectional area of the specimen.

Integrating between the time of initial permeation of chloride into solution B, to, and a subsequent time, t:

$$\int_{C_B=0}^{C_B=C_B} \frac{dC_B}{C_A - C_B} = \int_{t=t_o}^{t=t} \frac{Da\,dt}{V\ell}$$

hence, if C_A is constant $\left[-\log_e | C_A - C_B |\right]_0^{C_B} = \frac{Da}{V\ell}[t]_{t_o}^{t}$

therefore, $$\log_e \frac{C_A}{C_A - C_B} = \log_e \left[1 + \frac{C_B}{C_A - C_B}\right] = \frac{Da}{V\ell}(t - t_o)$$

Now for $0 < x \leq 2$ $\log_e x = (x-1) - \frac{(x-1)^2}{2} + \frac{(x-1)^3}{3} - \cdots\cdots$

putting $x = \left[1 + \frac{C_B}{C_A - C_B}\right]$ $\left[(<2 \text{ if } C_B < \frac{C_A}{2}\right]$,

$\log_e \left[1 + \frac{C_B}{C_A - C_B}\right] = \frac{C_B}{C_A - C_B}$ (if $C_B \ll C_A$)

therefore,

$$C_B \simeq \frac{Da}{Vl} C_A (t-t_o).$$

C_A and C_B are assumed to be equivalent to the concentration of solutions A and B respectively.

The requirement that C_A is constant and that $C_B << C_B$ must be achieved by careful experimental design.

In the test set up used (Figure 4.1) the specimens are necessarily larger than the internal cross-sectional area of the cells and hence diffusion may occur over an area > a. This "edge effect" means that the implicit assumption of one dimensional diffusion through the specimen is not strictly correct. Barrer, Barrie and Rogers (1962) examined the importance of the edge effect and produced a graph relating the relative difference in flux with specimen overlap, for various specimen thickness to cell internal radius ratios. Using the diffusion cells manufactured for this research, together with a 9.8mm thick (the thickest tested) 100mm diameter specimen, the edge effect results in an error in the diffusion coefficient of less than 7 per cent, which is negligible in the context of the present application.

A further implicit assumption is that D is constant. This is certainly not true, however, the results show that the variation in D is not sufficiently great to justify developing a model to take such variation into account.

Figure 4.3 shows a typical plot of C_B versus time.

Hence, at time $\frac{t_j + t_k}{2}$ $\qquad D \simeq \frac{Vl}{aC_A} \left[\frac{C_B(t_k) - C_B(t_j)}{t_k - t_j}\right]$.

4.3.3 Results

Figure 4.4 shows a typical set of C_B versus time results for 4 replicates of the same test (test reference D3). The curve passes through the average of the 4 values at each sampling time. The top set of curves in Figures 4.5 to 4.8 were constructed in similar fashion, although, for clarity, specific points are not shown; it should, however, be remembered that each curve is based on at least 30 readings. The lower set of curves in Figures 4.5 to 4.8 show the variation of diffusion coefficient (calculated from the slope of the top set

of curves) with time of exposure. The test references used in Figures 4.5 to 4.8 refer to Table 4.2.

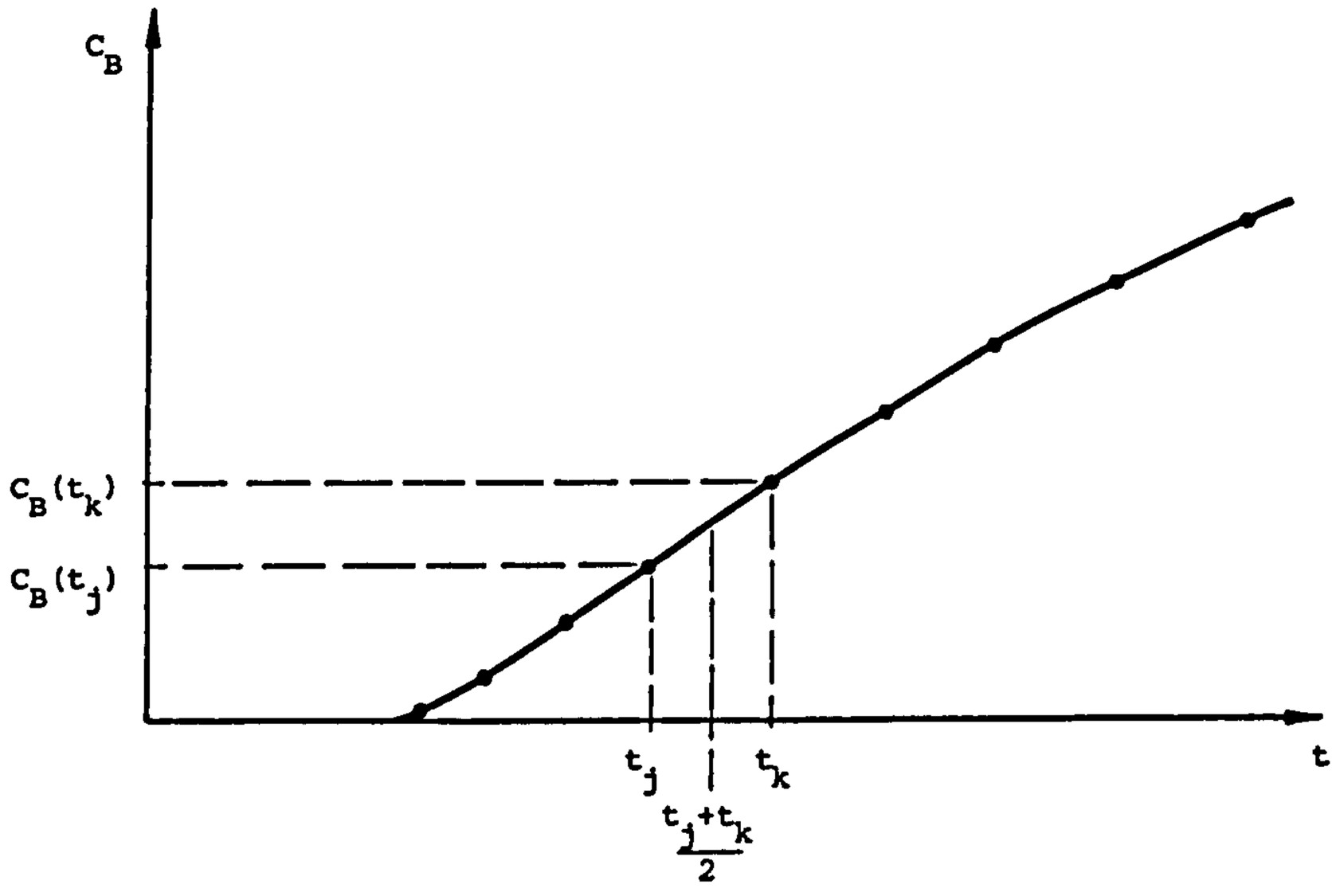

Figure 4.3: Typical graph of chloride accumulation in solution B with time.

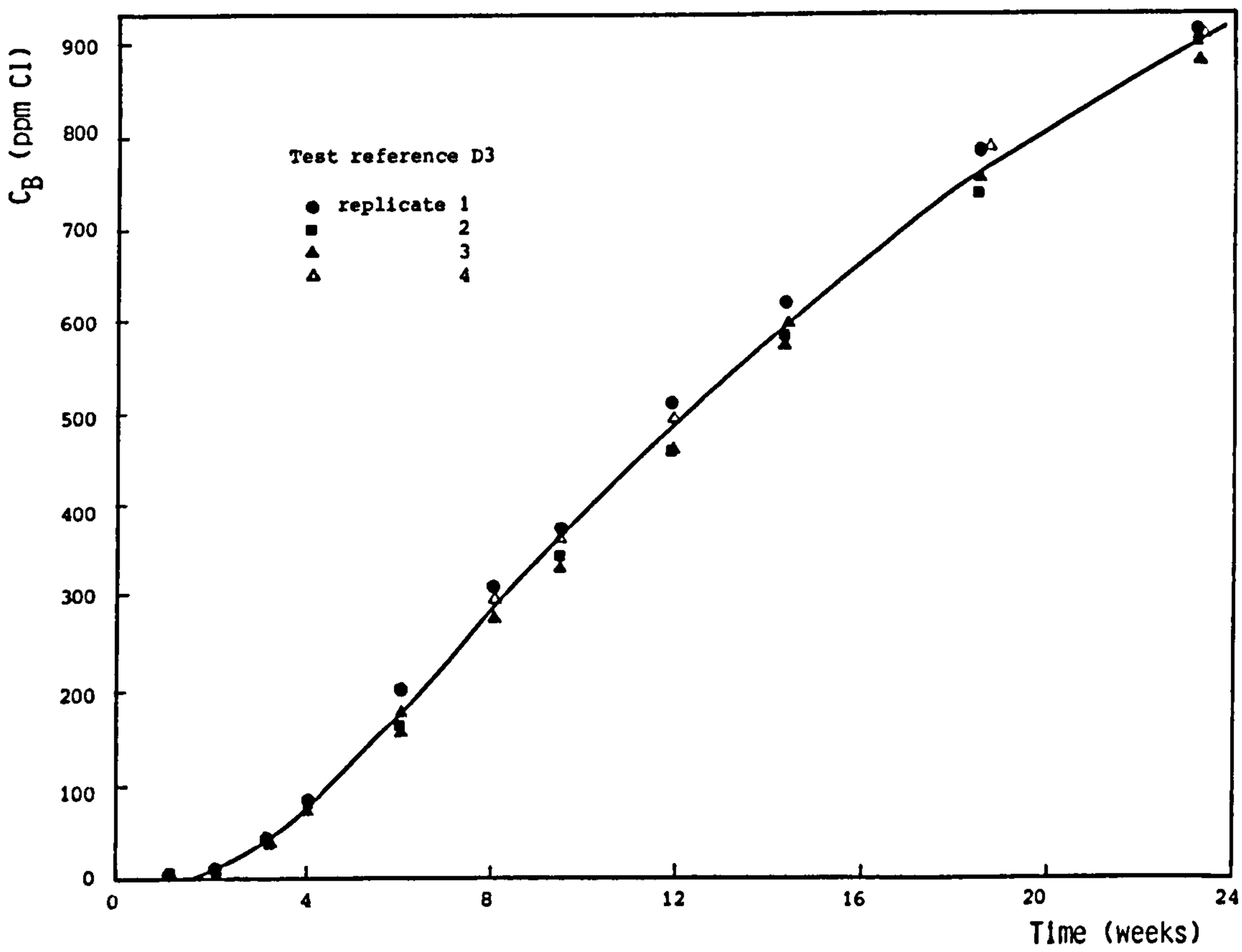

Figure 4.4: Variation of C_B with time for four replicates of test reference D3.

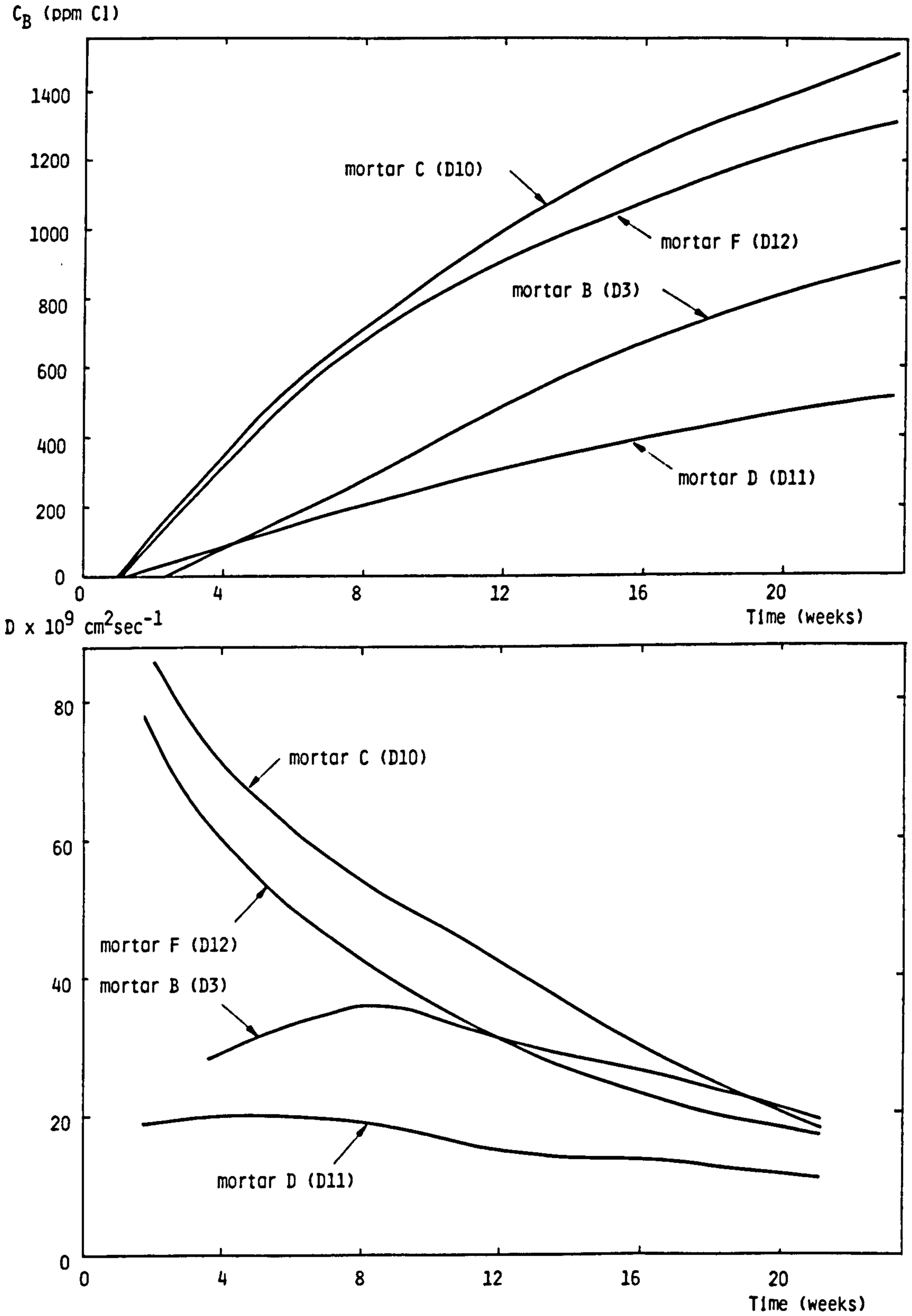

Figure 4.5: Effect of mortar composition on chloride ion diffusion from sea-water.

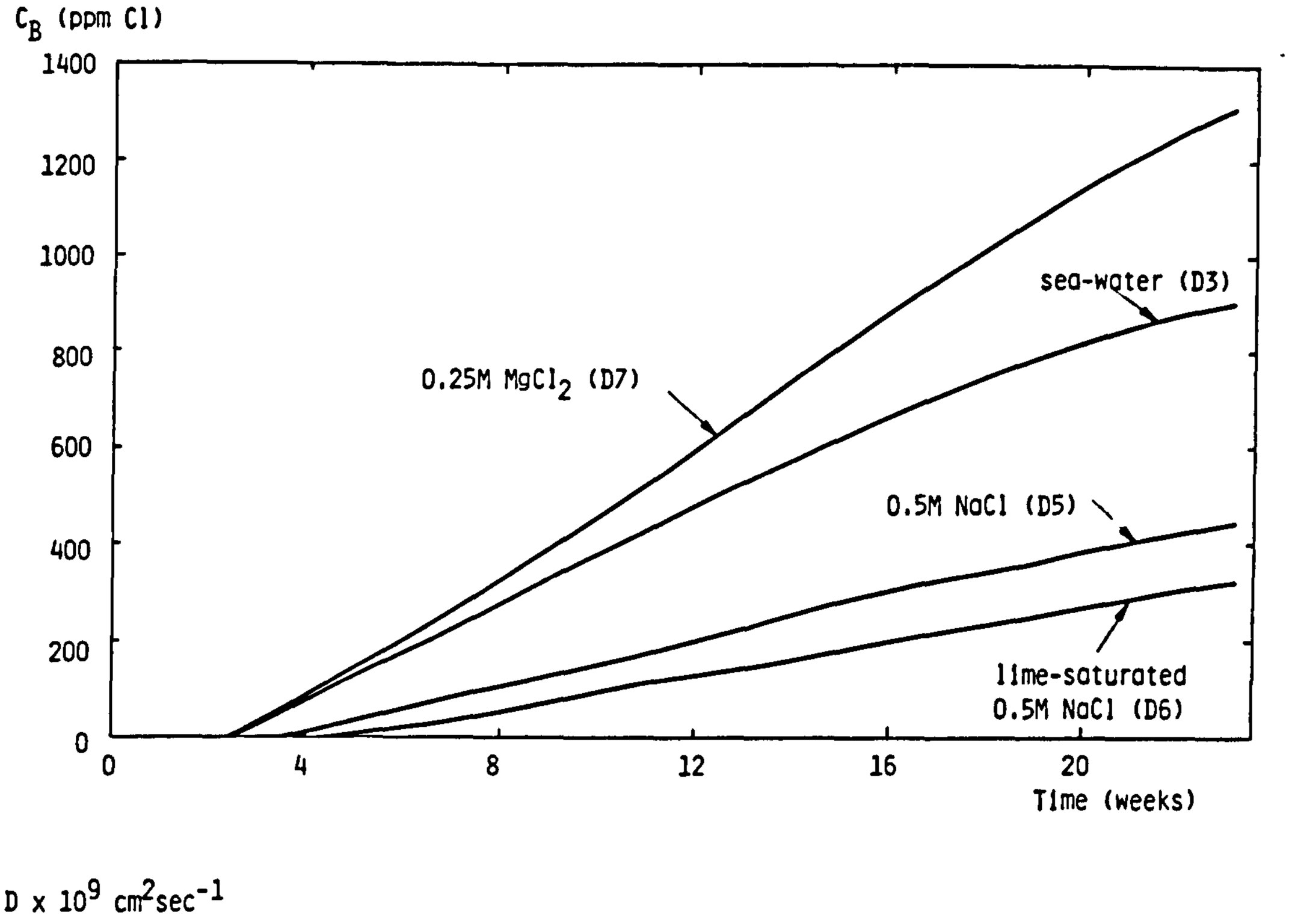

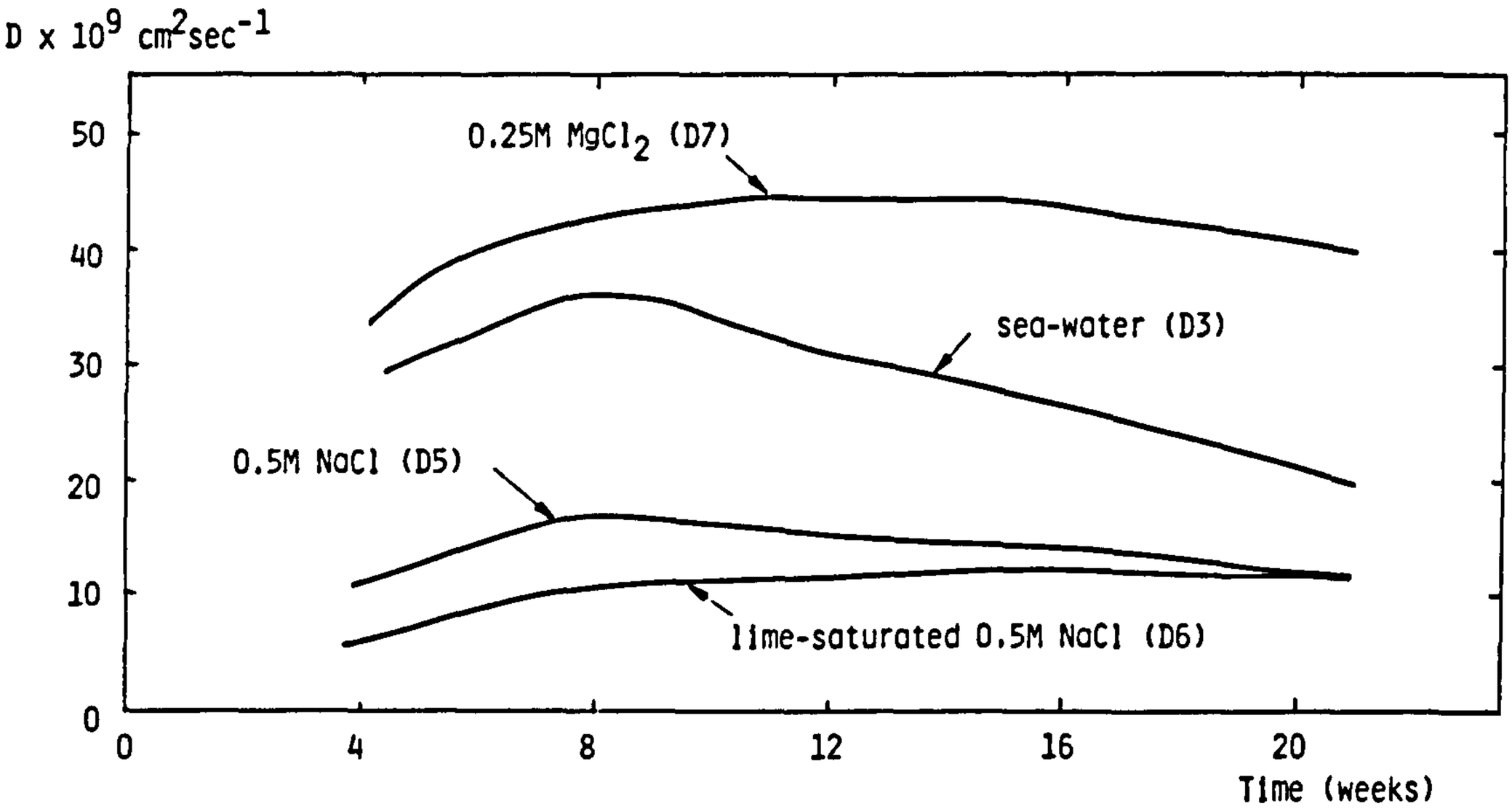

Figure 4.6: Effect of source of chloride ion on chloride ion diffusion.

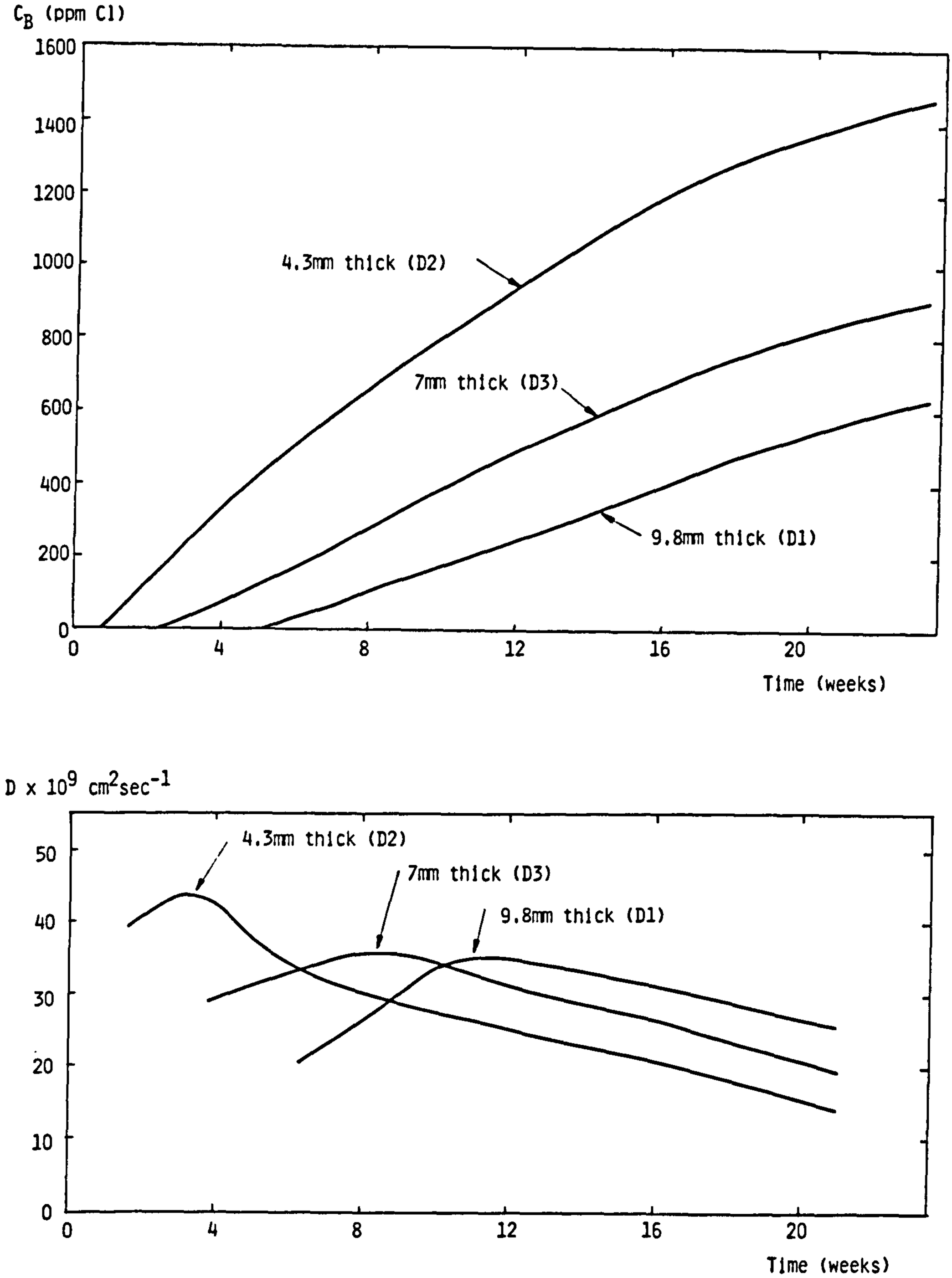

Figure 4.7: Effect of specimen thickness on chloride ion diffusion from sea-water.

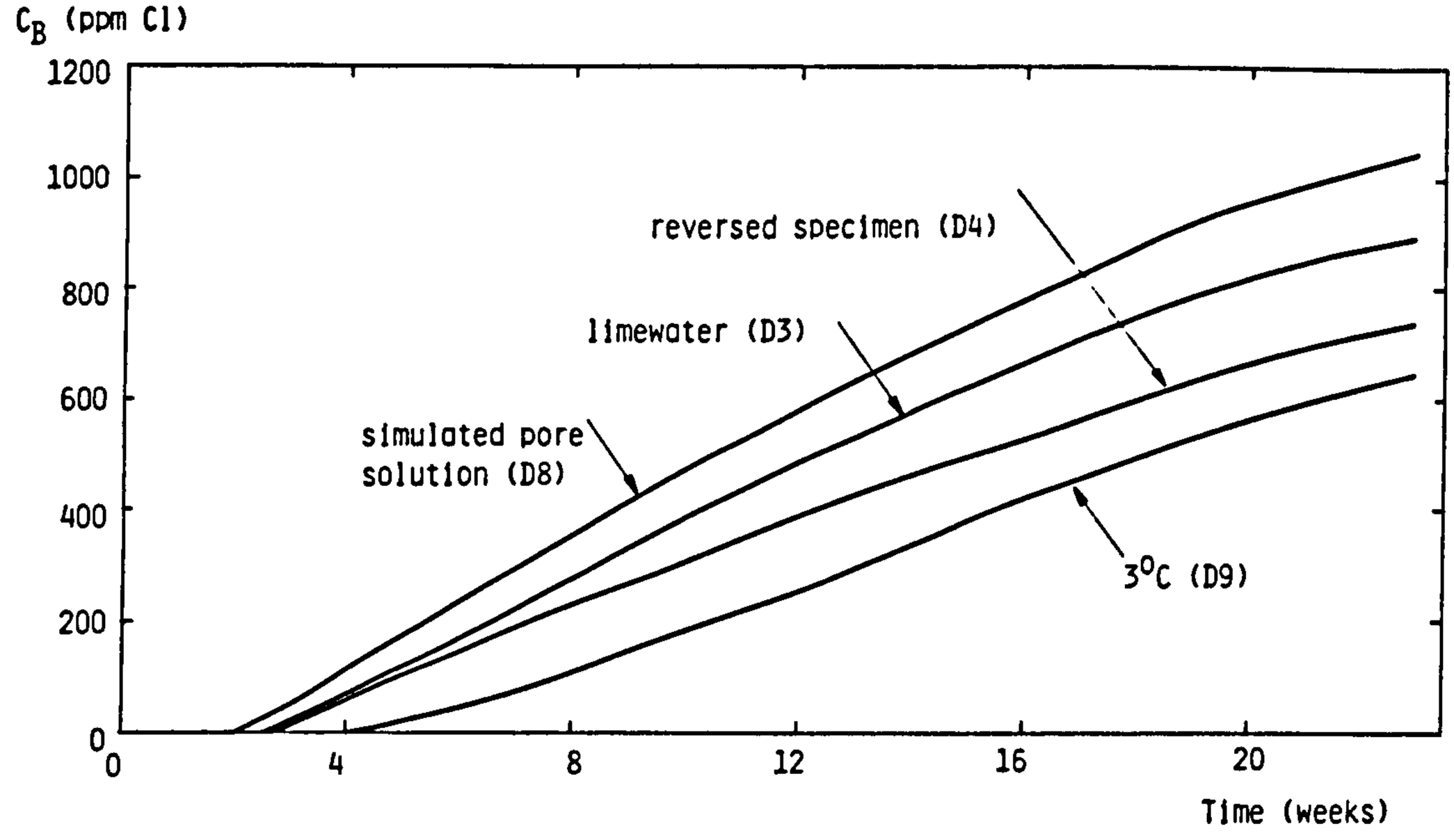

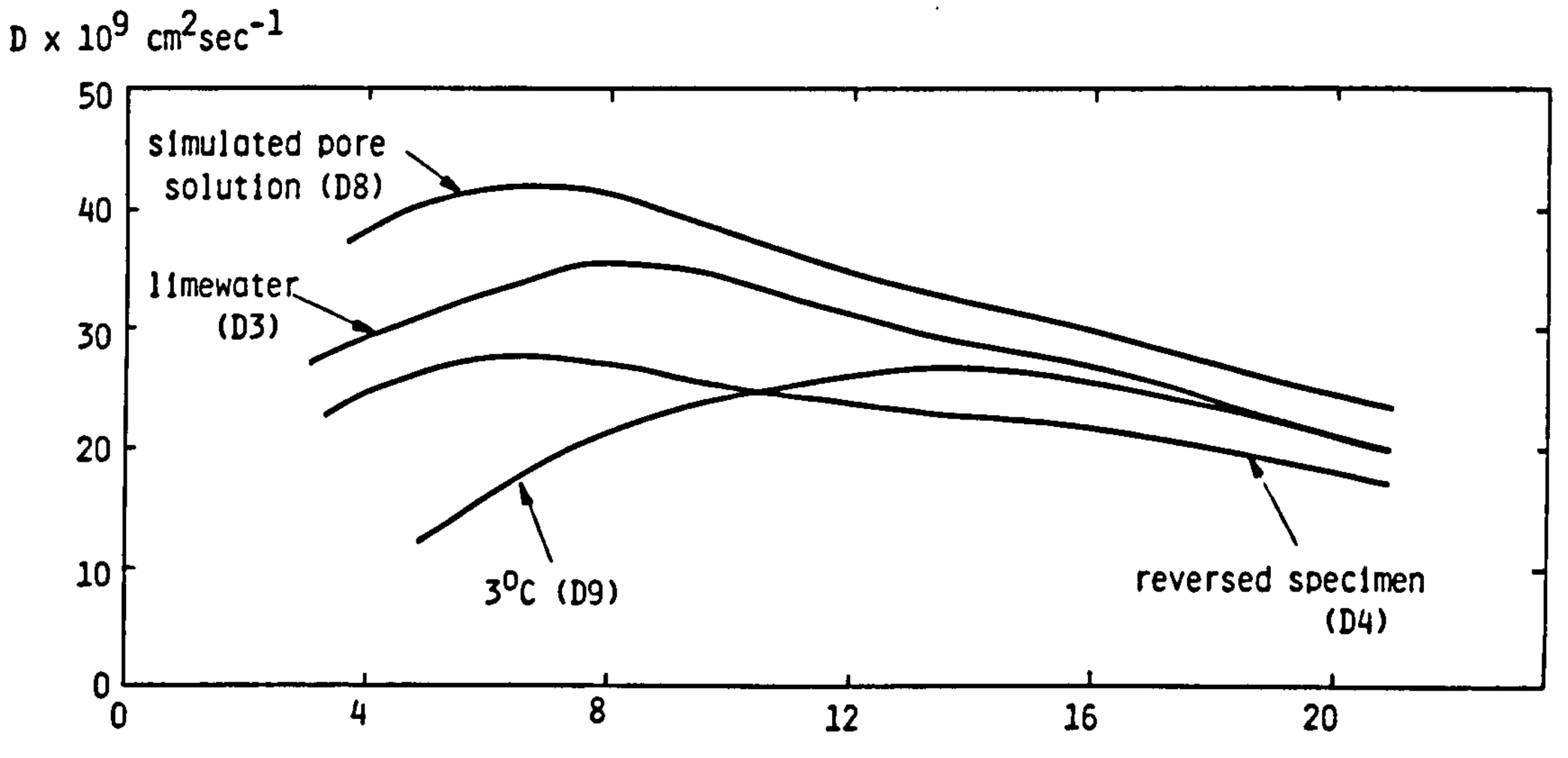

Figure 4.8: Effect of temperature, simulated pore solution composition and specimen orientation on chloride ion diffusion from sea-water.

4.3.4 Discussion

Figure 4.5 shows that the time from initial exposure to sea-water to chloride diffusion into solution B, t_o, varied from 7 days (for mortars C and F) to 16 days for mortar B. Interestingly, t_o for the pfa mix (mortar D) was only 9 days, despite the diffusion coefficient being lower than that for mortar B. Great care was taken to ensure that the specimens were still saturated when initially exposed to sea-water and so this phenomenon is unlikely to result from initial sea-water absorption. A possible explanation is that the pfa mix has a lower C_3A content and hence, at an early age, binds less of the diffusing chloride than an equivalent OPC mix, allowing the "chloride front" to penetrate more rapidly. This theory would explain the early gradual increase in diffusion coefficient up to 8 weeks of sea-water exposure for mix B, while the diffusion coefficient for mix D was relatively constant, but a more likely explanation for this observation is discussed later (see Figure 4.9 and related text).

There are no results in the literature that can be directly compared since very few workers have tested mortars or a comparable range of mixes and no work could be found in which sea-water had been used as the source of chloride ion. The most appropriate work with which to compare initial (i.e. before the permeabilty-reducing mechanism has had a significant effect) diffusion coefficients is that of Page *et al*. (1981), who tested hardened cement paste specimens exposed to 1M sodium chloride solution; these results are presented in Table 4.3. It can be seen that the diffusion coefficients are rather similar to the values obtained during the present work, although they refer to pastes rather than mortars. It is generally assumed that for normal aggregates diffusion is essentially through the cement paste, aggregate particles acting as obstacles to diffusion (5.3). Consequently mortars generally have lower diffusion coefficients than equivalent pastes. However, Figure 4.6 shows that when sodium chloride, particularly when lime- saturated, rather than sea-water, is the source of chloride ion, the diffusion coefficient through a similar specimen is considerably lower. The greater maturity of the paste specimens and the presence of cracks or voids associated with the paste-aggregate interface could also negate the blocking effect of the aggregate.

cement type	w/c ratio	$Dx10^9$ cm^2sec^{-1} 60 days old paste at 25°C 1.0M NaCl. (Page *et al*.1981) (at 25°C)	$Dx10^9$ cm^2sec^{-1} 41 days old mortar at 20°C Sea-water. (This study)
OPC	0.4	26	27 (mortar B)
"	0.6	124	85 (mortar C)
OPC/30% pfa	0.4		18 (mortar D)
"	0.5	15	
SRPC	0.4		75 (mortar F)
"	0.5	100	

Table 4.3: Diffusion coefficient of chloride ion in various pastes and mortars.

The results in Table 4.3 show the dependence of D on water/cement ratio; this is almost certainly a consequence of differences in pore structure. According to the classic model of Powers *et al*. (Table 7.1) all capillary pores in a 0.4 w/c ratio mix would be expected to have become segmented by gel after only 3 days, whilst in a similar mortar of 0.6 w/c ratio such segmentation would not be expected until around 6 months. Some indication of the relative pore size distributions of the mortars investigated in the present work may be obtained from the mercury intrusion porosimetry (MIP) data presented in Figure 7.1. It should be appreciated that these results do not accurately represent the condition of the mortars studied in these diffusion experiments since the samples were tested at an age of 5 months and drying would have modified the pore structure (7.2). Nevertheless, it can be seen that the mortar of 0.6 w/c ratio contained a greater volume of pores, particularly those with a minimum effective neck diameter greater than 1500 Å.

It is particularly interesting to compare the behaviour of mortars D and F. The two mortars have almost identical pore size distributions after 5 months and yet the diffusion coefficient for the SRPC mix is 4 times greater than that

of the pfa mix (Table 4.3). Furthermore, diffusion coefficients were taken at 6 weeks when it was likely that the slower hydrating pfa mix was more open-textured than the SRPC mix. Collepardi *et al.*(1972) observed a similar effect and concluded that the greater resistance offered by pozzolanic cement paste arose from "different types of interaction between the Cl^- ions and the pore surfaces of the materials studied". It was also suggested that the "difference in the diffusion coefficients could also be ascribed to a differing mobility of the water molecules present in the gel pores resulting from differences in the nature of the pore surfaces".

Mortars C and F exhibit very similar diffusion and electrical resistivity (5.9.1) behaviour, despite the difference in w/c ratio. Page *et al.* (1981) observed a similar trend and explained it in terms of similar pore size distributions. However,it can be seen from Figure 7.1 that the SRPC used in this work produced a less porous mortar with far fewer pores with effective neck diameters greater than 1000 Å. It is therefore suggested that chemical effects associated with C_3A content may also have an effect on chloride ion diffusion coefficients, possibly by complexation of chloride ions by aluminate phases (2.2.2.3).

It can be seen from Figure 4.5 that all the mixes tested exhibited a reduction in diffusion coefficient over the test period and that this was particularly significant for mixes C and F, each dropping to around one fifth of their original value. This reduction is equivalent to the specimen being 5 times its original thickness (Equation (4.1)) and therefore represents an apparent increase in specimen thickness of 28 mm.

Figure 4.6 shows the effect of the source of chloride on chloride diffusion. The dependence on cation ($D_{Cl^-(MgCl_2)} > D_{Cl^-(NaCl)}$) agrees with the work of Ushiyama and Goto (1974). The initial rate of diffusion of chloride ion from sea-water was considerably greater than that from the sodium chloride solution of equivalent chloride concentration. This was probably due to the combined effect of two independent mechanisms. Firstly, as shown by Vinograd and McBain (1941), the general effect of mixing electrolyte solutions is to speed up fast ions and to retard slow ones still further. Chloride ion diffusion is therefore accelerated due to the presence of other sea-water ions. The second mechanism is also likely to be responsible for the apparent initial increase in diffusion coefficient (mentioned earlier) exhibited by virtually all of the mortar B specimens tested. During early exposure, the

greater mobility of chloride ion over the corresponding cation (Ushiyama and Goto 1974) induces counter-diffusion of hydroxyl ions in order to maintain electrostatic equilibrium. This leaching of hydroxyl ions results in dissolution of $Ca(OH)_2$ from the hardened cement paste, thereby opening the cement paste pore structure and causing a gradual increase in D. Magnesium (and calcium) ions present in sea-water are less mobile than sodium ions and hence are likely to induce more rapid counter-diffusion.

The early increase in D was not observed by Page *et al.* (1981) when using lime-saturated sodium chloride solutions and the effect was certainly not as marked when specimens were similarly exposed in the present research. However, Ushiyama and Goto (1974) exposed very thin (0.8, 2 and 3mm thick) 0.4 water/cement ratio OPC paste specimens to various chloride solutions and observed a similar increase in D, particularly for specimens exposed to magnesium and calcium chloride solutions. Ushiyama and Goto suggest that a fixed structure is gradually established and hence, linear behaviour is eventually observed.

It is clear that the D versus time curves for sea-water exposed specimens are a combination of two characteristic trends (Figure 4.9), an early increase in D, as discussed above, and a gradual fall in D due to the permeability-reducing phenomena under investigation. Whether or not the early rise in D was primarily a result of testing unrepresentatively thin specimens remains to be elucidated (7.4). Unfortunately a diffusion cell technique is not suitable for testing specimens of thicknesses corresponding to typical cover to reinforcement (3.3.3); however, the phenomonon can be further investigated by analysing the results of tests on specimens of various thicknesses.

Figure 4.7 shows that the 4.3mm thick specimen exhibits a higher peak in D than the thicker specimens. However, this higher value occurs at an earlier time and is therefore probably due to the permeability-reducing mechanism having had less time to modify the mortar. The dependence of the drop in D with time on specimen thickness, suggests that the permeability-reducing mechanism is probably restricted to a limited thickness into the mortar and therefore, has a relatively more significant effect on thinner specimens.

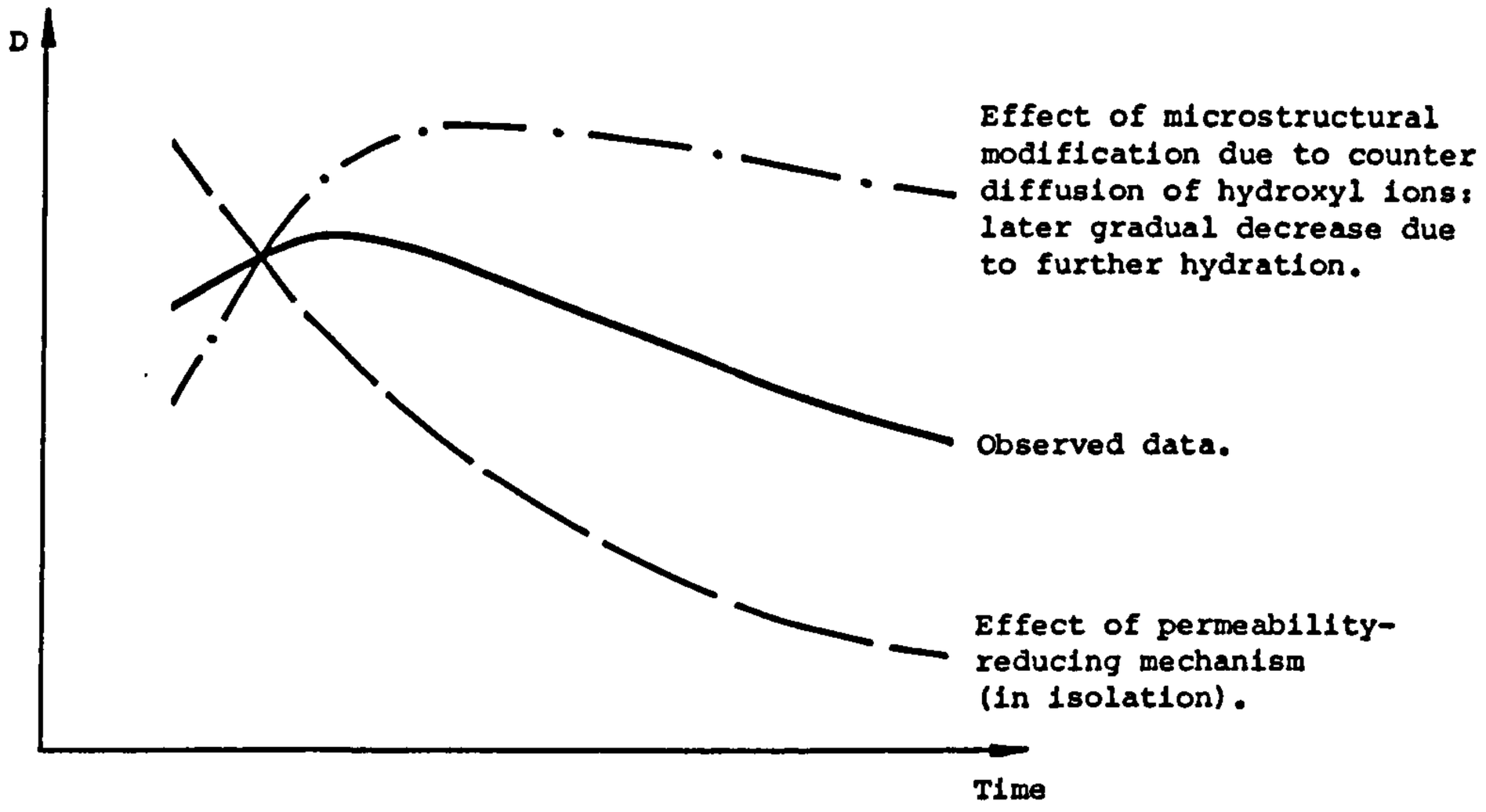

Figure 4.9: Component trends producing observed diffusion coefficient versus time curves.

Figure 4.8 shows the effect of other factors on chloride diffusion from sea-water. A reduction in temperature from 20°C to 3°C appears to moderate the permeability-reducing mechanism, which might have been expected since the rate of reaction between cement paste and sea-water reduces with temperature. However, these results should be interpreted with considerable caution. The diffusion coefficient of chloride ion in 0.4 water/cement ratio OPC paste at 3°C is approximately 40% of its value at 20°C (based on Page *et al.* 1981). This has the effect of greatly increasing the phase difference between a real change in permeability and chloride ion accumulaton in solution B. Figure 4.8 shows that at 3°C t_o is almost doubled and the peak in D is reached at a much later exposure time. Interpretation of results would have been easier if the specimens had been thinner, but this would have introduced other uncertainties.

Figure 4.8 shows that D is reduced when solution B is limewater rather than a solution correlating more closely with cement paste pore solution. Fortunately, the curves are sufficiently similar for the use of limewater to be acceptable.

Figure 4.8 also shows the effect of reversing the orientation of the specimen such that the sawn face was exposed to sea-water. t_o was unaffected, but the shape of the D versus time curve suggests that the permeability-reducing mechanism was more effective when acting on the sawn face.

Surface examination and analysis (6.2) and mercury intrusion porosimetry (7.4) of the specimens after the 23 week exposure period suggested that the drop in D associated with sea-water exposure was primarily due to the formation of an aragonite and/or brucite layer on the surface of the specimens. Theoretical studies (6.4) showed that precipitation of these minerals was likely to be sensitive to the partial pressure of carbon dioxide in the test environment. The tests described were carried out in sealed test cells, thereby limiting the availability of atmospheric CO_2. In case this had an effect on the results, 3 replicates of each of the 6 most important tests (D3, D5, D7, D10, D11, D12) were repeated using the modified test cell arrangement shown in Figure 4.10, in which the elongated access tube to solution A allow ed the solution to equilibrate with the atmosphere. Regular readings were taken up to 16 weeks of exposure. Although slight discrepancies, probably associated with testing specimens from different batches, were observed, the variation of D with time was, in all cases, very similar to the "sealed" test series.

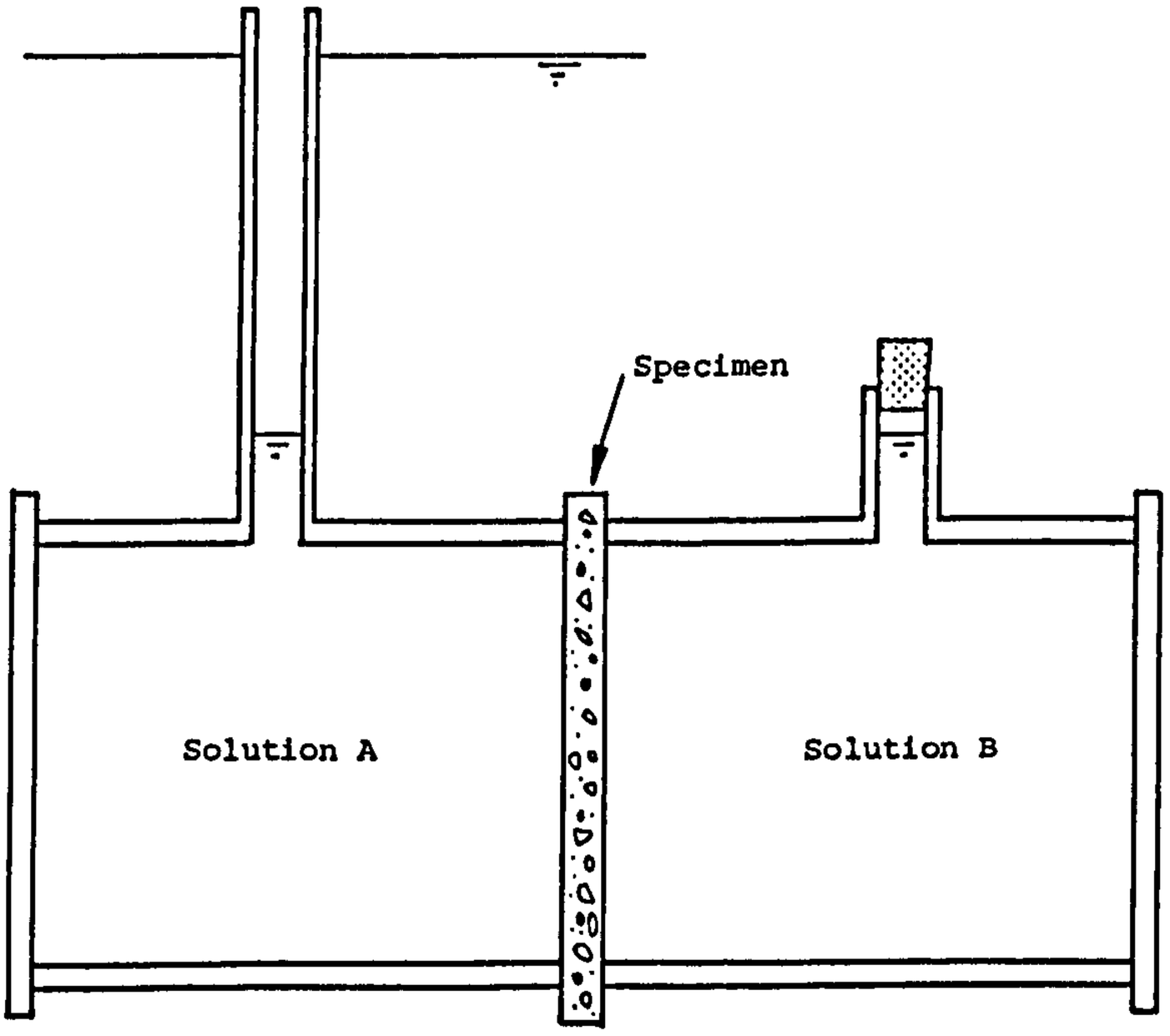

Figure 4.10: Diffusion cell for "open" test series.

The pH values of the test solutions, measured at the end of the exposure period for both the "sealed" and "open" test series, are presented in Tables 4.4 and 4.5 respectively. The most striking feature of these results is the high alkalinity of the sea-water. It would have been impractical to have

regularly replaced the sea-water, or to have dosed it with acid, but this increase in pH is undesirable (6.4) and close attention should be paid to pH control when developing more sophisticated techniques (Appendix 3). The relatively low pH in test reference D11 is due to the consumption of lime during the hydration of the pfa mortar, leaving less free lime available to be leached from the specimen. Indeed a further series of tests showed that the pH of a limited quantity of solution in contact with a mix containing pfa often reached a maximum and then actually reduced as hydroxyl ions were drawn back into the specimen.

Test Reference	Solution A	Solution B
D1	---	---
D2	11.41	12.24
D3	11.44	12.35
D4	---	---
D5	---	---
D6	12.51	12.41
D7	---	---
D8	---	---
D9	11.32	12.31
D10	11.60	12.37
D11	9.80	12.30
D12	11.79	12.38

Table 4.4: pH of "sealed" diffusion cell test solutions after 23 week exposure period.

Test Reference	Solution A	Solution B
D3	11.56	12.44
D5	10.00	12.51
D7	9.45	12.37
D10	9.94	12.46
D11	10.00	12.51
D12	11.94	12.44

Table 4.5: pH of "open" diffusion cell test solutions after 16 week exposure period.

4.3.5 Conclusions

(1) A theoretical study showed that the diffusion cell technique was not appropriate for monitoring sulphate ion diffusion from sea-water.

(2) The diffusion cell technique was found to provide a useful indication of changes in chloride ion diffusion coefficient over several months exposure to a chloride solution, provided an appropriate thickness of specimen was chosen.

(3) A chloride electrode was found to be a satisfactory means of determining chloride concentration (more accurately, activity), provided the solution was free of sulphide ion.

(4) The initial diffusion coefficients for the various mixes compare favourably with results found in the literature.

(5) All mixes tested showed an overall reduction in D over the 23 week sea-water-exposure period, with the more permeable mixes, mortar C & F, each dropping to around one fifth of their original value.

(6) Most D versus time curves have an early ascending portion which is believed to be associated with a modification of the cement paste microstructure due to counter diffusion of hydroxyl ions.

(7) The source of chloride ion was found to be extremely important in determining D. Diffusion from sea-water was considerably more rapid than diffusion from a sodium chloride solution of similar chloride concentration, although not as rapid as that from a magnesium chloride solution.

(8) The results were found to be less informative when the technique was used at lower temperatures (i.e. 3°C), due to the reduced mobility of ions.

(9) Repeating certain tests with solution A exposed to the atmosphere did not produce significantly different results from tests where the cells were sealed.

(10) Although simple to perform, the diffusion cell test has a number of drawbacks, all of which may be overcome by developing an electrical resistivity technique:

(a) there is little control of sea-water pH or composition;

(b) the specimens must be relatively thin;

(c) there is a delay between a change in permeability and chloride ion accumulation in solution B; i.e. an instantaneous indication of permeability is not afforded, particularly at low temperatures or for relatively impermeable mixes;

(d) "control" specimens must be exposed to chloride ions; and

(e) it is difficult to differentiate between surface and bulk effects.

Chapter 5: RESISTIVITY TESTING

5.1 Introduction

Comparatively little research has been undertaken on the electrical properties of cement pastes and even less on concretes. Most of the early work was concerned with the changes in electrical resistivity of cement paste during setting (e.g. Dorsch 1933, Calleja 1952, 1953) and readings were rarely taken beyond 24 hours after mixing. Several workers (e.g. Spencer 1937, Bhargava & Rehnstrom 1978, Woelfl & Lauer 1979) have investigated the relationship between resistivity and moisture content with a view to developing a practical non-destructive method of measuring the moisture content of concrete in situ. Research has also been directed at evaluating the insulating properties of concrete for use in specific applications such as railway sleepers (Monfore 1968), where inadequate resistivity affects the signalling system, or in structures in which concrete is used for protection from stray currents.

Concrete resistivity is one of the main factors controlling the corrosion of embedded steel (2.2.8) and yet, little research has been undertaken to elucidate the role of resistivity in this context. Furthermore, most of the large offshore concrete structures built so far have a variety of freely exposed steel components (anodes) in electrical contact with embedded steel (cathode), producing galvanic cells whose activity is primarily controlled by the resistivity of the concrete (Gjorv *et al.* 1977).

No instance could be found in the literature of resistivity measurements being taken as an indication of concrete permeability.

5.2 The concept of the resistivity of a material

The electrical resistivity of any material is defined as the resistance between opposite faces of unit cube of that material. Thus,

$$\rho = \frac{RA}{L} \qquad (5.1)$$

where ρ = resistivity (Ωm);
R = resistance (Ω);
A = cross-sectional area of specimen (m^2);
L = length of specimen (m).

Ohm's law states that the *direct* current through a metallic conductor is directly proportional to the potential applied and inversely proportional to the resistance of the conductor, i.e.:

$$I = \frac{E}{R}$$

where I = current (A);
E = potential (V).

If the conductor is an electrolyte, the passage of direct current causes *polarisation* and the establishment of a potential at the electrodes which opposes the applied voltage (Hansson & Hansson 1983). This *polarisation potential* results from reactions which form thin films of oxygen, hydrogen or other gases on the electrodes. In such a case the current is:

$$I = \frac{E_a - E_p}{R}$$

where E_a = applied potential (V);
E_p = polarisation potential (V).

Monfore (1968) demonstrated that E_p is effectively independent of E_a and hence R and E_p may be evaluated from measurements of I and E_a at two different values of E_a.

The effects of polarisation that are associated with direct current measurement can be avoided, provided the voltage is above a certain threshold level

(Gjorv *et al.* 1977), by using a four electrode system (3.2.8, Stratfull 1968).

For practical purposes, polarisation effects are eliminated by using alternating currents of sufficiently high frequency. Previous investigators (e.g. Hammond & Robson 1955, Monfore 1968) have assumed that a concrete or cement paste specimen subjected to an alternating current is electrically equivalent to a capacitance and a resistance in parallel. The current through such a combination is:

$$I = \frac{E}{Z}$$

where Z = impedance (Ω)

$$= \frac{R}{(1 + w^2C^2R^2)^{\frac{1}{2}}} \qquad (5.2)$$

and $w = 2\pi f$;

f = frequency (Hz);

C = capacitance (F).

5.3 Electrical conduction in concrete

An appreciation of the mechanism of electrical conduction in concrete is vital to enable changes in resistivity due to microstructural modification to be isolated from those due to other factors. A clear picture of the mechanism also aids in relating resistivity to permeability. A quantitative idea of the effect of mix variables and environmental factors on the resistivity of concrete serves to put into perspective changes due to the influence of sea-water.

Moist concrete behaves essentially as an electrolyte with a typical resistivity of 50 Ωm which is within the range associated with semi-conductors. When oven-dry, however, concrete has a resistivity of around 10^9 Ωm which classifies such concrete as a reasonably good insulator. This large increase in resistivity on removal of evaporable water is considered to mean that electric current is conducted through concrete by electrolytic means, that is by ions in the pore solution, with electronic conduction through the solid cement matrix and aggregate being negligible. Consequently it is not surprising that the following factors are of prime importance in determining concrete resistivity:

(1) Volume fraction occupied by pore solution, which is dependent upon:
   - (a) degree of saturation (see Figure 5.1);
   - (b) water/cement ratio (see Figures 5.1 and 5.2);
   - (c) aggregate/cement ratio;
   - (d) degree of hydration (see Figure 5.2).

(2) Ionic concentration of pore solution, which is dependent upon:
   - (a) cement content;
   - (b) alkali content of cement;
   - (c) ionic admixtures (e.g. chlorides);
   - (d) leaching of pore solution ions or ingress of ions from an external source (e.g. sea-water);
   - (e) degree of hydration (see Figure 5.2).

(3) Temperature (see A7.3).

The degree of saturation (moisture content) of the specimen, primarily controlled by environmental conditions, affects concrete resistivity more than

any other parameter (see Figure 5.1).

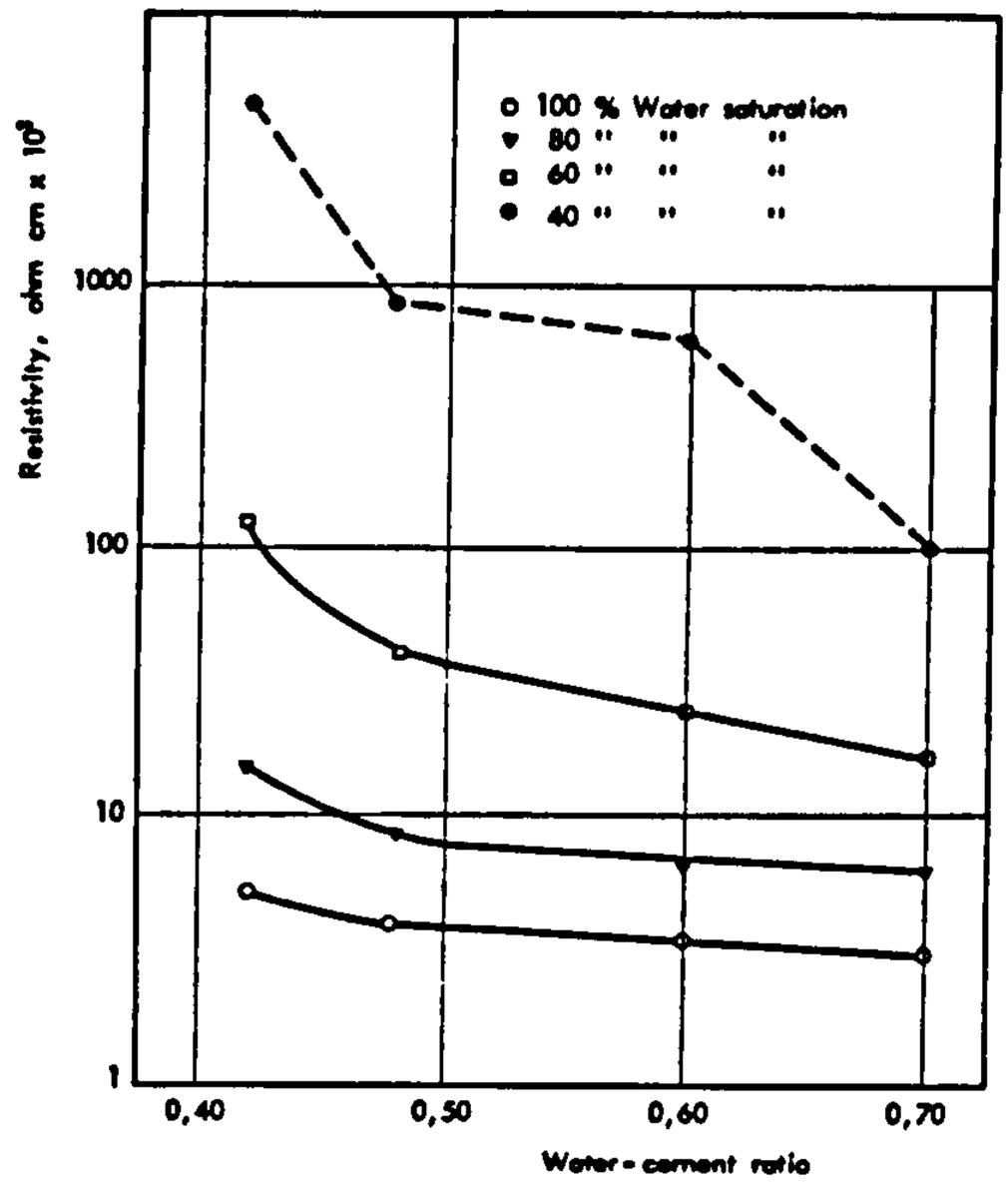

Figure 5.1: Effect of water/cement ratio and degree of saturation on the resistivity of concrete (Gjorv *et al.* 1977).

It should be noted that, while for a particular mix an increase in the volume fraction of pore solution will almost certainly result in a reduction in resistivity, if different cement types are used, the mix with the higher volume fraction of pore solution does not necessarily have a lower resistivity; this is analogous to certain concretes having a larger porosity but a lower permeabilty than concrete made with a reduced water/cement ratio but with a different cement.

The resistivities of aggregates commonly used in concrete are shown in Table 5.1. Comparison of these values with the resistivity of moist cement paste (typically 15 Ωm) and concrete (typically 50 Ωm) shows that most of the current is conducted through the paste, i.e. through the path of least resistance. This is confirmed by Whittington *et al.* (1981) who found that models representing cement mortar as a composite of non- conducting particles (aggregate) within a matrix of known resistivity (cement paste) agreed with the observed data to within a few percent.

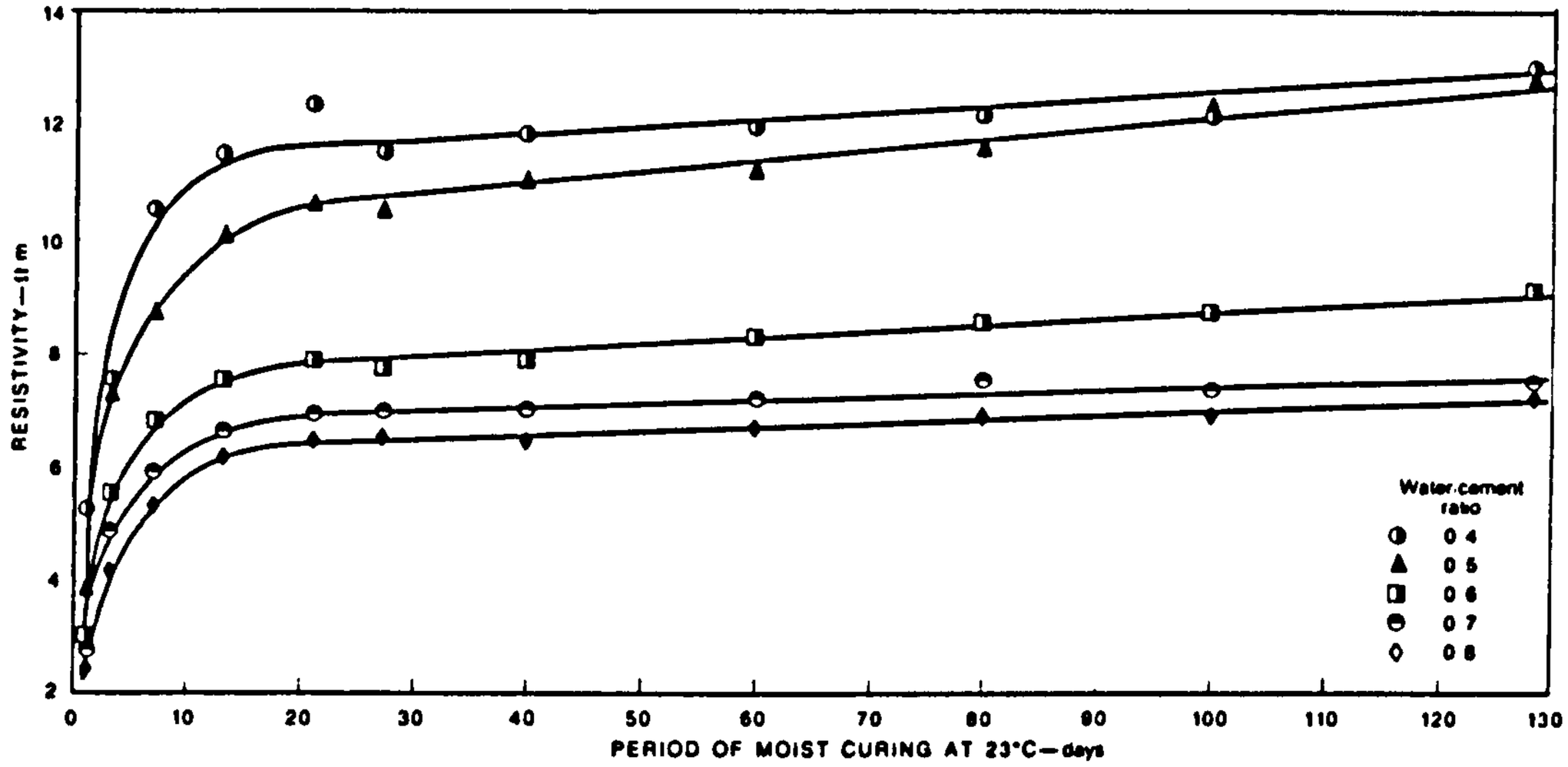

Figure 5.2: Effect of moist-curing on resistivity of concrete (Whittington *et al*. 1981).

Rock type	Resistivity Ωm	
	wet	dry
Basalt	$1.6x10^3$-$2.3x10^4$	$1.3x10^7$
Diorite	$2.8x10^4$	-
Gneiss	$6.8x10^4$	$3.2x10^6$
Granite	$3.0x10^5$-$1.6x10^6$	$3.0x10^{13}$-$3.2x10^{16}$
Granite porphyry	$6x10^3$	$1.0x10^5$-$1.3x10^6$
Limestone	$3x10^5$	$1.8x10^9$
Marble	$1.4x10^4$-$7.1x10^9$	$2.5x10^8$-$1.8x10^{18}$
Quartzite	$4.7x10^6$	-
Quartz porphyry	$9.2x10^5$	-
Sandstone	$2.3x10^2$-$1.4x10^5$	$3.1x10^5$-$6.4x10^8$

Table 5.1 : Typical resistivities of aggregates commonly used in concrete (based on Parkhomenko 1967).

As cement hydrates, water is consumed. If the mix is moist-cured there is generally a gradual increase in resistivity (Figure 5.2) associated with the reduction in pore space (7.1.2). If there is no external source of moisture, continued hydration leads to self-desiccation and the increase in resistivity is more rapid. It should be noted that changes in the cement paste pore solution, producing changes in resistivity, are also effected during hydration (5.5).

The ionic species present, as well as their concentrations, control resistivity since the current also depends upon ionic charge and velocity. The velocities of the main ions present in cement paste pore solution and sea-water in water

at 25°C due to a potential gradient are (Atkins 1983):

OH^-	20.6×10^{-8}	$m^2V^{-1}s^{-1}$
Ca^{2+}	6.2	" "
Na^+	5.2	" "
K^+	7.6	" "
Cl^-	7.9	" "
SO_4^{2-}	8.3	" "

The influence of mix water salinity (due to the addition of chlorides or the use of sea-water) on resistivity is found to be greatest in concretes with high water/cement ratios and is less marked in higher grade concrete (Henry 1964).

5.4 Resistivity test procedure

The test criteria outlined in 3.3.2, together with a number of practical and economic considerations, resulted in the development of the resistivity cell shown in Figures 5.3 and 5.4.

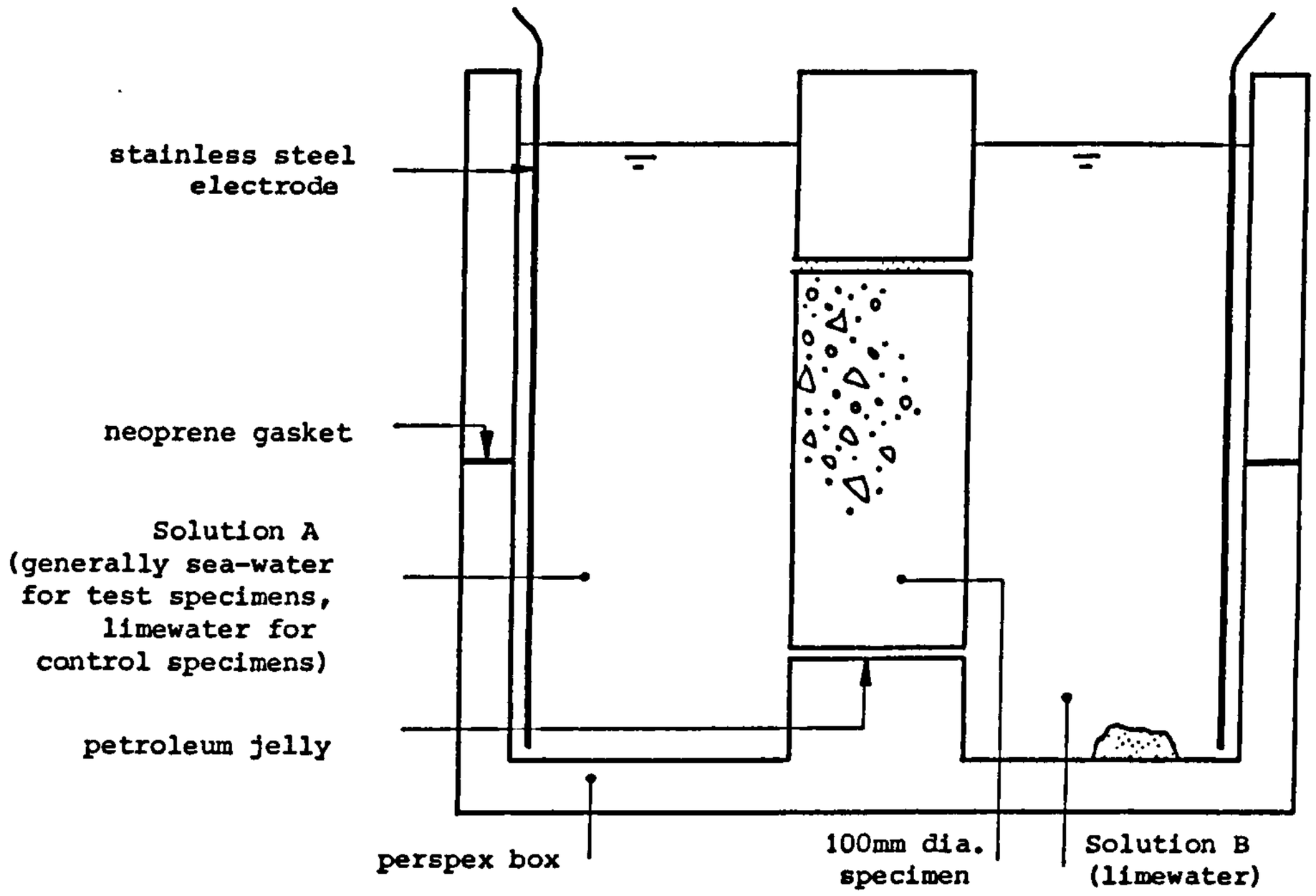

Figure 5.3: Section through resistivity cell.

After an initial curing period the 100 mm diameter cylindrical specimen *(resistivity specimen)* is installed between the two halves of the resistivity cell and is permanently housed for the full duration of the sea-water exposure period. The cell was designed to allow easy removal of the specimen since certain specimens were to be ground and subsequently retested (in order to identify surface effects). The gap (of approximately 1 mm) between the cell and the specimen is sealed using petroleum jelly applied to the curved face of the specimen and to the appropriate surfaces of the resistivity cell prior to fitting the specimen. Many materials were tested before petroleum jelly was adopted. Extensive preliminary testing showed that petroleum jelly provides a very efficient seal without penetrating the specimen or having any detrimental long-term effects. The two halves of the cell are clamped together, sealed with a neoprene gasket. Each side of the cell has a capacity of 2 litres and is fitted with a drainage point to permit simple replacement of electrolyte (i.e. sea-water, limewater etc.). The 20 gauge stainless steel electrodes are located in grooves formed in the sides of the perspex box.

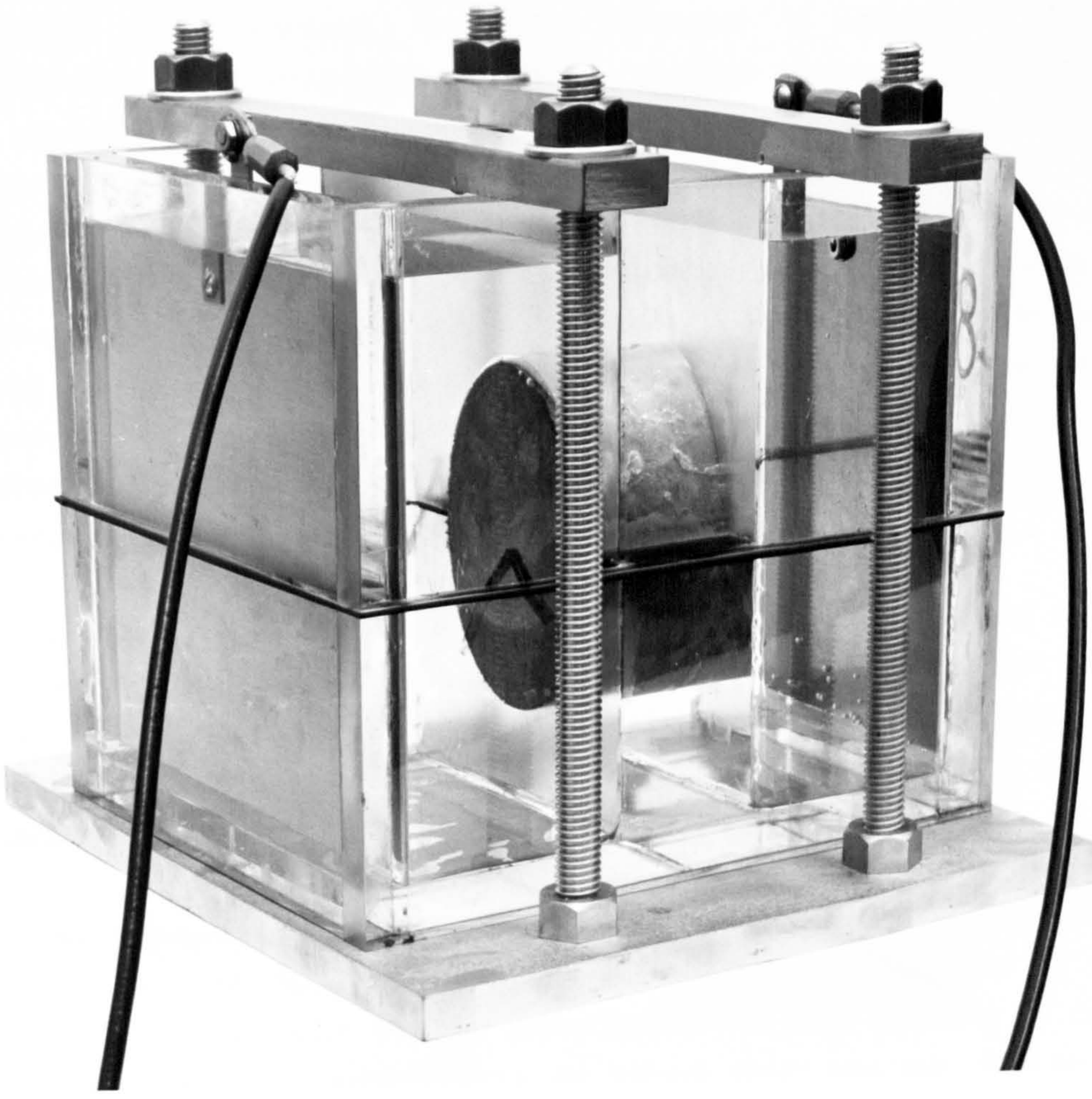

Figure 5.4 : Resisivity cell.

A universal bridge (Marconi TF2700) was used to take readings between the two electrodes. It was felt appropriate to take measurements using an alternating current in order to minimise polarisation effects (5.2). Polarisation manifests itself as an additional resistance, an effect which decreases with increasing frequency (Bhargava & Rehnstrom 1978). Consequently, as a preliminary experiment, a signal generator was linked to the universal bridge and the resistance and capacitance of typical concrete specimens were measured over a range of potentials (0.2 to 10 V) and frequencies (50 to 10,000 Hz). A fall in resistance of less than 5% was generally observed over the 50 to 10,000 Hz range and a very slight drop in resistance was exhibited as voltage increased. These data show similar, though less pronounced, trends to those of Monfore (1968) and Bhargava & Rehnstrom (1978). The maximum capacitance measured was only 85 pF (at a resistance of around 90 Ω) and this value included contributions from both the connecting leads and polarisation.

Impedance is the total opposition to the flow of alternating current and hence it might be regarded as a more appropriate parameter to monitor than resistance. However, the capacitance of concrete is so low that values of impedance, as calculated from Equation (5.2), are essentially equal to the measured resistances.

Bhargava & Rehnstrom (1978) noted that interference due to polarisation was negligible at 1000 Hz and, since this was the internal frequency of the universal bridge available for this work, resistances were measured at 1000 Hz. The bridge was powered by a 9V battery which was also felt to be acceptable.

In theory any electrolyte of relatively low resistivity could be used for solutions A and B (Figure 5.3), the resistance measured between electrodes requiring only minor correction (A7.2) to obtain the resistance of the specimen alone. Hence sea-water or other reasonably concentrated salt solutions are ideal for use as solution A. Solution B should be a simulated pore solution (4.3.1), but its precise composition is less significant than in the case of diffusion testing since the specimens are thicker. Limewater, having a sufficiently low resistivity, was therefore used as solution B in all tests.

The principal aim of this experimentation was to monitor any change in microstructure/permeability of concrete on exposure to sea-water. However, the microstructure of cement paste with a sufficient supply of moisture is constantly changing over at least the first 6 months (5.5) and hence control specimens are required to isolate changes due to the action of sea-water from those due to further hydration. The ideal environment for a control specimen would be, once again, a solution of identical composition to its pore solution, since the specimens would thereby be uninfluenced by the external environment. For reasons discussed earlier, in the context of limewater as a simulated pore solution (4.3.1), limewater was adopted as solution A for control specimens.

The laboratory in which most of the testing was undertaken was not temperature-controlled but, as suggested earlier, the resistivity of an electrolyte is temperature dependent. The temperature of solutions A and B was, therefore, recorded on each occasion a resistance reading was taken and the specimen resistance was corrected to the equivalent resistance at 21°C (A7.3).

5.5 Changes in specimen resistance during testing

Although the resistivity of concrete is dependent upon many factors (5.3), changes in the resistance of a particular specimen housed within a resistivity cell can be attributed to only 3 main parameters:

1. change in TEMPERATURE

2. change in PORE SOLUTION RESISTIVITY
   - (a) due to continued *hydration*: dissolution of ions from cement or replacement materials and removal of ions from pore solution by incorporation into solid hydration or reaction products.
   - (b) *external*: due to leaching or ingress of ions from an external source.

3. change in MICROSTRUCTURE
   - (a) due to continued *hydration*;
   - (b) due to *test solution - cement paste interaction*.

Changes in resistivity due to temperature variation are not a problem since specimen resistance at any temperature may be corrected to the equivalent resistance at a reference temperature (A7.3).

Changes in resistivity due to continued hydration (2(a) & 3(a)) may be accounted for by testing limewater-cured control specimens (5.4). Hence, if changes in pore solution resistivity due to the external environment (2(b)) are assumed to be negligible, the change in resistance due to test solution - cement past interaction is

$$R_s - R_\ell$$

where R_s = resistance of test specimen (i.e. specimen exposed to test solution); and

R_ℓ = resistance of control specimen (i.e. similar specimen, but exposed to limewater).

Alternatively, this change in resistance may be expressed in terms of an *apparent increase in thickness* of the specimen, calculated as

$$\left[\frac{R_s - R_\ell}{R_\ell}\right] \times \text{specimen thickness}$$

This results in a slight underestimation of the reduction in permeability since R_ℓ is not simply the resistance of the bulk material, but includes a contribution from the relatively more resistant cast face surface layer (5.8).

If the changes in pore solution resistivity due to the external environment were truly negligible, testing of 2 thicknesses of specimen would allow changes in resistance due to both test solution-cement paste interaction and further hydration to be apportioned between surface and bulk effects. Unfortunately, this assumption is only true in the case of extremely impermeable mixes or over very short test periods. The contribution due to a surface layer can, however, be determined by grinding off a predetermined thickness from the surface of the specimen and then remeasuring specimen resistance.

Electrolyte	Resistivity Ωm
Saturated $Ca(OH)_2$ solution (limewater)	1.1
Sea-water (North Sea)	0.2
Typical cement paste pore solution at 28 days (see Figure 5.13)	0.25 - 0.50

Table 5.2 : Electrolyte resistivities (at 20°C).

Table 5.2 presents typical resistivity values for the electrolytes involved. It can be seen that limewater-curing is likely to result in a fall in pore solution resistivity while sea-water exposure is likely to have the opposite, though less pronounced, effect. Consequently, the pore solution resistivity of the sea-water exposed test specimens will almost certainly be lower than the pore solution resistivity of the corresponding control specimen. Thus, if the pore solution resistivity changes are ignored, R_s-R_ℓ will represent an underestimation of the reduction in permeability.

Changes in the resistivity of a porous material due to variations in pore solution resistivity may be taken into account by measuring pore solution resistivity (5.7.2) and expressing results in terms of the Formation Factor (FF) of the material:

$$FF = \frac{\rho_C}{\rho_W} \qquad (5.3)$$

where ρ_C = resistivity of the saturated material; and

ρ_W = resistivity of its pore solution.

For a material with a non-conducting matrix (such as concrete, 5.3), FF is independent of ρ_W and provides a measure of the continuity of the pore system, being a measure of the relative ease with which ions can migrate through the material.

There are several complications associated with the direct application of Equation (5.3). For example, the surface resistances should be subtracted from the specimen resistance in order to calculate ρ_C and ρ_C and ρ_W (and hence FF) are likely to vary across the thickness of the specimen.

Another relationship that could be exploited is

$$FF = \frac{D_O}{D}$$

where D_O = chloride* ion diffusion coefficient in water

D = " " " " in the specimen under investigation

*or any other ion

This relationship is only an approximation for two main reasons. Firstly, FF is based on the diffusion (under an electrical potential gradient) of all ions present in the pore solution, while D is specific to a particular ion. Secondly, there are a number of factors, in particular the *relaxation effect* and the *electrophoretic effect* (see Appendix 9), which cause the mobility of ions driven by a potential gradient to be slightly different from the mobility of ions driven by a concentration gradient.

5.6 Preliminary testing

Calculations were undertaken to assess the magnitude of errors induced by various deviations from the standard test arrangement. The effects of imprecise cell dimensions, chipping of the specimen surface, electrode or specimen misalignment, the current passing for long periods and variations in the level of the electrolytes were found to be negligible. The only possible source of significant error was the existence of a leak between opposite sides of the cell, existed. A number of simple experiments were carried out to investigate the likelihood and consequences of such a leak occurring.

Substitution of a perspex disc for the concrete specimen gave a reading of effectively infinite resistance (though it should be noted that the surface characteristics of the disc were substantially different to those of a concrete specimen).

A concrete specimen was sealed into a resistivity cell, with only one side of the cell filled with solution (water containing a dye). Despite the appreciable hydraulic pressure (not experienced by the specimen under normal test conditions) there was no visible sign of leakage.

Testing 6 supposedly identical concrete specimens produced resistances of within ± 4% of the mean value.

Testing the same specimen in 5 different cells resulted in resistances of within ± 2.5% of the mean value.

These observations demonstrate the effectiveness and reliability of the seal. When a leak was deliberately produced by applying petroleum jelly to only part of the surfaces to be sealed, the subsequent resistance readings fluctuated with time in a manner that, it was felt, would have been detected had such a leak occurred during normal testing. Nevertheless, two specimens of each set of variables were always tested which had the dual function of aiding in identifying the presence of a leak and allowing one specimen to be discarded if such a leak were detected. Rather than testing two identical specimens, it was felt to be more advantageous to test specimens of two different thicknesses, thereby facilitating early differentiation between surface and bulk effects without sacrificing the benefits associated with replication.

Grinding away a predetermined thickness from the cast face of a specimen and then remeasuring specimen resistance was adopted as a means of isolating the source of the permeability-reducing phenomenon. The minimum thickness that

could be reliably ground from a 100 mm diameter resistivity specimen was found to be 1 ± 0.15 mm. However, the technique is only really appropriate for identifying relatively large changes in resistance since small changes are likely to be masked by the effects of the following "interfering" factors. The resistance values quoted are an estimation of the typical effect of each factor on the subsequent resistance reading, for a 25 mm thick mortar B specimen of 100 Ω resistance:

(1) microcracking and pore blocking due to grinding (±2Ω);
(2) microstructural damage due to partial drying of the specimen surface (+1Ω);
(3) variation in ρ_w due to the influence of the grinding lubricant (water) (+1Ω);
(4) further hydration of the specimen (+0.2Ω), (greater for mixes containing replacement materials, e.g. mortars D and E);
(5) errors associated with taking readings and making corrections for temperature and test solution resistivity (±2Ω).

Early results from the testing of 28 day limewater-cured specimens of different thicknesses seemed to suggest that resistivity was dependent upon specimen thickness, i.e. a 40 mm thick specimen had considerably less than double the resistance of a specimen only 20 mm thick. Although it was likely that this observation was due to leaching of cement paste pore solution ions being more significant for the thinner specimen, it was felt necessary to prove that the discrepancy was not due to there being an appreciable resistance associated with the specimen-electrolyte interface.

100 mm diameter specimens of 2 thicknesses of each of 5 different mortars (see Table 5.3) were cured at 100% relative humidity (but not in contact with an external source of water, thereby preventing leaching during curing) for 28 days. Several millimetres were then ground (using a minimal amount of water as a lubricant) from each of their flat faces, such that the exposed surface was representative of the bulk of the specimen. These specimens were then installed in resistivity cells with limewater on either side of the specimen and readings were taken over several days. The tendency was for the measured resistance to fall over the first few hours as the specimen was resaturated and then to gradually increase, probably due to further hydration (5.5). The lowest resistance reading was recorded (see Table 5.3) and the readings for each pair of specimens were used to calculate an *apparent surface resistance*,

using the equation

$$\text{apparent surface resistance} = \frac{R_t}{2} \cdot \frac{t(R_T - R_t)}{2\,(T - t)}$$

where t = thickness of thinner specimen;

T = thickness of thicker specimen;

R_t = resistance of thinner specimen; and

R_T = resistance of thicker specimen.

Table 5.3 shows that the apparent surface resistances so calculated were negligible.

Mix reference*	Specimen thickness mm	Resistance Ω	Apparent surface resistance Ω
Mortar B	24.4	96.9	
	41.5	164.8	-0.15
Mortar C	24.3	57.3	
	40.6	98.6	0.04
Mortar D	25.4	77.0	
	43.3	133.8	-2.03
Mortar E	25.3	231.9	
	40.6	368.3	2.51
Mortar F	25.1	67.5	
	42.3	114.2	-0.24

*see Appendix 1 for mix details.

Table 5.3 : Apparent surface resistances of various mortar specimens.

It should be pointed out that while test specimen replicates tested concurrently generally gave similar results, experiments repeated under apparently identical conditions, but at different times, often produced results showing similar trends but of a different magnitude.

5.7 Experimental details

5.7.1 General

Two consecutive series of tests were undertaken. In test series I (5.7.2) a concrete and a range of mortars were monitored during 18 weeks of immersion in sea-water. In test series II (5.7.3) the effects of a variety of other variables over a 12 week test period were assessed.

The following experimental details are common to both series I and series II:

Specimens were cast in purpose-made cylindrical steel moulds (A1.2). Ample specimens were cast to allow damaged specimens to be rejected. Specimens were demoulded after either one or two days in the mould and were cured in limewater at 20 ± 1°C (A1.2).

At 28 days specimens were rinsed with distilled water and fitted into resistivity cells. Solutions A & B were added simultaneously, thereby avoiding a pressure differential across the specimen. The maximum elapsed time from a specimen being taken out of the limewater curing tank to it being resaturated within the cell was 20 minutes and any surface drying of the specimen was therefore negligible. The cast face (the flat face that was at the bottom of the mould) was exposed to solution A. Solution B was always limewater (5.4) with additional lime being added every 2 weeks to replace that which was lost through precipitation of calcium carbonate due to carbonation.

Readings were generally taken every 2 weeks, but were only taken after the test solutions had been at constant temperature (± 0.2°C) for the previous hour (A7.1). A set of readings comprised:

resistance between electrodes (Ω);
resistivities of solutions A & B (using a dip conductivity cell) (Ωm);
temperature of solutions A & B (°C).

It was clearly important to test specimens that had been exposed in a natural marine environment. A number of such specimens were kindly made available for testing (5.7.4) by Mr M.B. Leeming, Technical Manager of the *Concrete in the Oceans* research programme.

5.7.2 Test series I

The mixes tested are shown in Table 5.4 and more comprehensive mix details are given in A1.1.

Mix reference	Free water/cement ratio	Cement type	Cement replacement materials
Concrete A	0.4	OPC	-
Mortar B	"	"	-
" C	0.6	"	-
" D	0.4	"	35% pfa
" E	"	"	70% bfs
" F	"	SRPC	-

Table 5.4 : Mixes tested

Two pairs of 25 and 45 mm thick specimens of each of the mixes in Table 5.4 were monitored in resistivity cells; one pair as *test specimens* with the cast face exposed to sea-water and the other face to limewater, the other pair as *control specimens* with both faces exposed to limewater. The sea-water was replaced every 4 weeks and the importance of this is discussed later (5.7.3). At the end of the 18 week exposure period the 25 mm thick mortar specimens were removed from their cells, 1 mm was ground from the cast face, the specimens were refitted and their resistances remeasured. Two additional 45 mm thick mortar B specimens (1 test specimen, 1 control specimen) were housed in resistivity cells and at the end of the exposure period were ground and retested more extensively in an attempt to more accurately determine the source of any increase in resistance.

In order to *truly* isolate changes in resistivity due to microstructural modification resulting from sea-water-cement paste interaction, it is also necessary to monitor changes in pore solution resistivity (5.5). The only feasible method of accomplishing this aim involves extracting the pore solution using a press. Unfortunately Imperial College did not have a suitable press,

but Dr. C. L. Page, Materials Research Group, Department of Construction, University of Aston, kindly offered to test a limited number of specimens.

Ideally, the resistivity of pore solution extracted from the *resistivity specimens* would have been measured. However, the technique is obviously destructive and many more resistivity specimens and hence resistivity cells would have been required. This was neither experimentally desirable (3.3.2) nor economically viable. Consequently *match-cured* "pore press" specimens were tested.

25 and 45 mm thick 49 mm (within the 2 inches limit of the press) diameter specimens of mortars B-F were cast in cylindrical PVC moulds. After demoulding, the curved face of all specimens (including the resistivity specimens) was sealed with plastic insulation tape. This was to restrict leaching and ion ingress to the flat faces of the specimens during limewater-curing so that the composition of the pore solution within the smaller pore press specimens was not more greatly affected than that of the resistivity specimens. All specimens were cured in limewater to 28 days. One 25 mm thick and one 45 mm thick specimen of each of the five mortars was then pressed. An additional specimen of each mix, having been sealed within its mould since casting, was also pressed. Of the remaining pore press specimens, half were exposed in specially manufactured curing cells (based on the resistivity cell design) with the cast face exposed to sea-water and the other face to limewater, while the other half were stored in a limewater-filled tank. After 8 and 16 weeks, specimens from both the sea-water-limewater curing cells and the limewater tank were pressed (2 thicknesses of each of 5 mixes).

The press was designed after a similar device reported by Longuet *et al.* (1973) except that a higher operating pressure was provided for. The insulation tape was removed and the specimens were rinsed with deionised water, dried with tissue and then confined between the piston and base of the cylindrical pressure vessel. The load applied through the piston was gradually increased to a value of 70 tonne. The expressed pore solution, which issued from the fluid drain at the base of the apparatus, was collected in a plastic syringe. Care was taken to avoid undue exposure of the solution to air and the samples obtained were stored in sealed plastic vials.

In anticipation of the expressed pore solution volume being very small, a

micro-conductivity cell was specially commissioned having a volume of only 0.2 ml. The cell was of the form of an inverted dip cell and was filled with solution by means of a micropipette. Readings were taken with a Pye Unicam MEL E7566/3 conductivity/resistance bridge. With such a small volume of solution it was not practical to attempt to measure temperature in the cell. Two different laboratories, where the ambient temperatures were reasonably constant, but significantly different (approximately 20 & 25°C), were used to take conductivity (reciprocal of resistivity) readings. The average of measurements on 3 samples of each solution was recorded at each temperature. These values were than corrected to the equivalent values at 21°C, using Equation (A7.1) with α = 0.018/°C (Glasstone 1948).

The expressed solutions were also analysed to determine concentrations of major ionic constituents using the following standard procedures:
OH^- titration with 0.01M HNO_3 using phenolphthalein indicator;
Cl^- spectrophotometry: mercury (II) thiocyanate method (Vogel 1978);
Na^+, K^+ flame photometry.

60 mm thick 49 mm diameter specimens of each mix, cast with the resistivity and pore press specimens and cured in limewater, were used to gain an indication of the change in porosity due to hydration continuing over the test period. At ages of 4, 12 and 20 weeks, specimens were weighed under water (W_w) and in a saturated surface-dry condition (W_{ssd}). They were then oven-dried at 105°C (to constant weight) and were reweighed (W_d). Porosity was defined as

$$\frac{W_{ssd} - W_d}{W_{ssd} - W_w} \times 100\%.$$

5.7.3 Test series II

The test variables are presented in Table 5.5. See Appendix 1 for specimen details.

Mix reference	Specimen thickness mm	Solution A	Other variables
Mortar B	25*, 45	limewater	-
"	25*, 45	0.5M NaCl	-
"	25*, 45	0.0185M $MgSO_4$	-
"	25*, 45	sea-water	3°C
"	45*	"	pH-controlled sea-water
Mortar C	45*	"	"
Mortar F	45*	"	"
"	25, 45	limewater	cracked
"	"	sea-water	"

Table 5.5 : Variables in resistivity test series II.

It was felt that a study of the individual effects of the main sea-water salts might elucidate the overall behaviour. Sodium chloride and magnesium sulphate solutions were used at typical ocean concentrations (Table 2.2).

Most of the resistivity cells were stored in the laboratory at a temperature of around 20°C. One pair of cells (see Table 5.5) were stored in a refrigerator at 3 ± 1°C, a temperature at the low end of the range of North Sea surface temperatures (A2.3).

Analysis of the sea-water exposed surface of diffusion specimens (6.2) and test series I resistivity specimens (6.3) identified the presence of layers of minerals, the chemical equilibria of which are sensitive to pH (6.4). It was therefore considered essential to undertake a series of tests in which the sea-water pH was confined within close limits of its normal value. The most appropriate method of achieving this requirement was found to be by dosing the sea-water at intervals with 1.0M HCl. Alternative methods of pH control are discussed in Appendix 3. Resistivity cells containing 45 mm thick specimens of the 3 mortars showing the most significant resistivity changes in test series I (mortars B, C & F) were checked, and dosed where necessary, every day for the first week, every three days for the following 3 weeks and every week for the rest of the test period. Whenever the sea-water pH was recorded as

greater than 8.30, dosing was used to return the pH to 8.15 ± 0.05. Using this regime, the maximum pH recorded for any of the 3 cells over the 80 day test period was less than 9.0. The increase in chloride ion concentration in the sea-water as a result of dosing was less than 2% in all 3 cases.

Several investigators in the reinforced concrete corrosion field have observed deposits within cracks in sea-water exposed concrete (e.g. Wilkins & Lawrence 1980) and it has been suggested that such crack-blocking is likely to reduce the rate of corrosion of embedded steel. It has also been proposed that crack-blocking may lead to improved structural performance, particularly under cyclic loading. Arthur *et al.* (1979) observed that reinforced concrete beams under cyclic loading in sea-water showed an increased endurance compared with beams tested in air. This was felt to be due to two effects resulting from crack-blocking. Firstly reduced corrosion, but also a reduction in cyclic deflection which, with the load range remaining unchanged, would have reduced the cyclic stress range. It was felt that the resistivity test might be an appropriate means of monitoring static crack-blocking phenomena. Several methods of introducing cracks into specimens were examined. Foil cast into the specimen and removed prior to testing has been used elsewhere, but it is likely to result in a portlandite-rich surface layer on the sides of the slot which would not be present in the case of a normal structural crack. Another possibility was to split the specimen in half by loading it in a compression testing machine, with its axis horizontal, until failure by splitting along the vertical diameter (i.e. as in an indirect tensile test). Unfortunately the damage incurred by the specimen was generally too great to allow the 2 halves to be "reassembled" and all attempts to contain the specimen, e.g. by wrapping tape around the circumference of the specimen prior to loading, proved unsuccessful. The method eventually adopted simply involved using a hammer and chisel to make a small groove along a diameter of the specimen on both faces and then applying a sharp blow to one side of the specimen while supporting the other, to split it in half. The two halves of the specimen generally fitted back together sufficiently well to allow easy installation into the resistivity cell.

At the end of the 12 week exposure period the specimens marked with an asterisk in Table 5.5 were removed from their cells, 1 mm was ground from the cast face, the specimens were refitted and their resistances remeasured.

5.7.4 Naturally exposed specimens

The *Concrete in the Oceans* programme provided specimens suitable for resistivity testing from 4 different exposure facilities:

(1) *Deep submersion* (Loch Linnhe): Loch Linnhe is a sea-water loch in Argyllshire, Scotland. Specimens were held at a depth of 140 m; at this depth the following parameters were measured (Leeming 1983):

temperature	7°C (winter)-13°C (summer);
salinity	32.3 g/kg;
dissolved oxygen	9.3 ppm;
pH	8.15.

These figures show that the sea-water at this facility was slightly less saline than the North Sea.

(2) *Shallow submersion* (Portland): specimens were held at a depth of 10 m in a man-made harbour with no major freshwater inlets, at Portland, Dorset.

(3) *Flowing tank* (Portland): specimens were submerged in a tank through which fresh sea-water was pumped.

(4) *Static tank* (Southall): specimens were submerged in a tank containing sea-water. The sea-water was replaced when the pH and dissolved oxygen level fell outside of "acceptable values" (Leeming 1983).

Ten 100 mm diameter cores cut from the deep submersion specimens were provided; 2 from each of the standard grade, low grade and pfa mixes (A1.1) after 2½ years exposure and 2 of each of the standard grade and low grade mixes after 5 years exposure. Unfortunately, prior to coring the surface of virtually all the specimens had been scraped to remove marine growth and this must inevitably have resulted in partial disruption of any surface formation. A large proportion of the surface of two of the cores was covered in a rubber latex material and most of the cores had suffered significant damage around the edge of the exposed surface due to vibration of the coring bit at the start of coring. However, 3 of the cores were resistivity tested. The 40 mm surface end section of each core was cut off using a diamond saw, the blade of which was lubricated with limewater. The

resistance of the specimen was then measured before and after the surface 1 mm was ground off, using limewater as both solutions A and B.

3 pairs of cores which were taken from standard grade concrete specimens which had been stored in exposure facilities (2), (3) or (4) for 2 years, were also provided. One core from each of the facilities was resistivity tested, in the manner described above, in order to compare the effects of *simulated* with *real* marine conditions.

The results and discussion are presented together in 5.9.3. The cores that were not resistivity tested were used for surface examination and analysis (6.7).

5.8 Results

5.8.1 Test series I

Figures 5.5 to 5.10 show the variation of resistance, increase in resistance and apparent increase in thickness of specimens of each of 6 different mixes over 18 weeks exposure to sea-water. The vertical dotted lines in Figures 5.6 to 5.10 represent the fall in resistance on grinding 1 mm from the cast faces of the 25 mm thick specimens.

Figure 5.11(a) presents a comparison of the resistance versus age relationships of the 25 mm thick limewater-cured control specimens of the 6 mixes under investigation. Figure 5.11(b) compares the increase in resistance, over 18 weeks of sea-water exposure, of 25 mm thick specimens of each of the mixes. Figure 5.11(c) compares the apparent increase in thickness, over 18 weeks of sea-water exposure, of 25 mm thick specimens of each of the mixes.

Figure 5.12 shows the resistivity (calculated using Equation (5.1) assuming the specimen to be homogeneous) of each of the resistivity specimens at ages of 4, 12 and 20 weeks. Figure 5.13 shows the pore solution resistivity of specimens, "match-cured" with the resistivity specimens, at ages of 4, 12 and 20 weeks. Figure 5.14 shows the variation in Formation Factor with time, on exposure to sea-water or limewater, for each of the resistivity specimens, calculated (using Equation (5.3)) from the data in Figures 5.12 and 5.13.

Table 5.6 shows the 28 day pore solution resistivities of mortar specimens stored in a sealed condition since casting.

Table 5.7 shows the porosity (determined by oven-drying) of limewater-cured specimens of each of the mortars at ages of 4, 12 and 20 weeks. Each result is the average of 2 specimens.

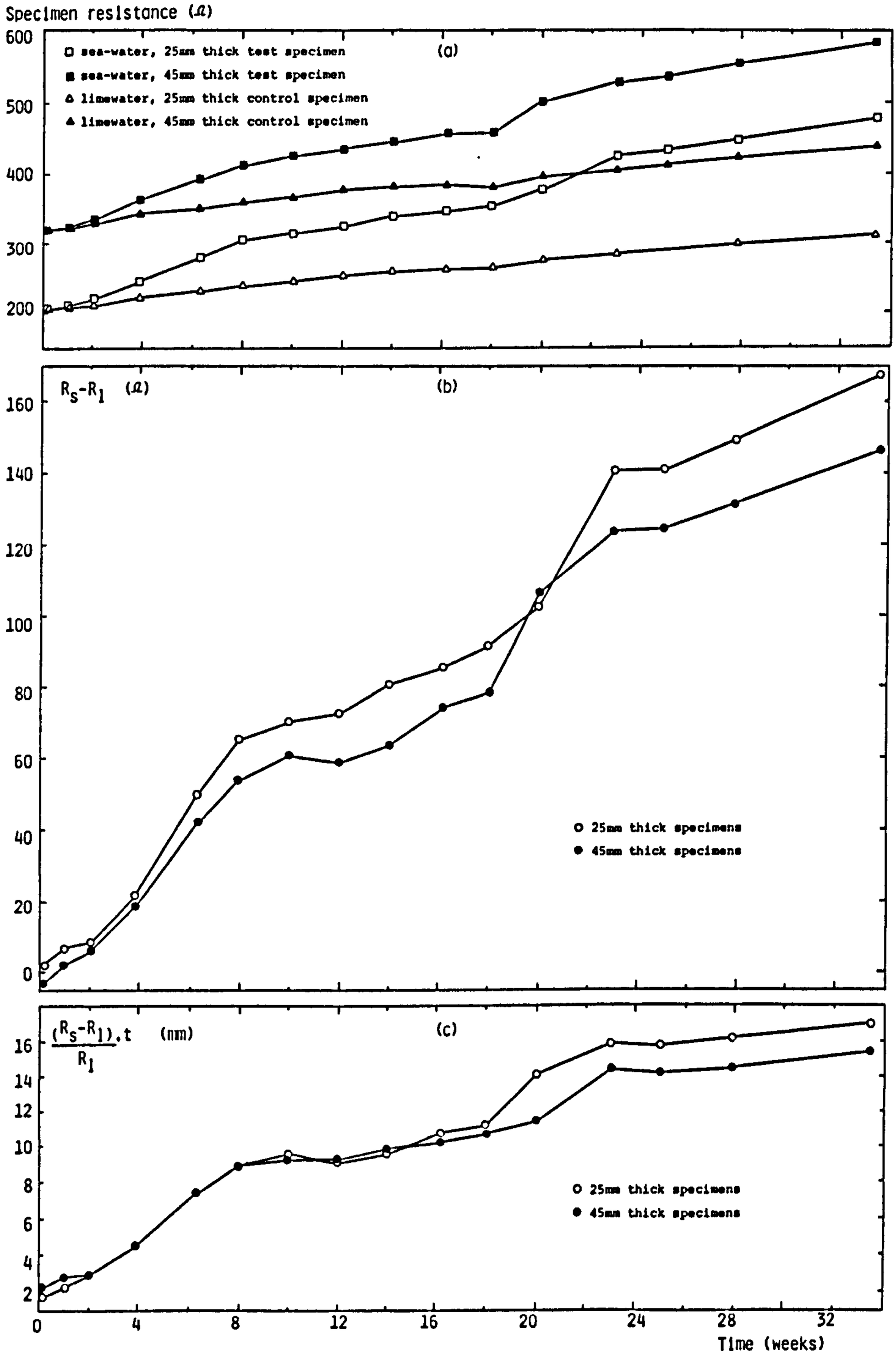

Figure 5.5: The effect of immersion in sea-water on the resistance of specimens of concrete A.

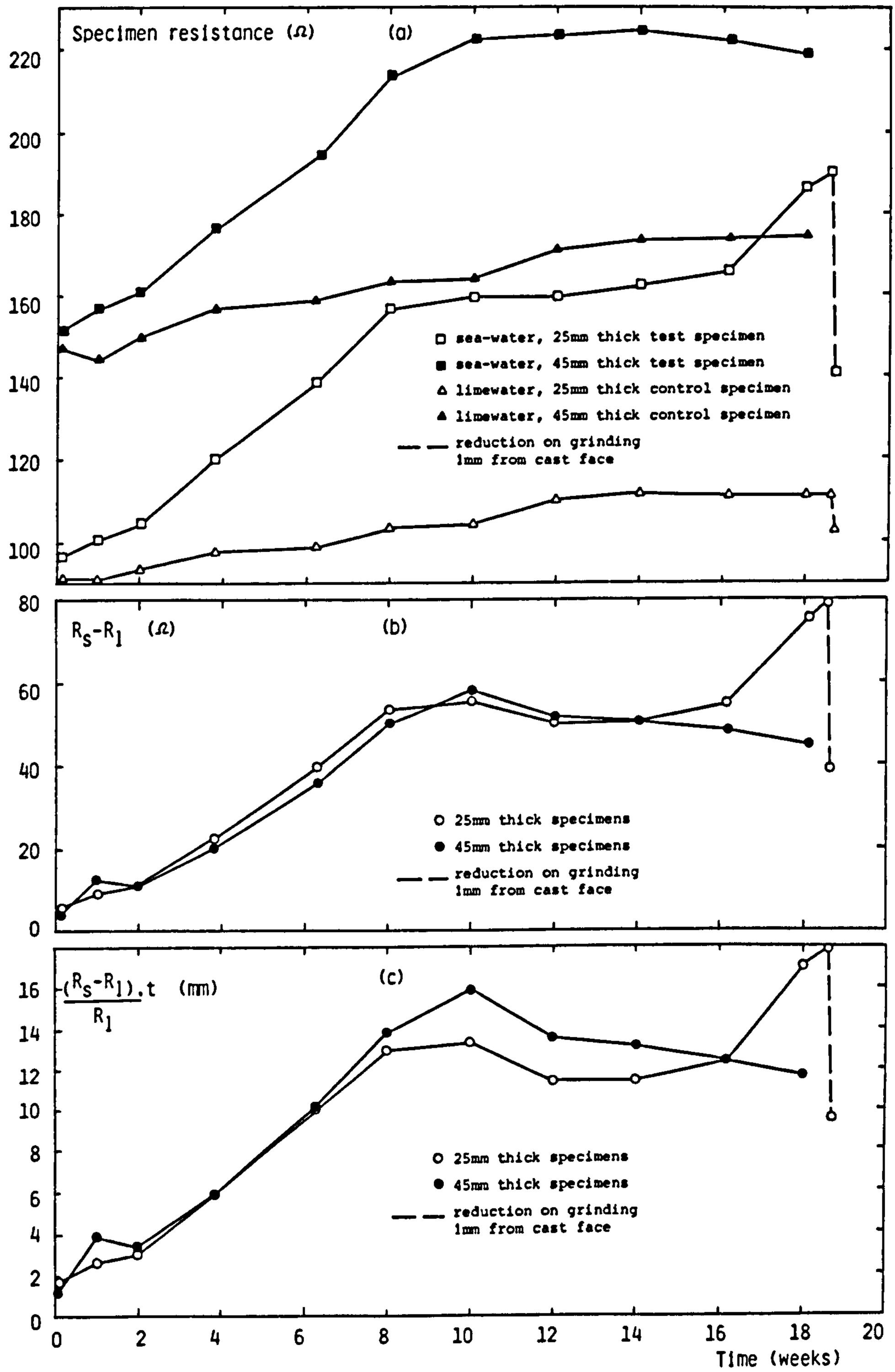

Figure 5.6: The effect of immersion in sea-water on the resistance of specimens of mortar B.

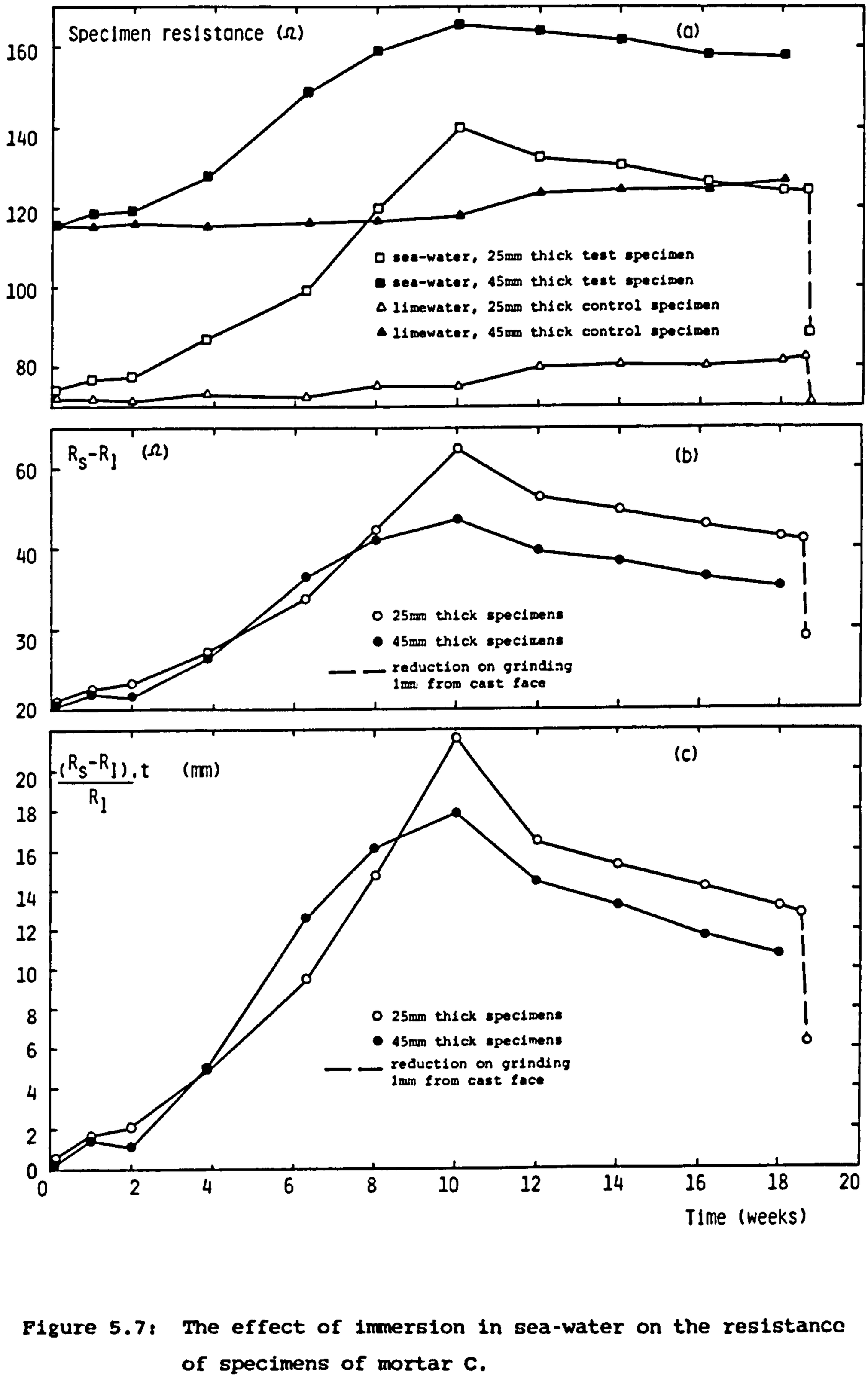

Figure 5.7: The effect of immersion in sea-water on the resistance of specimens of mortar C.

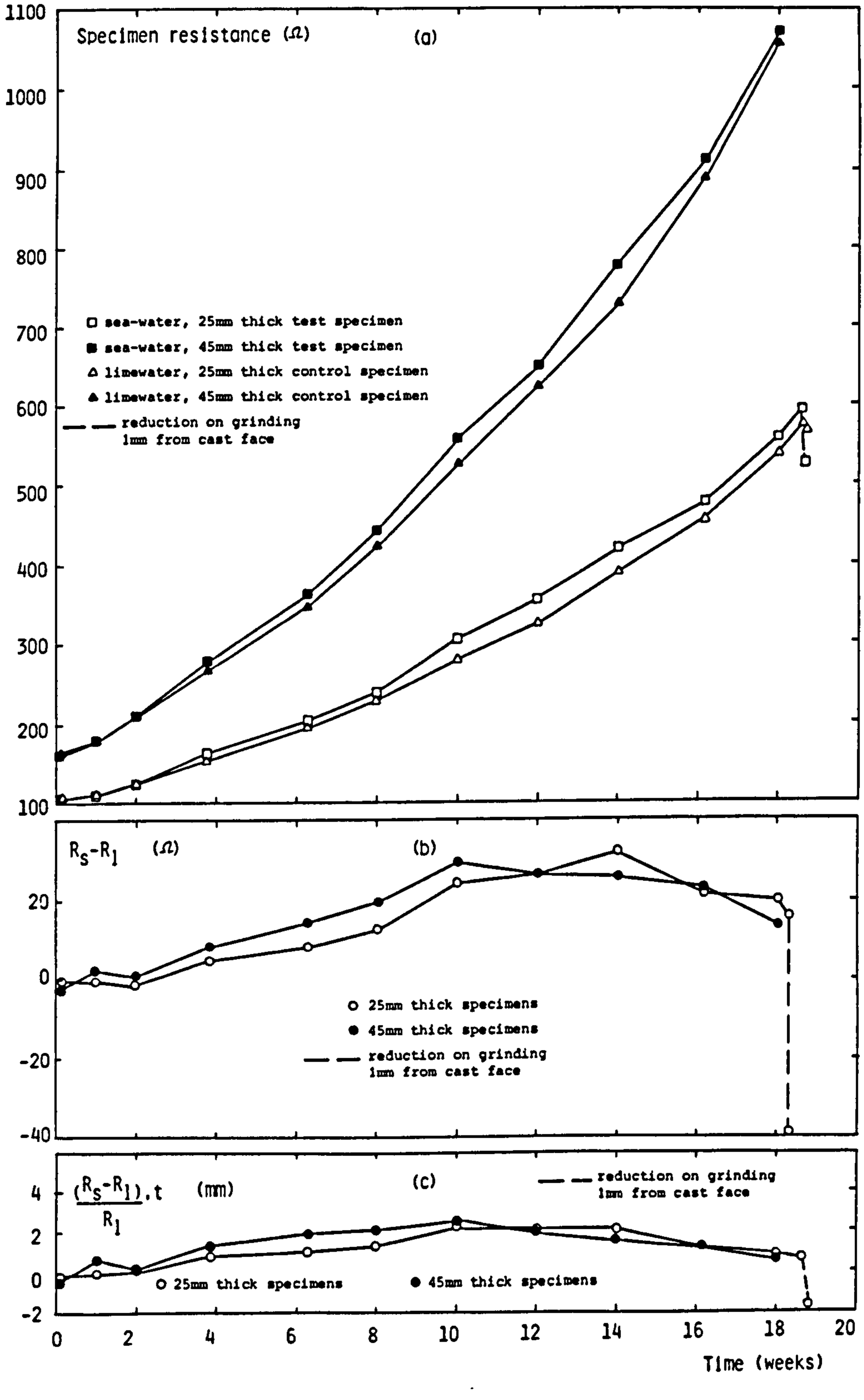

Figure 5.8: The effect of immersion in sea-water on the resistanco of specimens of mortar D.

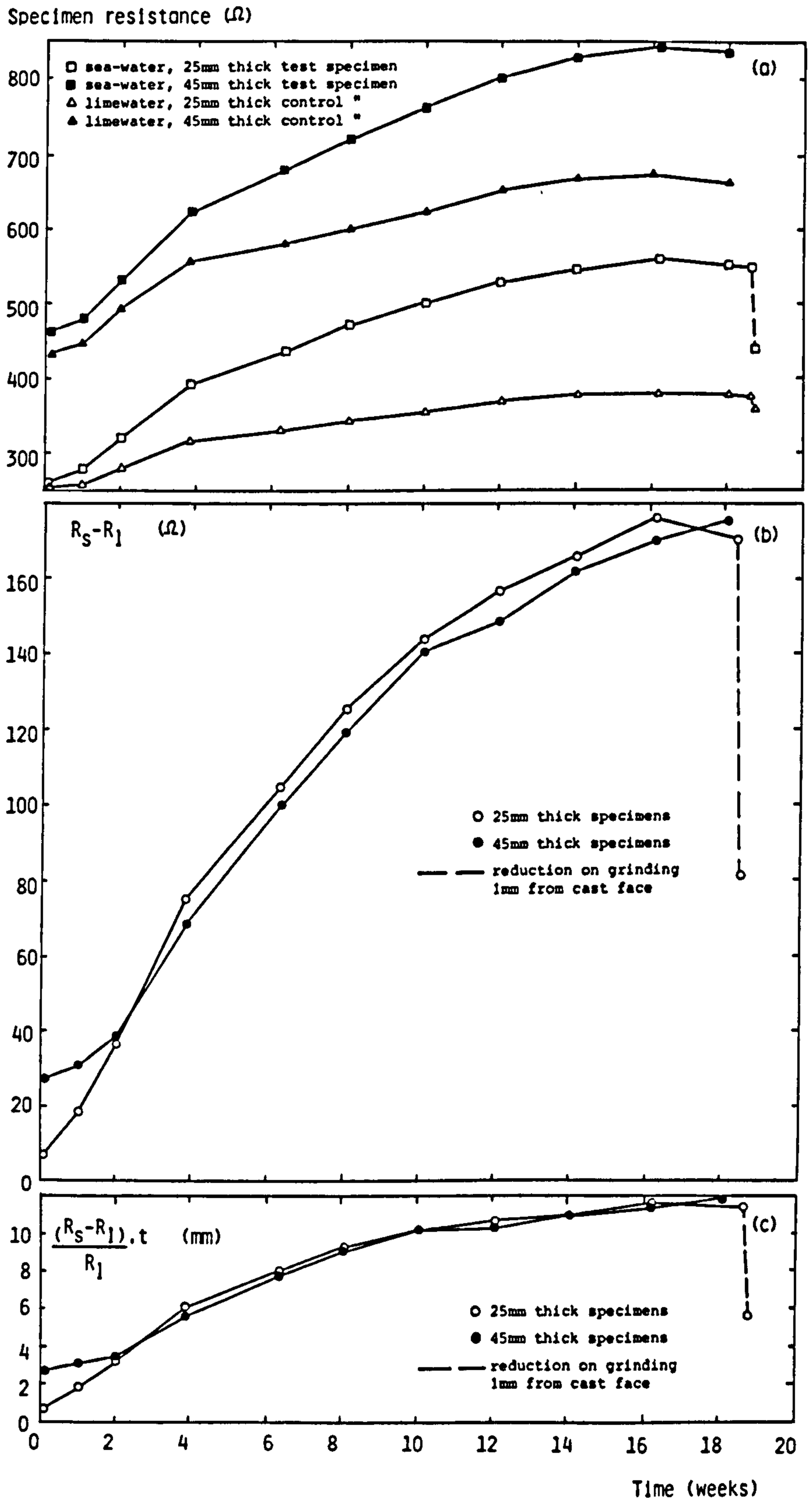

Figure 5.9: The effect of immersion in sea-water on the resistance of specimens of mortar E.

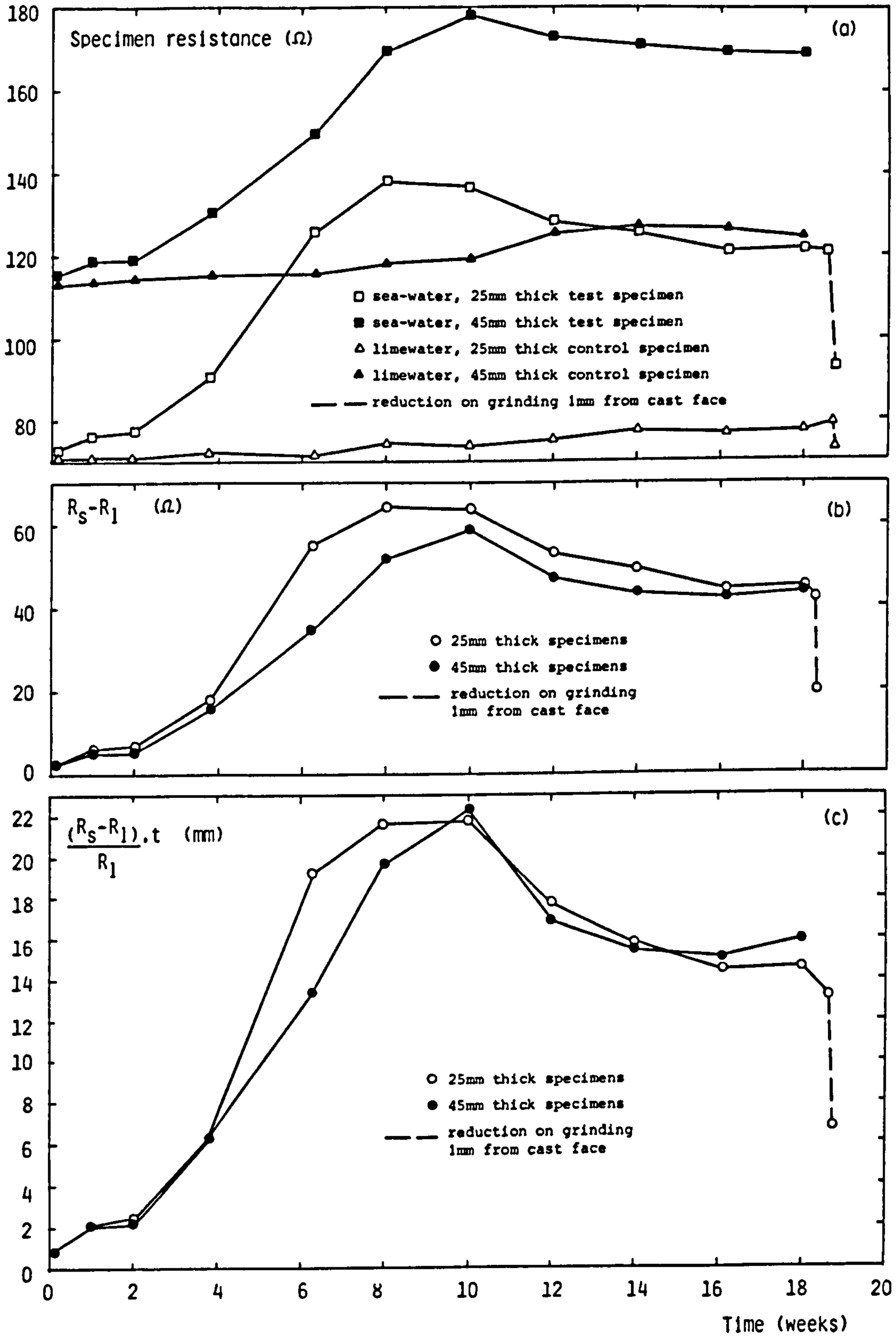

Figure 5.10: The effect of immersion in sea-water on the resistance of specimens of mortar F.

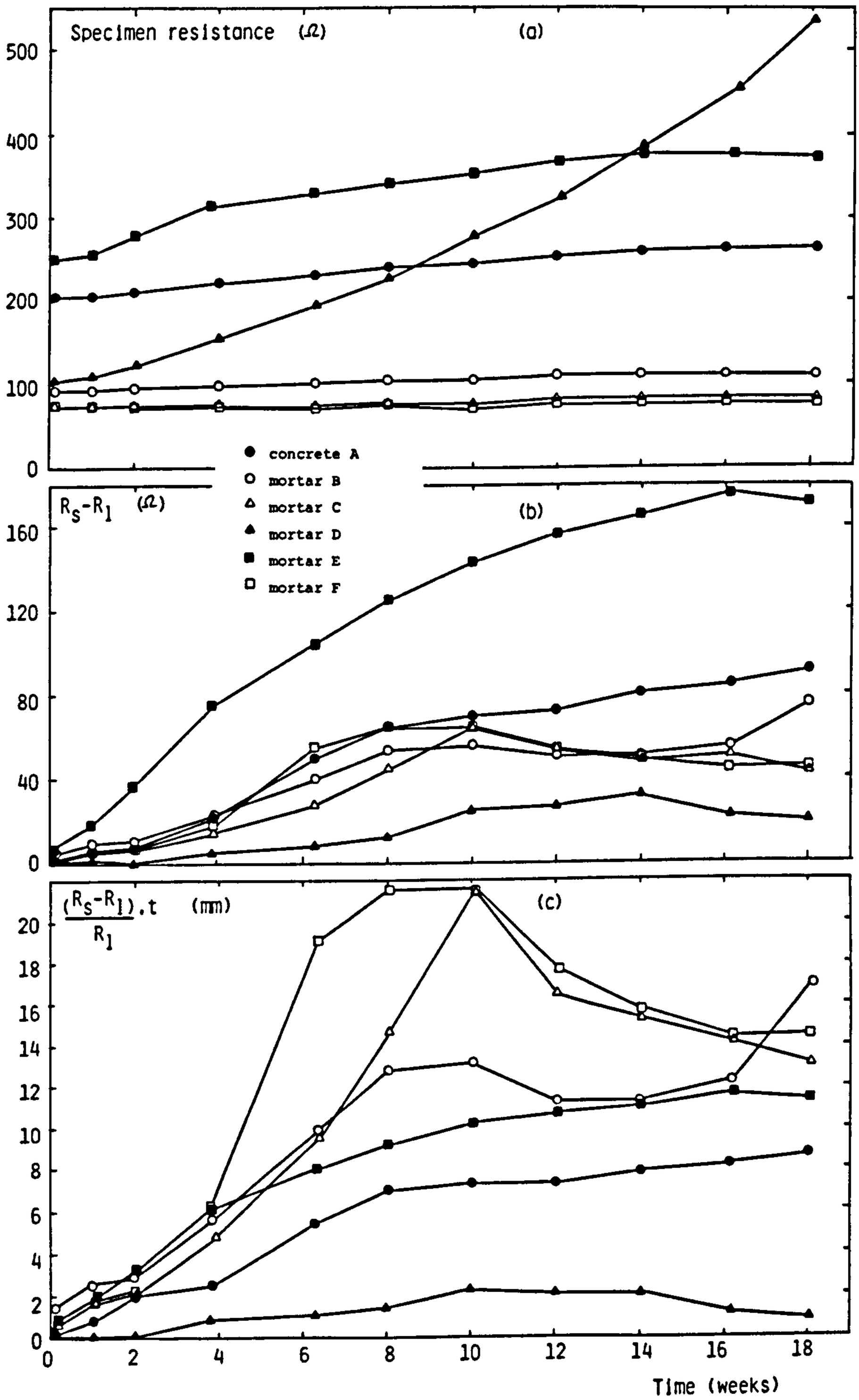

Figure 5.11: The effect of immersion in sea-water on the resistance of 25 mm thick specimens of various mixes.

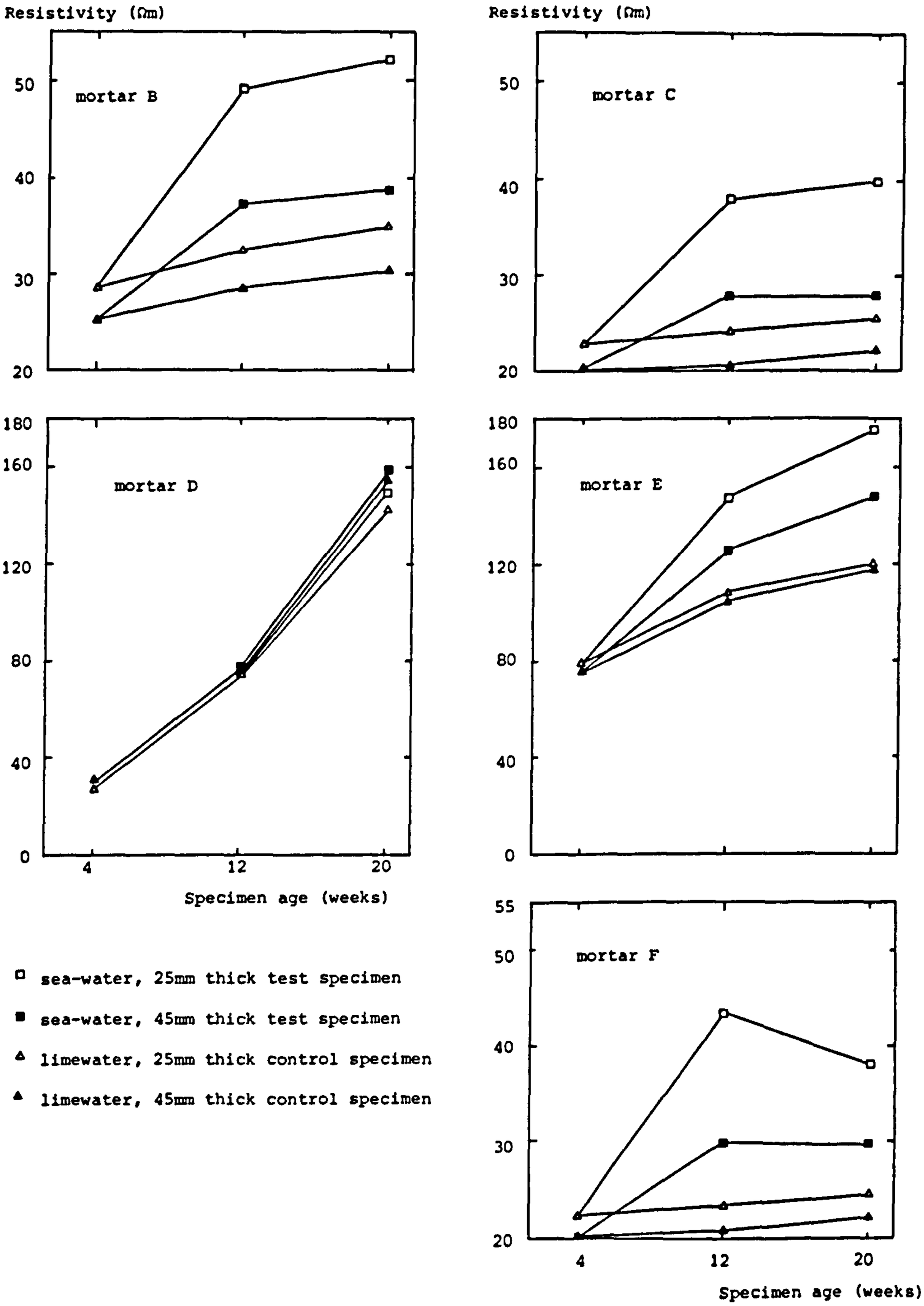

Figure 5.12: The effect of immersion in sea-water on the resistance of various mortars.

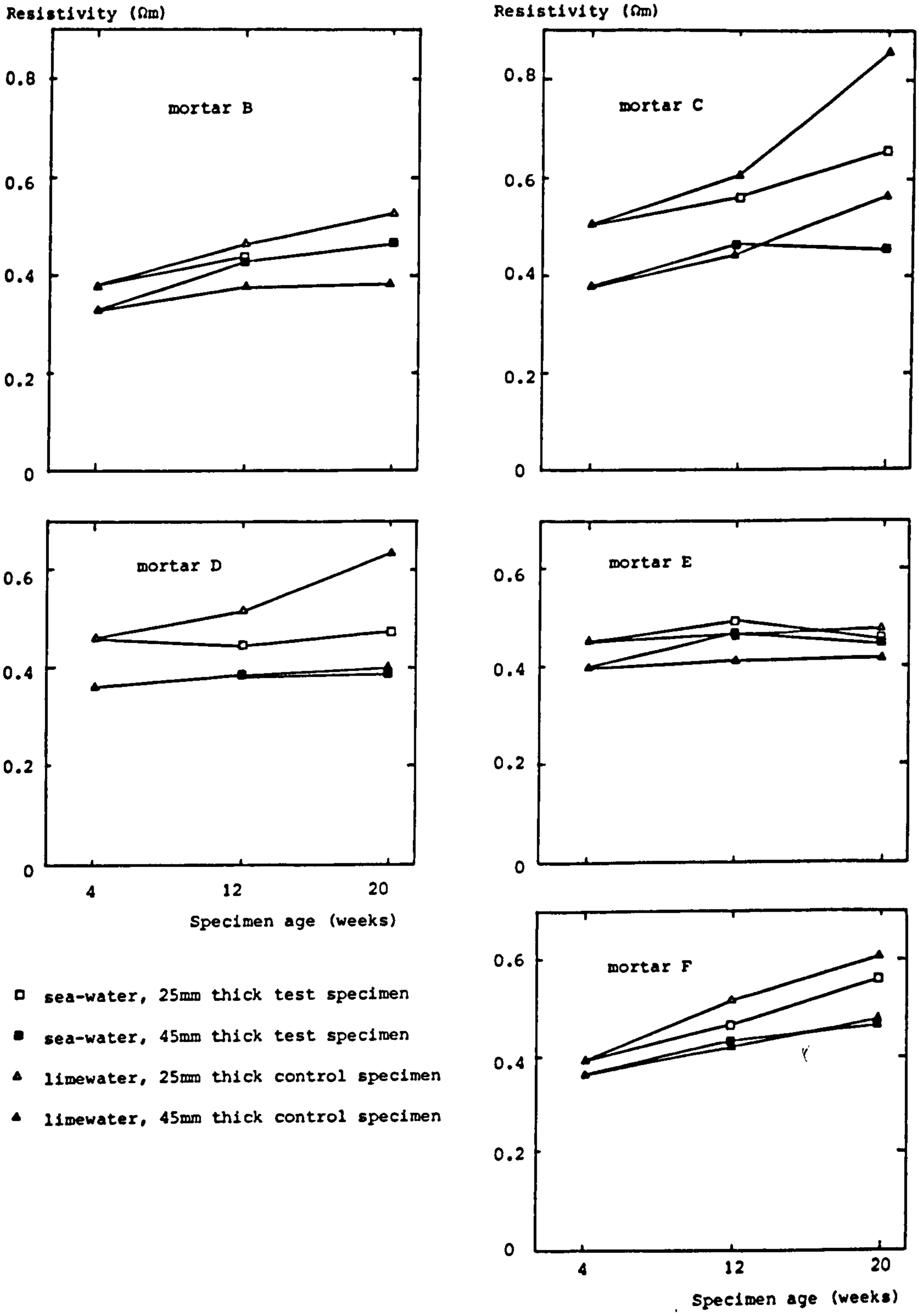

Figure 5.13: The effect of immersion in sea-water on the pore solution resistivity of various mortars.

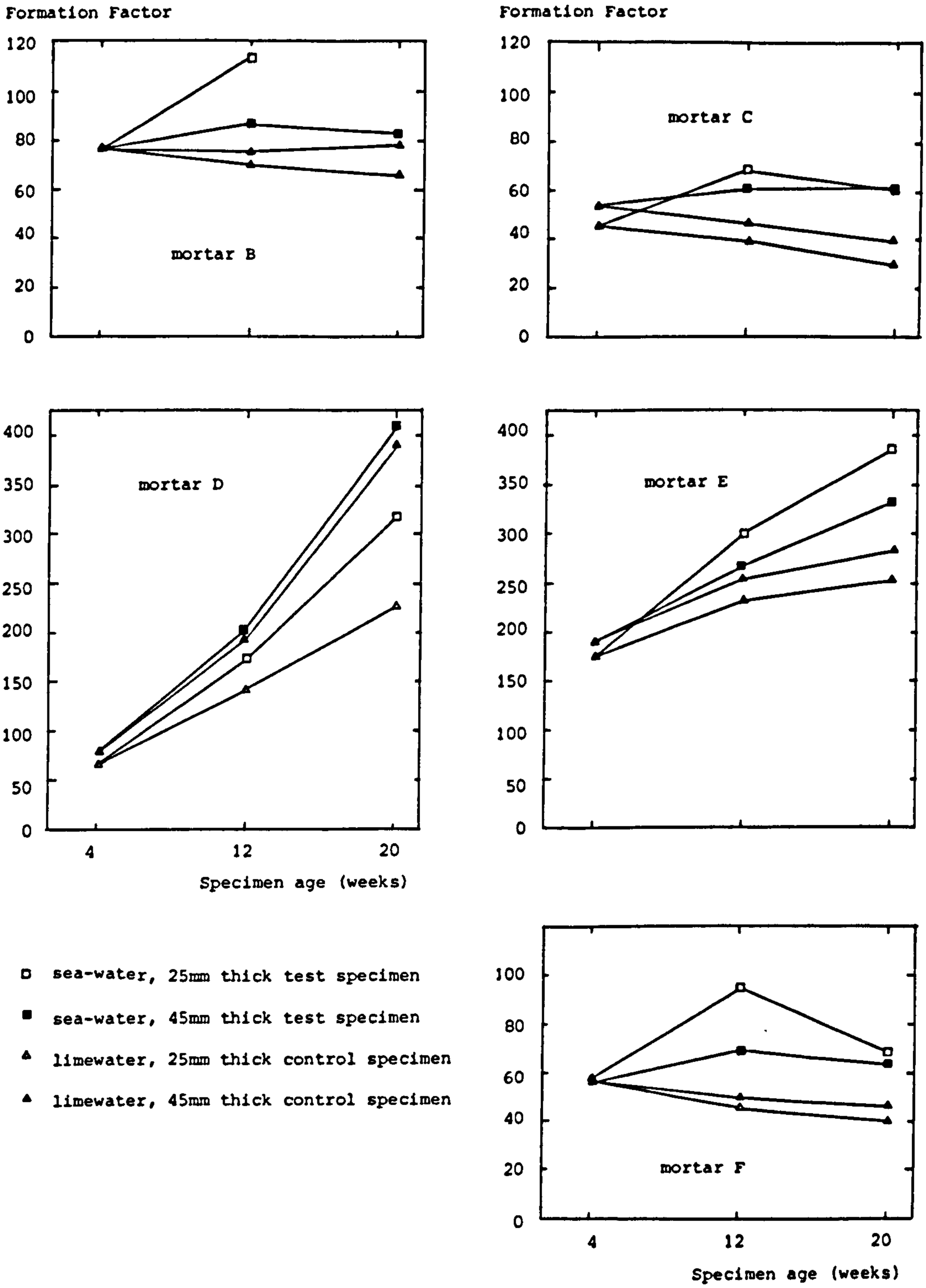

Figure 5.14: The effect of immersion in sea-water on the Formation Factor of various mortars.

Mix reference	Pore solution resistivity Ωm
Mortar B	0.25
" C	0.29
" D	0.27
" E	0.35
" F	0.26

Table 5.6 : 28 day pore solution resistivity of sealed mortars.

Mix reference	Porosity %		
	4 weeks	12 weeks	20 weeks
Mortar B	23.58	23.29	22.55
" C	29.16	28.57	28.46
" D	25.18	25.41	24.84
" E	23.50	23.51	22.50
" F	24.33	23.70	23.56

Table 5.7 : Porosities of limewater-cured mortars (determined by oven-drying at 105°C).

Chemical analyses of the pore solutions extracted from the pore press specimens are presented in Appendix 5.

5.8.2 Test series II

Figure 5.15 shows the variation of resistance, increase in resistance and apparent increase in thickness of specimens over 12 weeks exposure to 0.5M NaCl solution.

Figure 5.16 shows the variation of resistance, increase in resistance and

apparent increase in thickness of specimens over 12 weeks exposure to 0.0185M $MgSO_4$ solution.

Figure 5.17 shows the variation of specimen resistance with time of exposure to sea-water at 3 ± 1°C.

Figure 5.18 shows the variation of resistance with time of exposure to pH-controlled sea-water for 45 mm thick specimens of mortars B, C and F.

Figure 5.19 shows the variation of resistance, increase in resistance and apparent increase in thickness of cracked specimens over 12 weeks exposure to sea-water.

Note: The vertical dotted lines in Figures 5.15 to 5.19 represent the fall in resistance on grinding 1 mm from the cast faces of the specimens in question.

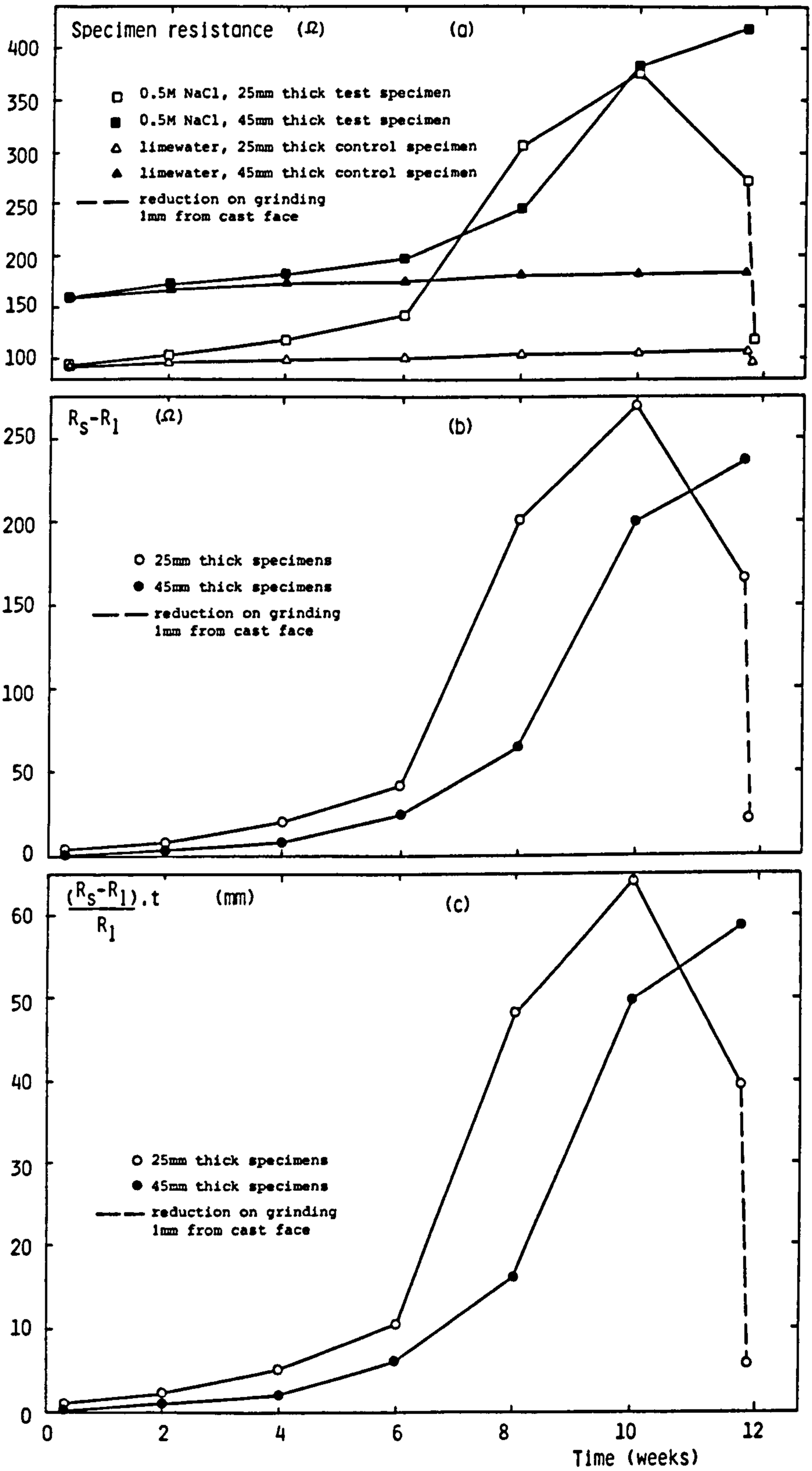

Figure 5.15: The effect of immersion in 0.5 M NaCl solution on the resistance of specimens of mortar B.

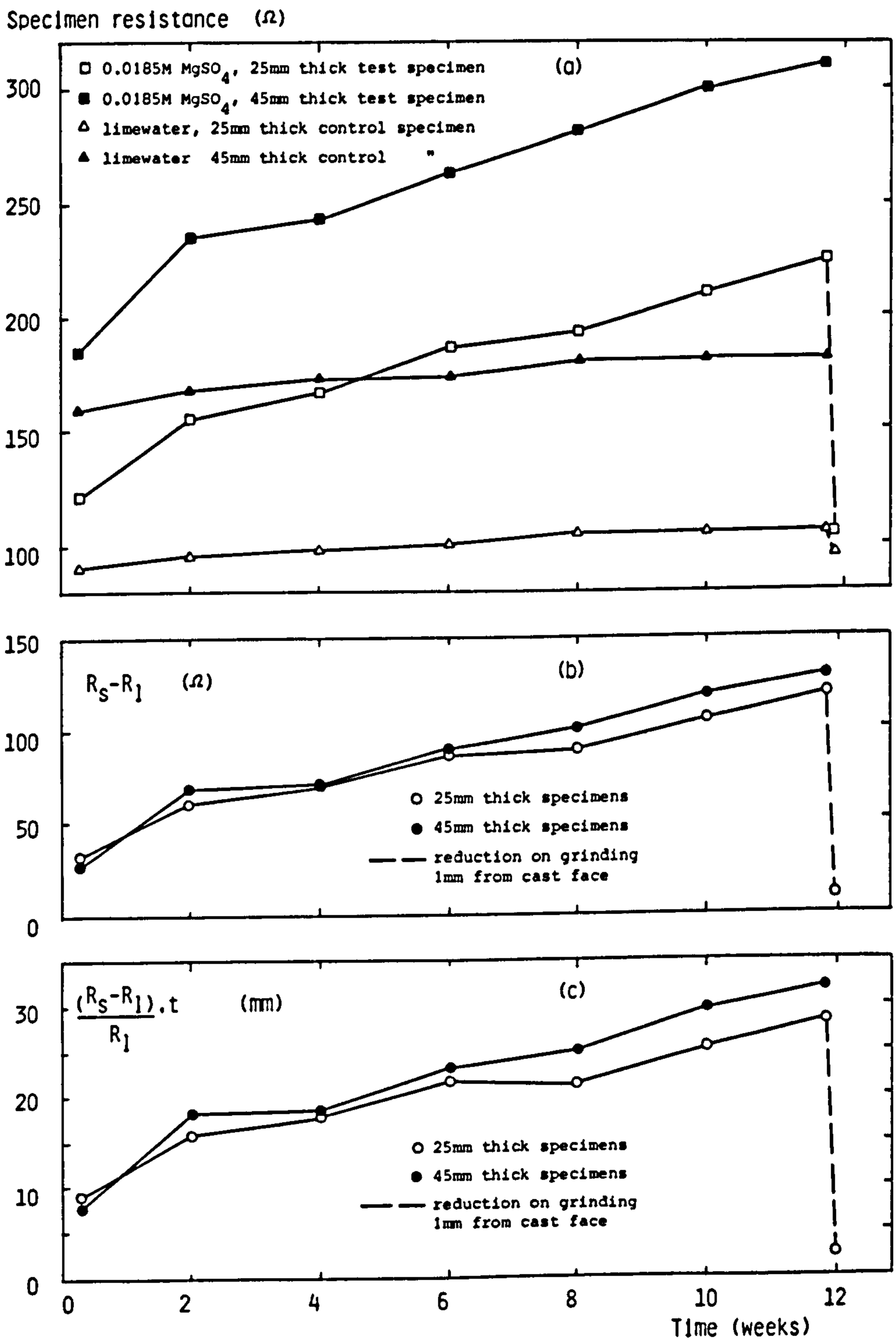

Figure 5.16: The effect of immersion in 0.0185 M $MgSO_4$ solution on the resistance of specimens of mortar B.

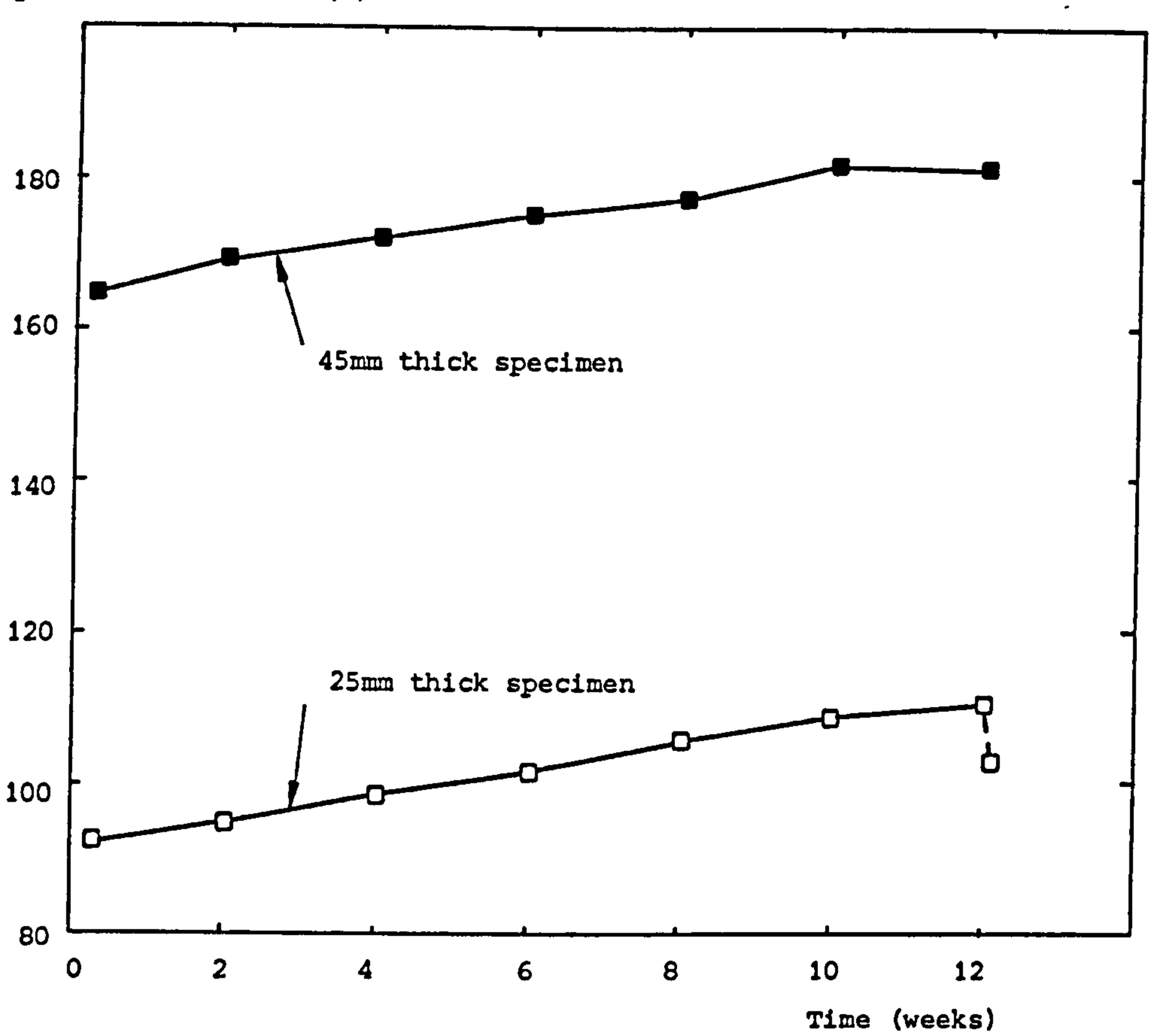

Figure 5.17: The effect of immersion in sea-water at 3 ± 1°C on the resistance of specimens of mortar B.

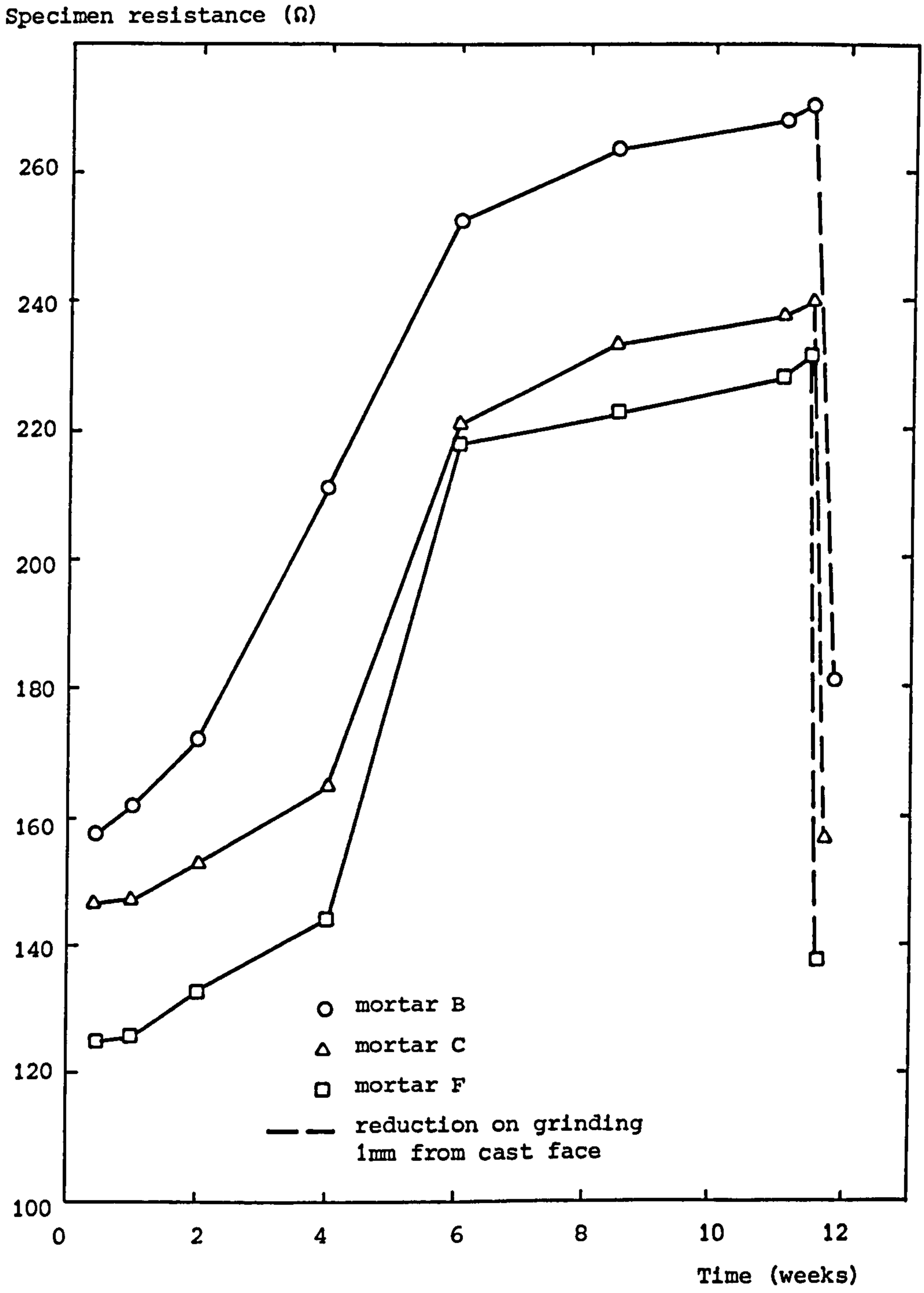

Figure 5.18: The effect of immersion in pH-controlled sea-water on the resistance of 45 mm thick specimens of mortars B, C and F.

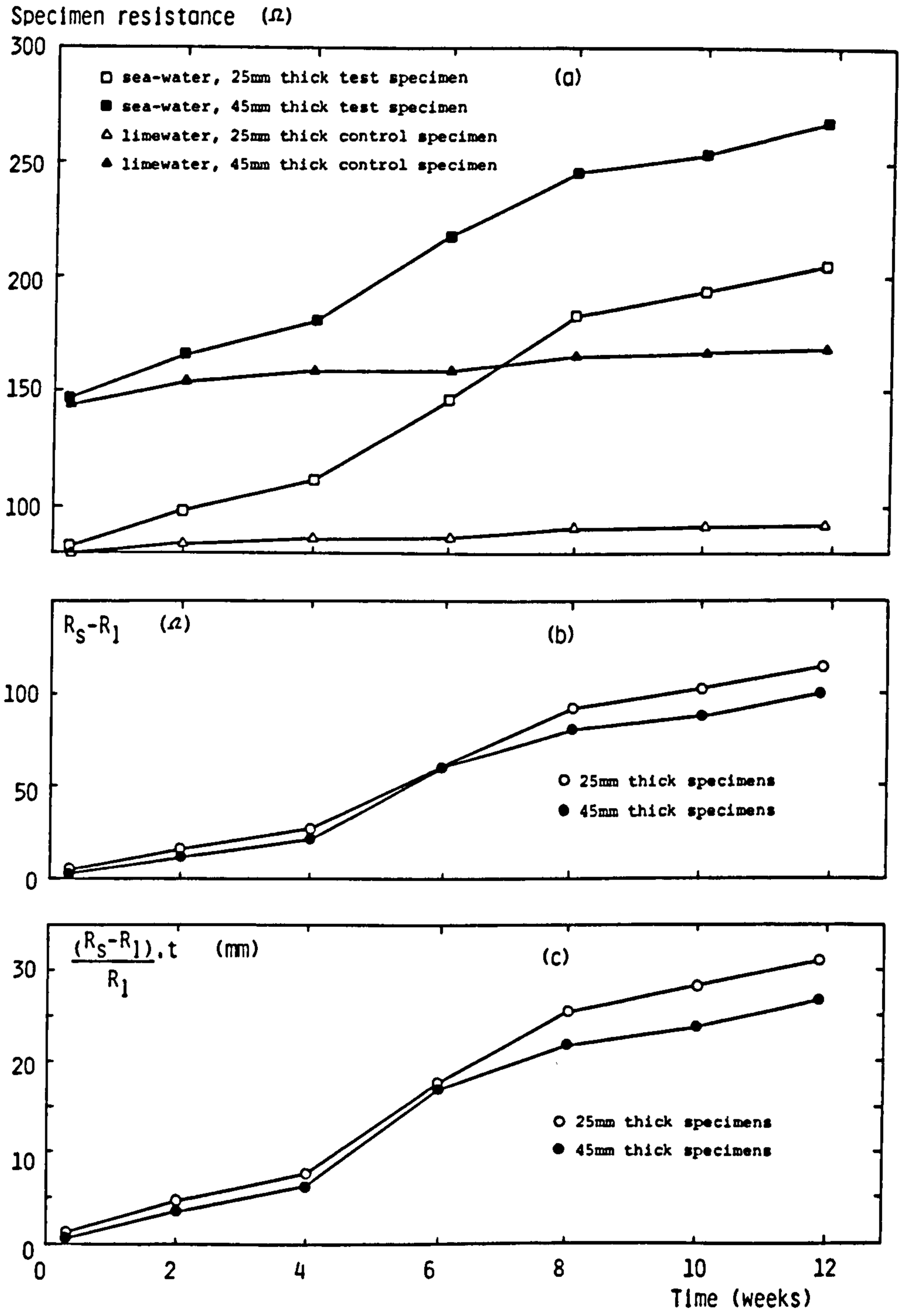

Figure 5.19: The effect of immersion in sea-water on the resistance of cracked specimens of mortar B.

5.9 Discussion

5.9.1 Test series I

It was mentioned earlier (5.7.2) that for the determination of pore solution resistivity (ρ_w) the average resistivity values of 3 samples of pore solution were taken at 2 different temperatures and that these were then corrected to give 2 equivalent values at the reference temperature of 21°C. These 2 values often differed by 15 or 20%, but were averaged to give the values of ρ_w plotted in Figure 5.13. The cause of this variation is probably associated with taking measurements on such a small quantity of solution. Carbonation of the solution may have had an effect and there may also have been a discrepancy between measured laboratory temperature and solution sample temperature. The conductivity cell volume was so small that even the presence of an air bubble between the electrodes was observed to produce spurious readings. The ρ_w (Figure 5.13) and Formation Factor (FF) (Figure 5.14) results are therefore interpreted with caution. It was felt that when attempting to monitor *small* changes in permeability *relative to a control specimen*, it would be prudent to base interpretation primarily on the specimen resistance data (i.e. without reference to ρ_w data) accepting that this is a conservative approach in the sense that any reduction in permeability is underestimated (assuming that the test solution is of lower resistivity than the limewater control solution; 5.5).

The graphs showing changes in specimen resistance over long exposure periods are smooth in comparison with similar data presented by other workers (e.g. Bernhardt & Sopler 1974, Gjorv *et al*. 1977). This is due to the correction made to account for resistance changes due to temperature variations.

It is immediately clear (Figure 5.11 (a)) that certain cements produce mixes of far higher resistivity than others. Figures 5.13 and 5.14 show that ρ_w is only partly responsible for this phenomenon, which is primarily a function of the cement paste pore structure. Hence, any reduction in permeability should be kept in perspective; certain mixes are, for the same water/cement ratio, inherently less permeable. It is for this reason that reductions in permeability are expressed in terms of both resistance and also as an apparent increase in specimen thickness.

At an age of around 6 weeks, the mixes rank in order of decreasing FF (increasing permeability) as follows:

Mortar E :	OPC/70% bfs	0.4 w/c
Mortar D :	OPC/35% pfa	"
Mortar B :	OPC	"
Mortar F :	SRPC	"
Mortar C :	OPC	0.6 w/c

This is the same order (with the addition of mortar E which was not included in the earlier study) as obtained by ranking the diffusion specimens at a similar age, in order of increasing chloride ion diffusion coefficient (4.3.4). Such correlation adds weight to the technique as a means of instantaneously identifying changes in diffusion coefficient / permeability.

The control specimens of the mixes without replacement materials (A, B, C & F) exhibit a very gradual increase in resistance over the duration of the experiment. One would expect this behaviour to be primarily due to a decrease in capillary porosity due to further hydration (5.5). The downward trend in FF shown in Figure 5.14 suggests, to the contrary, that this increase is due to an increase in pore solution resistivity and that, in fact, the pore structure is opening out. This would be very surprising in a lime-saturated solution and it is just conceivable that the increase in FF is due to the existence of a *surface conduction* mechanism (conduction at the cement paste - pore solution interface) whose contribution to total conduction becomes more significant as ρ_w increases. Such a mechanism has been observed in certain rocks by researchers in the well logging field (Worthington & Barker 1972, Winsauer & McCardell 1953). This case is a good example of a situation where a small change in permeability cannot be identified. The resistance readings cannot be related to those of a control specimen (since it is the behaviour of the control specimen that is being considered) and the changes monitored are sufficiently small to be masked by the experimental errors associated with evaluating ρ_w.

The resistivity of the pfa mortar (mortar D) exhibits a 5 to 6-fold increase over the test period. A small proportion of this is due to the slight increase in ρ_w (Figure 5.14), but the phenomenon is primarily associated with changes in the cement paste microstructure, probably due to continuing pozzolanic reaction. However, at the end of the exposure period the FF for the pfa mix is 7 times larger than that of the SRPC mix, even though their MIP pore size distributions are virtually identical (Figure 7.1). This suggests that the

difference could be due to different types of interaction between pore solution ions and pore surfaces as discussed with regard to differing rates of chloride ion diffusion (4.3.4). However, it has recently been suggested that pfa hydration products are far more fragile than the microstructure of OPC pastes and that thin films of hydration product, which may significantly reduce permeable porosity at lower pressures, are destroyed at the high pressures necessary for MIP. Consideration of "porosities" based on oven-drying at 105°C does not clarify the issue; the porosity of the pfa mix hardly changes over the test period (Table 5.7). This is almost certainly a function of the method used to determine porosity; oven-drying removes the capillary and most of the gel water, but also a proportion of the chemically bound water (7.1.2). Furthermore, the gel pore water has a greater specific gravity than free water and hence occupies a smaller volume than its weight suggests (7.1.2). Consequently porosity is probably progressively more overestimated as hydration proceeds.

Figure 5.12 shows the 25 mm limewater-cured specimens to have higher resistivities than the corresponding 45 mm thick specimens. This is partly because of the resistive surface layers making a relatively greater contribution to the resistance of the thinner specimen, but is primarily due to the pore structure of the thinner specimen being more exposed to leaching of cement paste pore solution ions and hence having a higher value of ρ_w (Figure 5.13).

The curves in Figures 5.5 to 5.11, showing the increase in resistance and the apparent increase in thickness of specimens due to sea-water exposure, do not necessarily pass through the origin since supposedly similar 28 days old specimens are rarely of identical resistance.

If the sea-water had not interacted with cement paste, it would have been expected that the resistance of the sea-water exposed specimens would fall below that of the control specimens due to lime leaching (2.2.3) and the relative reduction in ρ_w. However, it can be seen for all the mixes tested that sea-water exposure results in an increase in resistivity and FF and hence a reduction in permeability.

In terms of ohmic resistance, bfs mortar (mortar E) exhibited the greatest reduction in permeability (Figure 5.11(b)). However, the greatest relative

change was shown by mortars C and F, 25 mm thick specimens showing an increase in resistance equivalent to over 20 mm of additional thickness after only 10 weeks of sea-water exposure.

The resistivity of several of the more permeable mixes (particularly mortars C and F) reached a peak after 10 or 12 weeks of sea-water exposure and then gradually decreased. This phenomenon was originally thought to be due to a drop in ρ_w due to sea-water ion penetration. However, Figures 5.13 and 5.14 do not support this hypothesis. Surface examination and analysis (6.3) of the 45 mm thick resistivity specimens suggest that the increase in resistance of specimens exposed to sea-water is primarily due to the formation of a composite layer of aragonite and brucite on the sea-water exposed surface. Theoretical studies of the chemical equilibria of such minerals (6.4) suggest that their stability is very sensitive to sea-water pH. Cement paste pore solutions generally have a pH in excess of 12, while the pH of fresh sea-water is around 8.2 Hence the pH of the sea-water in the resistivity cell gradually increases. Therefore another hypothesis was that perhaps the layer had formed more densely as the pH of the sea-water increased and then when the sea-water was replaced (every 4 weeks) it partially dissolved to produce the observed drop in resistance. This theory is also suspect since it does not explain why the more permeable mixes are more susceptible to the mechanism and the reductions in resistivity do not generally coincide with replacement of the sea-water. A third explanation was that penetrating chloride ions react with lime in the cement paste to produce calcium chloride, which, being readily soluble in sea-water, is leached out (2.2.2.3), thereby producing a more porous, and hence less resistive, zone of cement paste below the surface layer. This theory is not supported by the mercury intrusion porosimetry results (7.3). The only conceivable mechanism to explain the observed data (and it is also supported by later resistivity tests using pure sodium chloride solution (5.9.2)) is again associated with the penetration of chloride ions. It is possible that a constriction of the cement paste pore system occurred in the surface zone of the sea-water-exposed specimen, due to the formation of calcium chloroaluminate (2.2.2.3), thereby contributing to the increase in resistance. Chloroaluminate is unstable at reduced pH and in sulphate environments and so, as the carbonation front and sulphate ions penetrated the specimen, the chloroaluminate may have decomposed causing a reduction in resistance.

Only a very slight increase in resistance due to sea-water exposure was

observed for the pfa mix (mortar D) specimens. This is a good example of how the resistance data alone represents a lower bound estimation of the decrease in permeability. Figure 5.14 shows that, with ρ_w taken into account, permeability, as represented by FF, is significantly reduced.

It can be seen from graph (b) of each of Figures 5.5 to 5.10 that, for each mix, the increase in resistance due to sea-water exposure is similar for the 25 mm and 45 mm thick specimens. This suggests that, during the test period, the permeability-reducing mechanism is confined to the first 25 mm of specimen thickness.

Grinding off 1 mm from the cast face of the 25 mm thick control specimens resulted in a fall in resistance equivalent to 2 or 3 mm thickness from the bulk of the specimen. However,grinding 1 mm from the cast face of the 25 mm thick *sea-water exposed* specimens generally caused a considerable reduction in resistance (graph (b), Figures 5.6 to 5.10), although in no case was a return to the resistance of the control specimen effected. In order to isolate the further source of increased resistance, further grinding and retesting of *all* the specimens was considered. After some deliberation it was felt to be more appropriate to save these specimens for mercury intrusion porosimetry so that the pore size distributions of the mortar below the surface 1 mm of the control and test specimens could be compared (7.3). Further increments of 1.5 mm were ground from the 2 additional 45 mm thick mortar B specimens. No dramatic reduction in resistance was observed, although the layers removed had higher resistivities than the average for the whole specimen. There also appeared to be a slight gradient, resistivity falling with distance into the specimen. However, the results should be treated with some caution as the changes being monitored were of the same order as the experimental errors inherent in the technique (5.6). It can, nevertheless, be concluded that the permeability-reducing mechanism is a combination of a surface and a more widespread *bulk* effect.

Gjorv *et al.* (1977) observed, on removing 1 mm from the sea-water face, a return to the original resistance prior to sea-water exposure. However, Gjorv *et al.* cured their specimens in water at 40°C for 2 months to eliminate any increase in resistance due to further hydration. Such complete hydration probably rendered the specimens so impermeable that sea-water ions were hardly able to penetrate, thereby permitting only a surface reaction of the type observed.

The solution contained within the pores of the 1 mm thickness removed from a sea-water exposed specimen is likely to be of much lower resistivity than the pore solution within the 1 mm removed from the control specimen, or indeed the pore solution within the bulk of the specimen (ρ_w). Consequently, the protection provided by the surface layer is likely to be underestimated for even the most impermeable of mixes. Table 5.8 shows the *minimum* individual contributions from the surface layer and the bulk effect to the increase in resistance and the apparent increase in thickness of 25 mm thick specimens after 18 weeks of sea-water exposure.

	Minimum increase in resistance (Ω) and Minimum apparent increase in specimen thickness (mm)			
Mix reference	due to surface layer		due to bulk effect	
	Ω	mm	Ω	mm
Mortar B	40	8.5	35	8.0
Mortar C	22	6.6	19	5.7
Mortar D	56	2.4	-40	-1.7
Mortar E	88	5.8	76	5.0
Mortar F	21	6.5	19	5.9

Table 5.8 : Minimum increase in resistance and minimum apparent increase in thickness of 25mm thick specimens after 18 weeks of sea-water exposure.

5.9.2 Test series II

The curves in Figures 5.15, 5.16 and 5.19, showing the increase in resistance and the apparent increase in thickness of specimens due to sea-water exposure, do not necessarily pass through the origin since supposedly similar 28 days old specimens are rarely of identical resistance.

Sodium chloride exposed specimens were originally tested in order to assess their value as alternative control specimens. The dramatic increase in resistance (Figure 5.15) is very surprising it being so great compared with the increase due to continued hydration that the limewater-cured control

specimens are virtually redundant. Consequently graphs (a), (b) and (c) are of almost identical shape.

The reduction in resistance on grinding off 1 mm from the sodium chloride exposed face shows that the phenomenon is almost entirely due to a surface effect. However, examination of the surface of the 45 mm thick sodium chloride exposed specimen showed no sign of a layer of the type observed on sea-water exposed specimens. The discrepancy between the results for 25 and 45 mm thick specimens in graphs (b) and (c) of Figure 5.15 suggests that observations are caused by a rather unpredictable mechanism. The only conceivable mechanism that could produce such results is the formation and subsequent partial decomposition of calcium chloroaluminate, as discussed in relation to the reduction in resistance exhibited by more permeable mixes after 10 or 12 weeks of sea-water exposure (5.9.1). However, no reference to appreciable pore blocking as a result of chloroaluminate formation could be found in the literature. This issue clearly merits further investigation (Chapter 11).

The increase in specimen resistance on exposure to magnesium sulphate solution was to be expected (Figure 5.16) and it is due to the formation of expansive reaction products (2.2.2.2) which have little effect when the test solution is sea-water, due to their increased solubility in the presence of chloride ions. The first reading was taken after the specimens had been in the resistivity cells for only 2 days, but the $MgSO_4$ solution had already had an appreciable effect (Figure 5.16, graphs (b) and (c)). The reduction in resistance on grinding off 1 mm from the $MgSO_4$ solution exposed face shows that the reaction was limited to the surface of the specimen.

Two resistivity cells containing test specimens were kept at 3 ± 1°C in a refrigerator to simulate the lowest likely temperature to be encountered in the North Sea (A2.3). Control specimens were not tested as it was assumed that any increase in control specimen resistance would be negligible due to the lower temperature inhibiting further hydration and leaching of pore solution ions. The increase in resistance due to sea-water exposure was far less than was initially expected (Figure 5.17). Surface examination and analysis of the 45 mm thick specimen (6.3) showed that a surface layer had been formed, but that it was rather porous, contained far less aragonite than the layer formed on an identical specimen exposed to sea-water at 20°C, and was of varying conformation at different locations on the same specimen. These observations

can be explained in terms of the chemical equilibria controlling the precipitation of aragonite (6.4.2.1).

At normal CO_2 concentrations, sea-water is just saturated with respect to aragonite at a temperature of 8°C and a pH of 8.0. Sea-water is buffered against small changes in pH, but under normal laboratory conditions the hydroxyl ions released by cement paste soon cause the pH of a relatively limited volume of sea-water to rise (methods of controlling this rise are discussed in Appendix 3). Rather surprisingly, the pH of the sea-water maintained at 3°C never exceeded 8.10, (it was measured prior to being replaced every four weeks). This was probably due to the decreased rate of leaching of cement paste pore solution ions into the sea-water, due to the lower temperature. Thus, at a temperature of 3°C, the sea-water was probably just on the brink of becoming undersaturated. The refrigerator was only opened when readings were taken and hence the partial pressure of CO_2 above the sea-water would almost certainly have fallen as CO_2 was consumed in producing aragonite. This would cause the sea-water to become undersaturated and hence would halt aragonite precipitation. It is felt that behaviour at a more typical North Sea temperature of say 7 or 10 °C is more likely to correlate with experiments undertaken at room temperature. However, more accurate simulation of offshore conditions is clearly an area that requires further attention (Chapter 11).

Comparison of Figure 5.18 with Figures 5.6, 5.7 and 5.10 shows that pH control did not reduce the increase in resistance due to sea-water exposure and that, in fact, the increase in resistance was more rapid than previously encountered. The drop in resistance on grinding off 1 mm from the sea-water exposed face shows, once again, that the permeability-reducing mechanism is primarily due to a surface effect.

It can be seen, by comparing Figure 5.19 (a) with the control specimens in Figure 5.16 (a), that the cracks only resulted in a drop in resistance of around 10%. Clearly the 2 halves of the broken specimen fitted together too well. The specimens are therefore effectively replicates of the mortar B specimens tested in test series I (Figure 5.6). Comparing these two sets of results shows that the permeability-reducing mechanism was far more effective for the test series II specimens. However, the behaviour of the 45 mm thick sea-water exposed specimen is very similar to that of the mortar B specimen exposed to pH-controlled sea-water. This is a typical example of an observation noted earlier (5.6); test specimen replicates tested concurrently

generally give very similar results, but experiments repeated under apparently identical conditions, but at different times, often produce results showing similar trends, but of a different magnitude. Similar variations were also apparent when studying surface layer development (6.5).

5.9.3 Naturally exposed specimens

The resistances of the deep submersion (Loch Linnhe) specimens before and after grinding the surface 1 mm from the sea-water exposed face are presented in Table 5.9. Sea-water exposure caused an increase in surface resistance of at least 230 Ω for all 3 specimens, despite the scraping and edge damage. This is equivalent to an additonal thickness of 22.5 mm for the least resistive mix. These results follow a very similar pattern to the behaviour of mortars B, C and D (Figures 5.6 to 5.8) in test series I.

The resistances of the various exposure facility specimens before and after the surface 1 mm was ground from the sea-water exposed face are shown in Table 5.10. The bulk specimen resistances (b-c) of the 3 specimens are similar. It is not surprising that the surface layer resistance of the naturally exposed specimen is lower than that of the static tank specimen; the swirling action of the sea would almost certainly have hindered layer formation. The similarity between the surface layer resistances of the specimens within the static and flowing tanks suggests that the flow rate was insufficient to cause significant water disturbance.

The results of examination and analysis of the sea-water exposed surfaces of similarly exposed specimens are presented in 6.7.

Mix reference	Age (years)	Specimen condition	a Specimen thickness (mm)	b Resistance before grinding (Ω)	c Resistance drop due to grinding (Ω)	ac/b-c Apparent thickness of surface layer (mm)
Standard grade concrete	5	surface badly scraped & approx. 7% of edge missing	41.2	865.8	238.7	15.7
Low grade concrete	5	surface scraped & 15% of surface ground away due to coring tube move-ment	41.7	700.4	245.2	22.5
pfa concrete	2½	surface scraped & 5% of surface covered with paint	40.5	3963	315	3.5

Table 5.9 : Resistivity testing of deep submersion (Loch Linnhe) specimen cores.

Exposure facility	a Specimen thickness (mm)	b Resistance before grinding (Ω)	c Resistance drop due to grinding (Ω)	ac/b·c Apparent thickness of surface layer (mm)
Shallow submersion	40.2	590.1	92.8	7.5
Flowing tank	39.7	658.7	157.3	12.5
Static tank	39.6	710.6	175.0	12.9

Table 5.10 : Resistivity testing of cores from standard grade concrete specimens stored in various exposure facilities for 2 years.

5.10 Conclusions

(1) Resistance measurement was found to be a useful method of monitoring changes in the permeability of mortar and concrete specimens. When the test solution (solution A) is sea-water, (or a comparable electrolyte significantly more conductive than limewater), resistance changes relative to a limewater-cured control specimen provide a lower bound indication of any increase in permeability.

(2) Despite practical difficulties in accurately measuring ρ_w of a small volume of a solution prone to carbonation, determination of FF proved useful by highlighting certain features not apparent from the specimen resistance data alone. A good correlation was found between FF and chloride ion diffusion coefficient, for the mortars tested.

(3) All the mixes tested showed a fall in permeability on sea-water exposure. In terms of ohmic resistance, bfs mortar exhibited the greatest reduction. However, the greatest relative change was shown by mortars C and F, 25 mm thick specimens showing an increase in resistance equivalent to over 20 mm of additional thickness after only 10 weeks of sea-water exposure.

(4) The reduction in permeability associated with sea-water exposure is primarily a surface effect, although accompanied by a more widespread bulk effect.

(5) pH control, by regularly dosing with HCl, had little effect on the phenomenon.

(6) Very little change in permeability was observed when the test was conducted in a refrigerator at 3°C. However, this was probably due to a reduced P_{CO_2} within the refrigerator together with the unusually low temperature (for the North Sea) causing the sea-water to be undersaturated with respect to aragonite - a situation not normally encountered offshore.

(7) Naturally exposed concretes developed appreciable surface resistances, although at a slower rate than laboratory exposed specimens, probably due to the swirling action of the sea.

(8) Specimens tested with NaCl solution, rather than sea-water, showed a

dramatic increase and subsequent decline in surface resistance. The only conceivable mechanism that would produce such results is the formation and subsequent partial decompositon of calcium chloroaluminate. Specimens of the more permeable mixes exposed to sea-water showed a reduction in resistance after reaching a peak after 10 or 12 weeks; this behaviour could be due to a similar mechanism.

(9) Specimens tested with $MgSO_4$ solution, rather than sea-water, showed a steady increase in resistance equivalent to around 30 mm of additional thickness after 12 weeks of exposure.

(10) It was frequently observed that test specimen replicates tested concurrently generally give similar results, but that experiments repeated under apparently identical conditions, though at different times, often produce results showing similar trends, but of a different magnitude.

Chapter 6: SURFACE LAYER FORMATION

6.1 Examination/analysis techniques

Resistivity testing (Chapter 5) showed that the permeability-reducing phenomenon exhibited by sea-water exposed concrete is primarily associated with the surface zone to a depth of less than 1 mm. It was therefore necessary to compare the surfaces of test and control specimens in order to determine the mechanism producing this decreased permeability.

Table 6.1 lists the techniques used to examine and analyse the surface of specimens. *Direct* examination of the specimen surface presented few problems. However, the nature of the surface layer could only be determined by examining the surface *in section*. A chip from a specimen, mounted at the appropriate angle, was rarely sufficient to enable detailed examination. A preparation technique was therefore developed, involving resin encapsulation, producing a *polished section* of the surface in section (Appendix 8).

	Technique	Sample	Technique enhanced by
VISUAL	Naked eye	direct: whole specimen in section: whole specimen	staining UV light (6.2)
	Optical microscopy	direct: whole specimen in section: polished section	X-polarised light
	Scanning electron microscopy (SEM)	direct: sample chipped from whole specimen in section: "	
ANALYTICAL	Electron-probe microanalysis (EPMA)	in section: polished section	
	X-ray diffraction analysis (XRDA)	powder	

Table 6.1 : Techniques used for the examination and analysis of surface layers.

X-ray analysis of powdered scrapings from the surface of sea-water exposed specimens often identified aragonite (6.2, 6.3). To allow *in situ* mineral identification (i.e. without the need to remove samples and undertake X-ray analysis) differential staining techniques, generally used by petrologists, were investigated. Differentiation between calcite and aragonite was achieved using Fiegl's solution (Friedman 1959), provided the layers present were reasonably thick. Some difficulty was encountered when the layers were thin, as the pre-stain etching necessary for staining to be effective removes an appreciable thickness of material.

Optical microscopy was undertaken using a Reichert Zetopan reflected light microscope generally at a magnification of 100X. Crossed polarised light often highlighted certain features.

SEM was undertaken using a Jeol JSM 35CF scanning electron microscope at 20 kV.

Electron-probe microanalysis was undertaken using the above scanning electron microscope with Link EDS analysis. This method allows the *analysis* of an extremely small area of sample. A particular wavelength of X-ray bombards the sample so that the material fluoresces. The emitted fluorescent wavelength and intensity are measured and the *elements* identified and quantified. The most appropriate application of the instrument in this context was the production of "digimaps" - maps showing the relative concentration of particular elements over the area of sample being examined.

X-ray diffraction analysis was undertaken using a Philips powder diffractometer with Cobalt K α-radiation. The crystal structure of different minerals causes a monochromatic X-ray beam to be diffracted at different angles. The *mineralogy* of a specimen can therefore be identified by simply measuring the position of the diffracted beam while the amount of each mineral is indicated by the intensity of the diffracted beam at the characteristic "d" spacing of the mineral.

6.2 Diffusion test specimens

At least one specimen from each diffusion test (Table 4.2; "sealed" cells, test references D1-D12; "open" cells, test references D2, D5, D7, D10, D11, D12) was examined.

All the sea-water exposed specimens had a thin surface deposit which was just visible with the naked eye on broken specimens viewed in section. Visibility was enhanced by illuminating the specimen with UV light. Polished sections viewed under the optical microscope showed the presence of a distinct surface layer, varying in thickness from 45 to 175 μm. EPMA showed that the layer was magnesium-rich, although there were often calcium-rich inclusions. XRDA of powdered scrapings taken from samples identified Mg-rich material as brucite ($Mg(OH)_2$), the inclusions being primarily aragonite often with minor quantities of calcite also present. Aragonite and calcite are polymorphs (different crystalline forms) of calcium carbonate (6.4.2.2).

Figures 6.1 (a) and (b) show the layer, after 23 weeks exposure to sea-water, on mortar B (OPC, 0.4 water/cement ratio). As can be seen, the surface of the layer varied from flat to spherulitic. Similar layers were observed on specimens of the other mixes not incorporating replacement materials (mortars C and F). Exposure at reduced temperature (3°C: test reference D9) produced no significant difference in layer formation. Exposure to 0.25M $MgCl_2$ solution, rather than sea-water, resulted in a very similar though slightly thicker (typically 180 μm) layer. The layer was of the same composition, but rather thinner (45-100 μm) on the sea-water exposed pfa mortar. Figure 6.1 (c) shows that there was a distinct aragonite layer beneath the brucite on the sea-water exposed bfs mortar. Figure 6.1 (d) shows how exposure to 0.5 M NaCl solution, rather than sea-water, had no visible effect on the mortar.

Specimens from the "open" cells exhibited very similar, though slightly less developed, layers to the corresponding "sealed" test specimens. This difference in development may be attributed to the exposure period for the "open" test specimens being only 16 weeks, 7 weeks shorter than the "sealed" test series.

Theoretical consideration of factors affecting the development of layers of the

type observed shows that changes in sea-water composition over the exposure period are likely to have influenced the nature of the layer produced.

The 0.5ℓ of sea-water held by the diffusion test cell contains approximately 0.63 g of magnesium ion. If all of this magnesium were available to produce pure brucite (S.G. = 2.39, Deer *et al.* 1965) the resulting layer on the 75 mm diameter exposed surface would be 143 μm thick. Clearly, therefore, availability of magnesium ion played an important part in controlling the thickness of the brucite layer.

A pH of 9.43 is required to precipitate brucite at laboratory temperatures and atmospheric pressure (6.4.3). During the course of the experiment this pH was exceeded in all the cells used (Tables 4.4 and 4.5), primarily due to leaching of alkalis from the cement paste pore solution. A high pH might prevail inside the pores and cracks within cement paste, but, in a true marine environment, the diluting effect of the sea, accelerated by swirling action, is likely to limit the pH of sea-water adjacent to a submerged concrete surface to a figure much nearer to its normal value of around 8.2.

It was therefore felt to be essential that in future tests sea-water composition should be controlled at least to the extent of the magnesium concentration being maintained within 10% of its original value and pH being kept below 9.43 and as little above 8.2 as possible. During resistivity testing sea-water was replaced every four weeks and more continuous pH control was provided in certain tests by dosing with HCℓ (5.7.3). The resistivity test specimen examination and analysis results are therefore likely to be more realistic than the findings described in this section and are therefore reported in greater detail (6.3).

(a)

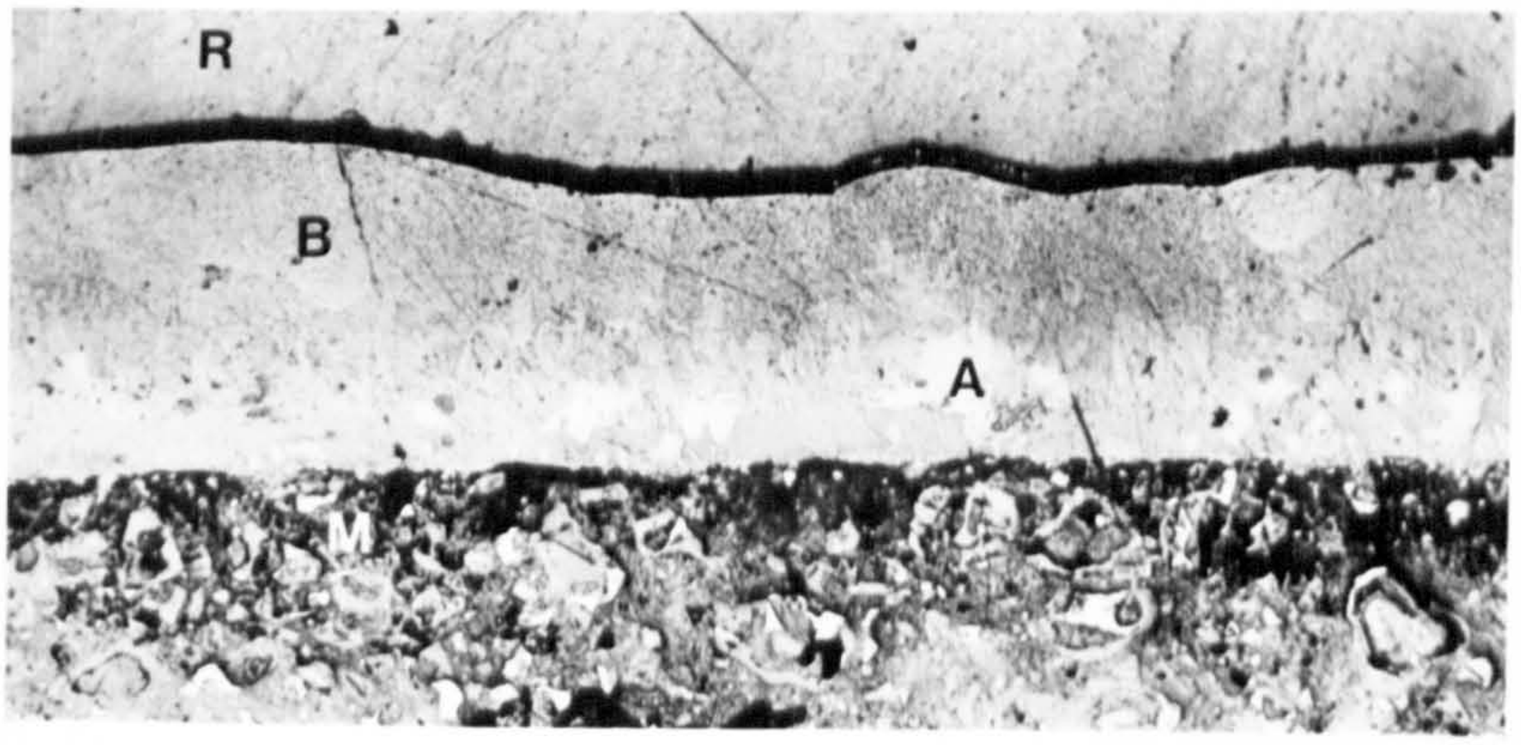

(b)

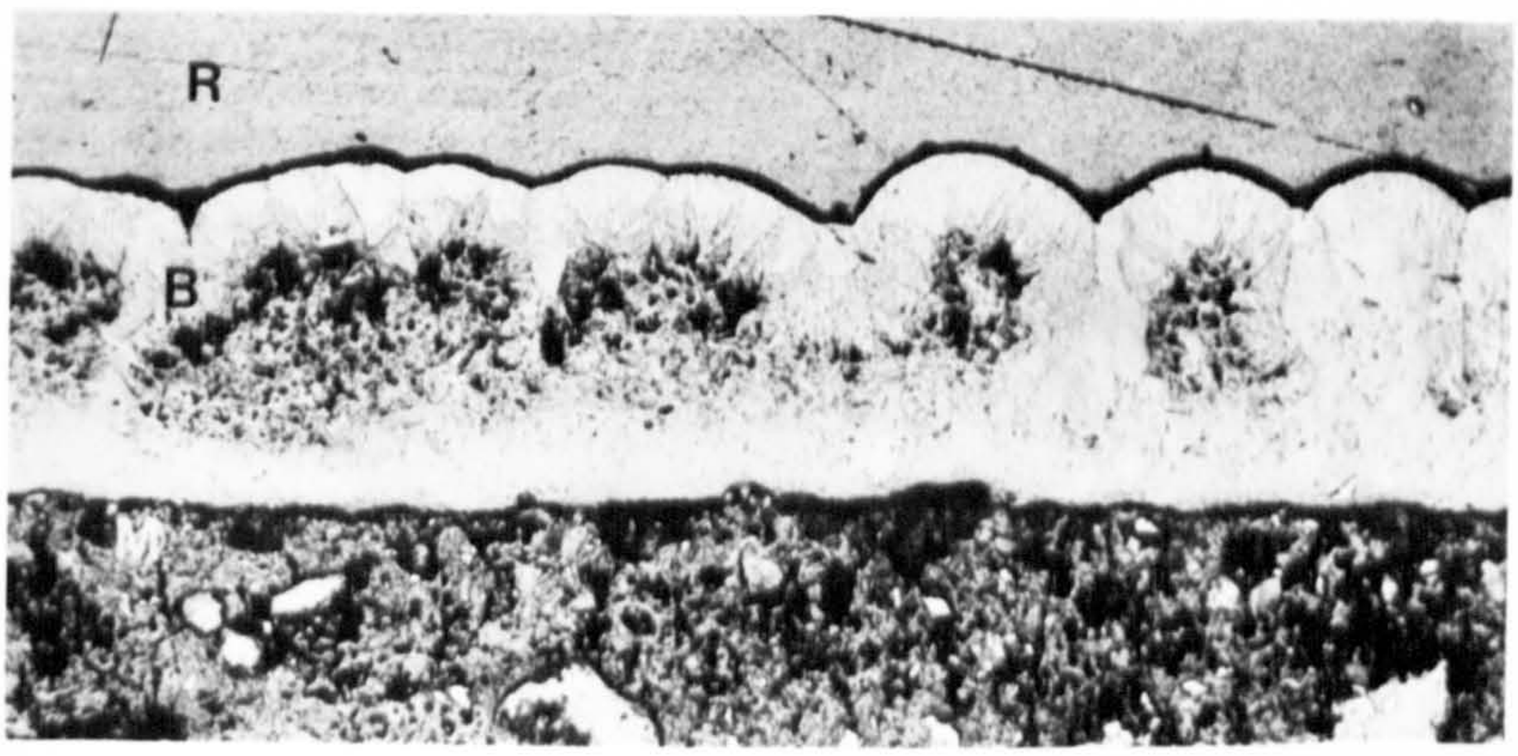

(c)

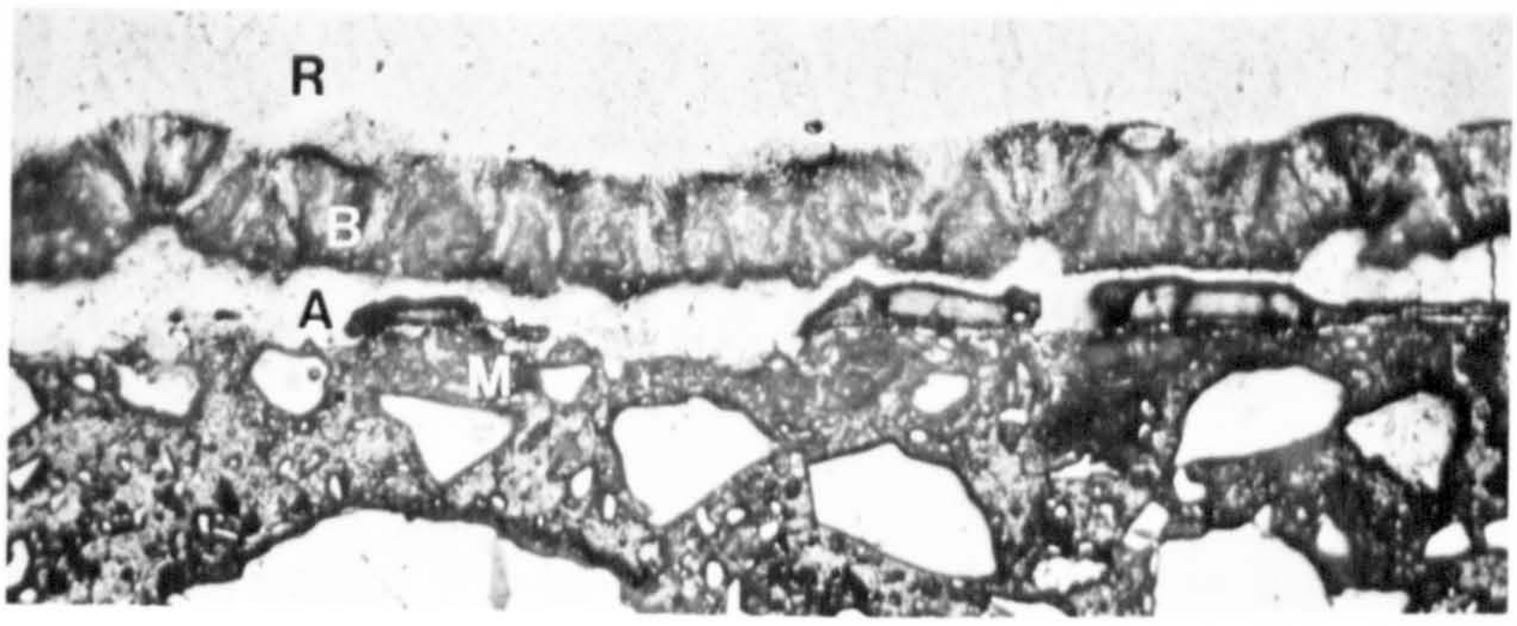

(d)

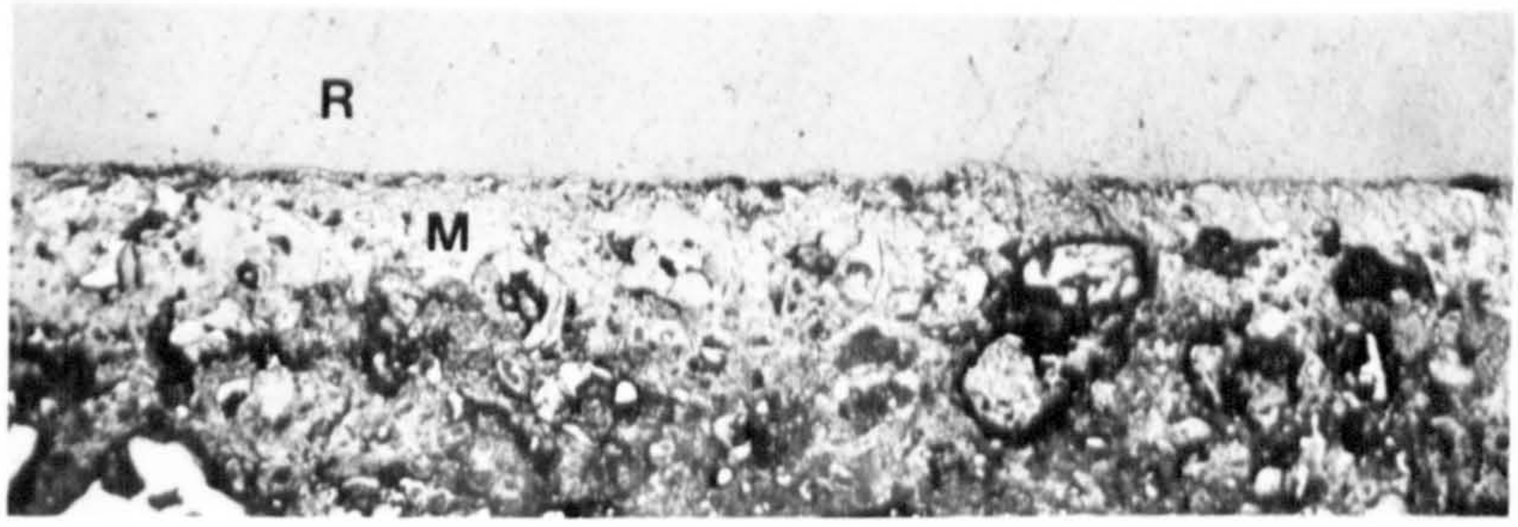

100 μm A = aragonite B = brucite M = mortar R = resin

Figure 6.1 : Sections through surface of diffusion test specimens:
(a) mortar B (0.4 w/c , OPC) after 23 weeks of immersion in sea-water;
(b) ———————————————— ————————————————
(c) mortar E (0.4 w/c , bfs/OPC) ———————— ————————————
(d) mortar B (0.4 w/c , OPC) after 23 weeks of immersion in 0.5M NaCl solution.

6.3 Resistivity test specimens

Resistivity specimens that were not surface ground were used for surface examination and analysis.

Low magnification SEM showed that 18 weeks of sea-water immersion resulted in a generally continuous spherulitic formation on the exposed face. Figure 6.2 compares the surfaces of sea-water and limewater conditioned specimens of mortar F. The thickness and precise form of the layer varied between mixes and even between different locations on the same specimen, but Figure 6.3 shows a typical example of what was observed. Clearly, the layer consists of two distinct components. EPMA showed the upper and lower layers to be Ca and Mg rich respectively. As with the formation on the diffusion specimens, XRDA showed the Ca-rich layer to be aragonite, often with traces of calcite and the Mg-rich layer to be brucite. The aragonite layer was typically 150 μm thick and the brucite layer 25 μm thick. EPMA showed that for the more permeable mixes (particularly mortars C & F) the brucite layer also penetrated the cement paste pores by up to 10 μm. The respective layers were significantly thinner and more variable on mortar D, a total layer thckness of 120 μm being typical. The aragonite spherulites on mortar F reached heights of over 300 μm. Closer examination (see Figure 6.4) showed that large aragonite spherulites had rather porous cores and that the underlying brucite was locally much thinner; this suggests very rapid nucleation and early growth. Figure 6.5 shows aragonite "urchins" at the base of a spherulite.

The layer formed on the surface of mortar E was rather different. The overall thickness was very variable, ranging between 25 and 150 μm and brucite was present not as a distinct layer, but finely dispersed within the aragonite (Figure 6.6). Brucite was also detected within the cement paste pores to depths of at least 60 μm.

Figure 6.7 shows the layer formed on concrete A after 33 weeks of sea-water exposure. The layers shown are very different despite the samples originating from locations only 5 mm apart on the same specimen. In places there appears to be a distinct third layer capping the aragonite spherulites, but this is simply due to the outer layer of aragonite being more dense, probably due to being precipitated more slowly.

12 weeks immersion in 0.5M NaCl solution resulted in a 10 to 50 μm thick

surface layer of calcite crystals. It would seem extremely unlikely that this very light deposit was solely responsible for the very large surface resistance exhibited during resistivity testing (5.8.2). However, no distinct chloride-rich layer, that might be associated with chloroaluminate formation, could be identified within the surface 2 mm of the specimen.

12 weeks immersion in 2.2 g/ℓ $MgSO_4$ solution resulted in a coating of crystalline aragonite, approximately 45 μm thick, on the specimen surface. This layer was extremely fragile and it proved difficult to obtain a polished section without causing partial disruption. The absence of a surface layer of brucite corresponds with the work of Baikov (reported by Biczok 1967 pp. 222-3) who observed only a loose and permeable skin of $Mg(OH)_2$ at 10 times the concentration of $MgSO_4$ used here. The reduction in permeability associated with the surface 1 mm (5.8.2) is almost certainly due to pore blocking by reaction products such as ettringite, gypsum and brucite (2.2.2.2). EPMA showed the presence of sulphur and magnesium at depths of at least 2 mm into the specimen, but did not isolate any *particularly* S-rich or Mg-rich layer within the surface 1 mm.

The layer on the specimen (mortar B) stored at 3°C was 50 to 75 μm thick, consisting largely of brucite but with discrete aragonite inclusions.

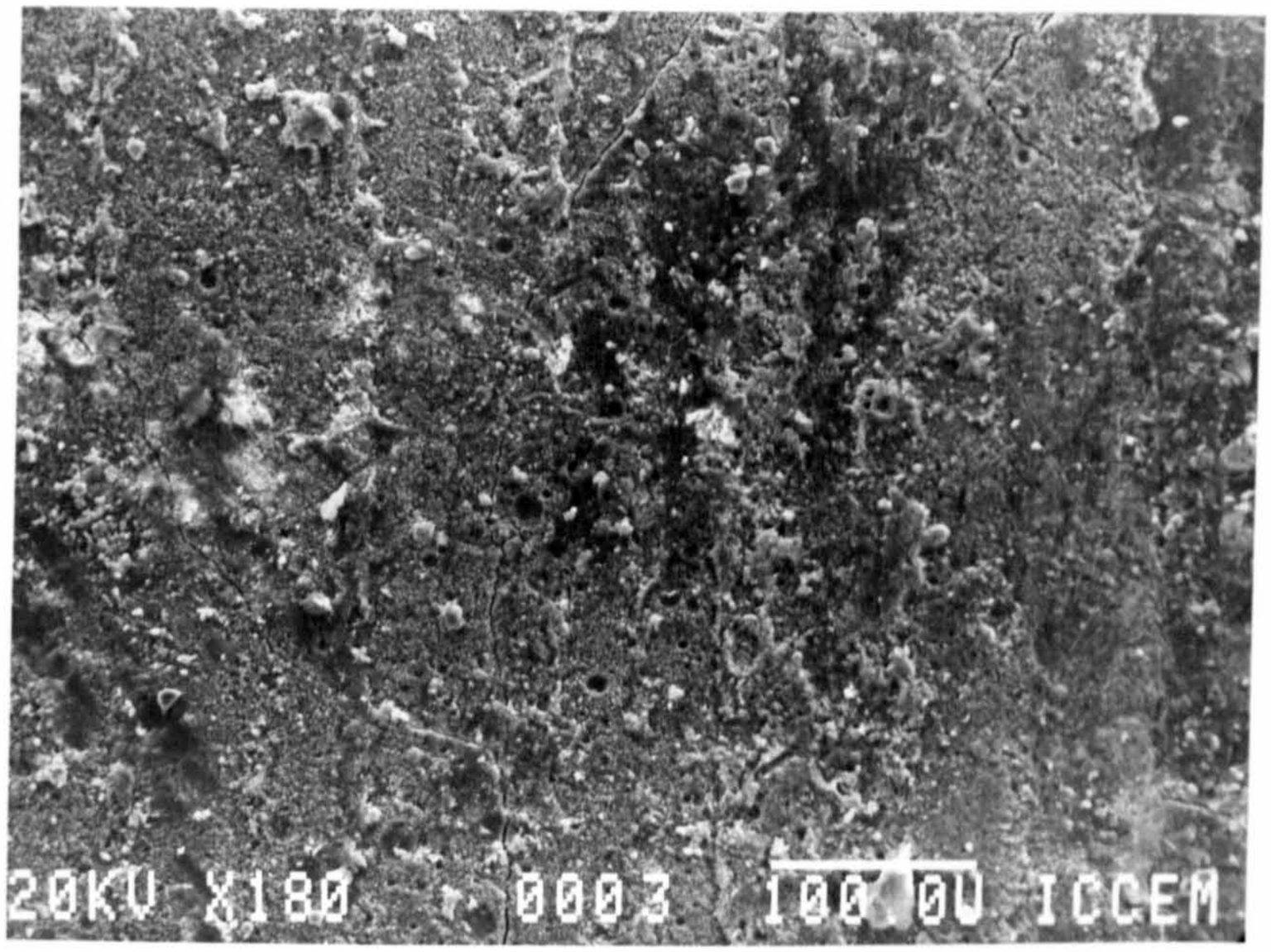

(a) Cured in limewater.

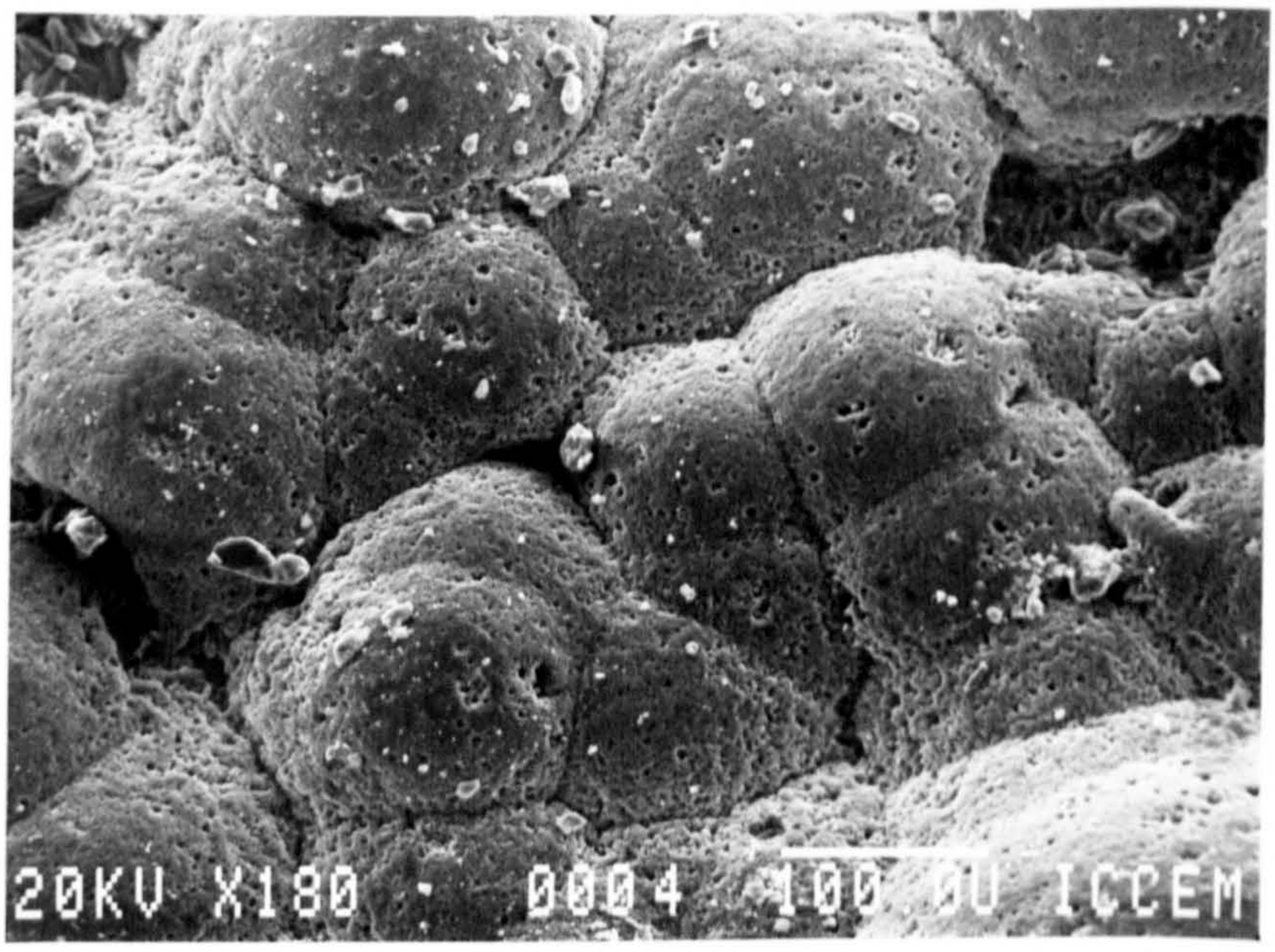

(b) Exposed to sea-water for 18 weeks.

Figure 6.2 : Scanning electron-micrographs of the surface of mortar F (0.4 w/c , SRPC).

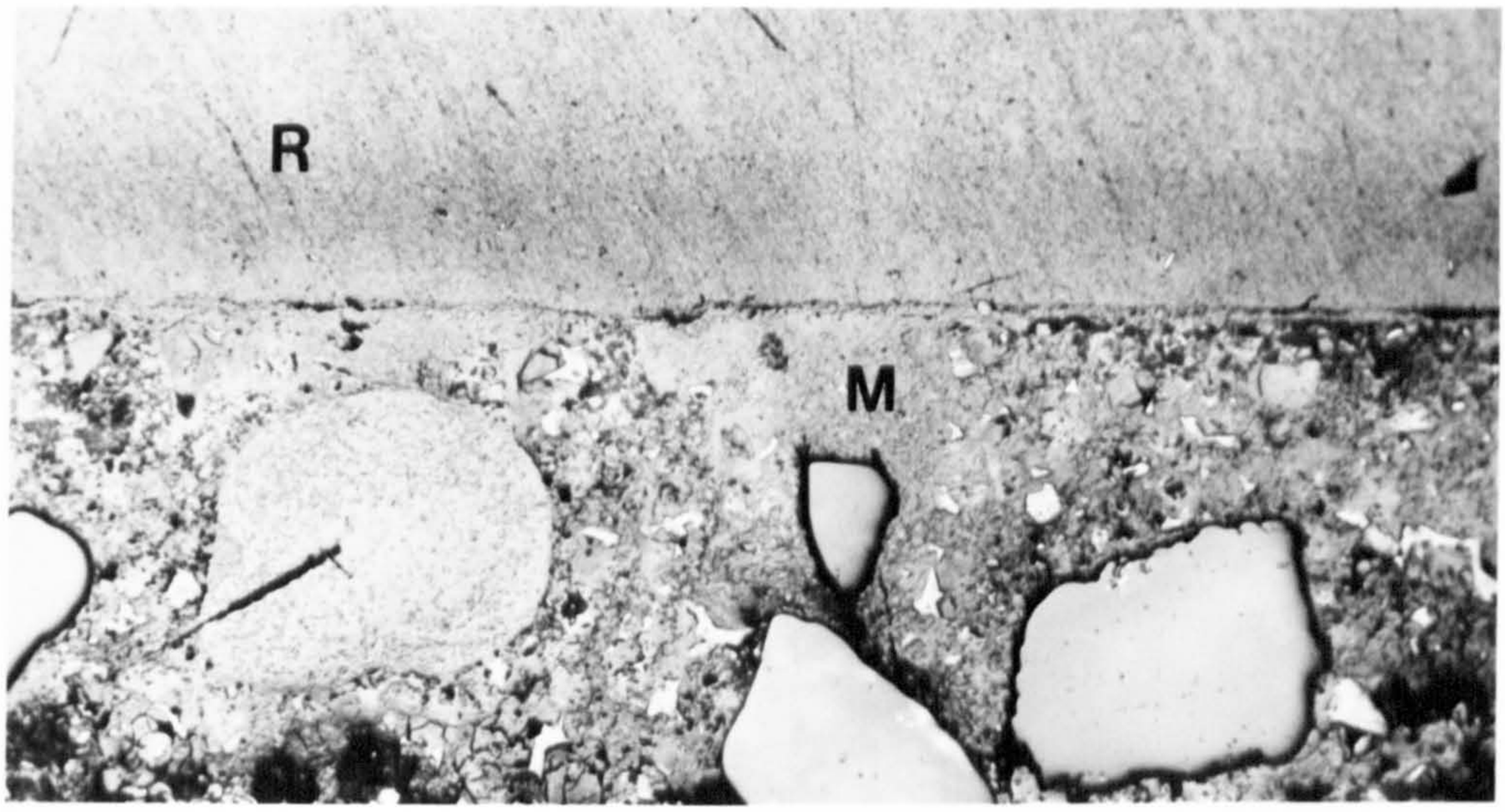

(a) Cured in limewater.

100 μm

A = aragonite
B = brucite
M = mortar
R = resin

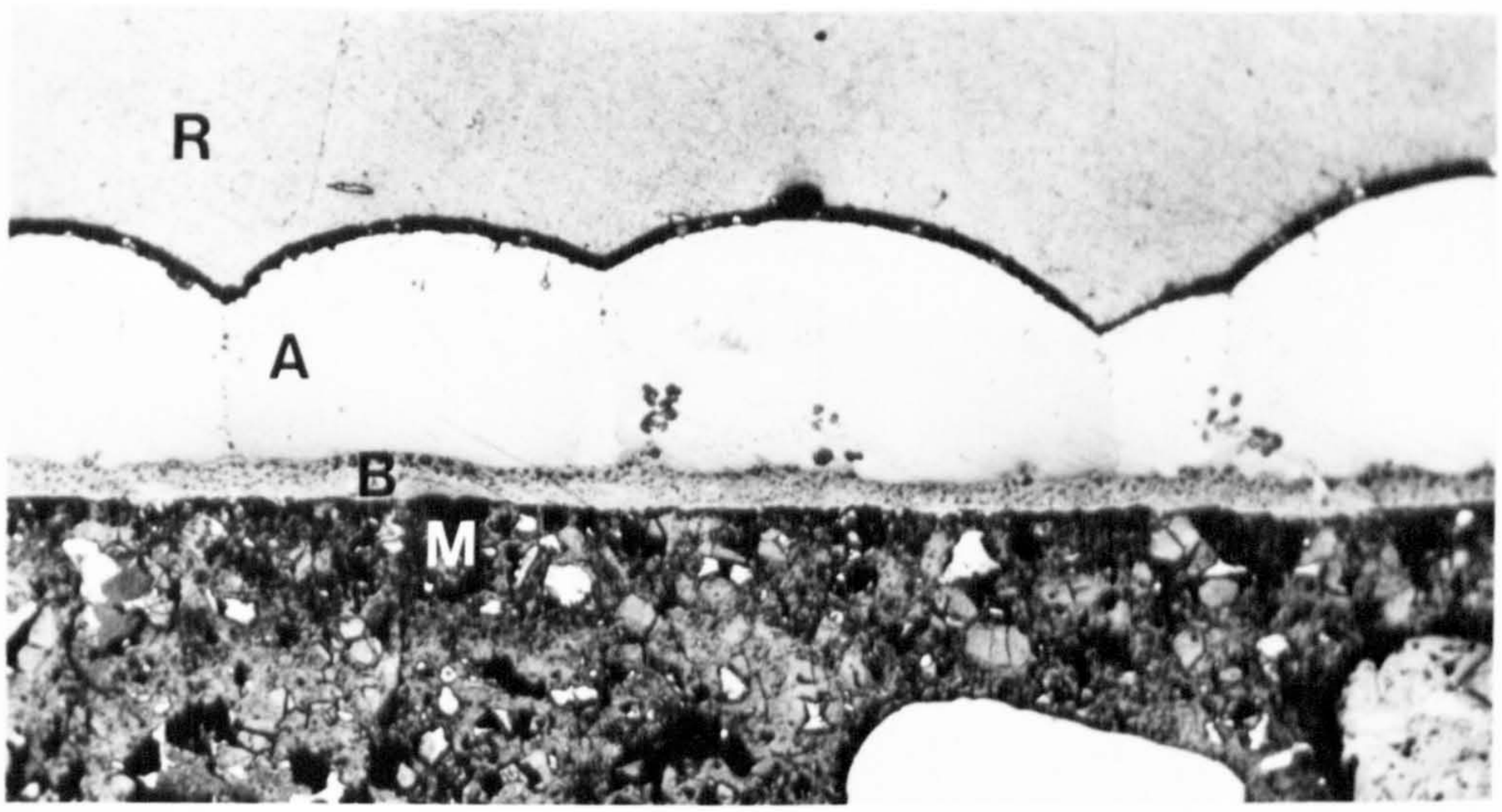

(b) Exposed to sea-water for 18 weeks.

Figure 6.3 : Sections through surface of mortar C (0.6 w/c , OPC).

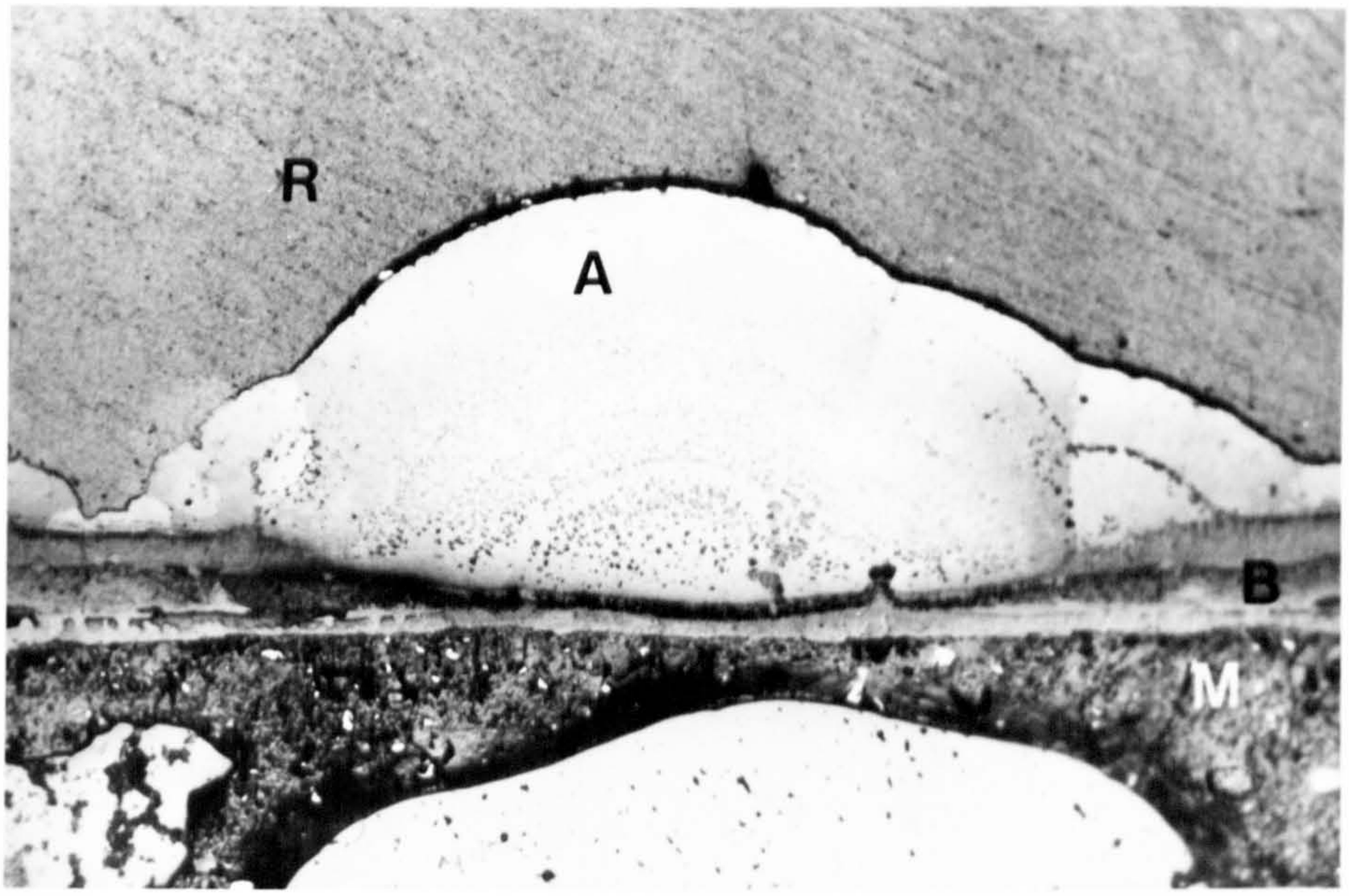

100 μm

A = aragonite M = mortar

B = brucite R = resin

Figure 6.4 : Section through large aragonite spherulite on the surface of mortar F (0.4 w/c , SRPC).

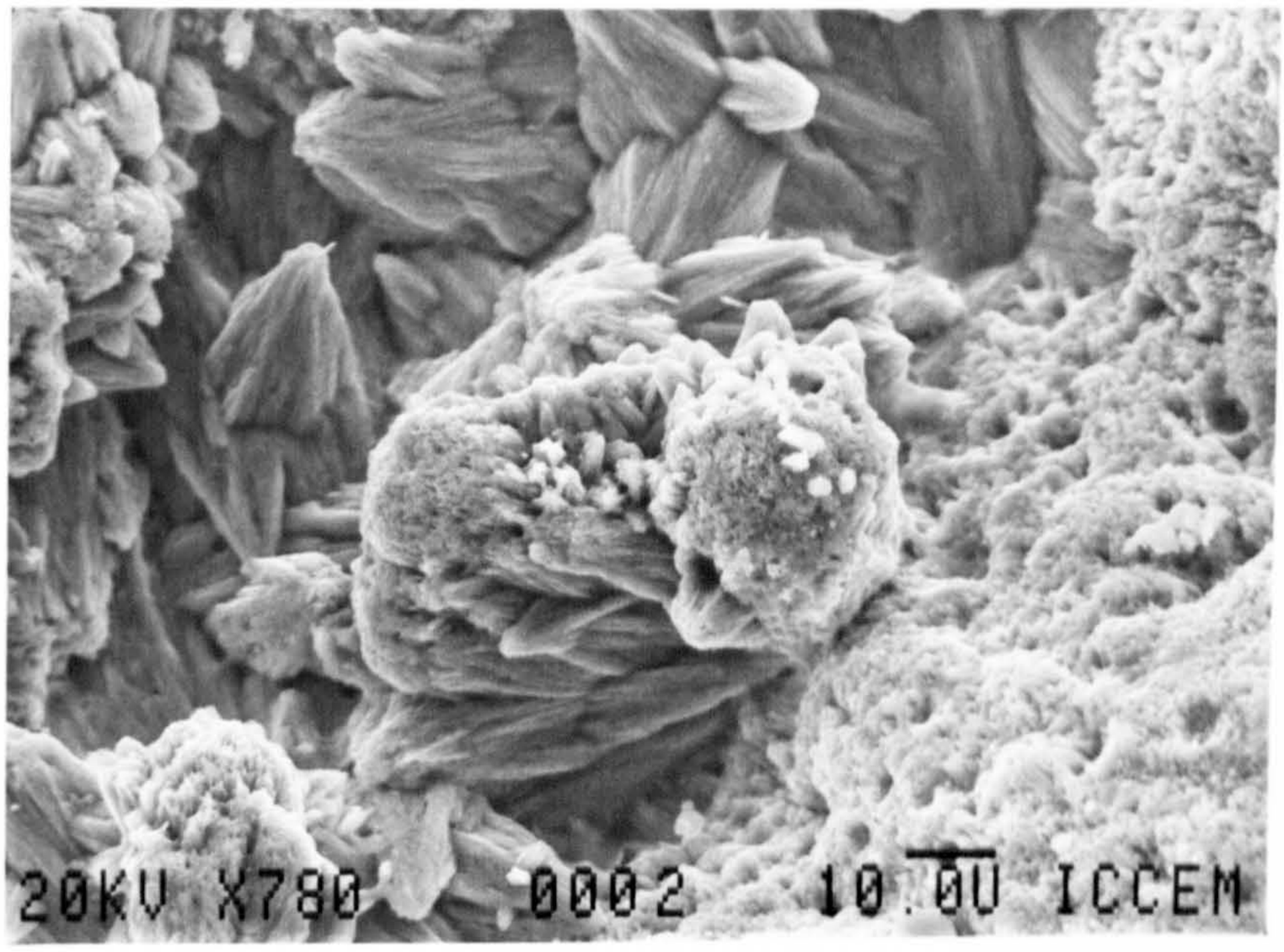

Figure 6.5 : Aragonite "urchins" at the base of a spherulite on the surface of mortar F (0.4 w/c , OPC) after 23 weeks of immersion in sea-water.

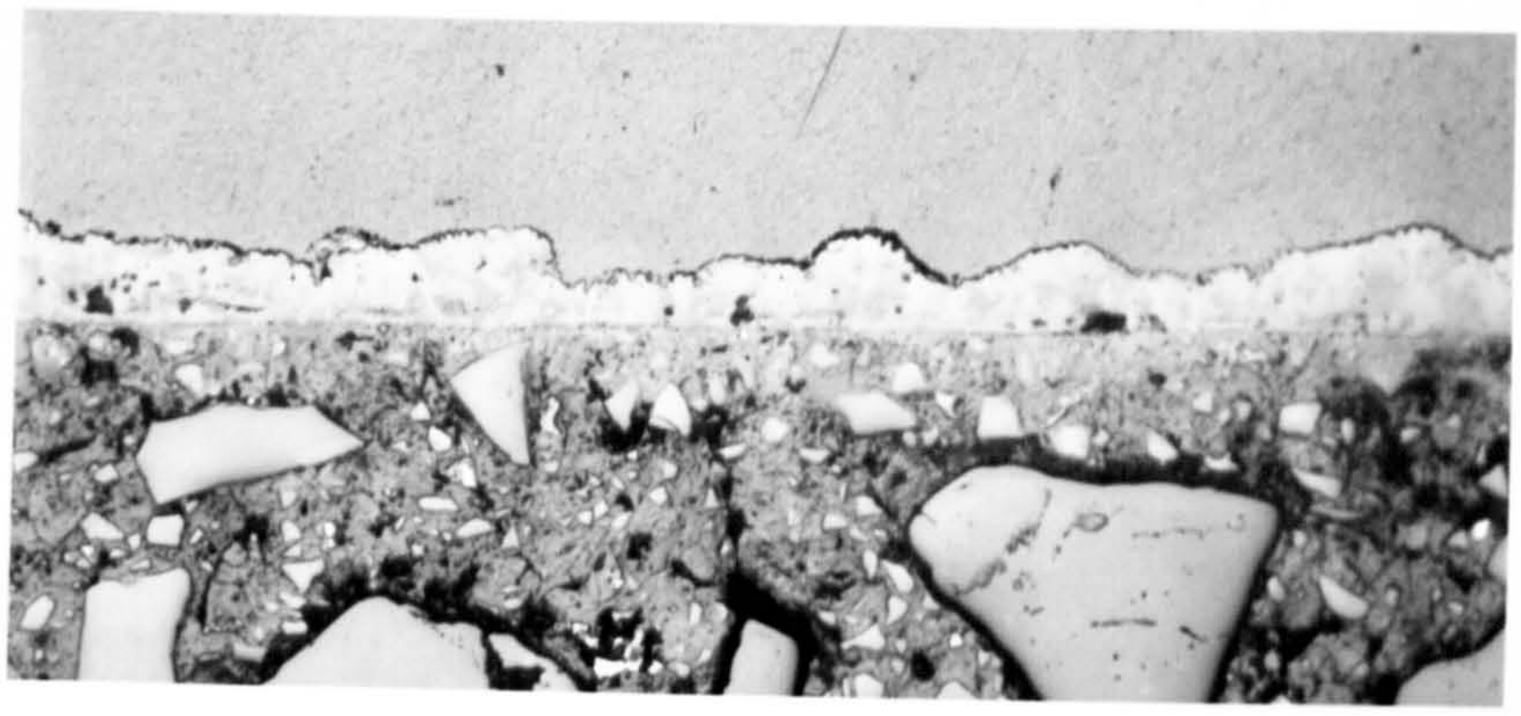

Figure 6.6 : Surface of mortar E (0.4 w/c , bfs/OPC) after 23 weeks of immersion in sea-water.

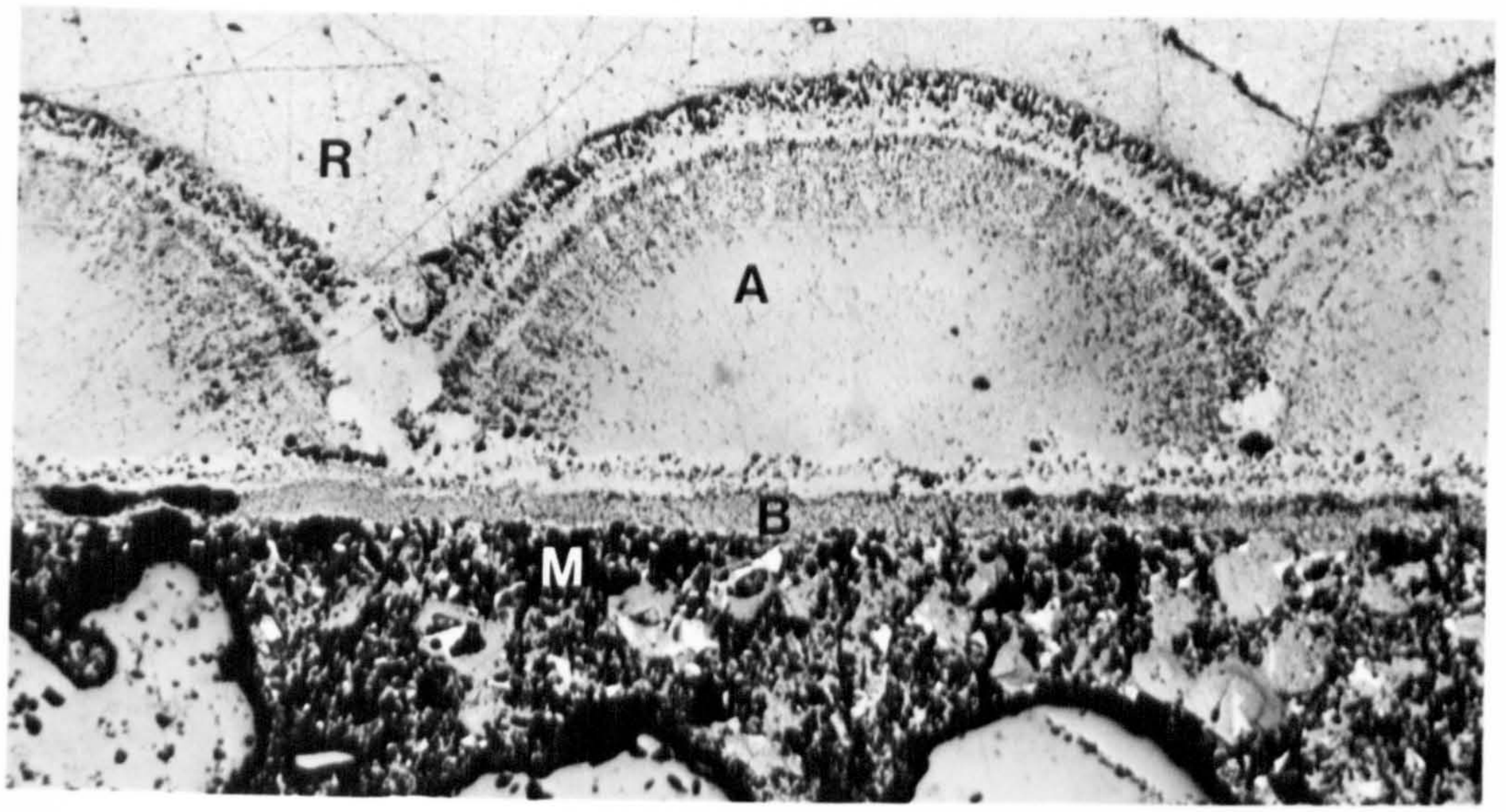

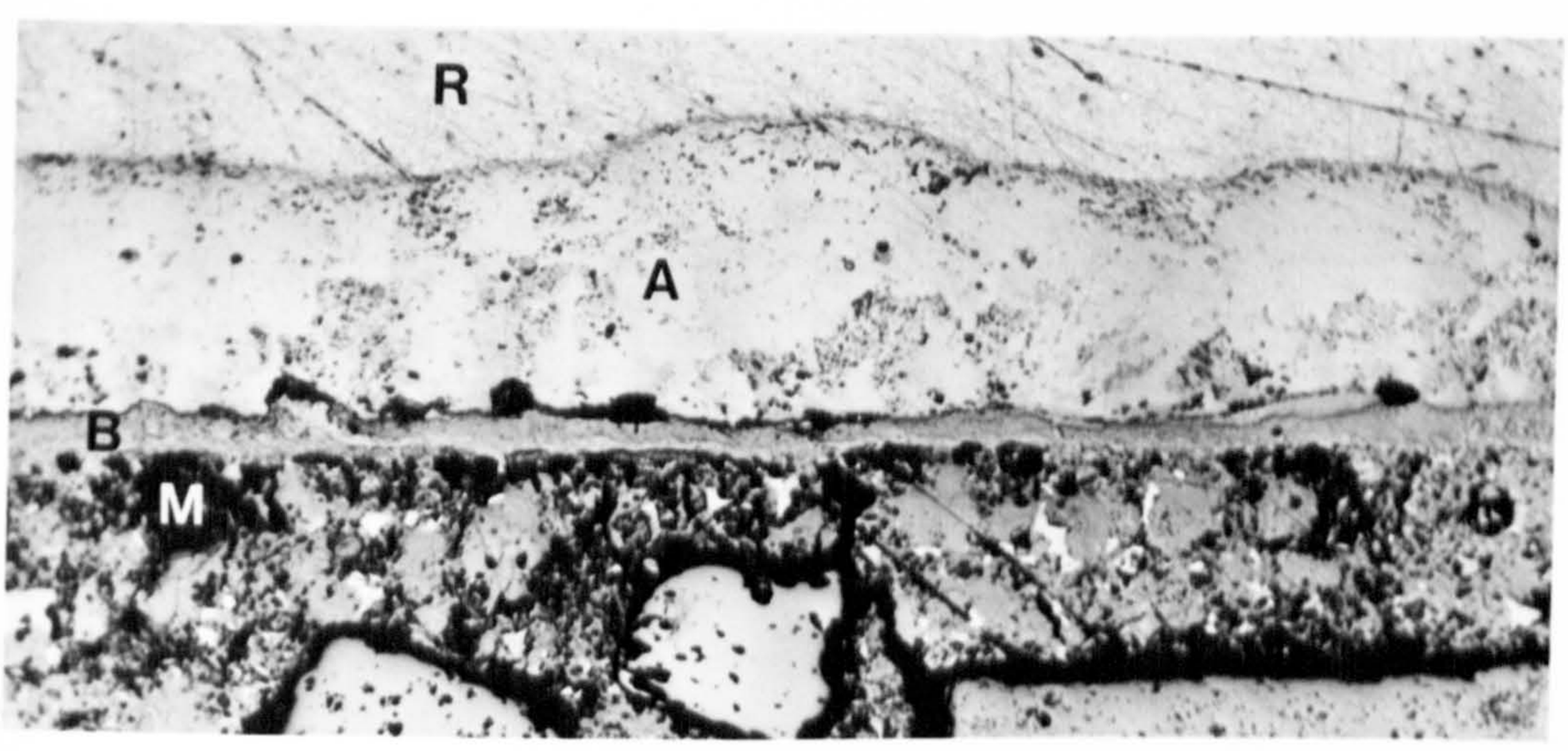

100 μm

A = aragonite
B = brucite
M = mortar
R = resin

Figure 6.7 : Sections through surface of concrete A (0.4 w/c OPC) after 33 weeks of immersion in sea-water.

6.4 Theoretical aspects of the development and stability of surface layers on concrete exposed to sea-water

6.4.1 Introduction

In very simple terms, calcium carbonate is precipitated due to saturation of the solution at the concrete/sea-water interface with calcium carbonate, and brucite is formed as a product of the reaction of magnesium salts present in sea-water with cement paste. However, an understanding of the factors affecting the development and stability of surface layers is necessary for the following:

(1) to allow laboratory experiments simuulating marine conditions in the most criticial areas to be designed. For example; must pH be accurately controlled?; are laboratory temperatures suitable or should all experiments be carried out at 8°C?; do pressure effects need to be considered?

(2) to allow prediction of likely layer formation under different conditions from those studied experimentally. For example, would denser layers be expected in the Persian Gulf where the sea-water salinity and temperature are higher than in the North Sea?

(3) so that specimens can be prepared and handled without the possibility of modification of the mineral layers.

(4) to enable methods of enhancing the formation to be developed.

The chemistry of precipitation in an environment as complex as that produced by the interaction of sea-water and cement paste pore solution is extremely formidable. The precipitation of calcium carbonate from sea-water is a subject of fundamental interest to geochemists, and intensive field and laboratory studies undertaken since 1960 have succeeded in resolving some of the major uncertainties (Blatt *et al*. 1980). Precipitation of brucite from sea-water is not a natural phenomenon and hence little could be found on the subject in the literature.

The main principle applied is that, for precipitation of a mineral to be possible, the aqueous solution in question must be supersaturated with respect to that particular mineral; i.e. the ion activity product (IAP) must exceed the solubility product (K_{SP}). The degree of saturation ($IAP/K_{SP} = S$) is probably the most important parameter governing the likelihood of precipitation. (Appendix 9 provides definitions of chemical terms).

6.4.2 Calcium carbonate

6.4.2.1 Carbonate equilibria

To understand the processes that culminate in the production of a carbonate layer on the surface of sea-water exposed concrete, the conditions in which crystals of calcium carbonate grow or are dissolved in aqueous solution must be studied. Unfortunately the combination of cement paste pore solution and sea-water provides an exceptionally complex environment to unravel. Initially therefore, consideration is restricted to the simplest possible system, CO_2-H_2O-$CaCO_3$.

The solubility of $CaCO_3$ in pure CO_2 free water is slight, about 14.3 mg/ℓ for calcite and 15.3 mg/ℓ for aragonite (Pobeguin 1954) in the pressure-temperature range of the surface of the sea. With the addition of CO_2 to the water, solubilities can reach hundreds of mg/ℓ. The solubility product $[Ca^{2+}],[CO_3^{2-}]$ increases with rising partial pressure of CO_2, decreasing temperature and increasing salinity (Deer *et al.* 1965).

The sequence of equations and corresponding eqilibrium constants (at 25°C and 1 atmosphere total pressure) in the H_2O-CO_2-CaO system are as follows:

$$H_2O + CO_2 \rightleftharpoons H_2CO_3 \qquad (1)$$

$$K = \frac{[H_2CO_3]}{[H_2O][CO_2]} = 10^{-1.47}$$

$$H_2CO_3 \rightleftharpoons H^+ + HCO_3^- \qquad (2)$$

$$K_1 = \frac{[H^+][HCO_3^-]}{[H_2CO_3]} = 10^{-6.35}$$

$$HCO_3^- \rightleftharpoons H^+ + CO_3^{2-} \qquad (3)$$

$$K_2 = \frac{[H^+][CO_3^{2-}]}{[HCO_3^-]} = 10^{-10.33}$$

Reactions (2) & (3) are very rapid. Reaction (1) is relatively slow but is followed by the instantaneous reaction

$$H_2CO_3 + OH^- \rightleftharpoons HCO_3^- + H_2O \qquad (4)$$

If the pH were to exceed 9, two other reactions would become important:

$$CO_2 + OH^- \rightleftharpoons HCO_3^- \qquad (5)$$

$$HCO_3^- + OH^- \rightleftharpoons CO_3^{2-} + H_2O \qquad (6)$$

Reaction (5) is slow, whereas (6) is instantaneous and raises the CO_3^{2-} content of the water.

The equilibrium constants associated with reactions (1)-(3) can be used to determine both the "total CO_2" in solution at any pH and the proportion of the total CO_2 represented by each molecular or ionic species.

$$KK_1K_2 = \frac{[H_2CO_3][H^+][HCO_3^-][H^+][CO_3^{2-}]}{[H_2O]P_{CO2}[H_2CO_3][HCO_3^-]}$$

Therefore

$$[CO_3^{2-}] = \frac{KK_1K_2P_{CO2}}{[H^+]^2}$$

(P_{CO2} is the partial pressure of carbon dioxide in water in equilibrium with the atmosphere, $10^{-3.5}$)

Also,

$$KK_1 = \frac{[H_2CO_3][H^+][HCO_3^-]}{[H_2O]P_{CO2}[H_2CO_3]}$$

Consequently,

$$[HCO_3^-] = \frac{KK_1P_{CO2}}{[H^+]}$$

Moreover,

$$KK_2 = \frac{[H_2CO_3][H^+][CO_3^{2-}]}{[H_2O]P_{CO2}[HCO_3^-]}$$

Therefore,

$$[H_2CO_3] = \frac{KK_2P_{CO2}[HCO_3^-]}{[H^+][CO_3^{2-}]} \cdot$$

Figure 6.8 shows the percentage of the total inorganic carbon represented by each of the carbon species plotted as a function of pH. The equilibrium constants decrease with increasing ionic strength, shifting the curves to the left as salinity increases. Clearly bicarbonate ion, HCO_3^-, is the most abundant species in the pH range of sea-water. The carbonate ion concentration is inversely proportional to the square of the hydrogen ion concentration and hence increases rapidly as pH increases.

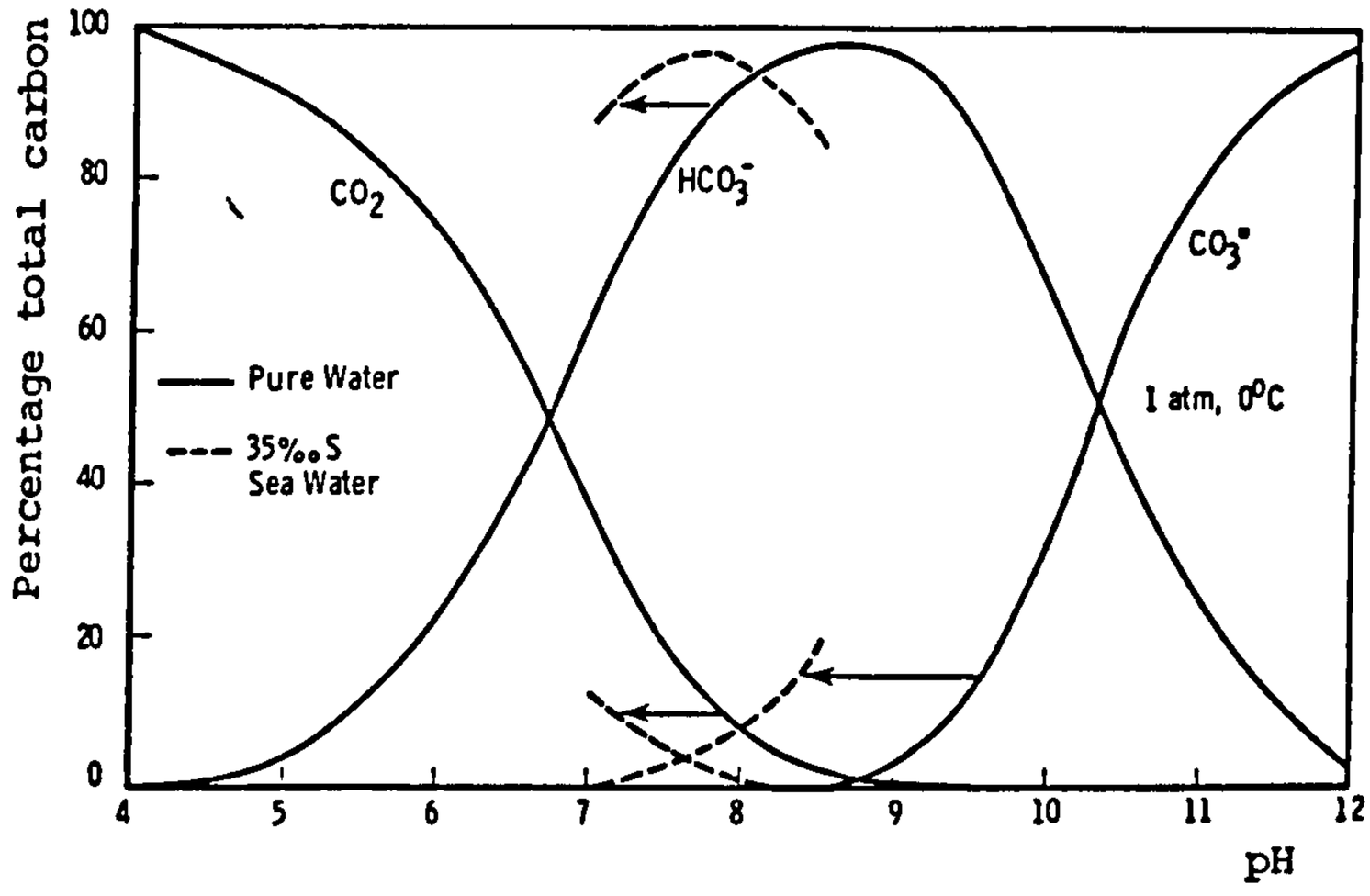

Figure 6.8: Dissolved carbon species as a function of pH (Horne 1969).

For each mole of water and newly dissolved CO_2 that react, a certain amount of H^+ and HCO_3^- is yielded, but a considerable portion forms undissociated H_2CO_3. In addition some of the CO_2 is held in CO_3^{2-}. Consequently, the addition of n moles of CO_2, instead of releasing 2n moles of H^+ in reaction (2), actually frees a much smaller quantity. Similarly an external source of OH^- (e.g. cement paste pore solution) results in a smaller increase in pH than might have been expected. In this way the system is *buffered*.

Most of the oceans are not at 25°C and 1 atmosphere total pressure. Berner (1971) presents a model (Appendix 4) that allows calculation of the IAP of (a) $CaCO_3$ in sea-water at varying temperature, pressure and pH and (b) $K_{calcite}$ at varying temperature and pressure, it being assumed to be independent of pH. Typical values for the pH of sea-water are discussed in A2.1.

Figure 6.9 shows the variation of IAP with pH at 8°C, 25°C and at a pressure equivalent to 2000 m ocean depth. The values at higher pH values are shown dotted since the asymptotic approach to an upper bound value disagrees with the theory presented earlier and is almost certainly a result of extrapolation to pH values beyond the range on which the model was based. It should, however, be noted that at higher pH values the degree of saturation is sufficiently high for its precise value to be of little significance.

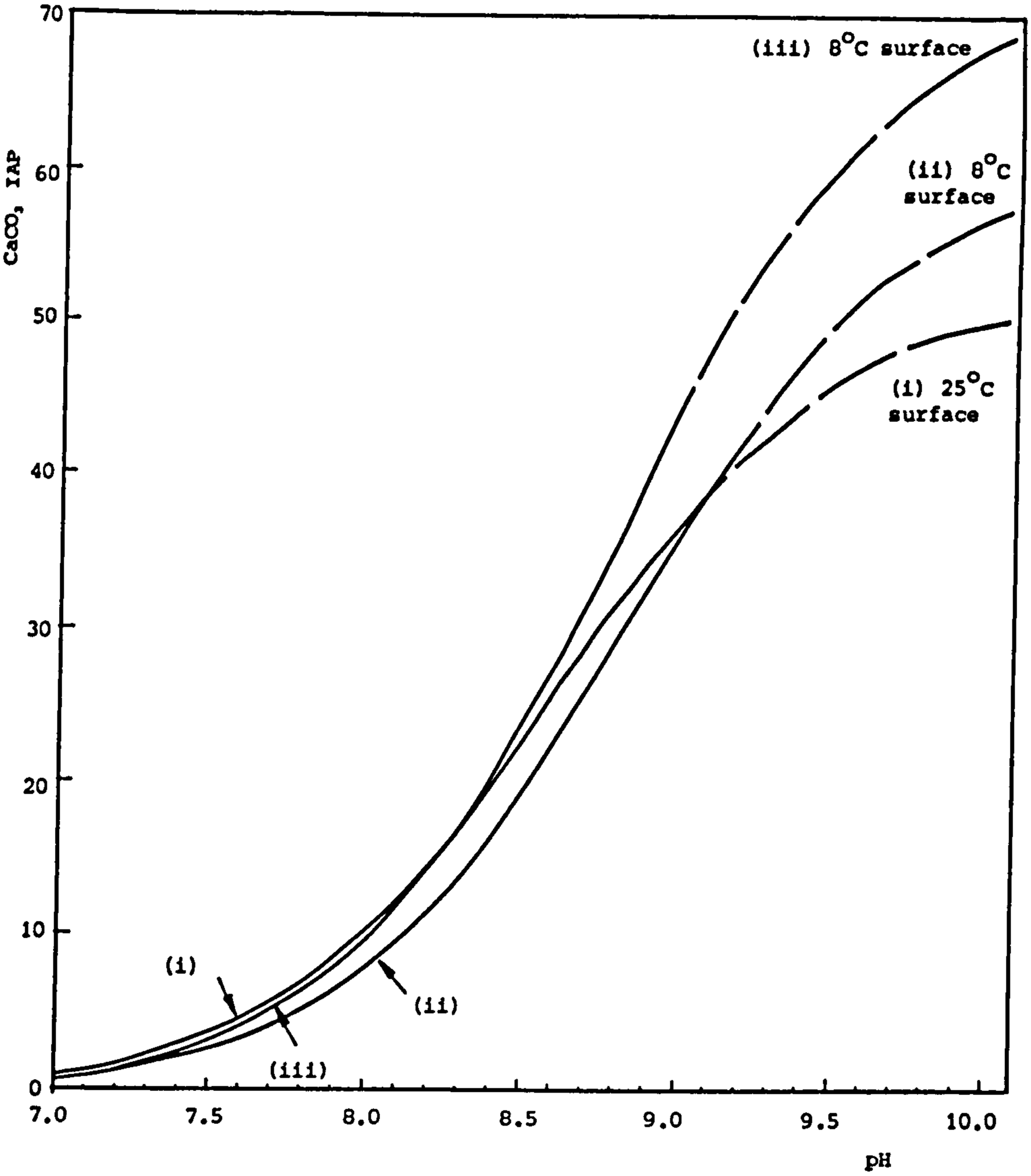

Figure 6.9: Variation of $CaCO_3$ IAP in sea-water with pH (based on Berner (1971) model - Appendix 4).

Figure 6.10 presents the degree of saturation of sea-water with respect to aragonite for the same variables considered in Figure 6.9. It has been assumed that over the range of pressure and temperature encountered in this context, the ratio $K_{aragonite}/K_{calcite}$ is constant. Although the IAP is dependent on pressure, $K_{aragonite}$ is similarly dependent and hence, pressure changes have little effect on the degree of saturation. However, the situation is further complicated by the fact that, due to biological CO_2 production, pH also tends to vary with depth. Figure 6.11 shows the degree of saturation with respect to calcite and aragonite as a function of depth in the Atlantic and Pacific Oceans; unfortunately, there is very little similar data relating to the North Sea, primarily due to the limited geological interest of North Sea

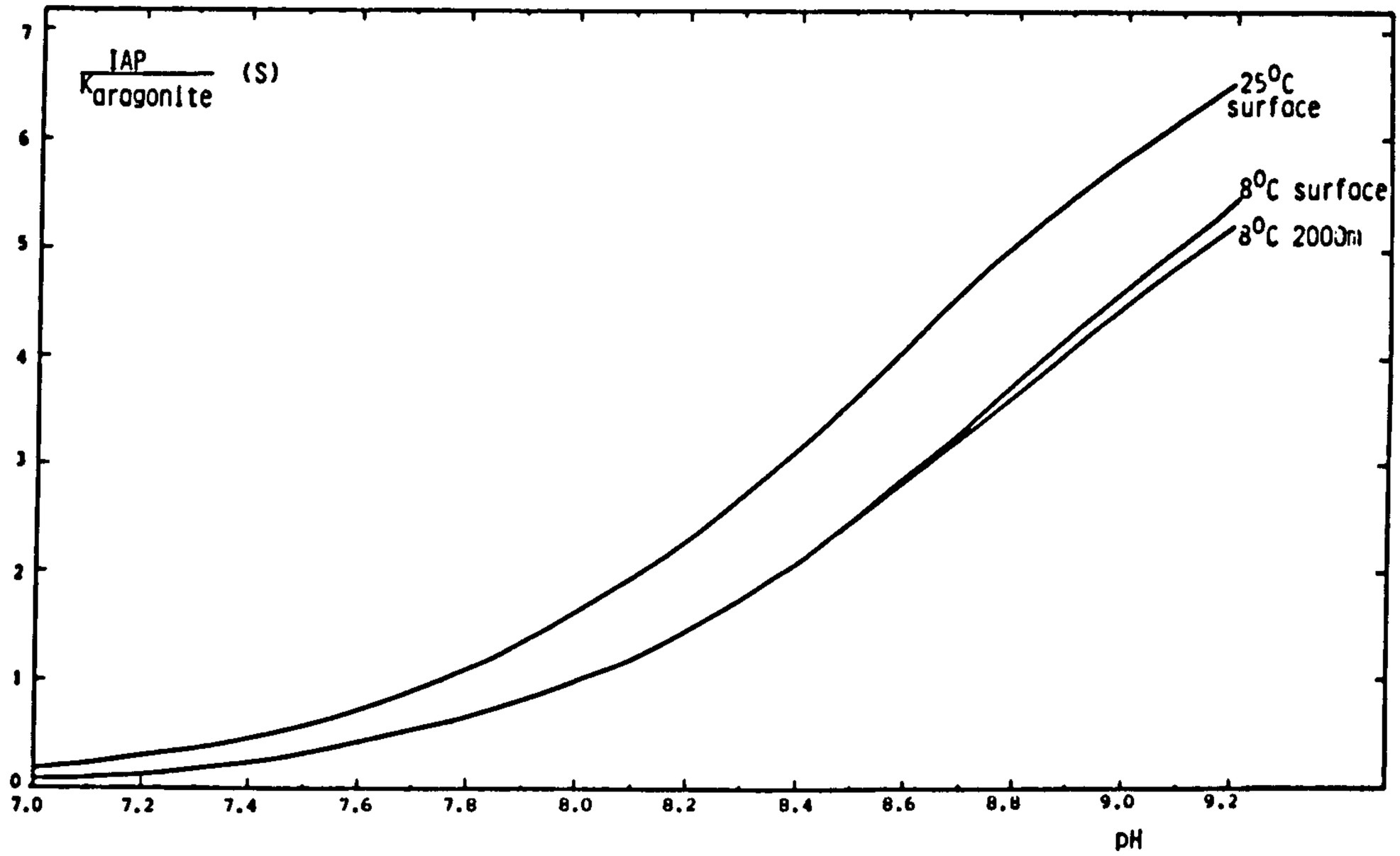

Figure 6.10: Variation of degree of saturation of sea-water with respect to aragonite, with pH (based on Berner (1971) model - see Appendix 4).

sea-water composition. The surface water of the ocean is highly supersaturated with respect to both calcite and aragonite. This degree of saturation reduces with depth, becoming undersaturated with respect to aragonite, in the range of 200-400 metres in the Pacific and at around 2000 metres in the Atlantic.

Up to now in this discussion, sea-water has been considered in isolation. The situation is far more complex at the surface of sea-water exposed concrete and particularly so within cracks or pores. The presence of cement paste pore solution ions causes a local increase in pH and Ca^{2+} ion concentration, thereby increasing the $CaCO_3$ IAP. Furthermore, the percentage of free ions changes and the number and complexity of ion pairs increases; species such at $Na_2CO_3^{\circ}$, $K_2HCO_3^{+}$ and $Ca(SO_4)_2^{2-}$ may be formed.

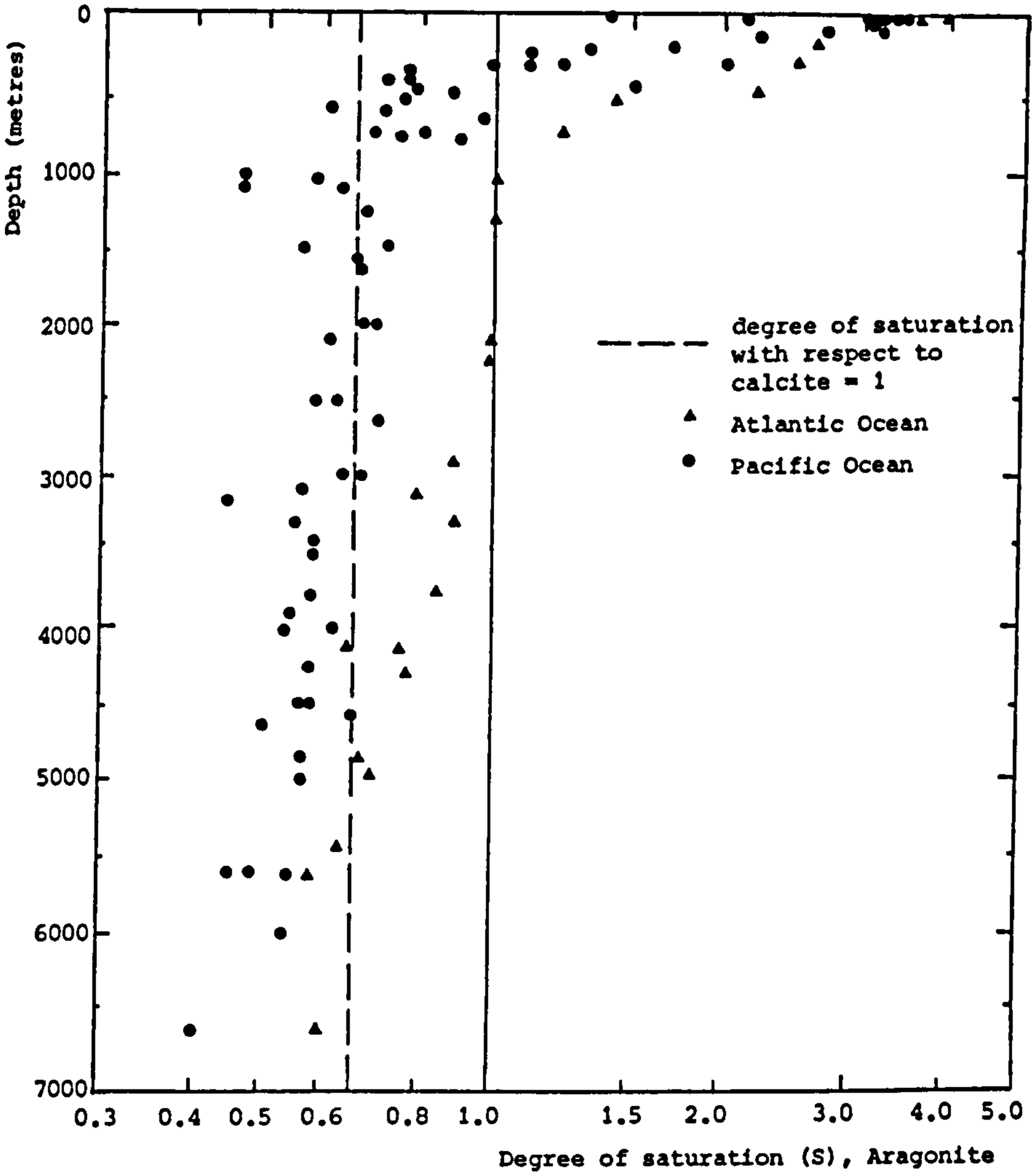

Figure 6.11: The degree of saturation with respect to aragonite as a function of depth in the Atlantic and Pacific Oceans (Broecker 1974).

The interaction of pore solution and sea-water makes it impossible to do more than generalise about the detailed chemistry of $CaCO_3$ precipitation. However, the following general conclusions can be drawn relating to the degree of saturation (S) of sea-water with respect to aragonite:

(1) S increases with temperature; at pH 8 and 8°C, S ≃ 1;
(2) the range of pressures likely to be encountered by an offshore structure have very little effect on S;
(3) S increases dramatically with pH;
(4) S increases with P_{CO_2};
(5) S > 1 for at least the first few hundred metres depth of normal sea-water.

Hence, the only circumstances under which concrete might come into contact with sea-water which is undersaturated with respect to aragonite are (a) in the laboratory at unrealistically low temperatures, pH values, or P_{CO_2}'s or (b) at great ocean depths.

6.4.2.2 Precipitation and stability of $CaCO_3$ layers

Calcium carbonate is polymorphous and exists in at least five modifications (Deer *et al.* 1965); calcite (trigonal system), aragonite (orthorhombic system) and vaterite (hexagonal system) being the three most important polymorphs.

Thermodynamic calculations indicate that pure calcite is the stable form of calcium carbonate and yet the layer is precipitated as aragonite. In fact there is no known instance of low-magnesium calcite nucleation in normal sea-water, although nucleation is known from freshwater lakes (Blatt *et al.* 1980). This suggests that one of the ions abundant in sea-water inhibits calcite nucleation and numerous experiments have identified this ion to be magnesium. Calcite forms at magnesium levels less than 5% of that in sea-water but, as the level increases, magnesium ion is incorporated into the calcite, thus distorting interatomic bonds so that thermal vibrations of ions are increased and the solubility increases. The incipient calcite particle dissolves into the water.

The cubic coordination between the calcium and oxygen atoms in aragonite precludes the substitution of small cations, such as magnesium, into the crystal structure. Large cations such as strontium can be accommodated and can interfere with the nucleation of aragonite in the same way that magnesium interferes with the nucleation of calcite. However the molality of strontium in sea-water is less than 0.2% that of magnesium and hence strontium is ineffective as a kinetic restraint on aragonite nucleation.

Another factor possibly inhibiting $CaCO_3$ precipitation is the presence in sea-water of dissolved and suspended organic matter. Suess (1970) has shown that small traces of dissolved polar organic molecules in sea-water are sufficient to bring about extensive adsorption on suspended $CaCO_3$. This can result in an effective blocking of nucleation sites and hence can retard

precipitation. It has been shown that organic coatings on aragonite, calcite and a variety of magnesium calcites completely inhibit the equilibration of these minerals with surface water of the Caribbean Sea, the Sargasso Sea and the Golf of Mexico (Suess 1970). Surface- active compounds in sea-water include fatty acids, proteins, lipids, fatty alcohols, fatty esters and unspecified polypeptides (Suess 1970). Accessible surfaces may also bear colonies of a variety of micro-organisms. Meadows and Anderson (1966, 1968) examined sand grains from different geographical locations, tidal levels and water depths. Micro-organisms and organic material were always present on the surfaces of grains. They were not evenly distributed though localised patches were particularly associated with surface hollows and cracks. Micro-organisms observed included bacteria, blue-green algae (Cyanophyceae), diatoms (Bacillariaceae) possibly yeasts (Ascomycetes) and early stages of brown seaweeds (Phaeophyta).

Aragonite is stable in sea-water, but out of an aqueous Mg^{2+} ion environment gradually inverts to calcite. Below 100°C the time required for completion of the dry reaction is of the order of tens of millions of years! Wet transformation of aragonite to calcite in water lacking free Mg^{2+} is much more rapid. The catalytic influence of water is great and reduces the activation energy which must be exceeded for the transformation to proceed. In pure water it has a rate curve of the form shown in Figure 6.12. A large number of salts which give strongly dissociated solutions act as accelerators at low concentrations. Thus, acceleration has been observed with aqueous NaCl, KCl, $CaCl_2$, $MgCl_2$ (0.001 M), $FeCl_2$, $NiSO_4$, $FeSO_4$ etc. (Fyfe & Bischoff 1965). An increase in the partial pressure of carbon dioxide has a similar effect. Alkali hydroxide solutions act as strong inhibitors.

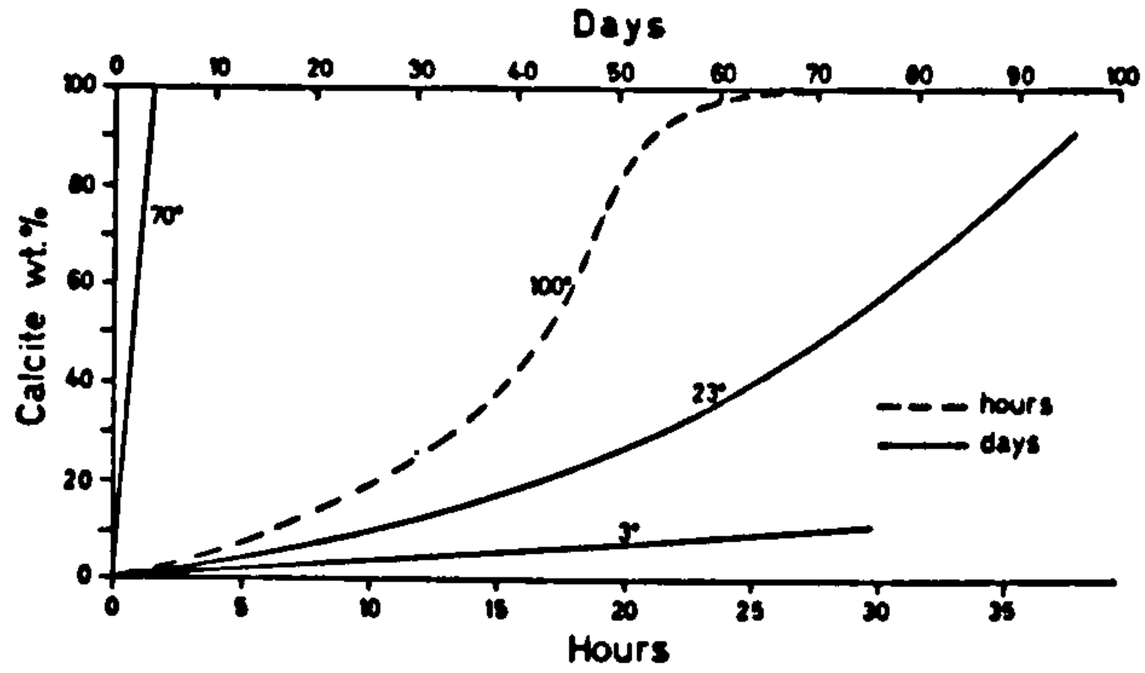

Figure 6.12: Rate curves for wet transformation of aragonite to calcite (Bathurst 1976; 100°C after Fyfe and Bischoff 1965, others after W.H. Taft in Chilingar *et al.* 1967).

6.4.3 Magnesium hydroxide

It has been seen (6.3) that brucite is generally deposited within cement paste pores as well as in a distinct layer beneath a protective aragonite layer. Thus, the environment in which brucite is generally precipitated is even further from pure sea-water than that in which the aragonite layer is deposited. It is, however, of value to consider the saturation state of sea-water with respect to brucite over a range of temperature, pressure and pH that might be encountered offshore or in the laboratory.

Figure 6.13 shows the dependence of the degree of saturation (S) on pH. It can be seen that sea-water is saturated with respect to brucite at a pH of greater than 9.43, but is undersaturated by at least two orders of magnitude over the normal pH range of sea-water. Brucite exhibits inverse temperature/solubility characteristics and hence at lower temperatures S is even less than the corresponding 25°C value. Calculations based on conventional partial molal properties of Mg^{2+} ion in sea-water (Millero 1976, Equation 4 and Table 49), show that the activity of magnesium ion is increased by only 1.1% at a pressure equivalent to 2000 m ocean depth. Any variation in S with depth is therefore likely to be associated with the effect of pH, rather than pressure variation.

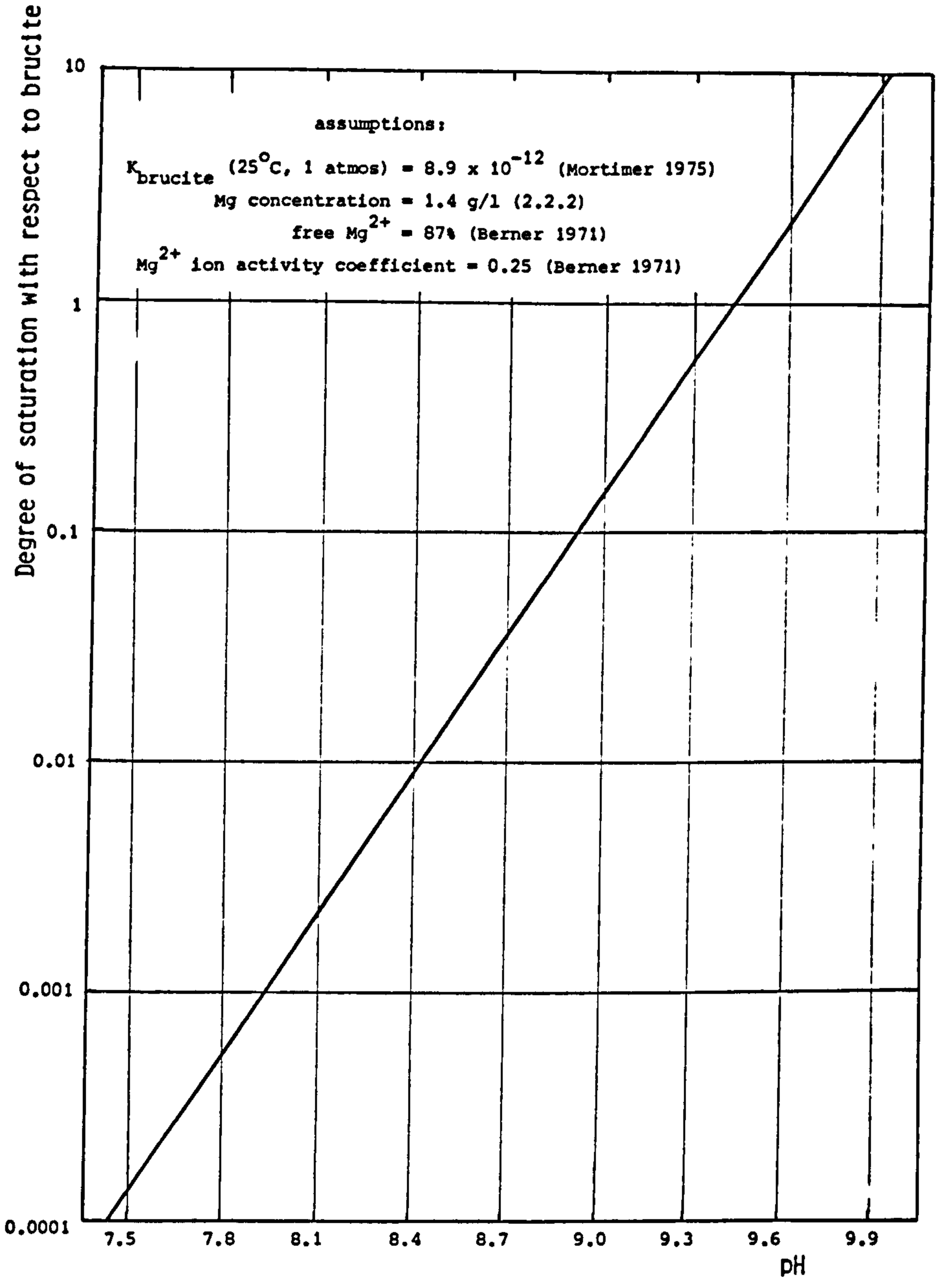

Figure 6.13: The degree of saturation of sea-water with respect to brucite as a function of pH.

It is clear that localised increases in pH within cracks or pores far outweigh any temperature or pressure effects.

6.5 Laboratory studies of layer development

In order to monitor the early-age development of surface layers, mortar specimens were exposed to sea-water for periods of 1 to 90 days, surface formations subsequently being examined.

A large proportion of these tests were combined with a programme concerned with comparing the effects of different curing regimes on chloride ion diffusion by measuring chloride ion concentration profiles after various periods of sea-water exposure (Appendix 6). The same specimens were used for both purposes and details are presented in Appendix 6.

Figure 6.14 shows typical layer development on a 28 day limewater-cured mortar B specimen. A 10 to 20 μm thick brucite layer is present after only 24 hours of sea-water exposure. After only 4 days the brucite layer has attained its ultimate thickness of 30 to 35 μm, and aragonite crystals are detected at the surface; this formation is extremely delicate and is therefore difficult to prepare in section. By 28 days a considerable layer of aragonite of typically 50 to 100 μm thickness has formed. However, the aragonite layer was found to vary greatly from specimen to specimen, from one face of a specimen to another and even from locations only 3 or 4 mm apart on the same face. On certain specimens aragonite did not appear until after 28 days of sea-water exposure and, as a result, the brucite layer was generally thicker.

It is difficult to isolate the individual contributions of aragonite and brucite to the reduction in permeability. There was an increase in specimen resistance on sea-water exposure before aragonite was in evidence, when there was only a thin layer of brucite present. Furthermore, 7mm thick mortar C and F specimens exhibited reductions in chloride ion diffusion coefficient equivalent to an increase in thickness of almost 30 mm (4.3.4), despite an accompanying increase in capillary porosity (7.4); this can only be due to the surface layer which was almost solely brucite (6.2). Clearly then, a brucite layer acts as an effective barrier. The mortar E resistivity specimen exhibited a high surface resistance (Table 5.8) due to a surface layer consisting predominantly of aragonite (6.3). Hence, it appears that both aragonite and brucite are able to effect a reduction in permeability and that neither is markedly more effective than the other.

Specimens immersed in sea-water immediately after demoulding formed layers more rapidly, the brucite layer being 30 μm thick after 24 hours exposure for the mortar B specimen. This was probably a consequence of $Ca(OH)_2$ being more readily available within the less mature cement paste.

Specimens cured in *distilled* water for 28 days prior to sea-water exposure developed thinner layers, probably due to their reduced $Ca(OH)_2$ content due to leaching during curing.

Specimens limewater-cured for a year before exposure produced less dense, but relatively thick, formations.

Specimens cast in moulds prepared with an excessive amount of mould oil exhibited thicker brucite layers with delayed crystallisation of aragonite.

Specimens were also immersed in sea-water that was pH-controlled by dosing with 1.0M HCl every day for the first week, every 3 days for the next 3 weeks and then every week for the remainder of the exposure period. All pH readings taken prior to dosing were less than 8.9 (see Appendix 3 for further details regarding pH-control of sea-water). Surface layers formed were similar to those observed on specimens stored in sea-water that was replaced every 4 weeks.

Figure 6.15 shows an automatic test rig devised to subject one face of up to four cylindrical concrete specimens to wetting and drying in sea-water, in an attempt to simulate a natural tidal zone environment. The specimens are housed in modified resistivity cells. The back face of the specimens is permanently in contact with limewater (solution B) and sea-water is pumped from a 25ℓ tank below the cells, regulated by domestic central heating controls. A cycle of 4 hours wet / 8 hours dry was found to allow the cast face to become visibly dry before rewetting.

Figure 6.16 shows that the layer formed after 12 weeks of cycling is effectively a scaled-down version of the layer observed on permanently immersed specimens, namely a 10-15 μm thick brucite layer covered by a 30 μm thick aragonite deposit.

0 days

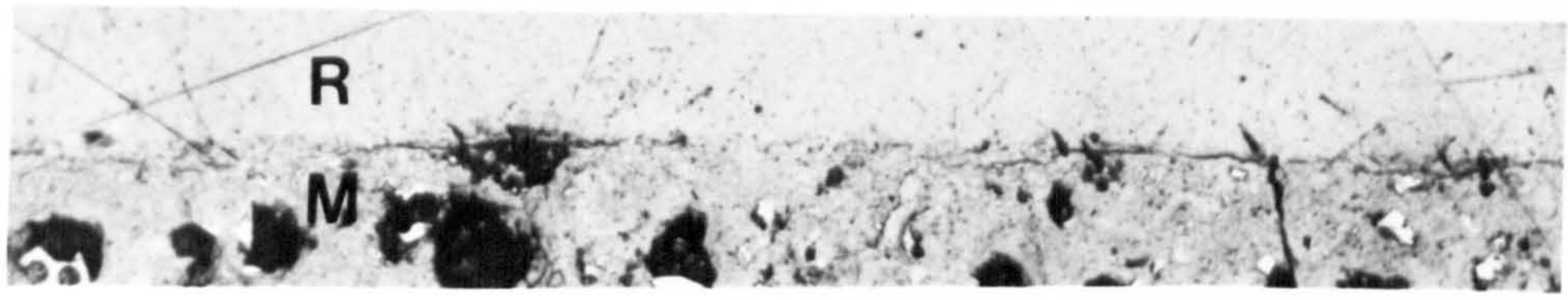

1 day

4 days

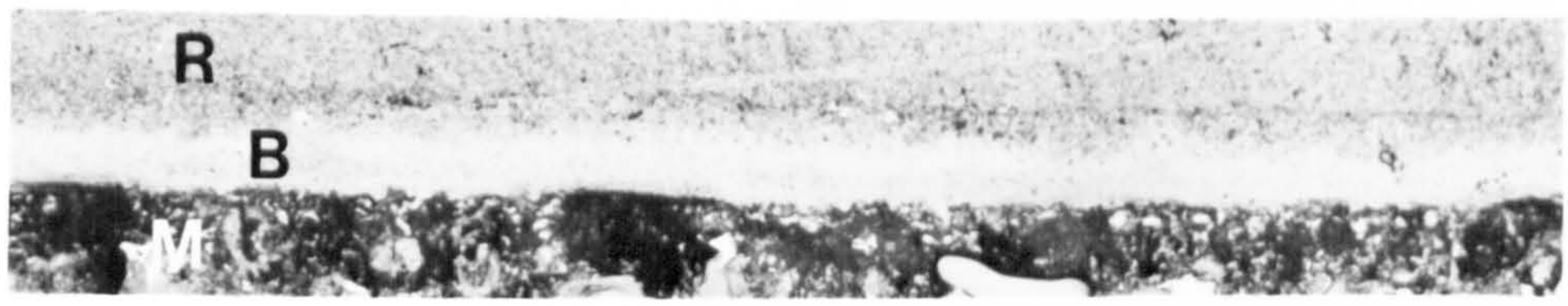

11 days

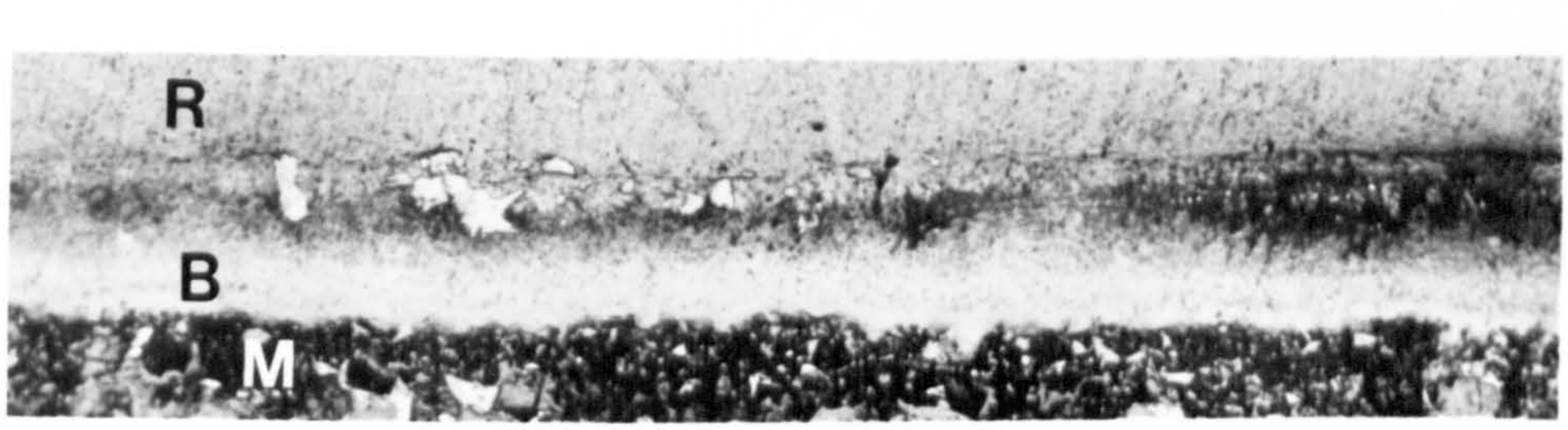

28 days

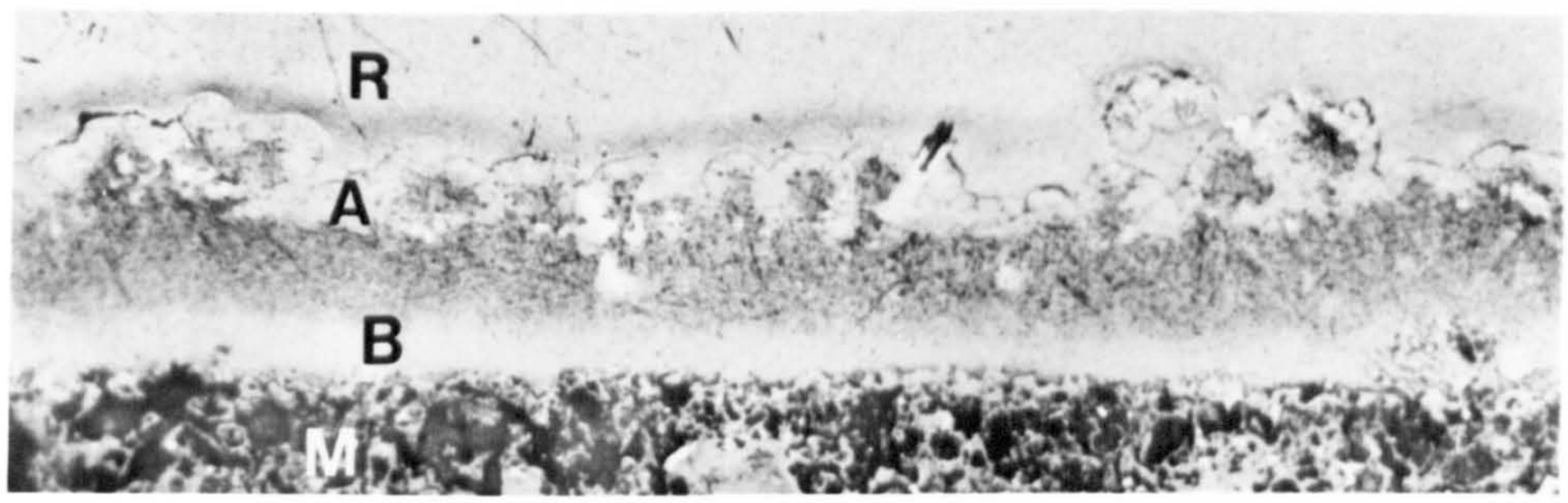

100 μm

A = aragonite M = mortar

B = brucite R = resin

Figure 6.14 : Early-age development of surface layer on mortar B (0.4 w/c , OPC) due to immersion in sea-water.

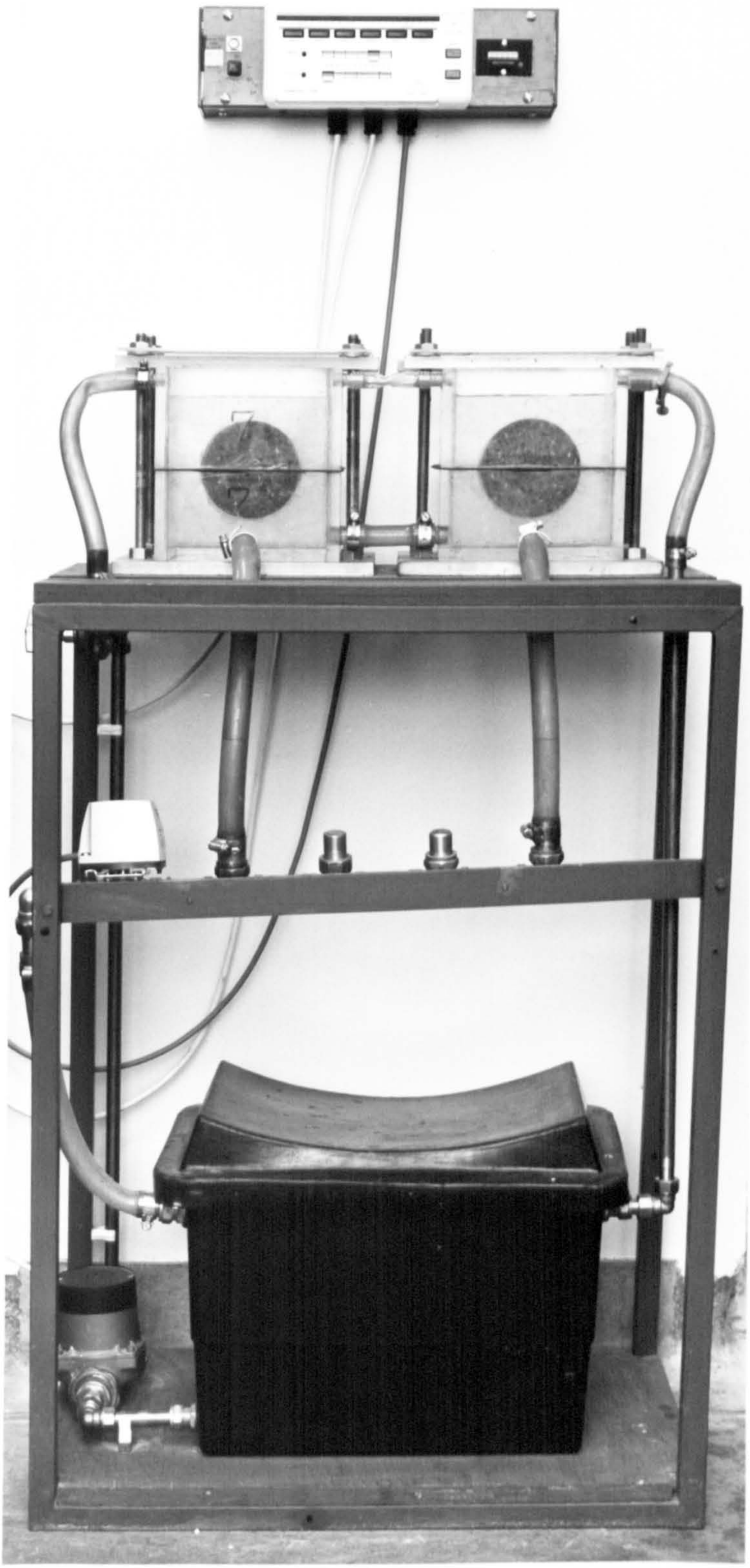

Figure 6.15 : Automatic wetting and drying test apparatus.

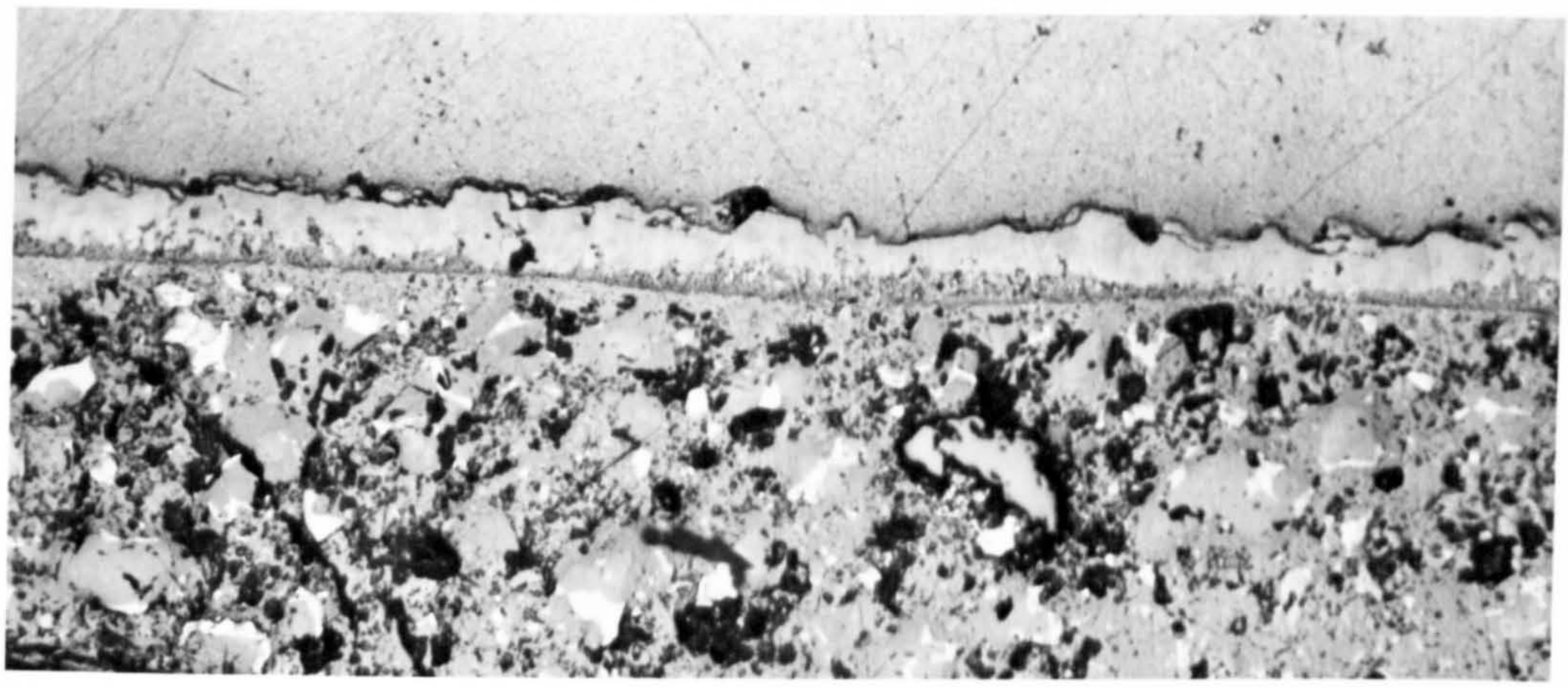

100 μm

Figure 6.16 : Section through surface of mortar B (0.4 w/c , OPC) after 12 weeks of exposure to wetting and drying in sea-water.

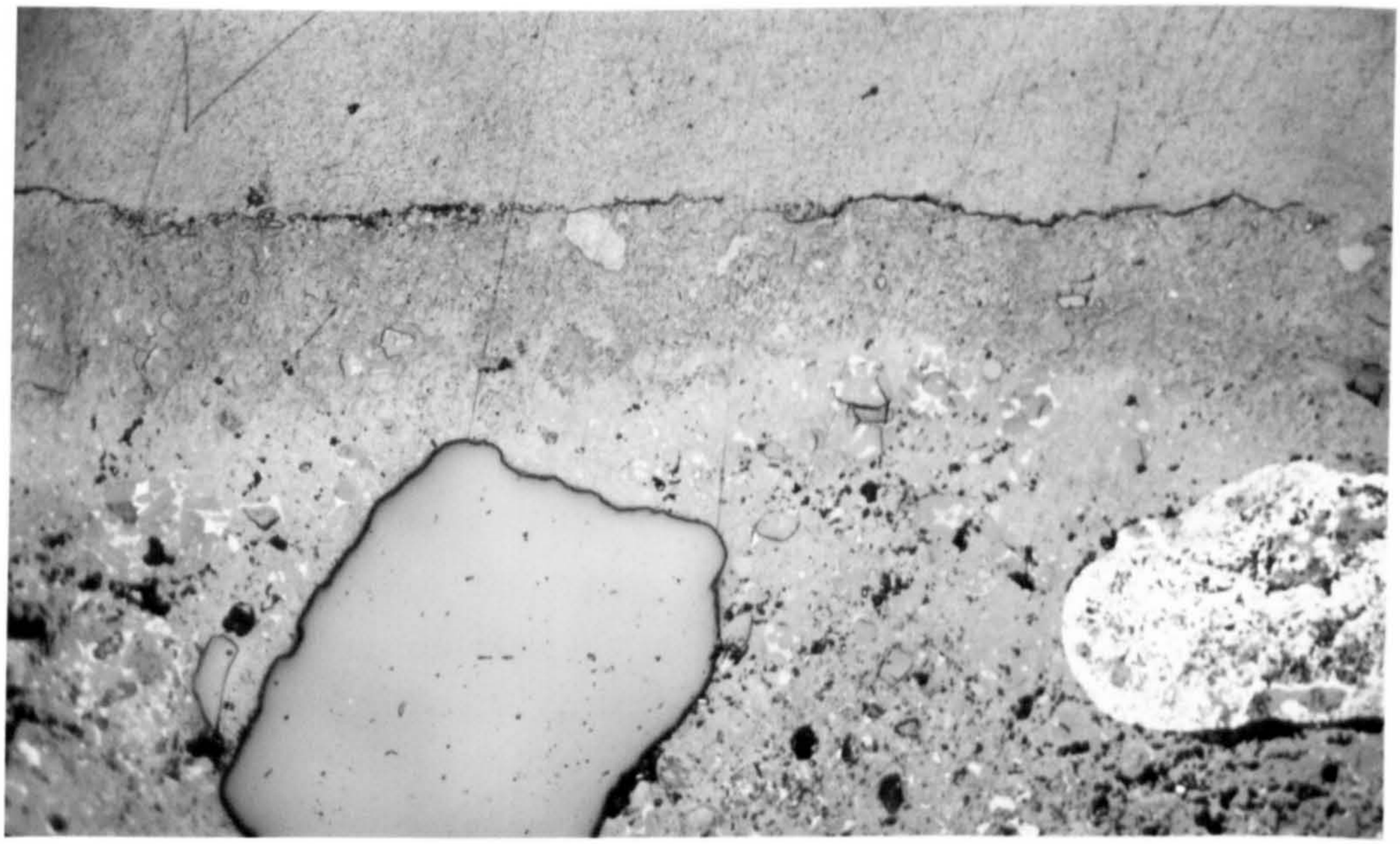

100 μm

Figure 6.17 : Section through surface of standard grade concrete (0.45 , OPC) after 2.5 years of deep submersion in sea-water.

6.6 *Concrete In the Oceans* laboratory specimens

36 cores taken from specimens tested within the *Concrete In the Oceans* "Efficiency of Cover" project were provided for examination and analysis.
The "Efficiency of Cover" project was concerned with investigating the factors within the cover zone controlling corrosion rate, and involved exposing 300 x 200 x 150 mm concrete slabs, of 9 different mixes and 3 curing regimes, to one of 4 laboratory simulated exposure zones for 2 years. Tidal, splash and atmospheric zones (Figure 2.1) were provided by arranging the specimens at three levels on racks within a large tank. The submerged specimens were placed in a second balancing tank which held the sea-water for most of the time. For 3 hours in every 12 the main tank was flooded to cover the lowest level of specimens to simulate the tidal zone. For 5 minutes at the end of this cycle the water level was raised above the next level of specimens to simulate the splash zone. The water was then pumped back into the balancing tank to begin the next cycle. The upper level of specimens was never covered, but air was bubbled though the water remaining in the bottom of the tank so that they remained in a salt-laden atmosphere with a relative humidity of approximately 96% (Leeming 1983).

A full factorial experiment (with no replication) was undertaken with the following variables:

water/cement ratio: 0.4, 0.5 and 0.6;
cement: 7% C_3A, 14% C_3A and 20% pfa replacement;

curing (42 days): air, fog and sea-water;
exposure zone: submerged, tidal, splash and atmospheric.

Thus there were 108 specimens in all. 50 mm diameter cores from each of the submerged zone specimens and also from each of the air-cured 0.5 water/cement ratio specimens (for all exposure zones and cement types) were provided, i.e. 1 core from each of 36 specimens.

At least one polished section was prepared (Appendix 8) from the sea water exposed surface of each core.

All specimens examined fitted neatly into one of 3 categories.
(1) All sea-water cured specimens exhibited the characteristic aragonite over

brucite surface formation regardless of water/cement ratio or cement type. (It should be noted that all the sea-water cured specimens provided were exposed in the *submerged* zone). The brucite layer was typically 50 μm thick, rather thicker than observed on the resistivity test specimens (6.3) and the aragonite thickness was very variable. Figure 6.18 (a) and (b) shows the variation in layer structure between two locations only 2 mm apart.

(2) Splash and tidal zone specimens exhibited a very thin surface layer of aragonite (e.g. Figure 6.18(c)), regardless of cement type; (only air-cured specimens were provided). The layer was typically 15 to 20 μm thick and often contained small brucite inclusions. The layer was absent in certain areas on some specimens; this could be a result of rough treatment during coring.

(3) All air and fog-cured submerged specimens showed no evidence of surface layer development, regardless of water/cement ratio or cement type (e.g. Figure 6.18 (d)).

Clearly environment (curing regime and exposure zone) rather than mix characteristics (water/cement ratio and cement type) was critical in controlling layer development. It would have been interesting to have tested sea-water cured specimens from other exposure zones.

Sea-water cured specimens had been cured for 42 days in troughs containing around the same volume of sea-water as the volume of the specimen (Baker 1984). No effort had been made to control pH, or to replace the sea-water, over the curing period. Hence leaching (2.2.3) would have caused a dramatic rise in pH (Appendix 3) which is likely to have resulted in enhanced aragonite and brucite precipitation. It is therefore likely that the sea-water cured specimens had developed substantial layers prior to being placed in the exposure tank.

The original pH of the sea-water in the exposure tank had been around 7.8 (Baker 1984), rather low for normal sea-water (A2.1). After around 6 months the pH had reached 8.2 and so, the sea-water was replaced. All later pH readings were less than 8.2 and hence the sea-water was not subsequently replaced. It therefore seems likely that the sea-water was undersaturated with respect to aragonite for a large proportion of the exposure period, a condition unlikely to obtain in a natural offshore environment (6.4.2.1). This could at least partly explain the absence of surface layers on the air and fog cured submerged specimens.

(a)

(b)

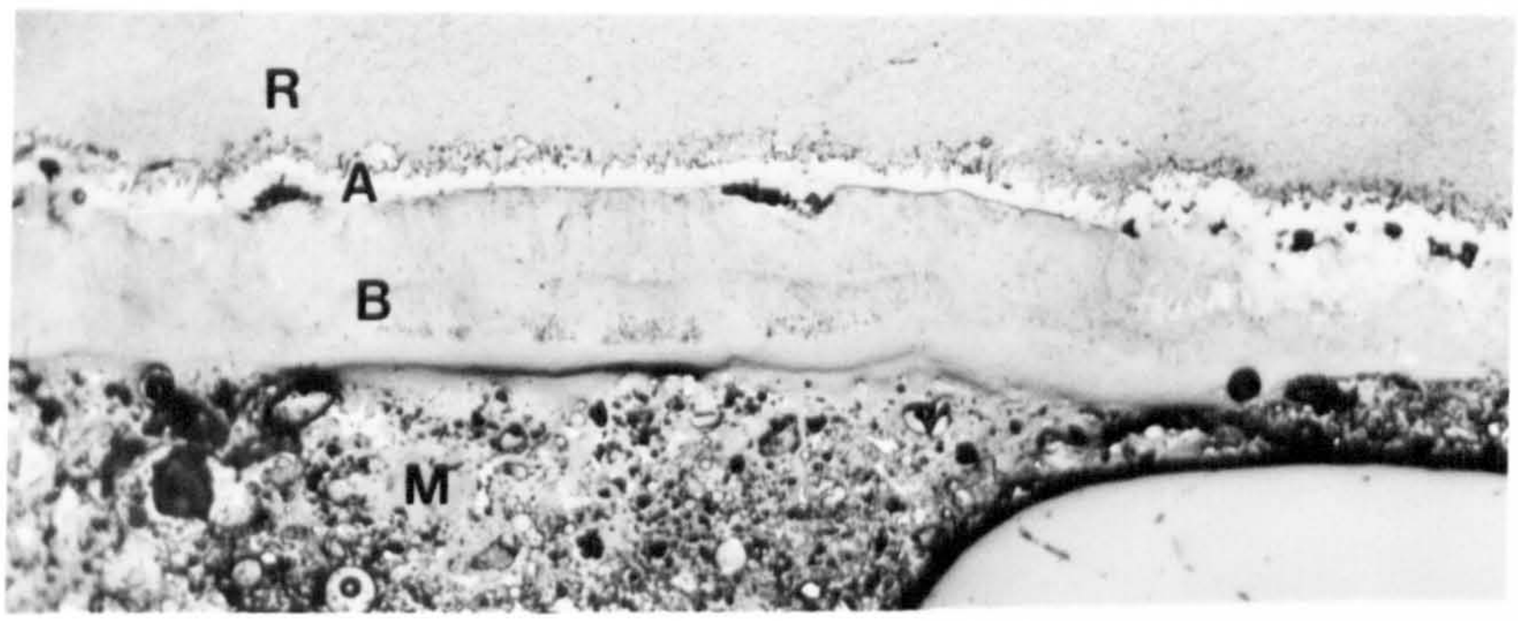

(c)

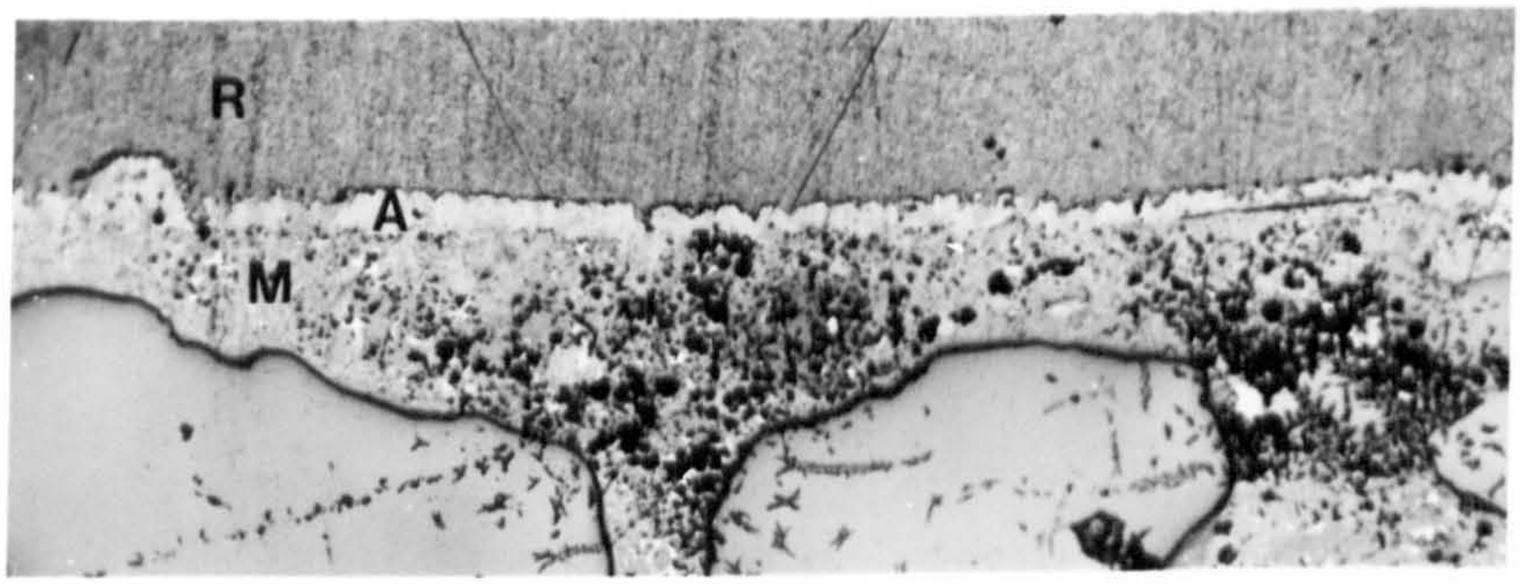

(d)

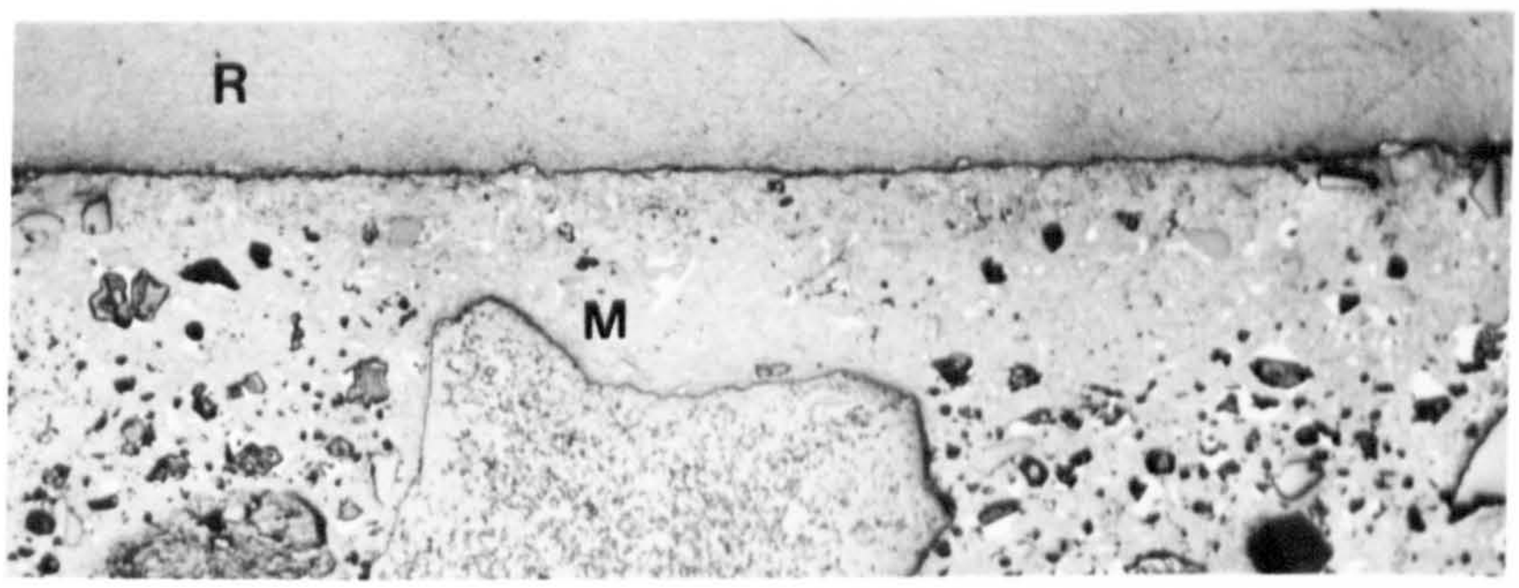

100 μm A = aragonite B = brucite M = mortar R = resin

Figure 6.18 : Sections through surface of Concrete in the Oceans specimens after 2 years of exposure to sea-water.
(a) & (b) 0.5 w/c , pfa/OPC , sea-water cured , submerged zone;
(c) 0.5 w/c , SRPC , air cured , splash zone;
(d) 0.4 w/c , SRPC , air cured , submerged zone.

6.7 Naturally exposed specimens

The *Concrete in the Oceans* programme provided cores taken from concrete specimens submerged for up to 5 years at the Loch Linnhe deep water exposure facility (5.7.4). Unfortunately the specimens had been surface-scraped to remove marine growth and further damage had occurred during coring. The least damaged cores were used for resistivity testing (5.9.3), but at least one polished section was prepared from the least disrupted area of the sea-water exposed face of each of the following cores (see A1.1 for mix details):

standard grade concrete : 2½ and 5 years exposure;
low grade concrete: 2½ and 5 years exposure;
pfa concrete: 2½ years exposure.

No distinct surface formation was present on any of the specimens, although the irregularity of the surface together with protruding aggregate particles suggested that, in places, an appreciable thickness of sample had been removed, presumably by scraping. Nevertheless, resistivity testing showed that, despite surface-scraping, a source of considerable resistance was still present within the surface 1 mm of specimens (5.9.3).

Examination of polished sections using crossed polarised light highlighted a brown surface zone within most of the specimens; its thickness was around 100 μm on the standard grade and pfa concretes exposed for 2½ years, increasing to 300 μm in places on the 5 years exposed low grade concrete. This brown area is just visible as a darker surface zone in Figure 6.17. Its rust-like appearance suggested that the surface zone might have been stained by haematite (red rust) from the tank in which the cores had aparently been stored prior to dispatch. Longer exposure to ferric ions might have produced ferrobrucite, a mineral with a brown tinge (Deer *et al.* 1965). However, this has not been verified by XRDA and the author is not aware of ferrobrucite being identified in the context of the corrosion of cracked reinforced concrete in sea-water. Furthermore EPMA in the "digimap" mode did not show this zone to be particularly iron-rich and indeed did not identify *any* unusually high element concentrations within the surface 1 mm.

The author could not find any analytical data in the literature to confirm the existence of an aragonite/brucite layer on the surface of concrete exposed to natural marine conditions. Generally only deteriorated concrete from offshore

structures is mineralogically analysed. If such a surface layer had been present, it is likely that its beneficial effects would have prevented significant deterioration and hence the concrete would not have been analysed and the layer identified. Additionally, severe handling could result in the layer flaking off prior to analysis or analysis of samples relatively thick in comparison with the surface layer could mask the presence of aragonite and brucite.

Clearly many more naturally exposed specimens must be examined and tested and future surveys of offshore structures should include tests specifically designed to investigate the nature and effect of the surface skin (Chapter 9). It would be particularly interesting to compare surface samples taken from each of the exposure zones of the same structure, since laboratory testing suggests that under certain conditions a surface layer may develop in the splash and tidal zones, but not in the submerged zone (6.6).

Chapter 7 : MERCURY INTRUSION POROSIMETRY

7.1 Introduction

7.1.1 Purpose of pore structure investigation

Resistivity testing (Chapter 5) showed that the permeability-reducing mechanism for concrete in sea-water was produced by the combination of a surface effect and a more widespread bulk effect. The aim of the testing reported within this chapter was to investigate the bulk effect by comparing the pore structures of sea-water exposed and control specimens. It was felt that such a study might also elucidate other more general aspects of resistivity and chloride ion diffusion behaviour.

7.1.2 Pore structure of concrete

Voids present in concrete vary in size from several millimeters to less than 20Å and for the purpose of this review they can be categorised as follows:

(1) air voids (entrapped and entrained air voids);
(2) aggregate voids;
(3) cement paste pores (capillary and gel pores);
(4) other voids.

Category, (4), represents voids that would not be expected to be present in laboratory-cast specimens; e.g. internal cracks from humidity and temperature changes, voids under aggregate particles created by bleed water in concrete with an excessive water/cement ratio, and "honeycomb" voids due to poor compaction.

(1) Air voids

Intentionally entrained air voids are air bubbles typically 0.1 mm in diameter and are distributed evenly throughout the cement paste. Accidentally entrapped air usually forms very much larger voids, often up to several millimeters in diameter. Entrained and entrapped air voids are distinct cavities isolated from one another and hence have little influence on the permeability of concrete.

(2) Aggregate voids

Normal-weight aggregates have a permeable pore space of typically 0.5 to 5.0%. The pores are much larger than those within the cement paste and hence, despite being less porous, aggregates are generally more permeable than cement paste (Powers 1958). However, since the aggregate particles are enveloped by the cement paste in fully compacted concrete, it is the permeability of the paste that controls concrete permeability (Neville 1978, Haynes 1980).

(3) Cement paste pores

Hardened cement paste consists of hydrates of the cement minerals referred to collectively as *gel*, of crystals of $Ca(OH)_2$, some minor components, unhydrated cement and the residue of the water-filled spaces in the fresh paste. Conventionally these water-filled spaces have been called *capillary pores* while the porosity of the gel itself has been accredited to *gel pores*.

At any stage of hydration the capillary pores represent that part of the gross volume which has not been filled by the products of hydration. Since these products occupy more than twice the volume of the original solid phase alone, the volume of the capillary system reduces as hydration proceeds. At water/cement ratios of higher than about 0.38 the volume of the gel is not sufficient to fill all the space available to it so that there will be some volume of capillary pores left even after full hydration. These form an interconnected system which is primarily, if not wholly, responsible for cement paste permeability. As hydration proceeds the solid content of the paste increases and the capillaries may become blocked by gel and segmented so that they are interconnected solely by the gel pores. For water/cement ratios above about 0.7 complete hydration would not produce enough gel to block all the capillaries (for extremely fine cement the maximum water/cement ratio would possibly be as high as 1.0, while for coarse cements it would be below 0.7). Table 7.1 shows the approximate age at which capillaries become segmented, assumed to correspond to the age at which a relatively abrupt reduction in permeability is observed.

Water/cement ratio	Age
0.40	3 days
0.45	7 days
0.50	14 days
0.60	6 months
0.70	1 year
> 0.70	impossible

Table 7.1: Approximate age at which capillaries become segmented (Powers *et al.* 1959).

Gel consists of particles of at least 4 morphologies (Diamond 1976). The predominent particles are "fibrous crystals", typically 0.5 to 2 μm long and less than 0.2 μm wide, which radiate outwards from cement grains. A second type of morphology, often existing contemporaneously with the fibrous particles, consists of elongated particles, of roughly the same cross section as the fibrous particles, which branch at considerable angles producing a continuous interconnected reticular network in three dimensions. A third common morphology consists of small irregularly flattened particles often no more than 0.3 μm across.

There are several theories as to the structure of the gel particles themselves. The Powers-Brunauer model (Ramachandran *et al.* 1981) considers gel to have a minimum porosity of 28% which is due to "gel pores" which are visualised as pores between gel grains of which the solid-to-solid distance is about 18Å with the diameter of the grains being around 100 Å. However, there is much recent evidence (Ramachandran *et al.* 1981) to suggest that cement gel consists of imperfectly aligned and possibly rumpled tobermorite-like layers; (this concept is not accepted universally (e.g. Diamond 1976)). In the Feldman-Sereda model (Feldman & Sereda 1968) the role of water is particularly important. The water within the interlayer spaces is a part of the structure and is more organised thus contributing to the rigidity of the system. Most of this *structural water* is lost at relative humidities below 10%, but only a part of it is lost at higher relative humidities. Accordingly it is not considered as pore water. Consequently, according to the Feldman-Sereda model, gel pores, as such, do not exist and the gel pores in the Powers-Brunauer model are considered to be a manifestation of interlayer spaces.

Water exists within cement paste in several forms:

(1) free water in capillary pores;

(2) "gel pore" water: (a) adsorbed water
(b) interlayer water
(c) lattice water - water of crystallisation which is not chemically associated with the principal constituents of the lattice;

(3) chemically combined water.

There is no technique available for determining how water is distributed between these different states. A convenient, though rather arbitrary, categorisation of water in hydrated cement paste is between evaporable and non-evaporable. Evaporable water *may* be defined as that which is lost on oven-drying at 105°C and is conventionally used to calculate "porosity". However this method almost certainly overestimates porosity, since drying at 105°C not only removes the capillary water and most of the "gel pore" water, but also removes some of the chemically combined water (Lea 1970). Furthermore, "gel pore" water has a specific gravity of around 1.1 (Powers & Brownyard 1946-7) and so occupies a smaller volume than suggested by its weight.

7.1.3 Methods of determining pore structure

The three structural properties which are fundamental to the description of porous materials are:

(1) *Porosity*: the fraction of the total volume which is occupied by pores. Porosity may be classified as open or closed and open pores may be further subdivided as permeable or saccate (dead-end).

(2) *Specific surface*: the surface area contained in unit mass of solid. In principle this may be derived from the porosity and the pore size distribution.

(3) *Pore size distribution*: the fraction of the total open pore volume in which the pores lie within a stated size range.

There is a wide variety of techniques available for studying pore structure (for review see Haynes 1973). Although methods exist whereby geometrical properties may be evaluated by direct observation, most techniques are indirect, being based on the observation of secondary or derived properties. It was considered desirable to limit the choice of technique to those whose use

on cement pastes was reasonably well documented. Table 7.2 presents such techniques, together with the pore parameters that may be determined.

Technique	Parameters determined
Helium pycnometry	open porosity, total porosity (if sample crushed).
Nitrogen or water vapour adsorption	micropore volume, specific surface, mean pore size (if porosity is also known).
Capillary condensation	open porosity, specific surface, pore size distribution.
Mercury intrusion porosimetry	open porosity, specific surface, pore size distribution.

Table 7.2 : Pore structure determination techniques.

In the context of a study on permeability it was felt that pore size distribution (together with porosity) would probably be the most informative pore parameter.

Helium pycnometry determines solid volumes by displacement principles, based on the gas laws. It does not give information on pore *sizes* and has mainly been applied to study the collapse or re-expansion of "interlayer space" within calcium silicate hydrates (e.g. Feldman 1973).

In adsorption techniques the amount of adsorpate (generally nitrogen or water vapour) lost or gained with changes in relative gas pressure at constant temperature (adsorption or desorption isotherms) is measured to enable estimates of porosity and surface area to be made. However, as with helium pycnometry, such techniques do not allow the evaluation of pore size distribution.

Capillary condensation techniques and mercury intrusion porosimetry (MIP) are based on measuring interfacial curvature (Haynes 1973) and by introducing a model (the equivalent radius of a pore of arbitrary shape is that of a cylindrical pore within which the interface would adopt the same mean curvature)

pore sizes can be estimated.

Capillary condensation methods generate pore size distribution information by applying the Kelvin equation (Diamond 1971) to either the adsorption or desorption isotherm. However, such methods are essentially limited to a maximum pore diameter of several hundred Å (Mikhail *et al.* 1975) which would neglect a large proportion of capillary pores which are primarily responsible for permeability. Furthermore, it is generally conceded that the Kelvin equation is not valid for "micropores". Harris (1965) cited data suggesting that the equation is invalid for pore diameters as large as 35 to 40 Å.

Mercury intrusion porosimetry is based on the principle that a non-wetting fluid (mercury) penetrates pores only if the resistance to wetting due to the surface tension of the fluid can be overcome by the applied pressure. Hence (Gregg & Sing 1967):

$$d = \frac{-4\gamma\cos\theta}{p}$$

where d = diameter of cylindrical pore;

γ = surface tension of fluid;

θ = constant angle between solid surface and fluid surface; and

p = absolute pressure.

Application of this relationship allows an estimate of pore size distribution to be made. The upper pore diameter limit can be as high as 1 mm, if an appropriate filling device is used, while the lower limit depends on the pressure capacity available and can be as small as 20 to 25Å (Diamond 1971).

There are interpretative problems associated with all these techniques (Ramachandran *et al.* 1981). However, most of these problems may be ignored if the techniques are being used for *comparative* purposes, e.g. comparing originally similar samples that have been exposed to different environments.

MIP enables the widest range of pore size distributions to be measured and was therefore selected as the technique to be used for the present study.

Unfortunately Imperial College does not possess a porosimeter, but Dr. D.

Bonner, School of Engineering, Hatfield Polytechnic, kindly offered to test a limited number of specimens.

7.2 Experimental details

Discs were cut from 100 mm diameter cylindrical mortar specimens using a diamond saw, the blade of which was lubricated with limewater. A "trim saw", lubricated with a very small quantity of limewater, was used to cut samples from the discs.

Several drying regimes were considered. Hardened cement pastes are subject to progressive partially irreversible changes during drying. Helium flow measurements on cement gel dried from 11% relative humidity suggest that "gel pores" (or interlayer spaces) progressively collapse (Ramachandran 1981). Parrott (1981) used methanol sorption to show that even drying at intermediate relative humidities, particularly in the range of 20 to 60%, resulted in capillary tension forces causing a partial collapse of pores in the size range up to 40Å diameter and a corresponding increase in the volume of larger pores. Such changes could apparently be avoided by using counter-diffusion to exchange the pore water with methanol, the methanol with n-pentane and then driving off the n-pentane by oven-drying. However, little is known of the long-term interaction of cement paste with such solvents and since the primary aim of the present study was simply to compare test specimens with control specimens, it was decided to adopt the more conventional preparation of oven-drying at 105°C. This regime also allows comparison of MIP data with "porosities" based on evaporable water content (Table 5.7, 7.1.2).

After oven-drying at 105°C to constant weight, specimens were stored over silica gel (to remove moisture) and soda lime (to remove CO_2) until tested.

A Carlo Erba Strumentazione Series 200 mercury intrusion porosimeter was used. A contact angle of 141.3°, as recommended by the manufacturers, was assumed.

7.3 Resistivity test specimens

One millimetre was ground from the cast faces of the 25 mm thick test series I resistivity specimens (sea-water exposed test specimens and limewater cured control specimens of mortars B-F) and their resistances were remeasured (5.7.2). A 5 mm thick disc was then cut from the ground face and 7 mm wide, 25 mm long, MIP samples were cut from near the centre of the disc.

The original intention had been to test at least 3 samples from each specimen, but early results were so consistent that in later tests only 2 samples from each specimen were tested. The results that follow represent the average values of replicated samples.

Figure 7.1 presents the pore size distributions of the limewater cured control specimens. Most of the results presented in Figure 7.1 are discussed earlier in the text, particularly in the context of the diffusion of chloride ions through specimens of these mixes (4.3.4).

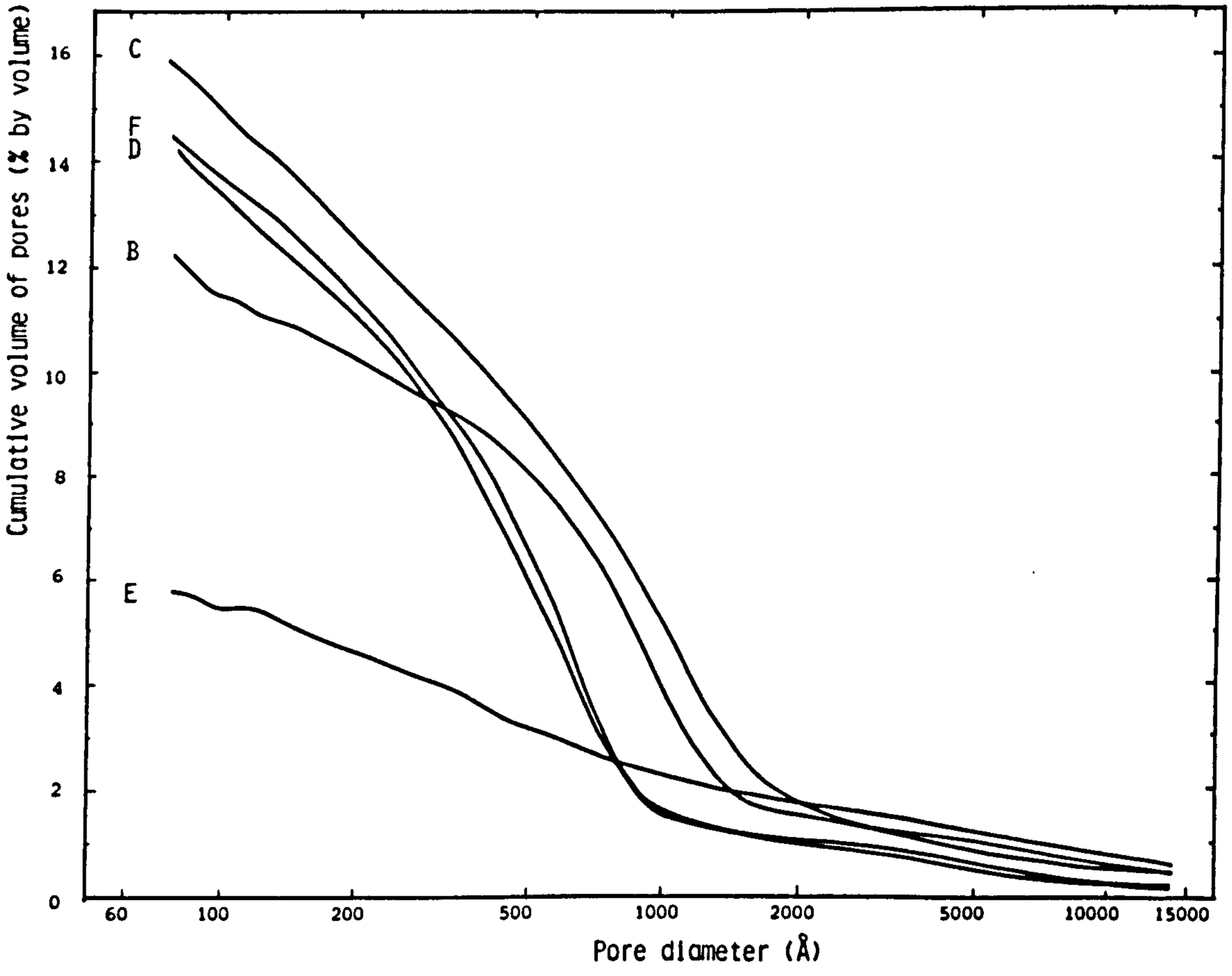

Figure 7.1: Pore size distributions of mortars after 22 weeks of limewater curing.

Table 7.3 shows the effect on the mortar of 18 weeks of sea-water exposure. Total porosity shows little variation. However, all the mortars that exhibited a *bulk* increase in resistance (Table 5.8, mortars B, C, E and F) show a reduction in the volume of pores with a minimum effective neck diameter of greater than 1000 Å. This modification is accompanied by an increase in the volume of the smaller pores, except for mortar F which shows a reduction in the volume of the smaller pores whilst only a nominal reduction in the larger pores.

It would seem likely that the reduction in volume of the larger pores is due to the formation of calcium chloroaluminate (2.2.2.3). This would explain the reduced effect on the zero-C_3A cement mix (mortar F). However, there is another mechanism that may be contributing to the shift in pore size distribution. Mehta (1980) observed a reduction in the volume of large pores as a result of the use of chloride salts as admixtures. Mehta suggests that this modification may be associated with the reticular structure of the calcium silicate hydrates (7.1.2) which are reportedly formed in the presence of chloride ions. It is, therefore, also conceivable that penetrating chloride ions alter the morphology of gel formed during the later stages of hydration.

Midgley and Illston (1980) exposed hardened OPC paste specimens to sodium chloride solutions for 6 months and then measured their pore size distributions using MIP. Chloride ion penetration caused little change in porosity but effected a shift in pore size distribution of a similar nature to that observed in the present work. Pastes with a w/c ratio of 0.47, exposed to a 30g/ℓ sodium chloride solution showed a marked reduction in the volume of pores of around 1000 Å diameter with a corresponding increase in the volume of pores with diameters of around 600 Å. The effect was more pronounced when a more concentrated chloride solution was used.

The pfa mix (mortar D) exhibited a bulk decrease in resistance (Table 5.8) as a result of sea-water exposure and this is reflected in the pore size distribution results. There is an increase in the volume of the larger pores and a reduction in the volume of pores with minimum effective neck diameters of less than 600 Å.

These shifts in pore size distribution would certainly cause changes in resistance (and hence permeability) but it is very difficult to ascertain whether

they are the *sole* cause of the "bulk effect" encountered during resistivity testing.

Mix reference	Exposure (Solution A)	Pore volume (% by volume) at various pore diameters								
		75-125Å	125-200Å	200-400Å	400-600Å	600-800Å	800-1000Å	1000-1600Å	>1600Å	Total
Mortar B	limewater	1.2	0.8	1.5	1.6	1.7	1.7	2.0	1.8	12.3
	sea-water	1.3	1.0	1.8	1.6	1.7	1.5	1.6	1.6	12.1
Mortar C	limewater	1.7	1.7	2.6	1.7	1.7	1.3	2.9	2.4	16.0
	sea-water	2.1	2.1	3.1	2.0	1.7	1.4	2.4	2.3	17.1
Mortar D	limewater	1.8	1.5	3.5	3.0	1.9	1.1	0.3	1.3	14.4
	sea-water	0.9	1.2	2.8	2.4	2.0	1.3	1.1	1.3	13.0
Mortar E	limewater	0.4	0.7	1.2	0.5	0.4	0.3	0.3	2.0	5.8
	sea-water	1.6	0.6	1.1	0.5	0.3	0.2	0.2	1.5	6.0
Mortar F	limewater	1.4	1.7	3.3	3.2	2.4	0.3	1.0	1.2	14.5
	sea-water	1.0	1.6	2.9	3.4	2.4	0.4	0.8	1.3	13.8

Table 7.3: Pore volume of limewater and sea-water exposed mortars at various pore diameters.

7.4 Diffusion test specimens

On completion of diffusion testing (4.3), samples were taken from 7 mm thick diffusion test specimens of mortars C and F (Table 4.2, test references D10 and D12). The surface layer (6.2) was removed using a scalpel and the samples were MIP tested.

7 mm thick discs were cut from cylinders of mortars C and F (cast from the same batch as the cylinders from which the diffusion specimens were taken) which had been limewater-cured since casting. Samples were prepared from these discs and they were MIP tested as control samples.

Table 7.4 shows the effect of 23 weeks of sea-water exposure on the diffusion test specimens, each result being the average of two samples. As can be seen, the pore volume of all but the finest pores of the mortar F specimen had increased. The observation of increased porosity supports the theory that the early increase in D is due to leaching of $Ca(OH)_2$ from the hardened cement paste as a result of the counter-diffusion of hydroxyl ions (4.3.4). This also suggests that the surface layer formed had a considerable permeability-reducing effect since it more than compensated for the increased porosity, producing an overall reduction in D (with time).

However, this opening of the pore structure is inconsistent with the behaviour of the resistivity specimens (7.3). The resistivity specimens do not appear to have been subject to such a phenomenon. The only possible difference in experimental details between the two testing techniques that might have caused these conflicting results is specimen thickness. A leaching mechanism peculiar to thin specimens could also explain the relative constancy in D (Figure 4.5) for the pfa mix (mortar D) despite its rapidly increasing FF (Figure 5.14).

It was initially considered that the mechanism producing this effect could be associated with the use of limewater, rather than a more realistic simulated pore solution, as solution B. However, Figure 4.8 shows that this was not the case. It would, nevertheless, appear that an extra thickness of mortar is a more efficient means of preventing leaching than a simulated pore solution reservoir. Hydroxyl ions cannot diffuse from solution B at a sufficient rate to prevent the dissolution of solid ($Ca(OH)_2$ from the paste matrix, whilst the hydroxyl ions within the cement paste pore solution appear to be more readily available. No mechanism can be envisaged that would explain this

observation.

Clearly it is advisable to test specimens that are reasonably thick in relation to expected depths of chloride penetration, in order to avoid the effect of such a mechanism which would seem to be a product of the experimental configuration. This is another factor favouring resistivity testing.

Reference	Exposure (Solution A)	Pore volume (% by volume) at various pore diameters								
		75-125Å	125-200Å	200-400Å	400-600Å	600-800Å	800-1000Å	1000-1600Å	>1600Å	Total
Mortar C	limewater	1.4	1.6	2.3	1.6	1.6	1.3	2.9	2.2	14.9
(test ref.D10)	sea-water	2.0	1.7	2.6	1.9	1.9	1.6	3.3	3.7	18.7
Mortar F	limewater	1.5	1.5	2.9	3.0	2.5	0.9	0.8	1.2	14.3
(test ref.D12)	sea-water	1.1	1.5	2.9	3.3	2.8	1.7	1.1	2.1	16.5

Table 7.4: Pore volumes of diffusion test specimens at various pore diameters

Chapter 8: INITIAL SURFACE ABSORPTION TESTING

8.1 Introduction

Specimens exposed to wetting and drying cycles (6.5, 6.6) exhibited surface layers of similar composition to those observed on corresponding submerged specimens, although the layers were generally thinner. This suggests that the permeability-reducing mechanism is also likely to be effected in the tidal zone. The principal purpose of this phase of testing was to obtain a "feel" for the effect of the mechanism on absorption, the predominant transport process in the tidal and splash zones (3.1).

The initial surface absorption test (ISAT) was felt to be the most appropriate method of monitoring changes in absorption characteristics (3.3.4). The ISAT was developed and assessed during the late 1950's and 1960's as a guide to the permeability of the surface layers of concrete (Levy 1960, Levitt 1970a, 1970b). ISA is defined as (BS 1881: Part 5: 1970) "the rate of flow of water into concrete per unit area after a stated interval from the start of the test and at a constant applied head and temperature".

In the present context the ISAT is used to compare the absorption characteristics of "conditioned" concrete specimens after various periods of limewater or sea-water submersion, (limewater was chosen as the control environment for the reasons discussed in 5.4). The resulting data is used to calculate changes in the volume of sea-water absorbed during the wetting phase of tidal zone exposure, over long periods of sea-water exposure.

BS 1881: Part 5: 1970 recommends oven-drying of test specimens prior to testing and indicates that laboratory conditioning leads to less accurate results. However, oven-drying would almost certainly result in cracking of the surface layer and subsequent testing would therefore underestimate the effectiveness of the layer in reducing absorption. Furthermore, oven-drying would modify the cement paste pore structure, negating the benefits of repeated testing of the same specimens (3.3.2). Consequently, a less severe drying regime was required that would produce minimal disruption of the layer and cement paste microstructure while rendering the specimen sufficiently dry to allow significant absorption. Preliminary tests were carried out in order to arrive at a suitable compromise.

BS 1881 states that specimens should be tested with distilled water. However, it was felt that sea-water might be a more appropriate permeating medium for the sea-water immersed specimens and hence preliminary tests were also undertaken to clarify this issue.

8.2 Preliminary testing

Test rigs as shown in Figure 8.1 were used. The funnel provides a 200 mm head of water which is applied to the concrete beam under test via a perspex cap clamped in position. When a reading is to be taken, a water-filled capillary tube is switched in to replace the funnel and the movement of the meniscus along the capillary tube over a specified period is recorded. Measurement of the cap and capillary tube areas allows the ISA to be calculated. The length of the 100 mm x 100 mm cross section test beams was chosen according to the number of test locations per beam required.

A temperature and humidity-controlled environmental chamber was initially considered to be the ideal means of conditioning specimens prior to testing. It was envisaged that, for the main test programme, each specimen would be tested in several locations and hence would be exposed in the laboratory for at least 6 hours. The humidity of the drying regime was therefore required to be very similar to the humidity of the laboratory in which the ISAT was being performed, in order to prevent spurious results due to the moisture state of the specimens changing between tests. Unfortunately the humidity control of the environmental chamber was very imprecise at temperatures near ambient. Unforced drying in the laboratory was therefore investigated. The main drawback of this latter regime is that conditions (temperature and relative humidity) are likely to be different on each occasion that testing is undertaken. However testing of limewater-cured control specimens helps to counteract this problem. Trial specimens (500 x 100 x 100 mm beams of concrete A (see A1.1 for mix details) were cured for 28 days in limewater and were then allowed to stand in the laboratory for 1, 3 or 7 days prior to ISA testing. 1 day of conditioning produced rather variable results on supposedly identical specimens, but the reproducibility of tests carried out after 3 and 7 days was relatively good. 3 days of laboratory air-drying was therefore adopted as the standard conditioning regime.

Preliminary tests were also undertaken to compare distilled water and sea-water as permeating media, to determine which face of the beams should be tested and to identify any other practical problems. Four 500 x 100 x 100 mm beams of concrete A (see A1.1 for mix details) were cast, demoulded after 1 day and cured in limewater for 28 days. They were then conditioned for 3 days. Each beam was tested with sea-water and distilled water in different locations on 2 different faces (Figure 8.2). Two ISAT rigs were used and, to eliminate any

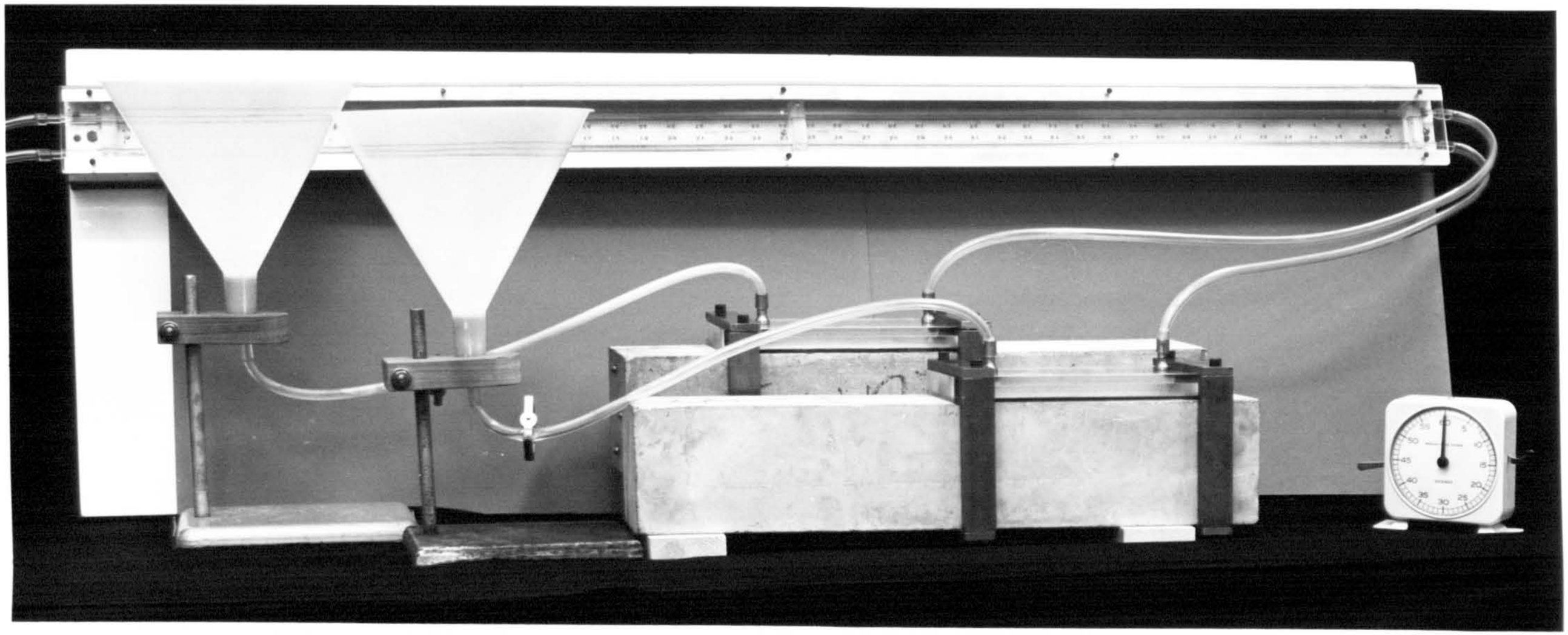

Figure 8.1 : ISAT rigs in operation.

discrepancies due to variation between the rigs, each rig was used for an equal number of distilled water and sea-water tests. Readings were taken between 3 minutes and over 2 hours.

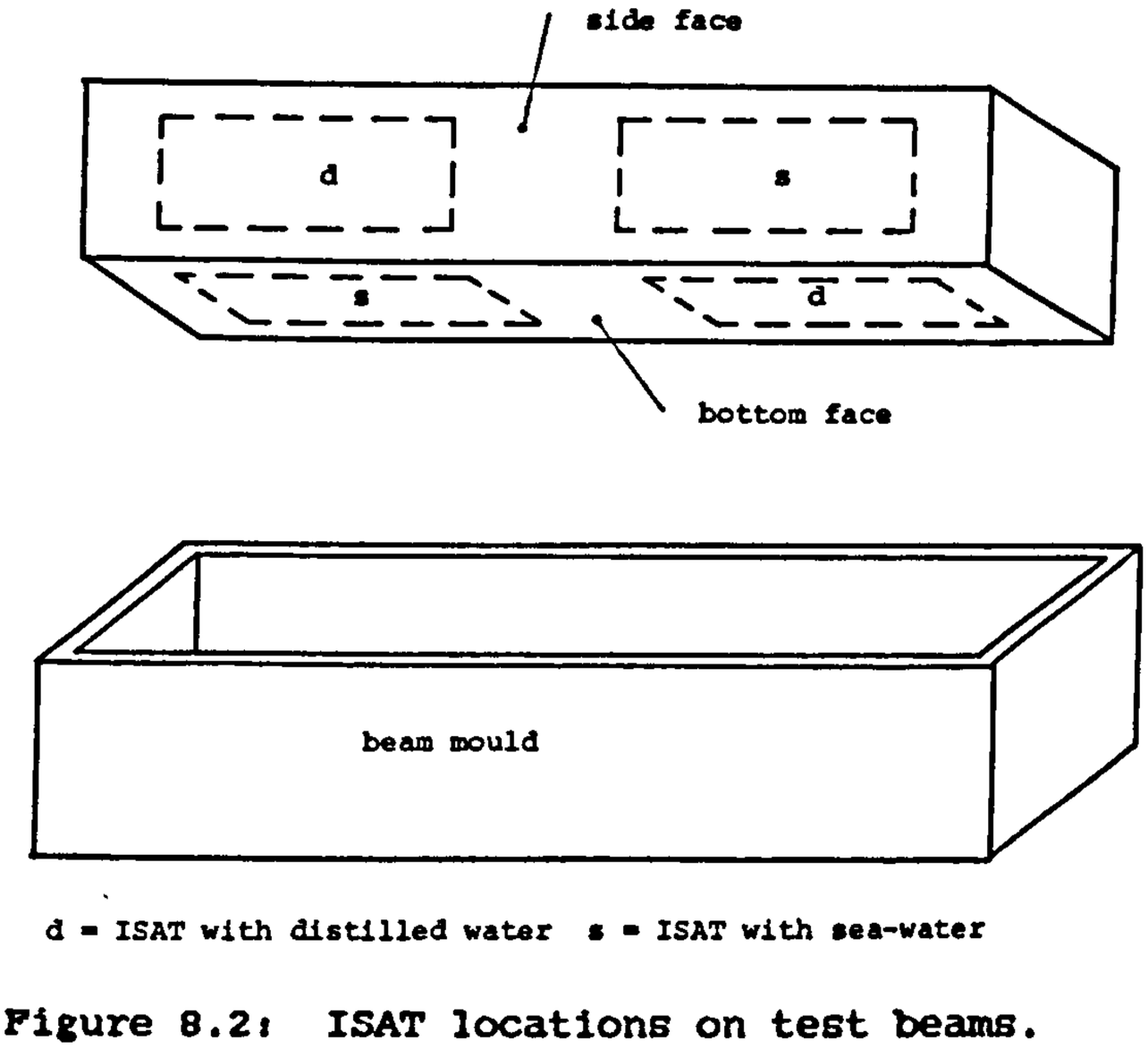

d = ISAT with distilled water s = ISAT with sea-water

Figure 8.2: ISAT locations on test beams.

As proposed by Levitt (1970b), the observed data corresponded closely to the relationship

$$ISA = a(time)^{-n}$$

where a and n are constants.

This is demonstrated by the linearity of the relationships between log ISA versus log time (see Figure 8.3). Each line in Figure 8.3 is the result of a linear regression analysis on the results of four tests. Clearly the bottom face was far less permeable than the side faces. Furthermore, the readings for the bottom face are more widely spread probably due to absorption being so low that secondary effects such as temperature variation, leaks and air in the system had a significant effect on meniscus movement in the capillary tube. Close visual examination of the beams showed the side faces to be more porous than the bottom faces, which were inevitably more thoroughly compacted. It was felt that the side faces corresponded more closely with typical *in situ* concrete and it was therefore the side faces that were tested in the main test programme, although the bottom faces were tested after oven-drying.

The Poiseuille equation for viscous flow through a fine capillary tube predicts that $ISA = a(time)^{-0.5}$. Levitt (1970a) found that, for concrete, n varied

between 0.3 and 0.7 and was constant for a specific concrete. In Figure 8.3, n varies between 0.8 and 1.1. Levitt proposed that the high rate of decay, n = 0.7, was due to silting up of pores, while the low rate of decay, n = 0.3, was associated with "capillary flushing action". Lydon (1980) reports values of n up to 0.88 for air-dried concretes, although the specimens tested were air-dried for at least 6 days and generally for around 10 weeks. Before equilibrium is obtained, an increasing humidity gradient exists between the surface and centre of a drying specimen. This is the probable cause of such high rates of decay.

Figure 8.3 also shows that sea-water is less rapidly absorbed than distilled water. This is probably primarily due to the greater viscosity of sea-water (see A2.2).

It was considered necessary to use either sea-water or distilled water for the main test programme, but to use sea-water on the sea-water exposed specimens and then distilled water on the limewater stored control specimens would be misleading. If sea-water were used as the permeating medium on control specimens the early stages of a surface layer might develop during the test period, thereby rendering the control specimens worthless. Furthermore, recalibration of the capillary tube after several 2 hour tests showed that the effective cross-sectional area of the tube reduced on using sea-water, probably due to deposition of sea salts onto the surface of the tube. It was felt to be extremely unlikely that distilled water if used as the permeating medium on a sea-water exposed specimen would cause significant inversion of aragonite to calcite (see 6.4.2.2) within the 2 hour duration of the test. Consequently distilled water was chosen as the permeating medium.

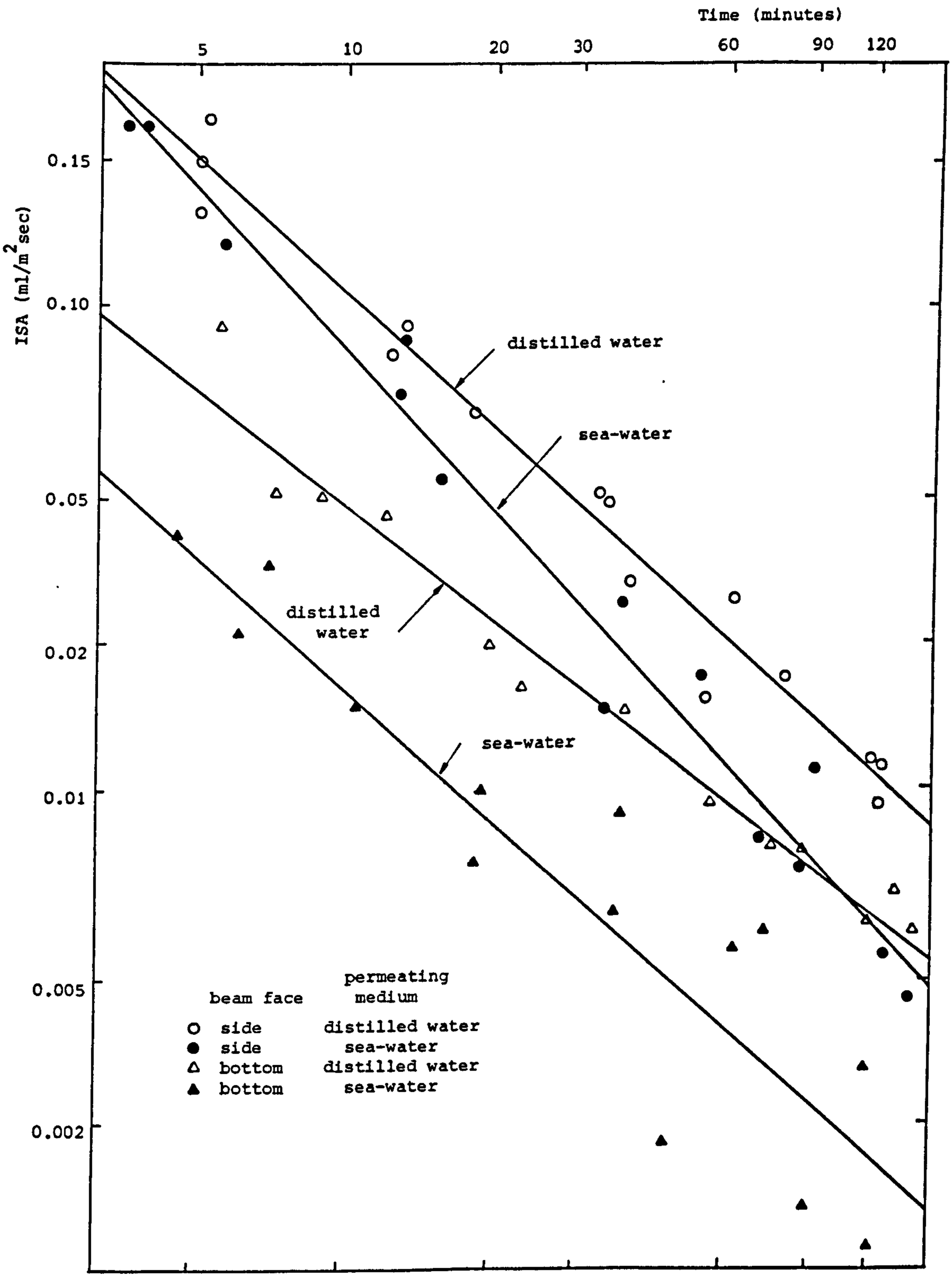

Figure 8.3: Variation of ISA with time using distilled water or sea-water as the permeating medium.

8.3 Main testing

Four 500 x 100 x 100 mm beams of plain concrete A (see A1.1 for mix details) were cast and cured in limewater for 28 days. They were then conditioned (8.2) for 3 days before each side face was ISA tested. Two test rigs were used (Figure 8.1), each beam being tested by both rigs. Readings were taken at approximately 10, 30, 60 and 90 minutes.

Although there was no visible difference, two of the beams were significantly more permeable than their counterparts, probably due to varying compaction. The two more permeable beams were immersed in a tank containing 85 ℓ of sea-water, the other two beams were immersed in limewater. The sea-water was replaced every 4 weeks. The beams were removed from the tanks, conditioned for 3 days, then retested after 9 and 23 weeks.

Figure 8.4 shows the log ISA versus log time plots for both the control and test beams at the 3 ages. Clearly little change occurred in the absorptive properties of the control specimens over the 23 week test period. However, it is clear that a very significant reduction in rate of absorption occurred in the case of the sea-water exposed specimens.

The results are made more understandable if presented as the volume of water per square metre absorbed (V) within a certain time period (t_2-t_1); (see Figure 8.5).

$$\log ISA = a + b \log t$$

where a and b are calculated from a linear regression analysis of the data.

Therefore, $ISA = 10^{a+b\log t} = 10^a t^b$.

Now $V = \int_{t_1}^{t_2} ISA\, dt = \frac{10^a}{b+1}(t_2^{b+1} - t_1^{b+1})$.

A sensible time to choose for t_2 is 6 hours, the average time that concrete in the tidal zone is submerged. Some of the preliminary tests were extended to 8 hours and the log ISA v. log time relationship was still linear. Levitt (1983)

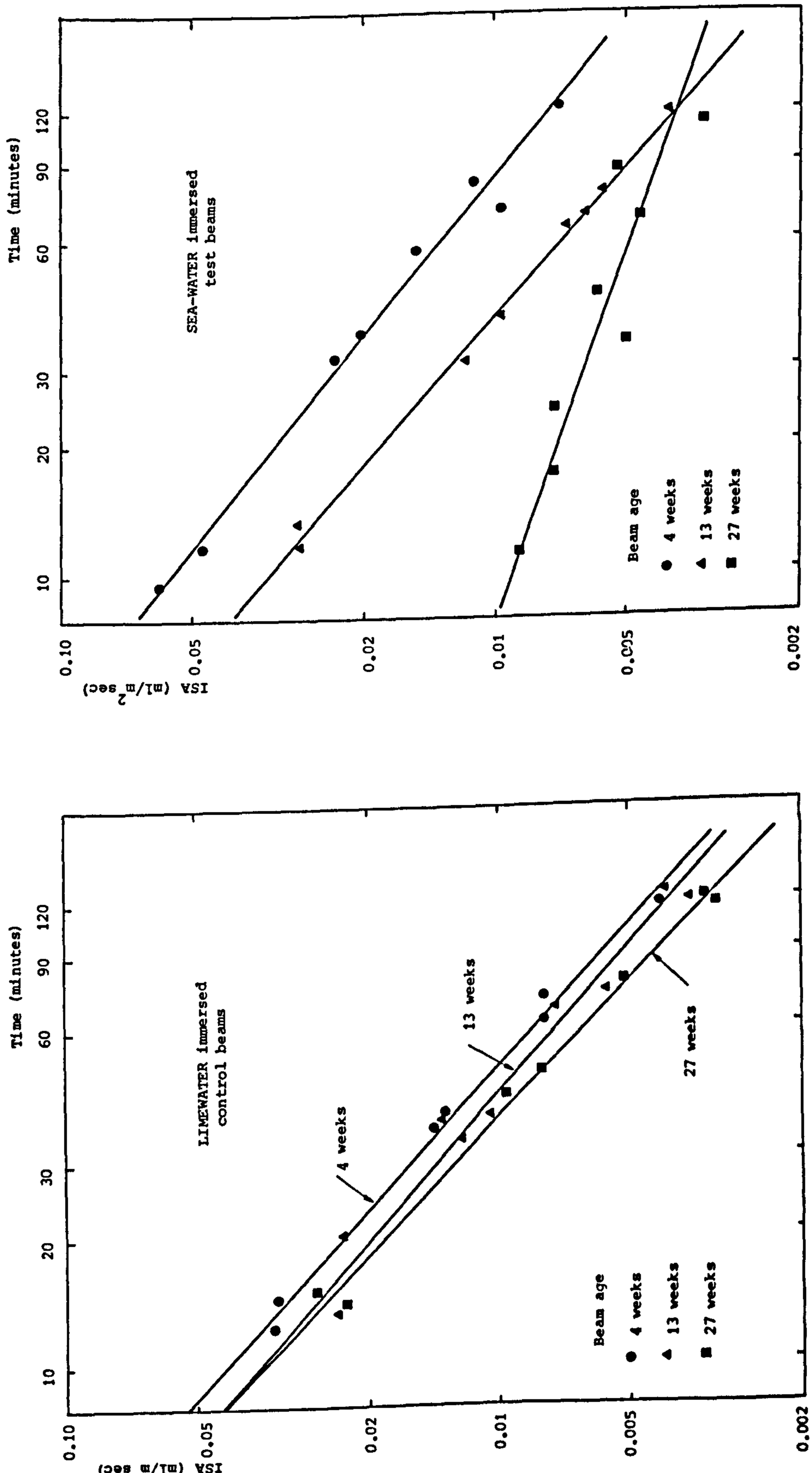

Figure 8.4: Progressive effect of sea-water immersion on ISA.

observed linearity for over 24 hours. Consequently it is reasonable to extrapolate the log ISA v. log time graph to 6 hours.

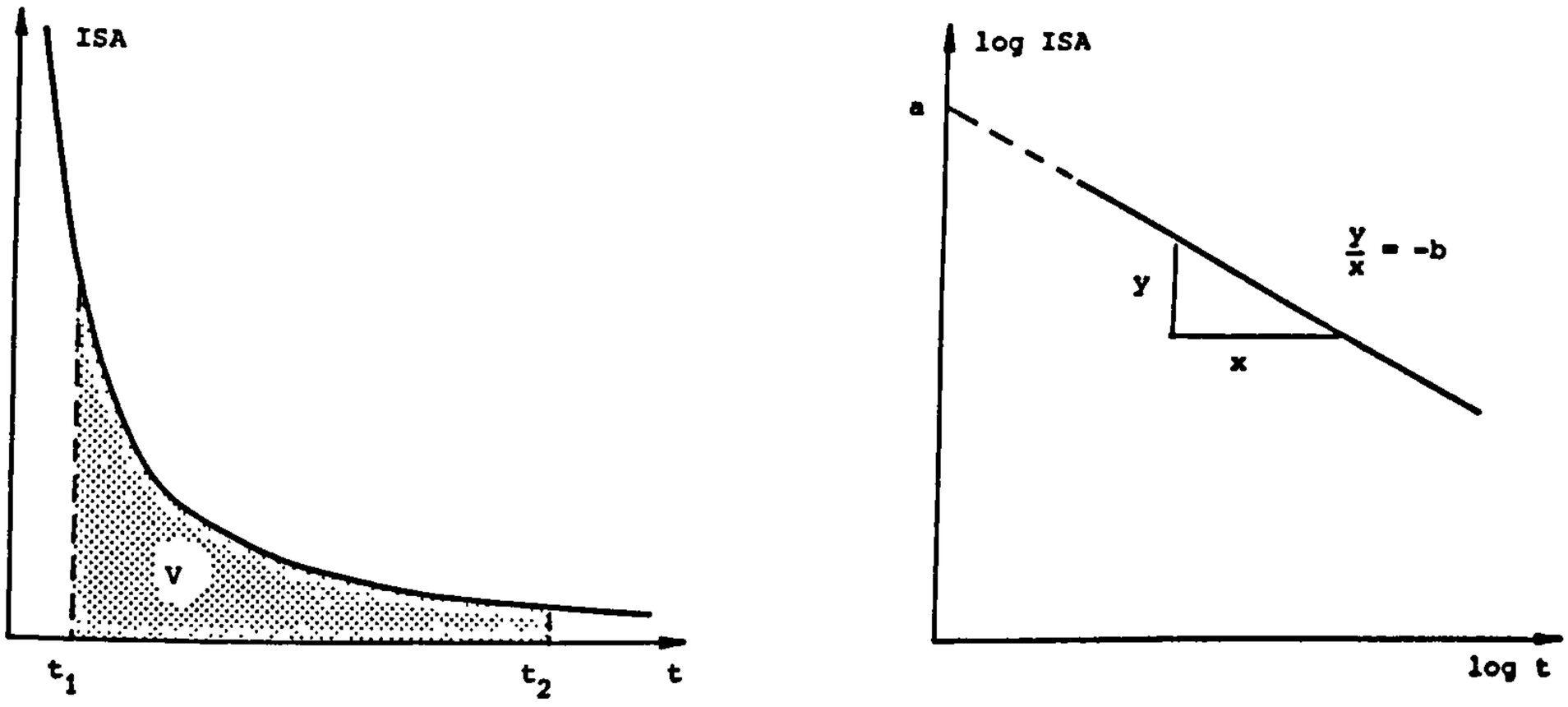

Figure 8.5: Calculation of total water absorbed from log ISA v. log time graph.

In theory t_1 should be set to zero. However, the first few seconds represent a relatively very large volume of water, which is extremely sensitive to a slight change in the slope of the linear regression line (b). A normally acceptable experimental error could cause a 30% change in the calculated first 5 seconds absorption at a relatively high value of b. Figure 8.6 shows the calculated water absorbed by the control beams over a 6 hour period for t_1 values of 0, 5 seconds and 1 minute. Clearly the values with the contribution from the first few seconds omitted are more sensible than the values with t_1 at zero.

Figure 8.7 shows the effect of sea-water exposure on subsequent absorption (t_1 = 5 seconds). The actual figures are of little consequence since different conditioning regimes would have given different values. However, the trend is clear; sea-water exposure results in a marked reduction in absorption.

After ISA testing the beams were oven-dried to constant weight at 105°C and their side and bottom faces were ISA tested; Figure 8.8 shows the corresponding log ISA v. log time plots. The most interesting aspect of this graph is that sea-water exposure reduces the rate of absorption of the side face to a value lower than that of the originally more dense bottom face. Table 8.1 shows the water absorbed over the initial 6 hour period with t_1 = 5 seconds.

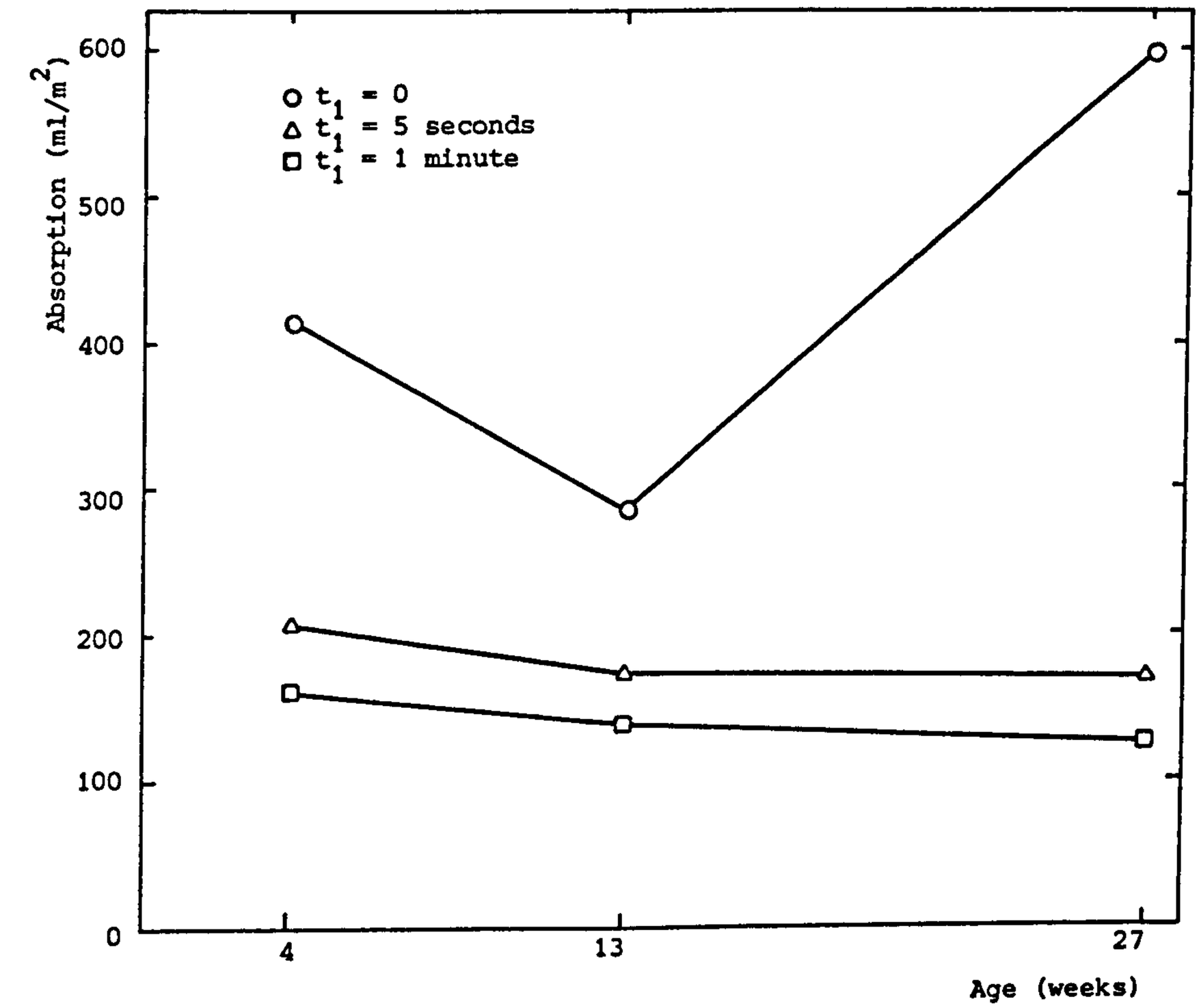

Figure 8.6: Calculated water absorbed in initial 6 hour period by control beams, at various ages, for different values of t_1.

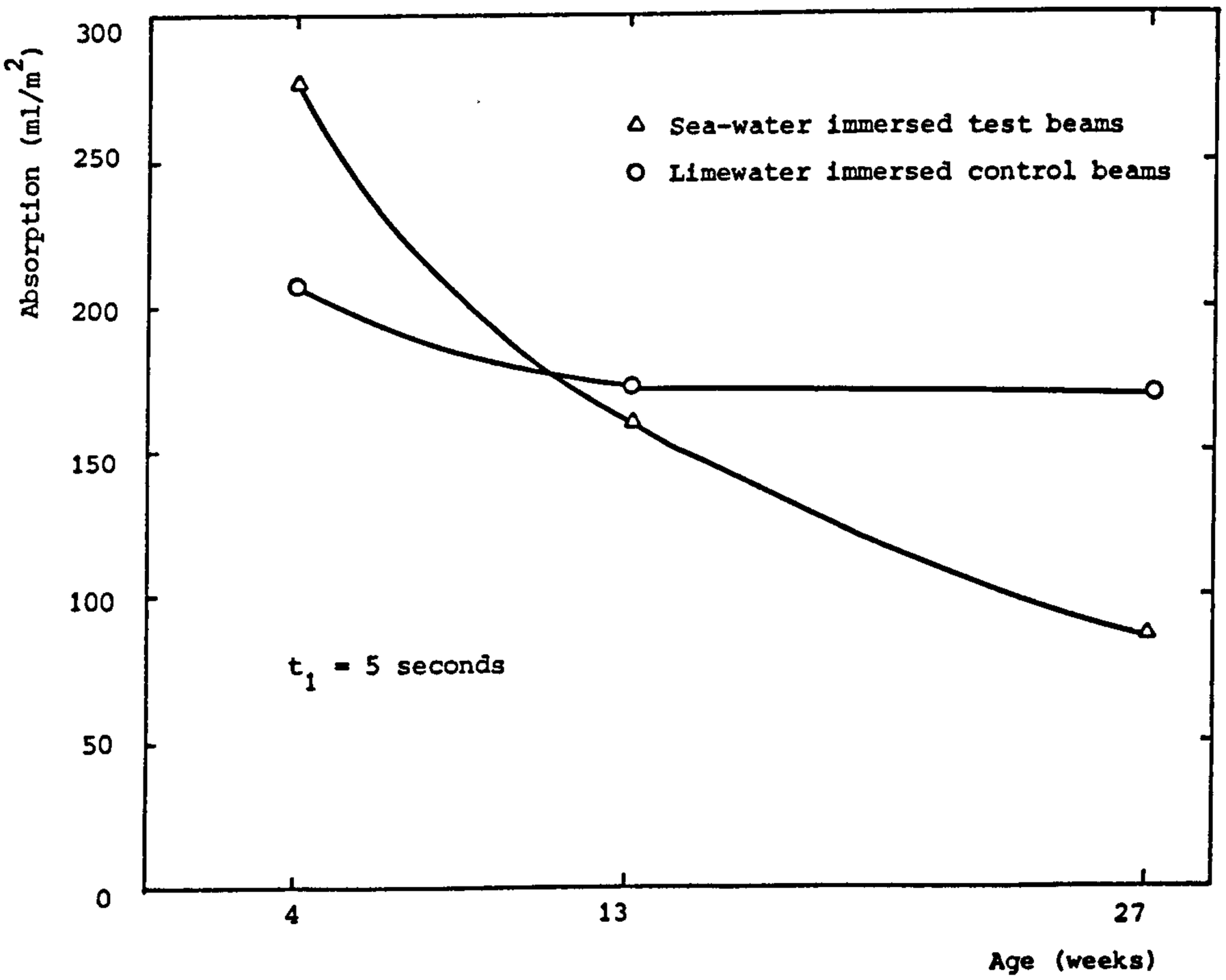

Figure 8.7: Water absorbed in initial 6 hour period by control and sea-water immersed beams at various ages.

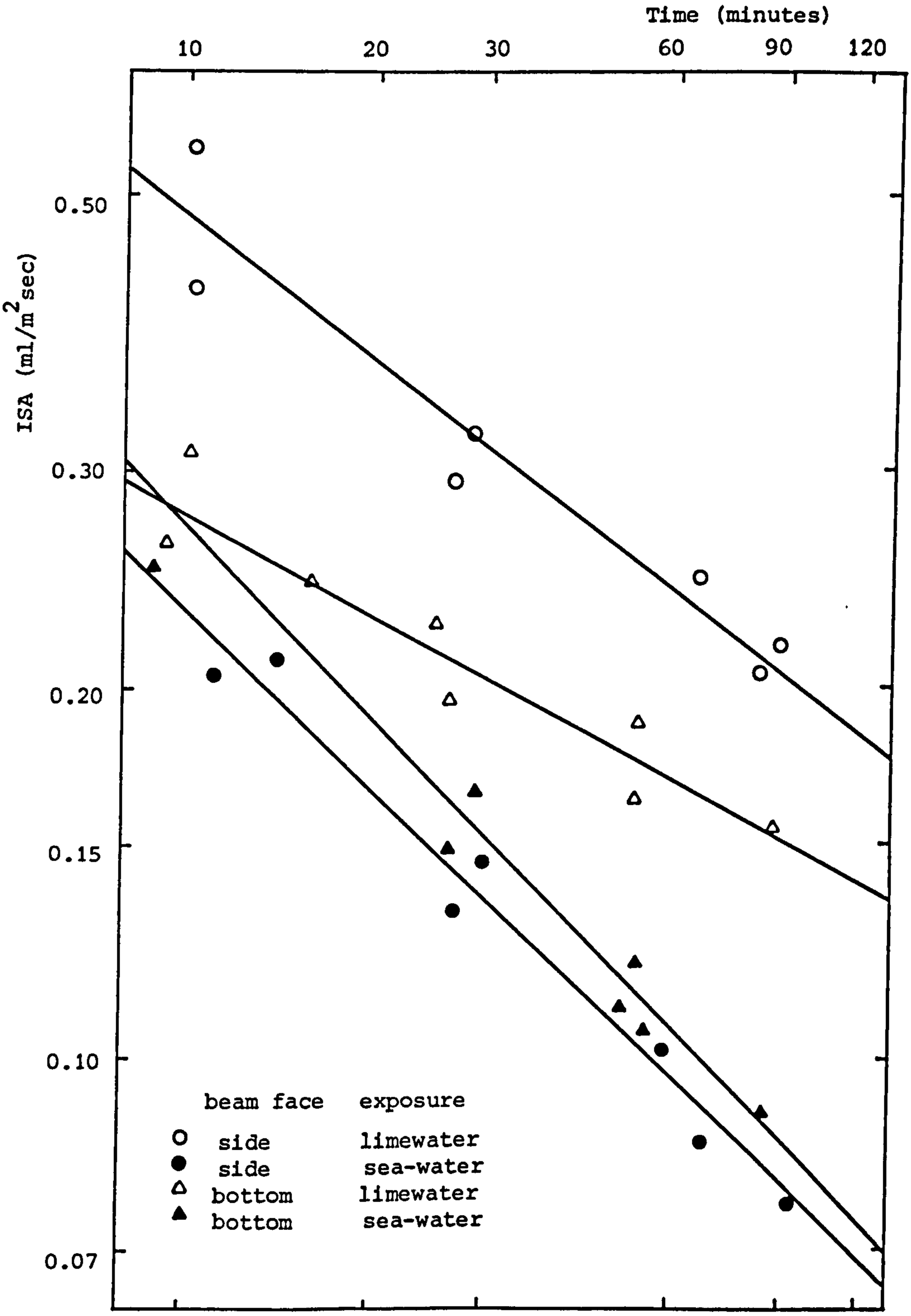

Figure 8.8: Effect of 23 weeks of immersion in sea-water on ISA (oven-dried beams).

	Water absorbed over initial 6 hours. ml/m^2	
	limewater control beams	sea-water test beams
side face	4183	1680
bottom face	3056	1845

Table 8.1: Effect of 23 weeks of sea-water exposure on water absorbed in initial 6 hour period (oven-dried beams).

It is concluded that the permeability-reducing mechanism induced by prolonged sea-water immersion significantly reduces the absorptive capacity of concrete.

Examination and analysis of wetting and drying test specimens (6.5, 6.6) suggest that the permeability-reducing mechanism is present, though less pronounced, in the tidal zone. Hence it is tentatively concluded that the volume of water (and hence ions) absorbed during the wetting phase of tidal zone exposure is also reduced over long periods of sea-water exposure.

Chapter 9 : THE SIGNIFICANCE OF THE PERMEABILITY-REDUCING PHENOMENON

A reduction in concrete permeability is likely to reduce the severity of almost all possible modes of degradation (see Table 2.5). Most importantly, reinforcement corrosion should be reduced as a consequence of the reduced ingress of chloride ion, carbon dioxide and oxygen and the increased resistivity.

The existence of the permeability-reducing phenomenon, and in particular the presence of the surface layer, should be appreciated when planning tests, or interpreting data from tests, on sea-water exposed concrete.

The surface layer is likely to have an effect on most *in situ* non-destructive test methods used to investigate the condition of offshore concrete structures. This is clearly to be expected since the layer also affects the performance of the concrete but if offshore concrete is compared with land-based concrete on the basis of such tests, misleading conclusions may be drawn. Electropotential measurements in the presence of a highly resistive layer could lead to smaller negative potentials than expected over the anode areas and consequent misinterpretation (Browne *et al*. 1983). Schmidt hammer measurements may give a misleading indication of concrete strength if the surface skin of the concrete is not removed prior to testing (Taylor Woodrow Research Laboratories 1980). A very dense surface layer might also affect the assessment of concrete density using ultrasonic pulse velocity and γ-ray backscatter techniques. If an area of concrete is water-jetted to remove marine growth (2.2.6) prior to examination, it should be appreciated that a large proportion of any surface layer will also be removed.

Permeability tests on relatively thin specimens cored from the surface of an offshore structure are likely to give an overestimation of the quality of the concrete as a whole.

Browne (1980) calculated the diffusion coefficient of chloride ion in concrete that had been exposed to a marine environment for 30 years from its chloride concentration profile as determined by analysing drillings. This data was then used to calculate profiles for different concretes at various ages. However, it is likely that the chloride profile at 30 years was not vastly dissimilar to the profile at 3 months, a large proportion of the chloride having entered before the permeability had been significantly reduced. It would be particularly

dangerous to use data acquired from a marine structure survey to predict the likely performance of concrete in a non-marine chloride environment (e.g. a bridge deck subjected to deicing salt) where the permeability-reducing mechanism is unlikely to be present.

It would be most informative if future surveys of offshore concrete structures included tests specifically designed to investigate the nature and effect of the surface skin. In particular:

(1) Examination and analysis of the concrete surface using SEM, EPMA, XRDA etc. (6.1).

(2) Resistivity measurements on short cores taken from sea-water exposed surfaces before and after grinding off the surface skin (5.9.3).

(3) Short term chloride ion diffusion tests (4.3.1) on discs cut from cores, at various depths into the structure.

(4) MIP of concrete samples (with large aggregate particles removed) at various depths into the structure.

The sensitivity of layer development to sea-water composition (6.4) should be taken into account when planning laboratory experiments involving the interaction of cement paste and sea-water. Clearly, particular care should be taken with the measurement of parameters dependent upon transport processes as, for example, in the case of reinforcment corrosion studies. However, even in structural performance tests, layer formation, or more accurately crack blocking, may have a very pronounced effect (5.7.3). The most important parameters to regulate would seem to be sea-water pH (Appendix 3) and magnesium ion concentration. Sea-water circulation is also to be recommended in order to eliminate local variations in sea-water composition.

Future corrosion models should take into account the likely decrease in rate of oxygen and chloride ion diffusion and the increase in resistivity of concrete exposed to sea-water.

Chapter 10 : CONCLUSIONS

An extensive literature survey of the performance of concrete in a marine environment disclosed a number of instances of concrete exhibiting a reduction in permeability as a result of exposure to sea-water (2.4.2). There were many conflicting proposals as to the mechanism producing such an effect.

A wide range of permeability test methods (3.2) were considered for use in investigating this permeability-reducing phenomenon. The first technique used to monitor permeability changes in concrete submerged in sea-water was an ion diffusion cell method (4.3). A theoretical study showed that the diffusion cell method was not appropriate for monitoring sulphate ion diffusion from sea-water, but the technique was found to provide a useful indication of changes in *chloride* ion diffusion over several months of exposure (4.3). Unfortunately however, the diffusion cell test had a number of drawbacks:

(a) there was little control of sea-water pH or composition;

(b) the specimens had to be relatively thin (which was later found to have caused a discrepancy with the behaviour of thicker specimens);

(c) there was a phase difference between a change in permeability and the accumulation of chloride ion being measured; i.e. an instantaneous indication of permeability was not afforded, particularly at low temperatures or for relatively impermeable mixes;

(d) control specimens had to be exposed to chloride ions (e.g. sodium chloride solution), and the diffusion coefficient was found to be dependent upon the source of chloride ion. Initial diffusion from sea-water was found to be considerably more rapid than diffusion from a sodium chloride solution of similar chloride concentration, although not as rapid as that from a magnesium chloride solution; and

(e) it was difficult to differentiate between surface and bulk effects.

All of these problems were overcome by developing an electrical resistivity technique.

Resistance measurement was found to be a useful method of monitoring changes in the permeability of mortar and concrete specimens. When the test solution is sea-water (or a comparable electrolyte significantly more conductive than limewater) resistance changes relative to a limewater-cured control specimen provide a lower bound indication of any increase in permeability.

Despite practical difficulties in accurately measuring the conductivity of a very small volume of pore solution, determination of Formation Factor (Equation 5.3) proved useful by highlighting certain features not apparent from the specimen resistance data alone (5.9.1).

All mixes studied showed a reduction in permeability on exposure to sea-water (4.3, 5.7-5.10, 8.3). In terms of ohmic resistance, a mortar incorporating blast-furnace slag exhibited the greatest reduction. However, the greatest relative change was shown by mortars C (OPC,0.6 w/c) and F (SRPC, 0.4 w/c), 25 mm thick specimens showing an increase in resistance equivalent to over 20 mm of additional thickness after only 10 weeks of sea-water exposure. This reduction in permeability was due to the formation of a discrete layer on the surface of the cement paste (Chapter 6) together with a more widespread bulk effect associated with a modification of the pore structure (Chapter 7).

A surface layer of brucite (magnesium hydroxide) was in evidence after only 1 day of submersion in sea-water, reaching its ultimate thickness of around 30 μm within 4 days (6.5). A continuous overlying layer of aragonite (calcium carbonate) was generally present after 28 days, having a thickness of around 100 μm after 3 months (6.5) and thickening on further exposure (6.3). The permeability of an OPC concrete was still reducing at an appreciable rate after 33 weeks of sea-water exposure (Figure 5.5). The precise thicknesses of the layers varied from specimen to specimen and, indeed, from location to location on the same specimen, but appeared to be more dependent upon environmental factors than on mix parameters. Theoretical considerations (6.4), confirmed by laboratory observations (6.6) suggest that layer development becomes more likely as sea-water pH increases. However, no reduction in surface resistance (5.9.2) or in surface layer thickness (6.5) was observed when sea-water pH was controlled by regular dosing rather than by sea-water replacement every 4 weeks. Both aragonite and brucite layers produce a reduction in permeability and it appears that neither is markedly more effective than the other.

The bulk effect was due to a shift in the pore size distribution of the cement paste. After 18 weeks of sea-water exposure there was generally a reduction in the volume of the pores with diameters (as measured by mercury intrusion porosimetry) greater than 1000 Å, accompanied by an increase in volume of the smaller pores (7.3). The mix incorporating pulverised fuel ash (mortar D) was an exception, exhibiting an *increase* in capillary porosity; this was

counteracted by the surface layer, producing an overall slight reduction in permeability (Figure 5.8).

Initial surface absorption testing showed that the absorptive capacity of 0.4 w/c ratio, OPC concrete is significantly reduced as a result of prolonged sea-water immersion (8.3).

Only a very limited number of naturally exposed specimens were tested and all were from the submerged zone. Unfortunately all specimens examined had been surface-scraped, to remove marine growth, prior to coring (5.7.4) and no distinct surface formation was identified (6.7). However, all specimens exhibited substantial surface resistances which were comparable with specimens submerged in sea-water in the laboratory.

The existence of the permeability-reducing phenomenon should be appreciated when planning tests, or interpreting data from tests on sea-water exposed concrete. It is also recommended that future surveys of offshore concrete structures should include tests specifically designed to investigate the nature and effect of the surface skin (Chapter 9).

The next phase of this research (Chapter 11) will be concerned with developing methods of deliberately enhancing the permeability-reducing phenomenon, which could, in due course, allow the specification of ultimately impermeable, and hence far more durable, concrete.

Chapter 11 : RECOMMENDATIONS FOR FURTHER WORK

This thesis reports part of an ongoing research programme. It is intended that most of the following research recommendations will be undertaken within the Concrete Section, Department of Civil Engineering, Imperial College.

The longest exposure period over which permeability was monitored in this work was 33 weeks, which is clearly a very small fraction of the likely life of an offshore structure. Laboratory tests are already planned to determine the effects of longer periods of sea-water exposure. 100 mm diameter mortar cylinders, with all faces except the cast face sealed, will be submerged in a carefully regulated sea-water tank. The tank will contain a very large volume of sea-water in relation to the volume of the specimens and will be accurately temperature-controlled which will allow effective use of a control module to regulate sea-water pH (Appendix 3). The sea-water will be vigorously circulated and will be replaced if the magnesium ion conmcentration should fall by 10%. Specimens will be tested after 3 months, 6 months, 1 year, 2 years and hopefully 5 years. Testing will involve sawing a 7 mm thick disc from the cast face end of the cylinder and measuring its chloride ion diffusion coefficient (4.3). The same specimen will then be used to determine pore size distribution (using MIP). This approach has the drawback of testing different specimens at each age, rather than monitoring changes in the permeability of a single specimen, but avoids problems associated with the long-term testing of unrepresentatively thin specimens (7.4).

A collaborative programme is planned in which more sophisticated quantitative techniques will be used to analyse the first few millimetres depth of sea-water exposed cement paste. This should shed light on the mechanism producing the shift in pore size distribution (7.3).

The marine environment can never be truly simulated in the laboratory and hence there is no substitute for the examination, analysis and testing of naturally exposed concrete. If such specimens were to become available, the most informative variable to embrace would be the exposure zone (Figure 2.1). It would also be interesting to test samples from coastal structures, ferrocement boats etc. The techniques that are recommended to investigate the nature and effect of the surface skin are outlined in Chapter 9.

Practical methods of enhancing the permeability-reducing phenomenon are shortly to be investigated. Surface layer development is likely to be more easily accelerated than modification of the cement paste pore structure. Methods of achieving rapid surface layer development are likely to involve early-age surface treatments rather than the use of admixtures.

No reference could be found in the literature to any investigation of the mechanisms producing the blocking of cracks in concrete in a marine environment, despite the enormous significance of such phenomena on the structural behaviour of reinforced concrete members subjected to cyclic loading (5.7.3), as well as the likely effect on reinforcement corrosion (2.2.8). Resistivity testing could be an effective means of investigating crack-blocking mechanisms. The main problem lies in producing realistic cracks whilst leaving specimens sufficiently intact to allow installation into the resistivity cells (5.7.3). Specimen encapsulation prior to taking samples should allow the preparation of polished sections (Appendix 8) of cracks, thereby facilitating examination and analysis of crack deposits.

The dramatic increase in the surface resistance of OPC mortar specimens exposed to sodium chloride solution (Figure 5.15) merits further investigation. It was thought to be likely that the mechanism producing such a phenomenon was associated with the formation of calcium chloroaluminate (5.9.2). Resistivity testing of specimens incorporating cements with various C_3A contents should clarify this issue. Certain cells should be adapted so that CO_2 may be bubbled through the sodium chloride solution; this will accelerate carbonation of the specimens and should shed light on whether the increased surface resistance is a permanent effect, or whether it is a transient phenomenon which is negated as the chloroaluminate in the surface zone decomposes due to the reduced pH.

The almost linear increase in resistivity (and Formation Factor) of the limewater-cured pfa mortar over the 18 week test period (Figure 5.8), despite the apparent constancy of pore structure (as measured by MIP), merits further research. Determination of open porosity using helium pycnometry or of pore size distribution using a capillary condensation method (7.1.3) should show whether this apparent ambiguity is due to the pfa/OPC hydration products being particularly fragile and hence partially destroyed at the high pressures necessary for MIP. It would also be interesting to determine the chloride ion diffusion coefficient of pfa mortars at various ages to show whether a progressive reduction is effected, as is implied by the resistivity test results.

REFERENCES

AMERICAN CONCRETE INSTITUTE, Standard 357R-78 (1978): Guide for the design and construction of fixed offshore concrete structures.

AMERICAN SOCIETY FOR TESTING AND MATERIALS, Standard C355-64 (1964): Standard test methods for water-vapor transmission of thick materials.

ARTHUR, P.D., EARL, J.C. and HODGKIESS, T. (1979) Fatigue of reinforced concrete in sea-water. Concrete, Vol. 13 (5), p. 26.

ARUP, H. (1983) The mechanisms of the protection of steel by concrete. In: CRANE, A.P., ed. Corrosion of reinforcement in concrete construction. The Society of Chemical Industry/Ellis Horwood Ltd., pp. 151-157.

ASKHEIM, N.E. and RØLAND, B. (1983) The relevance of present criteria for corrosion resistance of marine R.C. structures. Conference on Corrosion of Reinforcement in Concrete Construction. The Society of Chemical Industry, London, 20 pp.

ATKINS, P.W. (1983) Physical chemistry, 2nd ed. Oxford University Press, p. 897.

ATWOOD, W.G. and JOHNSON, A.A. (1924) The disintegration of cement in sea-water. Transactions of the American Society of Civil Engineers, Vol. 87, Paper No. 1533, pp. 204-230.

BAKER, A.F. (1984) Private communication.

BARRER, R.M., BARRIE, J.A. and ROGERS, M.G. (1962) Permeation through a membrane with mixed boundary conditions. Transactions of the Faraday Society, Vol. 58, pp. 2473-83.

BATHURST, R.G.C. (1976) Carbonate sediments and their diagenesis. Developments in sedimentology 12. 2nd ed. Elsevier Scientific Publishing Company.

BERNER, R.A. (1965) Activity coefficients of bicarbonate, carbonate and calcium ions in sea-water. Geochimica et Cosmochimica Acta, Vol. 29, pp. 947-965.

BERNER, R.A. (1971) Principles of chemical sedimentology. McGraw-Hill Book Company.

BERNHARDT, C.J. and SØPLER, B. (1974) An experimental study of steel in reinforced concrete in marine environment. Nordisk Betong, Vol. 2, pp. 22-32.

BHARGAVA, J. and REHNSTROM, A. (1978) Electrochemical aspects of electrical resistance gages for concrete. Swedish Council for Building Research, Stockholm, 35 pp.

BICZOK, I. (1967) Concrete corrosion and concrete protection. Budapest, Publishing House of the Hungarian Academy of Sciences.

BLATT, H., MIDDLETON, G. and MURRAY, R. (1980) Origin of sedimentary rocks. 2nd ed. Prentice-Hall, Inc.

BOGUE, R.H. and LERCH, W. (1934) Hydration of Portland cement compounds. Industrial and Engineering Chemistry, Vol. 26, pp. 837-842.

BRITISH STANDARDS INSTITUTION, BS 1881: Part 5: 1970, Methods of testing hardened concrete for other than strength.

BRITISH STANDARDS INSTITUTION, BS 1881: Part 122: 1983, Methods for determination of water absorption.

BRITISH STANDARDS INSTITUTION, BS 6235: 1982, Code of practice for fixed offshore structures.

BROECKER, W.S. (1974) Chemical oceanography. New York, Harcourt Brace Jovanovich.

BROWNE, R.D. (1980) Mechanisms of corrosion of steel in concrete in relation to design, inspection and repair of offshore and coastal structures. In: Performance of concrete in marine environment. Detroit, American

Concrete Institute, ACI Special Publication SP-65, pp. 169-204.

BROWNE, R.D. and BAKER, A.F. (1980) The performance of structural concrete in the marine environment. In: LYDON, F.D. ed. Developments in concrete technology. Barking, Applied Science Publishers Ltd., pp. 111-149.

BROWNE, R.D., GEOGHEGAN, M.P. and BAKER, A.F. (1983) Analysis of structural condition from durability results. In: CRANE, A.P., ed. Corrosion of reinforcement in concrete construction. The Society of Chemical Industry/Ellis Horwood Ltd., pp. 193-222.

CALLEJA, J. (1952) New techniques in the study of setting and hardening of hydraulic materials. Journal of the American Concrete Institute, Vol. 23, p. 525.

CALLEJA, J. (1953) Determination of setting and hardening time of high-alumina cements by electrical resistance techniques. Journal of the American Concrete Institute, Vol. 25, p. 249.

CHILINGAR, G.V., BISSELL, H.J. and FAIRBRIDGE, R.W., eds. (1967) Carbonate rocks: origin, occurrence and classification. Amsterdam, Elsevier, 471 pp.

COLE, W.F. (1953) A crystalline hydrated magnesium silicate formed in the breakdown of a concrete sea-wall. Nature, Vol. 171, pp. 354-5.

COLLEPARDI, M., MARCIALIS, A. and TURRIZIANI, R. (1972) Penetration of chloride ions into cement pastes and concretes. Journal of the American Ceramic Society, Vol. 55 (10), pp. 534-5.

CONJEAUD, M.L. (1980) Mechanism of sea-water attack on cement mortar. In: Performance of concrete in marine environment. Detroit, American Concrete Institute, ACI Special Publication SP-65, pp.39-61.

CONJEAUD, M.L. (1981) Private communication.

CORROSION INSTITUTE, DENMARK (1978) Galvanised steel in concrete, a necessary warning. Electroplating and Corrosion Newsletter.

CRANK, J. (1975) The mathematics of diffusion. 2nd ed. Oxford, Clarendon Press.

DÄRR, G.M. and LUDWIG, U. (1973) Determination of permeable porosity. Materials and Structures: Research and Testing, Vol. 6 (33), pp. 185-190.

DEER, W.A., HOWIE, R.A. and ZUSSMAN, J. (1965) Rock-forming minerals, Vol. 5: Non-silicates. 4th impression, Longmans.

DET NORSKE VERITAS (1977) Rules for the design, construction and inspection of offshore concrete structures.

DIAMON, M., AKIBA, J. and KONDO, R. (1971) Through pore size distribution and kinetics of carbonation reaction of Portland cement mortars. Journal of the American Ceramic Society, Vol. 54 (9), pp. 423-428.

DIAMOND, S. (1971) A critical comparison of mercury porosimetry and capillary condensation pore size distributions of Portland cement pastes. Cement and Concrete Research, Vol. 1, pp. 531-545.

DIAMOND, S. (1976) Cement paste microstructure - an overview at several levels. In: Hydraulic cement pastes: their structure and properties, Proceedings of a conference held at University of Sheffield, April 1976. Cement and Concrete Association, pp. 2-30.

DISTECHE, A. and DISTECHE, S. (1967) The effect of pressure on the dissociation of carbonic acid from measurement with buffered glass electrode cell. Journal of the Electrochemical Society, Vol. 114, pp. 330-340.

DORSCH, K.E. (1933) The hardening and corrosion of cement. Cement and Cement Manufacture, Vol. 6 (4), pp. 131-142.

DORSEY, N.E. (1940) Properties of ordinary water-substance. New York, Reinhold Publishing Corp.

DUEDALL, I.W. and WEYL, P.K. (1967) The partial equivalent volumes of salts in sea-water. Limnology and Oceanography, Vol. 12, pp. 52-59.

ERDEY-GRUZ, T. (1974) Transport phenomena in aqueous solutions. London, Adam Hilger Ltd.

EVERETT, L.M. and TREADAWAY, K.W.J. (1980) Deterioration due to corrosion in reinforced concrete. BRE Information Paper IP 12/80.

FAIRBRIDGE, R.W. (1966) The encyclopaedia of oceanography. New York, Reinhold Publishing Corp.

FEDERATION INTERNATIONALE DE LA PRECONTRAINTE (1977) Recommendations for the design and construction of concrete sea structures. 3rd ed.

FELDMAN, R.F. (1973) Helium flow characteristics of rewetted specimens of dried hydrated Portland cement paste. Cement and Concrete Research, Vol. 3 (6), pp. 777-790.

FELDMAN, R.F. and SEREDA, P.J. (1968) A model for hydrated Portland cement paste as deduced from sorption-length change and mechanical properties. Materials and Structures, Vol. 1 (6), pp. 509-519.

FIDJESTØL, P. and NILSEN, N. (1980) Field test of reinforcement corrosion in concrete. In: Performance of concrete in marine environment. Detroit, American Concrete Institute, ACI Special Publication SP-65, pp. 205-221.

FIGG, J.W. (1973) Methods of measuring the air and water permeability of concrete. Magazine of Concrete Research, Vol. 25 (85), pp. 213-219.

FIGG, J.W. (1983) Chloride and sulphate attack on concrete. Durable Concrete Symposium, The Institute of Concrete Technology, London.

FLUSS, P.J. and GORMAN, S.S. (1958) Discussion of "Use of concrete in marine environments" by Wakeman *et al.*. Journal of the American Concrete Institute. Proceedings, Vol. 54, pp. 1309-1346.

FORTEATH, G.N.R., PICKEN, G.B. and RALPH, R. (1984) Patterns of macrofouling on steel platforms in the central and northern North Sea. In: LEWIS, J.R. and MERCER, A.D., eds. Corrosion and marine growth on offshore structures. Ellis Horwood Publishers, pp. 10-22.

FRIEDMAN, G.M. (1959) Identification of carbonate minerals by staining methods. Journal of Sedimentary Petrology, Vol. 29 (1), pp. 87-97.

FYFE, W.S. and BISCHOFF, J.L. (1965) The calcite-aragonite problem. In: PRAY, L.C. and MURRAY, R.C., eds. Dolomitization and limestone diagenesis: a symposium. Society of Economic Paleontologists, Special Publication No. 13, pp. 3-13.

GJORV, O.E. (1968) Durability of reinforced concrete wharves in Norwegian harbours. The Norwegian Committee on Concrete in Sea-water, Ingeniorforlaget A/S, Oslo.

GJORV, O.E. (1971) Long-time durability of concrete in sea-water. Journal of the American Concrete Institute. Proceedings, Vol. 68, pp. 60-67.

GJORV, O.E. (1973) Durability of concrete structures in the ocean environment. FIP Symposium: Concrete Sea Structures, Tbilisi, September 1972. London, Federation Internationale de la Precontrainte, pp. 141-145.

GJORV, O.E. and VENNESLAND, O. (1979) Diffusion of chloride ions from sea-water into concrete. Cement and Concrete Research, Vol. 9, pp. 229-238.

GJORV, O.E., VENNESLAND, O. and EL-BUSAIDY, A.H.S. (1976) Diffusion of dissolved oxygen through concrete. Corrosion 76, Paper No. 17, Houston, National Association of Corrosion Engineers, 13 pp.

GJORV, O.E., VENNESLAND, O. and EL-BUSAIDY, A.H.S. (1977) Electrical resistivity of concrete in the oceans. Proceedings: Ninth Offshore Technology Conference, Houston. OTC paper No. 2803, pp. 581-588.

GLANVILLE, W.H. (1931) The permeability of Portland cement concrete. Department of Scientific and Industrial Research. Building Research Technical Paper No. 3.

GLASSTONE, S. (1948) Textbook of physical chemistry. 2nd ed. London, Macmillan and Co. Ltd.

GOTO, S. and ROY, D.M. (1981) Diffusion of ions through hardened cement pastes. Cement and Concrete Research, Vol. 11, pp. 751-7.

GREGG, S.J. and SING, K.S.W. (1967) Adsorption, surface area and porosity. London, Academic Press.

HAMMOND, E. and ROBSON, T.D. (1955) Comparison of electrical properties of various cements and concretes. The Engineer, Vol. 199, pp. 78-80 and 114-115.

HANSSON, I.L.H. and HANSSON, C.M. (1983) Electrical resistivity measurements of Portland cement based materials. Cement and Concrete Research, Vol. 13, pp. 675-683.

HARNED, H.S. and SCHOLES, S.R. (1941) The ionisation constant of HCO_3^- from 0 to 50°C. Journal of the American Chemical Society, Vol. 63, pp. 1706-1709.

HARRIS, M.R. (1965) A source of error in the computation of pore size data from nitrogen sorption isotherms. Chemistry and Industry, Feb. 6 1965, pp. 268-9.

HAYNES, H.H. (1974) Long-term deep ocean test of concrete spherical structures, part I: Fabrication, emplacement and initial inspections. Technical Report R-805, Civil Engineering Laboratory, NCBC, Port Hueneme, California, 35 pp.

HAYNES, H.H. (1979) Long-term deep ocean test of concrete spherical structures - results after 6 years. Technical Report R-869, Civil Engineering Laboratory, NCBC, Port Hueneme, California, 48 pp.

HAYNES, H.H. (1980) Permeability of concrete in sea-water. In: Performance of concrete in marine environment. Detroit, American Concrete Institute, ACI Special Publication SP-65, pp. 21-38.

HAYNES, H.H. and KAHN, L.F. (1972) Behaviour of 66-inch concrete spheres under short- and long-term hydrostatic loading. Technical Report R-774, Civil Engineering Laboratory, NCBC, Port Hueneme, California, 85 pp.

HAYNES, H.H. and ZUBIATE, P.C. (1973) Compressive strength of 67-year old concrete submerged in sea-water. Technical Note N-1308, Naval Civil Engineering Laboratory, Port Hueneme, California.

HELMUTH, R.A. (1962) Capillary size restrictions on ice formation in hardened Portland cement pastes. Proceedings: Fourth International Symposium on the Chemistry of Cement, Washington 1960. Washington, National Bureau of Standards, Vol. II, pp. 855-869.

HENRY, R.L. (1964) Water vapor transmission and electrical resistivity of concrete. Technical Report R-314, Naval Civil Engineering Laboratory, Port Hueneme, California.

HOHN, R. (1973) On the climatology of the North Sea. In: GOLDBERG, E.D., ed. North Sea science. MIT press.

HORNE, R.A. (1969) Marine chemistry: the structure of water and the chemistry of the hydrosphere. Wiley-Interscience.

KALOUSEK, G.L. and BENTON, E.J. (1970) Mechanism of sea-water attack on cement pastes. Journal of the American Concrete Institute. Proceedings, Vol. 67, pp. 187-192.

KHOURY, G.A. and SULLIVAN, P.J.E. (1984) The effect of elevated temperatures on concrete. To be published by Applied Science Publishers.

KING, C.A.M. (1975) Introduction to physical and biological oceanography. London, Edward Arnold.

KING, R.A., DAWSON, J.L. and GEARY, D. (1979) On the detection, repair and prevention of corrosion of steel reinforcements in marine reinforced concrete structures. In: Corrosion of steel reinforcements in concrete construction. The Society of Chemical Industry, London, pp. 135-143.

KONDO, R., SATAKE, M. and USHIYAMA, H. (1974) Diffusion of various ions in hardened Portland cement. Review of the 28th General Meeting, The Cement Association of Japan, Tokyo. pp. 41-43.

LAWRENCE, C.D. (1981) Durability of concrete: molecular transport processes and test methods. Slough, Cement and Concrete Association, Technical Report 544, 25 pp.

LAWRENCE, C.D. (1982) Permeability measurements on concretes. Cement and Concrete Association, Departmental Note DN/4038.

LEA, F.M. (1970) The chemistry of cement and concrete. 3rd ed. Edward Arnold.

LEEMING, M.B. (1983) Corrosion of steel reinforcements in offshore concrete - experience from the Concrete in the Oceans Programme. In: CRANE, A.P., ed. Corrosion of reinforcement in concrete construction. The Society of Chemical Industry/Ellis Horwood Ltd., pp. 59-78.

LEVITT, M. (1970a) Non-destructive testing of concrete by the initial surface absorption method. Proceedings: Symposium on Non-Destructive Testing of Concrete and Timber. London, Institution of Civil Engineers, June 1969. Institution of Civil Engineers, pp. 23-26.

LEVITT, M. (1970b) The ISAT - a non-destructive test for the durability of concrete. The British Journal of Non-Destructive Testing, Vol. 13 (4), 7 pp.

LEVITT, M. (1983) Private communication.

LEVY, M. (1960) The permeability and absorption of precast concrete products. Civil Engineering, January and February, 8 pp.

LI, Y-H. (1967) The degree of saturation of $CaCO_3$ in the oceans. PhD thesis, Columbia University, New York, 176 pp.

LONGUET, P., BURGLEN, L. and ZELWER, A. (1973) La phase liquide du ciment hydrate. Revue des Materiaux de Construction et des Travaux Publics, Vol. 676, pp. 35-41.

LYDON, F.D. (1980) A note on the initial surface absorption test applied to lightweight concrete. Precast Concrete, August 1980, pp. 367-369.

LYMAN, J. (1956) Buffer mechanism of sea-water. PhD thesis, University of California, Los Angeles, 198 pp.

LYSE, I. (1961) Durability of concrete in sea-water. Journal of the American Concrete Institute. Proceedings, Vol. 57, pp. 1575-1584.

MACINTYRE, W.G. (1965) The temperature variation of the solubility product of calcium carbonate in sea-water. Fisheries Research Board, Canada. Report Series No. 200, 153 pp.

MAKITA, M., MORI, Y. and KATAWAKI, K. (1980) Performance of typical protection methods for reinforced concrete in marine environment. In: Performance of concrete in marine environment. Detroit, American Concrete Institute, ACI Special Publication SP-65, pp. 453-471.

MATHER, B. (1982) Concrete in sea-water. Concrete International, Vol. 4 (3), pp. 28-34.

MEADOWS, P.S. and ANDERSON, J.G. (1966) Micro-organisms attached to marine and freshwater sand grains. Nature, Vol. 212, pp. 1059-1060.

MEADOWS, P.S. and ANDERSON, J.G. (1968) Micro-organisms attached to marine sand grains. Journal of the Marine Biological Association of the United Kingdom, Vol. 48, pp. 161-175.

MEHTA, P.K. (1973) Mechanism of expansion associated with ettringite formation. Cement and Concrete Research, Vol. 3, pp. 1-6.

MEHTA, P.K. (1980) Durability of concrete in marine environment - a review. In: Performance of concrete in marine environment. Detroit, American Concrete Institute, ACI Special Publication SP-65, pp. 1-20.

MEHTA, P.K. (1983) Mechanism of sulphate attack on Portland cement concrete - another look. Cement and Concrete Research, Vol. 13, pp. 401-406.

MEHTA, P.K. and HAYNES, H. (1975) Durability of concrete in sea-water. Journal of the American Society of Civil Engineers, Structural Division, Vol. 101 (ST8), pp. 1679-1686.

MIDGLEY, H.G. and ILLSTON, J.M. (1980) Effect of chloride penetration on the properties of hardened cement pastes. Proceedings: Seventh International Symposium on the Chemistry of Cements, Paris, Vol. 3, pp. VII 101-103.

MILLERO, F.J. (1979) Effects of pressure and temperature on activity coefficients. In: PYTKOWICZ, R.M., ed. Activity coefficients in electrolyte solutions. Florida, CRC Press, Inc., Ch. 2, Vol. II, pp. 63-151.

MONFORE, G.E. (1968) The electrical resistivity of concrete. Journal of the Portland Cement Association, Research and Development Laboratories. Vol. 10 (2), pp. 35-48.

MORRISON, G.L., GILLILAND, W.J., BUKOVATZ, J.E., JAYAPRAKASH, G.P. and SEITZ, R.D. (1979) An evapo-transmission method for determining relative permeability of concrete. Federal Highway Administration, U.S. Dept. of Transportation, Washington. Research report FHWA-KS-79-1.

MORTIMER, C.E. (1975) Chemistry - a conceptual approach. 3rd ed. D. van Nostrand Co.

MURATA, J. (1965) Studies on the permeability of concrete. RILEM Bulletin, No. 29, pp. 47-54.

NEVILLE, A.M. (1978) Properties of concrete. 2nd ed. Pitman Publishing Ltd.

PAGE, C.L. (1975) Mechanism of corrosion protection in reinforced concrete marine structures. Nature, Vol. 258, pp. 514-5.

PAGE, C.L., SHORT, N.R. and EL TARRAS, A. (1981) Diffusion of chloride ions in hardened cement pastes. Cement and Concrete Research, Vol. 11, pp. 395-406.

PAGE, C.L. and TREADAWAY, K.W.J. (1982) Aspects of the electrochemistry of steel in concrete. Nature, Vol. 297, pp. 109-115.

PARKHOMENKO, E.I. (1967) Electrical properties of rocks. New York, Plenum Press.

PARKINSON, J. (1982) Durability conflict gains strength. New Civil Engineer, 19th May 1983, pp. 24-25.

PARROTT, L.J. (1981) Effect of drying history upon the exchange of pore water with methanol and upon subsequent methanol sorption behaviour in hydrated alite paste. Cement and Concrete Research, Vol. 11, pp. 651-658.

PHILIP, J.R. and DE VRIES, D.A. (1957) Moisture movement in porous materials under temperature gradients. Transactions of the American Geophysical Union, Vol. 38, pp. 222-232.

POBEGUIN, T. (1954) Contribution a l'etude des carbonates de calcium, precipitation du calcaire par les vegetaux, comparaison avec le monde animal. Annales des sciences naturelles. Botanique et biologie vegetale, Vol. 15, pp. 29-109.

POPOVICS, S., SIMEONOV, Y., BOZHINOV, G. and BAROVSKY, N. (1983) Durability of reinforced concrete in sea-water. In: CRANE, A.P., ed. Corrosion of reinforcement in concrete construction. The Society of Chemical Industry/Ellis Horwood Ltd., pp. 19-38.

POWERS, T.C. (1958) Structure and physical properties of hardened Portland cement paste. Journal of the American Ceramic Society, Vol. 41, pp. 1-6.

POWERS, T.C. (1979) The specific surface area of hydrated cement obtained from permeability data. Materials and Structures, Vol. 12 (69), pp. 159-168.

POWERS, T.C. and BROWNYARD, T.L. (1946-7) Studies of the physical properties of hardened Portland cement paste, (Nine parts). Journal of the American Concrete Institute, Vol. 43.

POWERS, T.C., COPELAND, L.E., HAYES, J.C. and MANN, H.M. (1954) Permeability of Portland cement paste. Journal of the American Concrete Institute, Vol. 51, pp. 285-298.

POWERS, T.C., COPELAND, L.E. and MANN, H.M. (1959) Capillary continuity or discontinuity in cement pastes. Journal of the Portland Cement Association, Research and Development Laboratories, Vol. 1 (2), pp. 38-48.

PREECE, C.M., FROLUND, T. and BAGER, D.H. (1981) Chloride ion diffusion in low porosity silica cement paste. Proceedings: Nordisk miniseminar on silica in concrete, Cement and Concrete Research Institute, NTH, Trondheim, Norway.

OST, B. and MONFORE, G.E. (1966) Penetration of chloride into concrete. Journal of the Portland Cement Association, Research and Development Laboratories, Vol. 8, pp. 46-52.

OWEN, B.B. and BRINKLEY, S.R. (1941) Calculation of the effect of pressure upon ionic equilibria in pure water and in salt solutions. Chemical Reviews, Vol. 29, pp. 1540-1541.

RAMACHANDRAN, V.S., FELDMAN, R.F. and BEAUDOIN, J.J. (1981) Concrete science, treatise on current research. Heydon.

REGOURD, M. (1975) The action of sea-water on cements. Annales de l'Institut Technique du Batiment et des Travaux Publics, No. 329, pp. 86-102.

RICHARDS, P.W. (1982) A laboratory investigation into the water permeability and compressive strength properties of plain concretes produced with and without pulverised fuel ash as affected by curing temperature. Slough, Cement and Concrete Association, Advanced Concrete Technology Project.

ROBINSON, R.A. and STOKES, R.H. (1959) Electrolyte solutions. 2nd ed. London, Butterworths.

ROSE, D.A. (1965) Water movement in unsaturated porous materials. RILEM Bulletin, No. 29, pp. 119-123.

RUBENCHIK, L.I. (1942) Microorganisms as a factor in the corrosion of cement and concrete. Chemical Abstracts, Vol. 36 (6770).

SCHIESSEL, P. (1975) Relationship between crack width and corrosion on the reinforcement. Beton + Fertigteil-Technik, Heft 12.

SPENCER, R.W. (1937) Measurement of the moisture content of concrete. Journal of the American Concrete Institute, Vol. 9 (1), pp. 45-61.

SPINKS, J.W.T., BALDWIN, H.W. and THORVALDSON, T. (1952) Tracer studies of diffusion in set Portland cement. Canadian Journal of Technology, Vol. 30 (1), pp. 20-28.

STILLWELL, J.A. (1983) Exposure tests on concrete for offshore structures. Published for the Concrete in the Oceans Management Committee by the Cement and Concrete Association, Slough. 59pp.

STRATFULL, R.F. (1968) How chlorides affect concrete used with reinforcing steel. Material Protection, Vol. 7 (3), pp. 29-34.

STRATFULL, R.F. (1983) Criteria for the cathodic protection of bridge decks. In: CRANE, A.P., ed. Corrosion of reinforcement in concrete construction. The Society of Chemical Industry/Ellis Horwood Ltd., pp. 287-331.

SUESS, E. (1970) Interaction of organic compounds with calcium carbonate: I association of phenomena and geochemical implications. Geochimica et Cosmochimica Acta. Vol. 34, pp. 157-168.

TAYLOR WOODROW RESEARCH LABORATORIES, (1980) Marine durability survey of the Tongue Sands Tower. Published for the Concrete in the Oceans Management Committee by the Cement and Concrete Association, Slough. 141 pp.

TEYCHENNE, D.C., FRANKLIN, R.E. and ERNTROY, H.C. (1975) Design of normal concrete mixes. London, HMSO.

THORVALDSON, T. and WOLOCHOW, D. (1938) The action of sulphate solutions on steam-cured composite cement mortars. Journal of the American Concrete Institute. Proceedings, No. 34, pp. 241-265.

TUUTTI, K. (1980) Service life of structures with regard to corrosion of embedded steel. In: Performance of concrete in marine environment. Detroit, American Concrete Institute, ACI Special Publication SP-65, pp. 223-236.

UEG, (1982) Applications for concrete offshore. UEG Report UR20. 147 pp.

USHIYAMA, H. and GOTO, S. (1974) Diffusion of various ions in hardened Portland cement paste. Proceedings: Sixth International Congress on the Chemistry of Cement, Moscow. Vol. II-1, pp. 331-337.

VASSIE, P.R. (1980) A survey of site tests for the assessment of corrosion in reinforced concrete. Transport and Road Research Laboratory, Laboratory Report 953.

VERBECK, G.J. (1968) Field and laboratory studies of the sulphate resistance of concrete. In: SWENSON, E.G. ed. Performance of concrete. Canadian Building Series No. 2, University of Toronto Press, pp. 113-124.

VICAT, L.J. (1857) Recherches sur les causes physiques de la destruction des composes hydrauliques par l'eau de mer, etc. Bulletin de la Societe d'Encouragement pour l'Industrie Nationale.

VINOGRAD, J.R. and McBAIN, J.W. (1942) Diffusion of electrolytes and of their mixtures. American Chemical Society Journal, Vol. 63, pp. 2008-2015.

VOGEL, A.I. (1978) A textbook of quantitative inorganic analysis, 4th ed. London, Longman, p.754.

WELTY, J.R. (1974) Engineering heat transfer. Wiley.

WHITING, D. (1981a) Rapid determination of the chloride permeability of concrete. Federal Highway Administration, U.S. Department of Transportation, Washington. Research Report FHWA/RD-81/119, p.9.

WHITING, D. (1981b) Rapid measurement of the chloride permeability of concrete. Public Roads Magazine, Vol. 45 (3), pp. 101-112.

WHITTINGTON, H.W., McCARTER, J. and FORDE, M.C. (1981) The conduction of electricity through concrete. Magazine of Concrete Research, Vol. 33 (114), pp. 48-60.

WILKINS, N.J.M. and LAWRENCE, P.F. (1980) Fundamental mechanisms of corrosion of steel reinforcements in concrete immersed in sea-water. Concrete in the Oceans Technical Report No. 6, Cement and Concrete Association.

WINSAUER, W.O. and McCARDELL, W.M. (1953) Ionic double-layer conductivity in reservoir rock. Transactions of the American Institute of Mining and Metallurgical Engineer, 198, pp. 129-134.

WINSLOW, D.N. and DIAMOND, S. (1974) Specific surface of hardened Portland cement paste as determined by small angle X-ray scattering. Journal of the American Ceramic Society, Vol. 57 (5), pp. 193-197.

WOELFL, G.A. and LAUER, K. (1979) The electrical resistivity of concrete with emphasis on the use of electrical resistance for measuring moisture content. Cement, Concrete and Aggregates, Vol. 1 (2), pp. 64-67.

WORTHINGTON, P.F. and BARKER, R.D. (1972) Methods for calculation of true formation factors in the bunter sandstone of northwest England. Engineering Geology, Vol. 6, pp. 213-228.

Appendix 1: Specimens

A1.1 Mix details

Although it was strongly suspected that the permeability-reducing mechanism was associated with the cement paste, it was regarded as essential to relate the effects being monitored to the likely performance of offshore concrete. Furthermore, it was expected that the presence of aggregate-paste interfaces would influence the transport processes being investigated. However, most of the test techniques used involve relatively small specimens and 10 mm was regarded as the maximum size of aggregate that would be acceptable within a 25 mm thick resistivity specimen (Chapter 5). Even 10 mm was too great for ion diffusion (Chapter 4), MIP (Chapter 7) and chloride ion concentration profile specimens (Appendix 6). It was therefore decided to test concrete with a maximum aggregate size of 10 mm and mortars with the same mix proportions but with the coarse aggregate omitted.

Table A1.1 shows details of the mixes tested. Table A1.2 shows the mix proportions, strengths and workabilities of either the mixes tested, or of the concretes on which the mortars tested were based. Mortars B, D, E and F are simply the corresponding concretes with the 10 mm aggregate omitted.

Mix reference	Free water/cement ratio	Cement type	Cement replacement materials
Concrete A	0.4	OPC 1	-
Mortar B	"	"	-
" C	0.6	"	-
" D	0.4	"	35% pfa
" E	"	"	70% bfs
" F	"	SRPC	-
C_iO* standard grade concrete	0.45	OPC 2	-
C_iO low grade concrete	0.70	OPC 2	-
C_iO pfa concrete	0.44	OPC 2	20% pfa

*C_iO = *Concrete in the Oceans* programme

Table A1.1: Mixes tested.

The OPC concrete (concrete A) was designed according to "Design of Normal Concrete Mixes" (Teychenne *et al.* 1975) with a water/cement ratio of 0.4. If a coarser aggregate had been used the aggregate/cement ratio would have been increased to around 4.0 and the resulting cement content would have been around 440 kg/m^3.

In terms of comparing the behaviour of different mixes, water/cement ratio and cement content are rather meaningless parameters when cement replacement materials are used. The pulverised fuel ash (pfa) and blast furnace slag (bfs) concretes were therefore designed to be practical alternatives to the OPC mix, i.e. with 28 day characteristic strengths greater than 50 N/mm^2 and slumps of around 75 mm.

Mortar C was designed to have a w/c ratio of 0.6, but with the same paste/ aggregate ratio as mortar B to allow comparison of the behaviour of the respective pastes. The need for this mortar to correspond to a concrete is not important, since a 0.6 w/c ratio concrete would rarely be used offshore (see Table 2.4), the comparison being primarily of "scientific" interest.

Table A1.3 shows the chemical composition of the cements, pfa and slag used.

Granite aggregate was used throughout.

	Concrete A, (B & F)	Mortar C	Concrete D	Concrete E	C_jO Concrete grades		
					standard	low	pfa
cement	1.00	1.00	0.65	0.30	1.00	1.00	0.80
pfa	-	-	0.35	-	-	-	0.20
bfs	-	-	-	0.70	-	-	-
20mm aggregate	-	-	-	-	1.70	2.55	1.70
10mm "	1.80	-	1.64	1.86	0.80	1.20	0.80
sand	1.50	1.71	1.34	1.42	1.50	2.25	1.50
free water	0.40	0.60	0.38	0.38	0.45	0.70	0.44
Slump	85mm	-	70mm	80mm	40mm	100mm	50mm
Mean 28 day cube strength	70 N/mm^2	-	54 N/mm^2	59 N/mm^2	65 N/mm^2	35 N/mm^2	63 N/mm^2

Table A1.2: Mix proportions, strengths and workabilities of mixes tested.

	OPC 1	OPC 2	SRPC	pfa	blast furnace slag
CaO	64.6	63.0	64.5	1.6	41.6
SiO_2	19.7	20.5	20.7	52.5	35.9
Al_2O_3	5.8	4.9	3.6	26.5	10.1
Fe_2O_3	3.2	2.3	5.9	9.1	0.24
MgO	1.2	1.2	1.05	1.6	-
MnO	-	-	-	-	0.25
TiO_2	-	-	-	-	0.45
Na_2O	0.23	*	0.18	0.9	0.66
K_2O	0.47	*	0.47	4.2	0.52
SO_3	2.7	2.6	2.39	0.65	0.25
S^{2-}	-	-	-	-	1.66
C	-	-	-	-	0.04
Free CaO	1.7	*	-	-	0.12
Ignition loss	1.4	2.8	0.80	2.9	2.48 gain
Insoluble residue	0.4	0.8	0.35	-	0.13
C_3S	55.2	59.7	65.8		
C_2S	14.8	13.8	9.7		
C_3A	9.9	9.0	(-0.5)		
C_4AF	9.7	7.0	17.9		

*not measured

Table A1.3: Composition of cements, pfa and slag (% by weight).

A1.2 Casting and curing

Specimens were cast in moulds as outlined in Table A1.4 using minimal mould oil. 25 mm thick specimens were compacted (by vibration) in one layer. 45 and 55 mm thick specimens were compacted in 2 layers. The ISAT beams were compacted in 3 layers.

Test method	Mould	Specimen
Diffusion (Chapter 4)	see Figure A1.1	4-10mm thick discs cut from 55mm thick cylinder
Resistivity (Chapter 5)	"	entire 25-45mm thick cylinder
Pore press (Chapter 5)	49mm diameter cylindrical PVC pot	"
ISAT (Chapter 8)	500 x 100 x 100mm beam mould	entire beam: see Figure 8.2
Cl^- concentration profile (Appendix 3)	see Figure A1.1	entire 55mm thick cylinder

Table A1.4: Mould and specimen details.

To allow comparison between the results of the various test methods, it was considered important to have a standard curing regime.

Curing regimes for offshore construction vary considerably though, with the exception of tremie-placed concrete, the surface zone is virtually always allowed to partially dry out prior to sea-water exposure.
Unfortunately, if the diffusion test specimen had been allowed to dry before being exposed to chloride solution the ensuing absorption would have resulted in a misleadingly low value of t_o and an erroneous diffusion coefficient (4.3.2, 4.3.4).

Figure A1.1 : 100 mm diameter cylindrical specimen moulds.

Any drying of resistivity specimens prior to testing results in a subsequent relatively long period of reducing resistivity as the specimen is gradually resaturated on testing. Although, in theory, the effects of this phenomenon should be eliminated by testing identically-cured control specimens, the resistivity changes observed are typically of an order of magnitude greater than changes due to further hydration and therefore tend to reduce the accuracy of the technique. Even specimens stored at 100% relative humidity have been observed to show a similar, though less pronounced, trend.
Unsaturated curing may even distort ISAT results; the adopted pretest drying period is sufficiently short that it would not reduce specimens that had been dry-cured for several weeks or immersed in sea-water for several months to a similar moisture state. Consequently, if unsaturated curing were adopted the first absorption measurements, taken before sea-water exposure, would be unrealistically high.

It was, therefore, necessary to cure specimens under water. Freshwater-curing would have caused lime leaching (2.2.3) and hence specimens were cured in saturated calcium hydroxide solution (limewater). This was convenient since limewater was also used as a simulated pore solution for diffusion (4.3.1) and resistivity (5.4) testing and as the control environment for resistivity (5.4) and ISA (8.3) testing.

There is no *typical* age at which offshore concrete is first exposed to sea-water, it can vary between a few minutes and several years. 28 days was felt to be a reasonable compromise, allowing pfa and bfs mixes to approach the strength of comparable OPC mixes, while leaving sufficient unhydrated cement in all the mixes to participate in reactions with the sea-water.

Mix reference	Days in mould	Days in limewater at 20 ± 1°C
Concrete A	1	27
Mortar B	1	27
Mortar C	2	26
Mortar D	2	26
Mortar E	1	27
Mortar F	1	27

Table A1.5: Curing regimes

Appendix 2: Sea-water properties

A2.1 pH value

The pH of "*in situ*" sea-water depends on many factors and in particular on the amount of dissolved oxygen, which in turn depends on photosynthetic activity and thence on the amount of solar radiation. It is not surprising, therefore, to find systematic seasonal and diurnal variations in pH. However, sea-water is *buffered* (6.4.2.1) and hence under normal conditions its pH is only subject to very slight variation and it is rare for the pH of sea-water to fall outside the range 7.8 - 8.3 (Bathurst 1975). A pH at the higher end of this range generally tends to occur near the surface where the water is in equilibrium with the CO_2 of the atmosphere.

There is little data relating to the North Sea, but monthly average pH of the English Channel varies between around 8.14 and 8.29 (Horne 1969).

Nevertheless, pH values of as high as 8.9 sometimes occur in the relatively shallow water of tidal pools, bays and estuaries, while pH values as low as 7.0 are encountered in diluted sea-water and in basins where H_2S is produced (Horne 1969).

A2.2 Viscosity

Temperature °C	Viscosity centipoise		η_S/η_p
	sea-water η_S	pure water η_p	
0	1.887	1.787	1.056
5	1.592	1.516	1.050
10	1.380	1.306	1.056
15	1.206	1.138	1.060
20	1.070	1.002	1.068
25	0.952	0.890	1.069

Table A2.1: Comparison of the viscosities of pure water and 30g/kg salinity sea-water at 1 atmosphere (based on Dorsey 1940, Robinson and Stokes 1959).

A2.3 North Sea average sea surface temperatures

The average temperature of the sea surface is presented in the form of isotherms in Figure A2.1 for January, April, July and October.

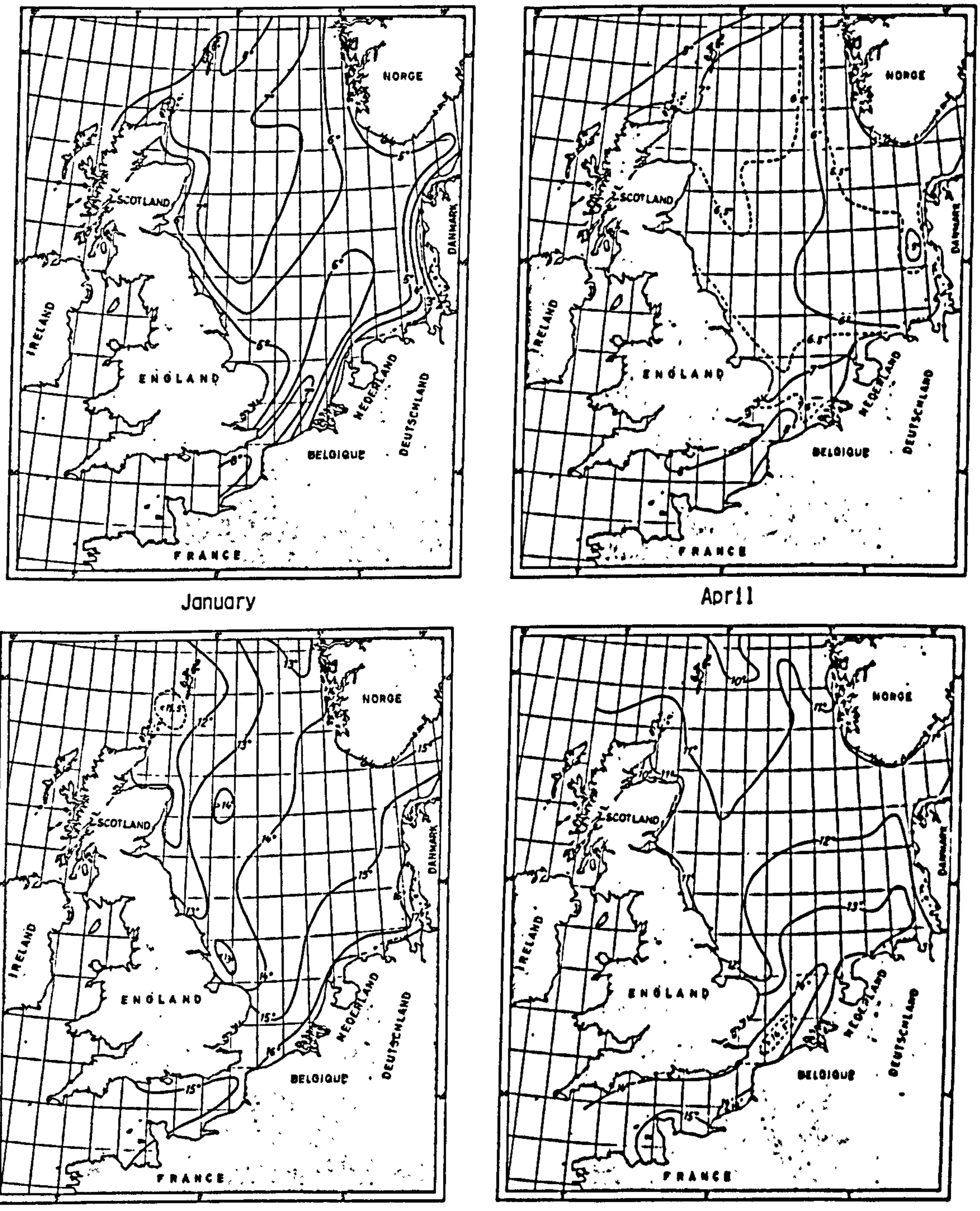

Figure A2.1: North Sea average sea surface temperatures (°C, Hohn 1973).

Appendix 3: Controlling the pH of sea-water

The pH of sea-water is typically 8.1 (A2.1), while the pH of cement paste pore solution is generally greater than 12.5. Consequently, although sea-water is naturally buffered (6.4.2.1), if a concrete specimen is placed within a limited volume of sea-water (as is the case in most laboratory experiments) there is a tendency for the pH of the sea-water to rise.

A theoretical study of the factors affecting the precipitation of brucite and particularly aragonite (6.4) suggests that, in the context of the present research, sea-water should be maintained at as near its original pH as is practically possible. For this reason a range of pH-control methods was investigated. Figure A3.1 shows the pH versus time graphs, using each of the methods, based on a 45 mm thick specimen of 84 day old limewater-cured mortar B.

Figure A3.1 (a) shows the variation of pH with time with no pH-control. Some of the reactions involved in sea-water buffering are relatively slow and hence the initial release of alkalis from the specimen cannot be counteracted and pH increases. After around 6 hours pH reaches a peak as alkali release has reduced and the buffering reactions are under way. pH then falls, reaching a value only slightly higher than its original value after around 60 hours. Over several weeks the pH gradually climbs as the buffering mechanism is unable to compensate for the continued leaching. The dotted line shows the result of using only 1.5 ℓ of sea-water.

In method (b) the initial "hump" is not controlled, but the long term gradual increase in pH is countered by regularly replacing the sea-water.

Dosing (method (c)) is unlikely to reduce the initial peak, but the "recovery time" may be shortened as well as long term pH changes being controlled. Attempts to reduce the initial peak by early dosing generally resulted in the pH dropping significantly below its initial value; only extraordinary circumstances could cause this to occur in the vicinity of a concrete surface offshore and hence this was regarded as more undesirable than a short-term increase in pH. Hydrochloric acid is the most appropriate acid for dosing, since a small addition of chloride ion is unlikely to have a significant effect on the phenomenon under investigation, whereas a small addition of the anions associated with other acids would significantly alter the sea-water composition.

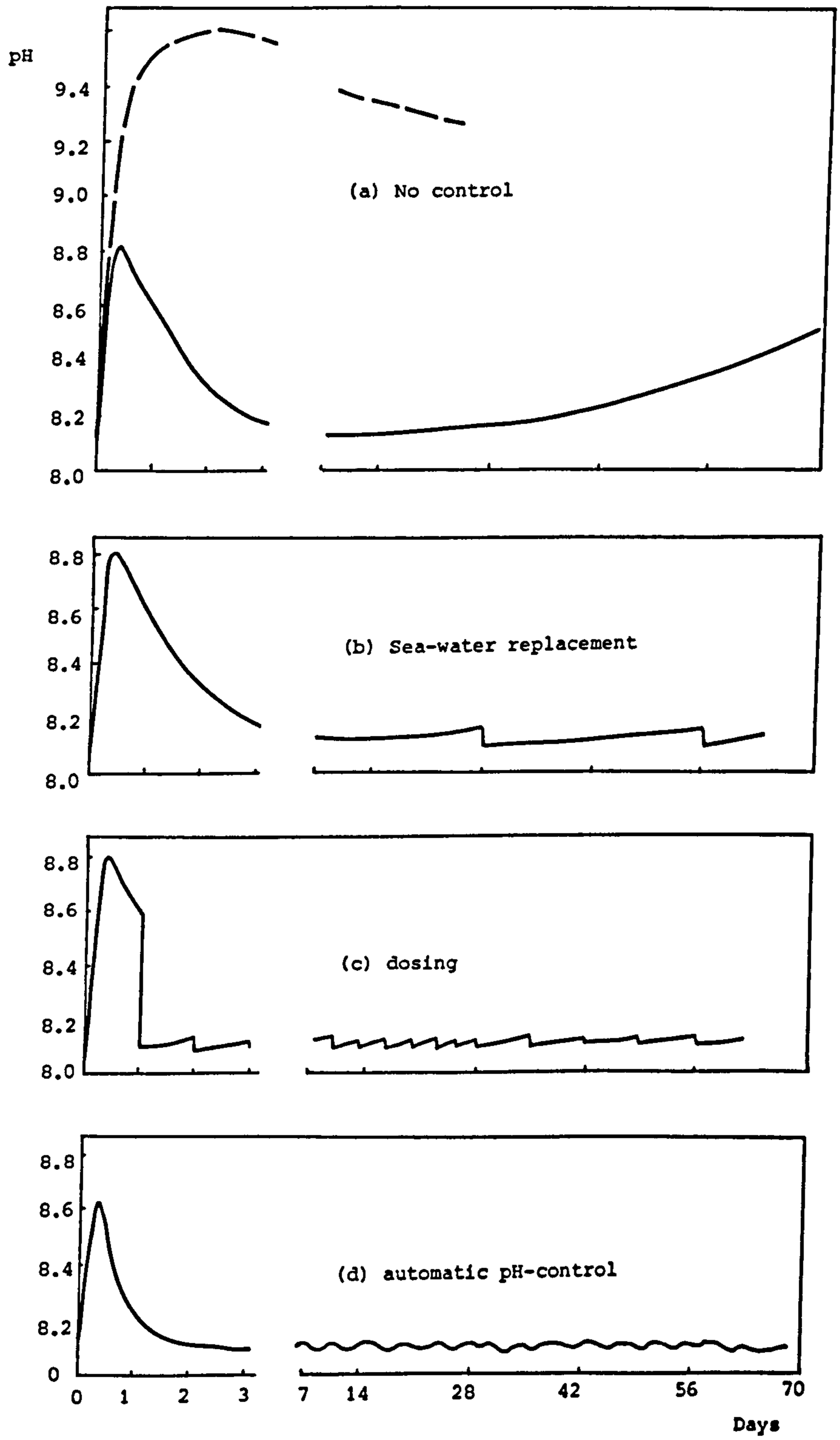

Figure A3.1: Variation of pH of 6 litres of sea-water, containing an OPC mortar specimen, with time, using various pH-control methods.

Method (d) uses an automatic pH-controller. Figure A3.2 shows a commercially available pH-control module in operation. pH is continuously monitored and when the pH reading exceeds a pre-set value (say 8.1) acid is pumped into the trough until the pH reading falls below the pre-set value. A second pump is used to circulate the sea-water to prevent excess acid being introduced into the trough before having an effect on the sea-water adjacent to the pH electrode (near to the specimen). Attempts to completely eliminate the initial peak by using a relatively concentrated acid once again caused the pH to drop below its initial value, but with more dilute acids the method reliably reduced both the initial peak and the recovery time. However, variation in laboratory temperature caused the *measured* pH to vary (although the actual pH was probably virtually constant) and hence often resulted in acid being pumped and *actual* pH being reduced, when not required. The laboratory in which most of the experimentation was undertaken was not temperature-controlled and daily fluctuations in pH of 0.25 were not unusual (not shown in Figure A3.1(d)).

The only feasible method of eliminating the initial peak would appear to be by using an extremely large sea-water/specimen volume ratio and to circulate the water vigorously. This was not practical in the context of diffusion or resistivity testing and may even result in a lower pH at the concrete surface than encountered offshore.

The significance of pH control was not appreciated prior to analysis of layers on the diffusion specimens (6.2). However, sea-water was replaced every 4 weeks during testing for resistivity (5.7), surface layer development (6.5), ISA (8.3) and chloride penetration (Appendix 6). Where more precise pH-control was required sea-water was dosed with HCl every day for the first week, every 3 days for the following 3 weeks and then every week for the remaining exposure period. (5.7.3, 6.5).

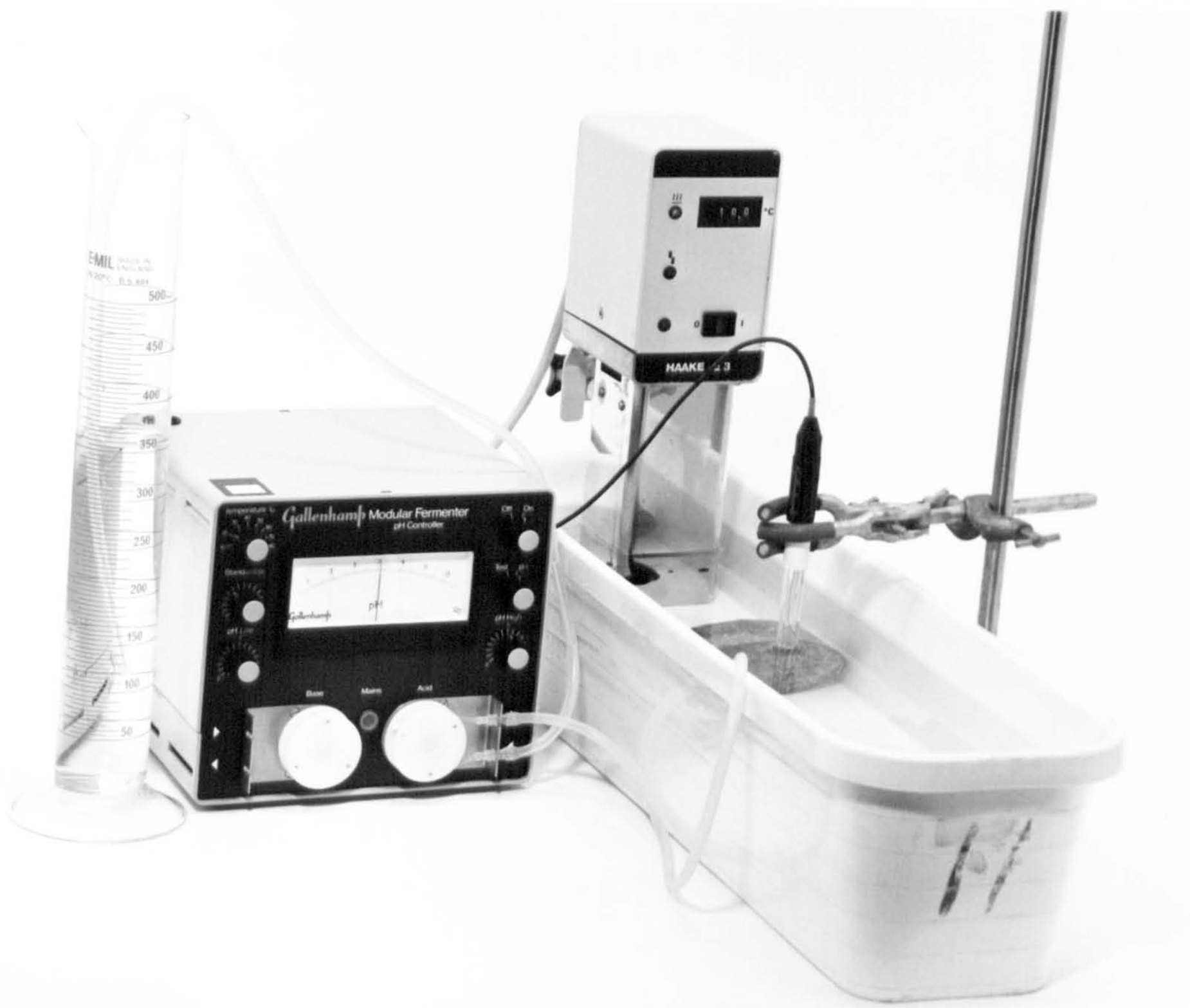

Figure A3.2 : Automatic pH-control apparatus.

Appendix 4: Calculation of the state of saturation with respect to $CaCO_3$ of sea-water as a function of temperature, pressure and pH

Berner (1971) presents a model allowing calculation of IAP of $CaCO_3$ at any temperature (T), pressure (P) and measured *in situ* pH.

$$IAP = 2.47 \times 10^{-5} \frac{\gamma_{T_{Ca}^{2+}}}{\frac{2}{\gamma_{T_{CO_3^{2-}}}} + \frac{a_{H^+}}{\gamma_{T_{HCO_3^-}} K_2}}$$

where:

a_{H^+} (H^+ activity) is obtained directly from measured pH; and the effects of temperature (Harned & Scholes 1941) and pressure (Owen & Brinkley 1941) on K_2 result in the following expressions:

$$\log \left[\frac{K_T}{K_{298^\circ}}\right] = 4980 \left[\frac{1}{298} - \frac{1}{T}\right] + 32.5 \log \frac{298}{T} \quad ;$$

$$\log \left[\frac{K_P}{K_a}\right]_2 = \frac{P-1}{6.8\ T} - 1.54 \times 10^{-7} \left[3000(P-1) - 2.07 \times 10^7 \log\left[\frac{3000+P}{3000}\right]\right].$$

subscript a refers to value at atmospheric pressure.

The effect of temperature on $\gamma_{T_{Ca}^{2+}}$, $\gamma_{T_{CO_3^{2-}}}$ and $\gamma_{T_{HCO_3^-}}$ has been calculated by Li (1967) using experimental measurements by Lyman (1956) and MacIntyre (1965) for carbonate equilibria in sea-water at different temperatures. For the temperature range in the ocean there is negligible variation in $\gamma_{T_{CO_3^{2-}}}$.

$$\gamma_{T_{HCO_3^-}} = 0.55 - 0.003(298-T) \quad ;$$

$$\gamma_{T_{Ca}^{2+}} = 0.20 - 0.002(298-T) \quad .$$

It can be shown that at all depths in the ocean the effect of pressure on $\gamma_{T_{Ca}^{2+}}$ is negligible (Duedall & Weyl 1967). The pressure effect on $\gamma_{T_{HCO_3^-}}$ and $\gamma_{T_{CO_3^{2-}}}$ has been calculated from measurements of the pressure effect on carbonate equilibria in seawater (Disteche & Disteche 1967). The resulting equations

for 22°C are:

$$\log\left[\frac{\gamma_{Tp}}{\gamma_{Ta}}\right]_{HCO_3^-} = 1.13 \times 10^{-4}\,(P-1)\ ;$$

$$\log\left[\frac{\gamma_{Tp}}{\gamma_{Ta}}\right]_{CO_3^{2-}} = 3.76 \times 10^{-4}\,(P-1)\ .$$

$K_{calcite}$ may be calculated at any temperature (Berner 1965) and pressure (Owen & Brinkley 1941) using the following expressions:

$$\log\left[\frac{K_T}{K_{298°}}\right]_{calcite} = 5860\left[\frac{1}{298} - \frac{1}{T}\right] + 50.2 \log\frac{298}{T}\ ;$$

$$\log\left[\frac{Kp}{K_a}\right]_{calcite} = \frac{P-1}{6.8T} - 2.78 \times 10^{-7}\left[300(P-1) - 2.07 \times 10^{7}\log\left[\frac{3000+P}{3000}\right]\right].$$

Appendix 5: The effect of sea-water exposure on the chemical composition of mortar pore solutions

Tables A5.1 - A5.4 present the chemical analyses of pore solutions extracted from the "pore press" specimens. (See 5.7.2 for further details including analytical procedures used).

The following general conclusions can be drawn from this data:

(1) Leaching (2.2.3) causes a loss of pore solution ions and a fall in pH for both control and sea-water exposed specimens and, as would be expected, the thinner specimens are more greatly affected.

(2) Sea-water exposure results in a more rapid fall in pH than limewater-curing.

(3) The 25 mm thick sea-water exposed specimens appear to reach an equilibrium pH, often showing an increase in pH between 84 and 140 days. This rather unexpected behaviour may be a result of experimental error.

(4) There is less loss of sodium and potassium ions from the sea-water exposed specimens than from the control specimens.

Mix reference	Age (days)	Control specimens 45mm	25mm	Test specimens 45mm	25mm	sealed specimens
Mortar B	28	13.28	13.22			13.45
	84	13.23	13.13	12.96	12.75	
	140	13.19	13.03	12.85		
Mortar C	28	13.21	13.05			13.33
	84	13.14	12.97	12.84	12.62	
	140	12.95	13.25	12.81	12.62	
Mortar D	28	13.22	13.09			13.36
	84	13.18	13.07	13.03	12.70	
	140	13.15	13.00	12.86	12.96	
Mortar E	28	13.21	13.05			13.33
	84	13.14	12.97	12.84	12.62	
	140	12.95	13.25	12.81	12.62	
Mortar F	28	13.25	13.19			13.42
	84	13.15	13.06	12.91	12.64	
	140	13.08	12.98	12.87	12.81	

Table A5.1 : pH (by titration).

Mix reference	Age (days)	Control specimens 45mm	25mm	Test specimens 45mm	25mm	sealed specimens
Mortar B	28			3410	4440	
	84			4440	-	
	140					
Mortar C	28			4440	6035	
	84			3375	2840	
	140					
Mortar D	28			4260	7210	
	84			5505	1775	
	140					
Mortar E	28			3090	3195	
	84			2875	890	
	140					
Mortar F	28			3550	3975	
	84			3950	4665	
	140					

Table A5.2 : Chloride content ppm.

Mix reference	Age (days)	Control specimens 45mm	25mm	Test specimens 45mm	25mm	sealed specimens
Mortar B	28	2100	1850			2700
	84	1500	1000	2300	1500	
	140	1500	1000	1650	-	
Mortar C	28	1600	1200			2100
	84	1150	900	1800	1600	
	140	850	500	1450	1100	
Mortar D	28	1400	900			2100
	84	1300	1200	2000	1900	
	140	700	950	1650	1050	
Mortar E	28	2000	1800			2700
	84	2000	1650	2300	3000	
	140	1975	2050	2000	1450	
Mortar F	28	1200	1200			1700
	84	1100	800	1400	1000	
	140	650	625	1250	950	

Table A5.3 : Sodium content ppm.

Mix reference	Age (days)	Control specimens 45mm	25mm	Test specimens 45mm	25mm	sealed specimens
Mortar B	28	4500	4300			7750
	84	3150	1900	3100	2400	
	140	3200	1750	2950	-	
Mortar C	28	3900	2800			5500
	84	2200	1150	2800	1600	
	140	1750	875	2250	1200	
Mortar D	28	3800	2800			6400
	84	3250	2300	4600	3700	
	140	2600	2750	4350	2650	
Mortar E	28	2300	2000			3200
	84	1650	1050	1750	1750	
	140	1700	1750	1000	1200	
Mortar F	28	4900	4400			8100
	84	3150	2100	3800	2300	
	140	3050	1850	3550	2050	

Table A5.4 : Potassium content ppm.

Appendix 6: Chloride ion concentration profiles

A6.1 Introduction

One of the most important parameters controlling the durability of offshore reinforced concrete structures is the rate at which chloride ion reaches the embedded steel (2.2.8). The experimentation reported in Chapters 4 - 8 suggests that the rate of chloride penetration almost certainly reduces with time of exposure to sea-water.

During the early stages of this research programme some considerable effort was directed at developing a method of monitoring permeability changes based on measuring the concentration of chloride ion at various depths into specimens after various periods of sea-water exposure. Such a method would be *direct* in the sense that actual chloride levels at depths corresponding to concrete cover to reinforcement could be monitored. Unfortunately a number of major problems were encountered in interpreting such data in this way and these problems are outlined in A6.2. However, it was felt that the technique had value as a simple means of *comparing* the behaviour of different specimens and hence enabling the effect of a variety of factors to be evaluated and the effect of the permeability-reducing phenomenon to be put into perspective. The results of a test programme comparing the effects of different curing regimes are reported in A6.3.

A6.2 Interpretation of chloride ion concentration profiles

There are several approaches that may be taken when attempting to interpret chloride concentration profiles.

The most basic method simply involves a visual comparison with other profiles to gain a measure of the relative permeability of different concretes to chloride ion (e.g. Stillwell 1983, Gjorv & Vennesland 1979, Ost & Monfore 1966). Few workers have attempted more sophisticated interpretative procedures than this and this is the approach used in A6.3.

More sophisticated approaches aim to determine a diffusion coefficient (D) calculated from the measured concentration profile. However, it should be emphasised that the value of D calculated at a particular time does not relate

to the diffusion characteristics of the specimen at that time, but is based on the entire exposure history of the specimen.

The diffusion of a species into a semi-infinite medium is represented by the relationship (Crank 1975):

$$\frac{C}{C_o} = \text{erfc}\ [x/2\sqrt{Dt}] \qquad \text{(A6.1)}$$

where x = distance from the surface of the medium;

t = time;

D = diffusion coefficient of the species in the medium;

C = concentration of the species at position x and time t;

C_o = concentration of the diffusing species at the surface of the medium;

erfc = an error function (obtained from mathematical tables).

Generally x and t are predetermined and C is measured and hence if a value of C_o is assumed a "D profile" may be calculated for each value of t. In practice C_o is not the concentration of chloride ion in the test solution, but is a considerably lower value which must be estimated by extrapolating the concentration profile to $x = 0$. Alternatively, an iterative computer method may be used to calculate "best fit" values of C_o and D for each concentration profile (Taylor Woodrow Research Laboratories 1980).

However, the ingress of chloride ion into most cement pastes involves reaction (2.2.2.3) as well as diffusion. Consequently, if values of D are calculated at discrete points within a specimen using Equation (A6.1), based on measured total chloride concentrations, there is an *apparent*, very pronounced fall in D with increasing depth into the specimen. Equation (A6.1) would be more appropriately applied to chloride within the pore solution, i.e. water-soluble chloride. However, measurement of water-soluble chloride levels alone could not be used to indicate changes in permeability since, even if permeability were constant, the amount of chloride ion entering the pore solution is likely to increase with time as less aluminate remains free to bind diffusing chloride.

Theoretical diffusion plus reaction models exist (Crank 1975) which could perhaps be applied to concrete. Lawrence (1981) demonstrated the use of a linear absorption isotherm (bound chloride is a constant proportion of total

chloride) model but conceded that the assumption of a linear isotherm is unlikely to be correct for chloride diffusion in concrete.

It was felt that the development and application of a more sophisticated model could not be justified in the context of the present research.

A6.3 The effect of curing regime on chloride ion diffusion

100 mm diameter, 55 mm long, mortar B (see A1.1 for mix details) cylinders were cast. These were demoulded after 24 hours. Five curing regimes were used prior to sea-water immersion:

(1) immediate sea-water immersion;
(2) 28 days limewater immersion;
(3) 1 year limewater immersion;
(4) 28 days distilled water immersion;
(5) 28 days 100% relative humidity.

Specimens were stored in tanks containing sea-water which was replaced every 4 weeks.

At the end of the predetermined exposure period, specimens were removed from their tanks, rinsed with distilled water and allowed to dry in laboratory air for at least 48 hours. The cast faces were then wire brushed and blown with compressed air to remove any remaining chloride from the surface of the specimens.

Drilled samples were extracted using a 6.5 mm diameter bit with a flattened end. Samples were generally taken from the central 45 mm diameter core of the specimen to avoid chloride that had penetrated biaxially but this was not strictly adhered to for specimens exposed for very short durations (< 11 days). Samples were taken down to 20 mm depth in 5 mm increments. Fifteen 5 mm deep holes generally produced a sample of approximately 5g. The holes were then flushed out with compressed air before the next depth was drilled. The 0-5 mm depth holes were drilled slightly wider than the 5-10 mm depth holes etc. to avoid including dust from material nearer to the surface in with samples taken at greater depth.

Total chloride was determined as follows:

The sample was accurately weighed and 50 ml of 1.0 N nitric acid was added. The mixture was stirred for 5 minutes. The solution was then brought to a pH of around 5 by adding sodium carbonate. 25 ml of the solution was then filtered off and 5 ml of buffer (2.0 M ammonium acetate plus 2.0 M acetic acid) was added. This solution was then thoroughly stirred before being analysed with a calibrated chloride electrode.

Figure A6.1 compares the effect of immediate sea-water exposure with 28 days of limewater-curing. Clearly at early ages chloride diffusion into the "uncured" specimens was far more rapid. However, after 3 months of exposure the concentration profiles are virtually identical. This decreased penetration is possibly associated with the more rapid surface layer formation observed on the "uncured" specimens (6.5).

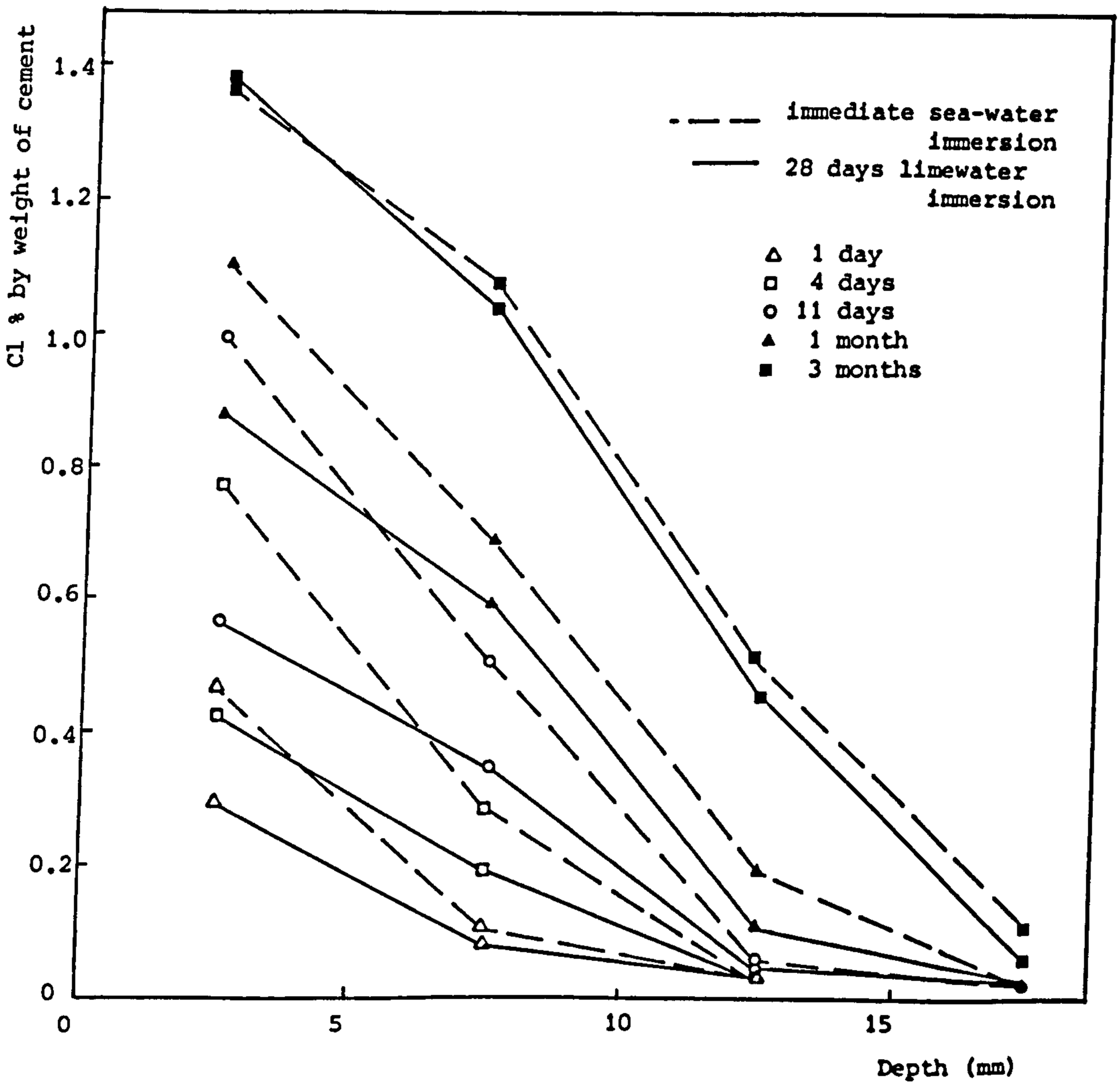

Figure A6.1: Chloride concentration profiles for specimens subjected to two different curing regimes, after various periods of immersion in sea-water.

Figure A6.2 compares the effects of 5 different curing regimes on the concentration profiles at one and 3 months. The spread of results for each exposure period is surprisingly narrow. Long-term curing resulted in the least chloride penetration. Distilled water curing caused the greatest chloride levels at 3 months; this is likely to be due to the combined effects of thinner surface layer development (6.5) and increased porosity, both effects due to lime leaching during curing.

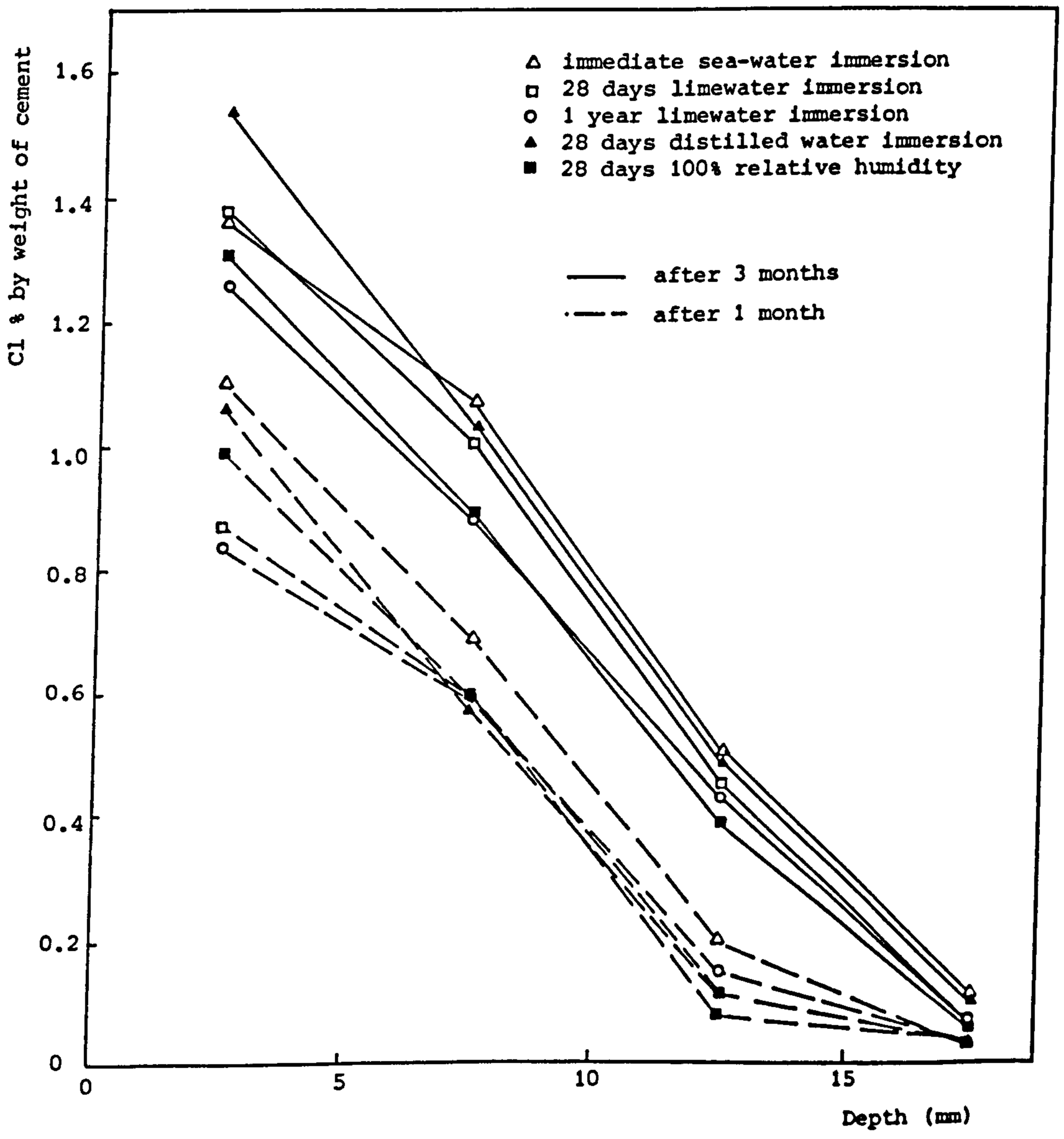

Figure A6.2: Chloride concentration profiles for specimens subjected to various curing regimes after 1 and 3 months of immersion in sea-water.

Appendix 7: Taking and correcting resistivity readings

A7.1 Correlation between solution and specimen temperatures

For obvious practical reasons the temperature of the test solution, rather than the specimen, is measured. This introduces the question of how long the solution temperature must be constant to be sure that the specimen is at the same temperature. This may be treated as a problem of transient heat conduction in a large flat slab.

Initially the slab is at uniform temperature T_o ; then the adjacent medium is raised to, and maintained at, temperature T_∞ . By assuming certain physical properties, the time taken for a particular point within the slab to reach a chosen temperature T can be calculated.

The following are conservative estimates:

concrete thermal conductivity 3 $Wm^{-1}{}^oC^{-1}$ (Khoury & Sullivan 1984)

concrete/mortar thermal diffusivity 0.7 x 10^{-6} m^2S^{-1} (")

convective transfer coefficient 275 $Wm^{-2}{}^oC^{-1}$ (Welty 1974)

$$T_o - T_\infty = 3^oC$$

Standard charts (Welty 1974) show that T at the centre of the specimen is within 0.1°C of T_∞ within 40 minutes.

The temperature at the centre of a number of mortar specimens was monitored (with a thermocouple and data logger) after a steep increase in solution temperature. The results suggested that the above calculations are conservative.

During normal testing resistance readings were only taken after the solution temperatures had been constant (± 0.2°C) for the previous hour.

A7.2 Correction of measured resistance for test solution resistivity

Notation

R measured resistance

R_a error in measured resistance due to solution A

R_b " " " " " " " B

R_x specimen resistance

R_A conductivity "dip" cell resistance reading in solution A

R_B " " " " " " " B

R_S " " " " " " standard solution

t thickness of central plate of resistivity cell

ρ_a resistivity of solution A

ρ_b " " " B

ρ_s " " standard solution

The contributions of the solutions on either side of the specimen to the measured resistance were often significant, particularly for more conductive mixes or where relatively dilute solutions were used.

During early preliminary testing, when a resistance reading was taken and the temperature of the solutions measured, the resistivity of the solutions would be read from pre-plotted graphs of resistivity versus temperature; these graphs were based on laboratory measurements of the resistivity of sea-water, saturated limewater etc., over a range of temperatures. This method was later found to be imprecise because ion migration into, or more often out of, the specimen resulted in the composition of the solutions changing and the pre-plotted graphs became inapplicable. Consequently, in subsequent testing, the resistivities of the solutions were measured directly (at the same time as the resistance and temperature were measured) using a "dip" conductivity cell and the correction was based on this value.

Figure A7.1 shows the likely region through which the current is conducted; the precise flow path is unimportant.

$$R = R_a + R_x + R_b \quad \text{(resistances in series).}$$

$$\text{Correction} = R_a + R_b = \frac{L}{A}(\rho_a + \rho_b) \quad \text{(from Equation (5.2))}$$

$$\text{and} \quad \rho_a = \rho_s \frac{R_A}{R_S} \quad \& \quad \rho_b = \rho_s \frac{R_B}{R_S}$$

$$\text{therefore,} \quad \text{correction} = \frac{L}{A} \frac{\rho_s}{R_S}(R_A + R_B)$$

ρ_s is known, R_A , R_B & R_S are measured.

$\frac{L}{A}$ *(half cell constant)* is a geometrical property of the resistivity cell and is more conveniently measured rather than calculated.

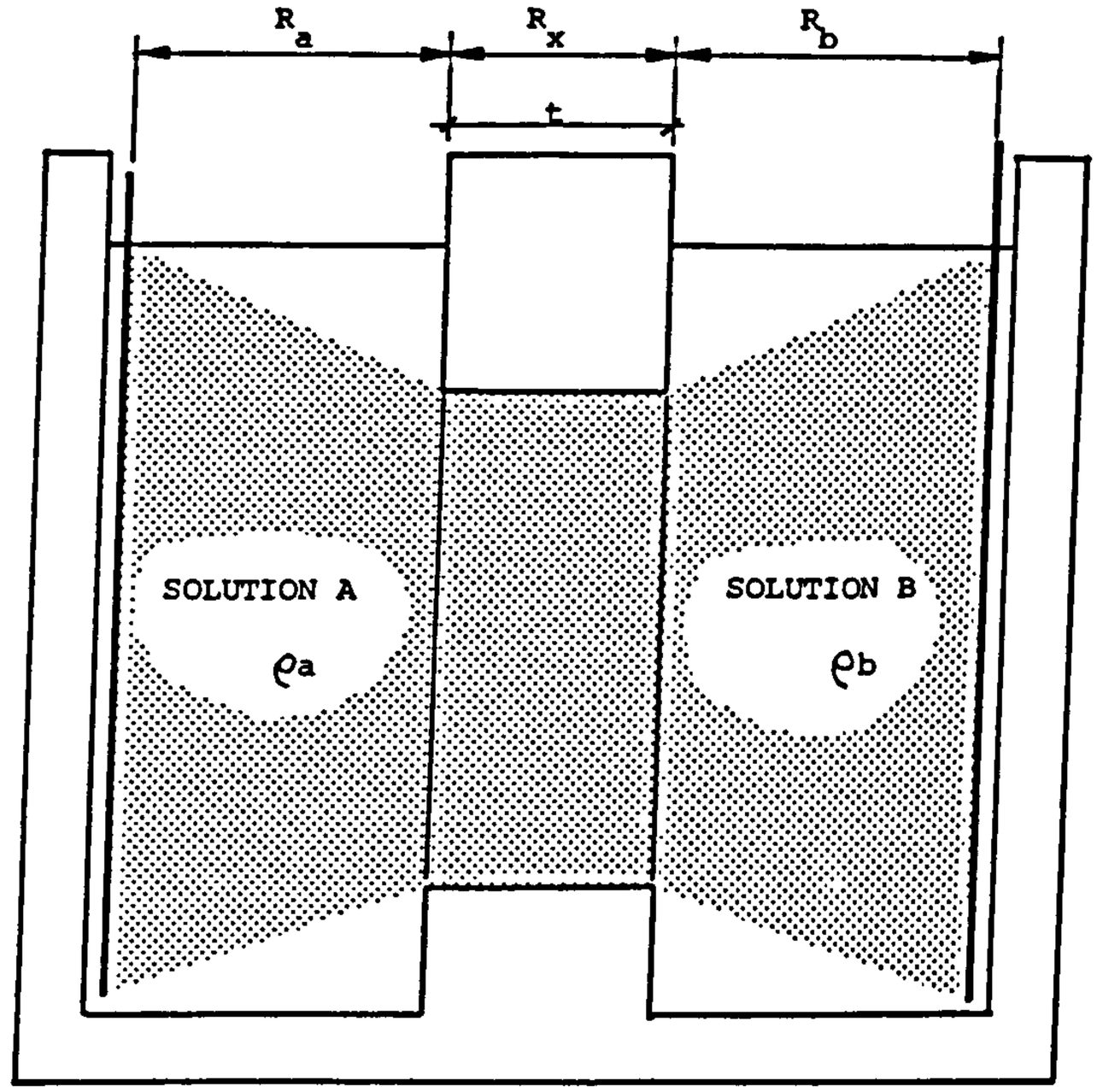

Figure A7.1: Idealised electrical flow path through resistivity cell.

A standard solution of 7.4789 g KCl/kg H_2O was used to measure the resistance (R) between electrodes of resistivity cells with no specimen present. A layer of petroleum jelly of the same thicknesss as would be present if a specimen were under test, was applied.

Resistance of solution in volume normally occupied by specimen $= \frac{0.001\ \rho_S}{(0.1016)^2\ \frac{\pi}{4}} = 0.1233\ \rho_S\ \Omega/\text{mm thickness}$

therefore, $R = 0.1233\ \rho_S t + 2\frac{L}{A}\rho_S$

therefore, $\frac{L}{A} = \frac{R}{2\rho_S} - 0.06165\ t$.

Standard solution temperature = 19°C therefore $\rho^S = 0.8772\ \Omega m$.

t = 25 mm R = 10.9Ω (average of 3 cells), therefore $\frac{L}{A} = 4.67$.

t = 45 mm R = 13.15Ω (average of 3 cells), therefore $\frac{L}{A} = 4.72$.

Therefore, $\frac{L}{A}$ taken as 4.7 (regardless of t).

Hence, correction = $4.7 \frac{\rho_S}{R_S} (R_A + R_B)$.

Corrections ranged from 6Ω for sea-water - limewater to 25Ω for 0.0185M $MgSO_4$ solution - limewater.

A7.3 Correction of measured resistance for temperature variation.

The resistivity of concrete is temperature dependent. To allow comparison of readings taken at different temperatures it was therefore necessary to convert measured specimen resistance to the equivalent resistance at a reference temperature.

The electrical resistivity of moist concrete (and other electrolytes) at a temperature t, can be related to its resistivity at a reference temperature θ, by the formula

$$\rho_\theta = \rho_t + \rho_t \alpha (t - \theta) \qquad \text{(A7.1)}$$

where ρ_θ = resistivity at θ°C;

ρ_t = resistivity at t°C;

α = temperature coefficient of resistivity.

An alternative relationship, which is based on the Hinrichson-Rasch Law and is applicable to most refractory materials, has also been applied to concrete (Hammond & Robson 1955, Whittington *et al.* 1981).

$$\rho_\theta = \rho_t e^{a\left[\frac{1}{\theta} - \frac{1}{t}\right]}$$

where θ & t are in degrees absolute and

a is a constant.

The data in the literature relating to the effect of temperature on the resistivity of concrete are extremely sparse. Most workers in this field have given the phenomenon only very superficial attention, typically testing one specimen at each of 3 or 4 temperatures. Only Spencer (1937) has tested a significant number of specimens, producing a "temperature reduction chart" to fulfil the

same function of reducing resistance readings to a reference temperature of 70°F. Spencer found that concrete type had little effect on the relationship.

Spencer's data was found to be very closely approximated over the range 5 - 35°C by Equation (A7.1) with α = 0.025/°C (see Figure A7.2). Whittington *et al.* (1981) derived a value of 0.022/°C, though apparently based on only 6 readings. Monfore observed that "an average increase in temperature of one degree F caused an average decrease in resistivity of one percent." This is equivalent to α = 0.018/°C which is the value that one would expect of cement paste pore solution, being primarily a solution of bases (Glasstone 1948); a correction curve based on α = 0.018/°C is also shown in Figure A7.2.

Temperature corrections were duly based on Equation (A7.1) with α = 0.025/°C and a reference temperature of 21°C. However, this issue clearly merits further study.

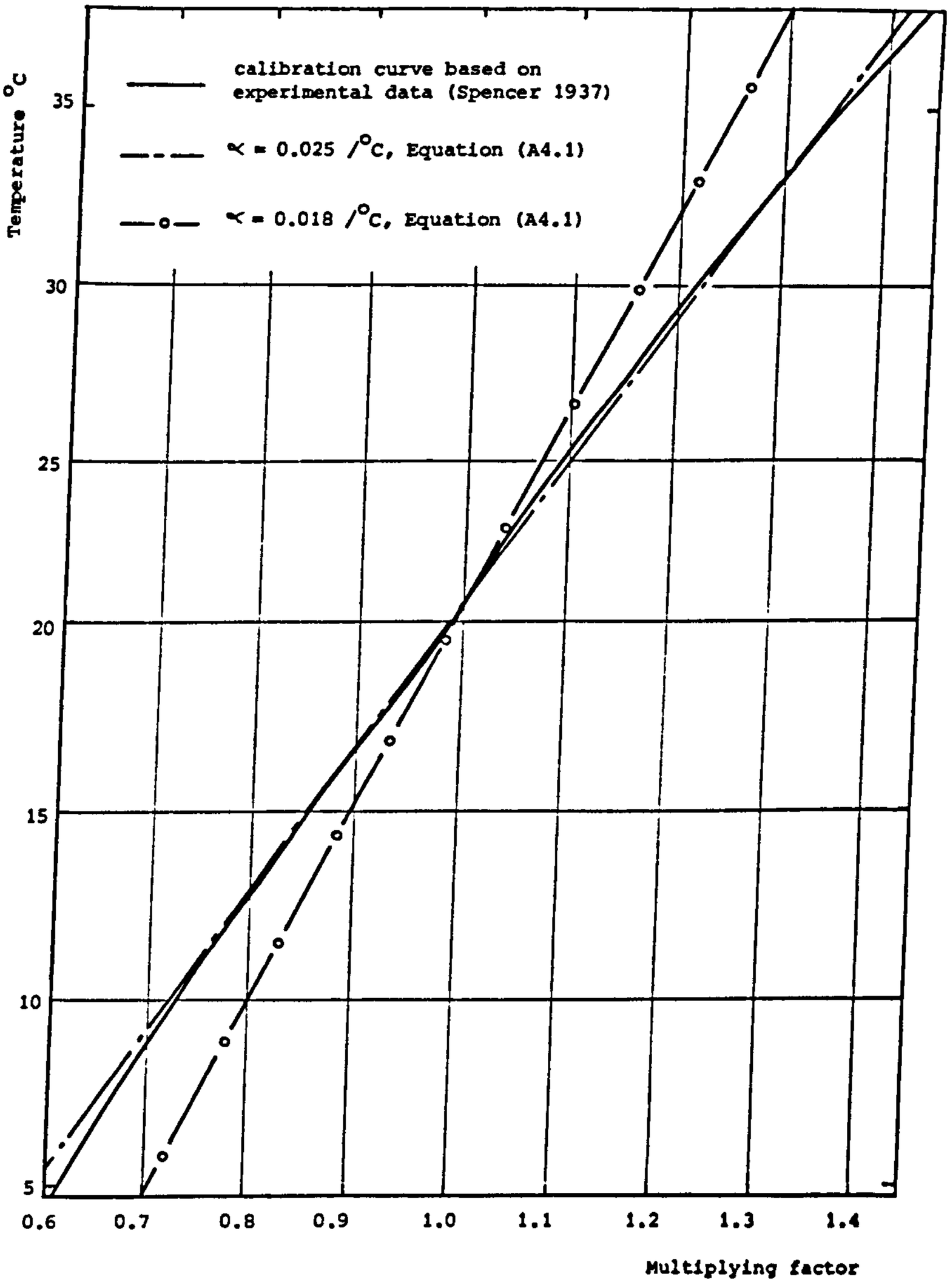

Figure A7.2: Multiplying factor for reducing specimen resistance to equivalent value at 21°C.

Appendix 8 : Preparation of polished sections

Difficulty was encountered in developing a preparation technique that rendered the specimen in a suitable condition for EPMA without disrupting the surface layer. This was particularly difficult since little was known of the form or properties of the layer. Early attempts resulted in dissolution, fracture or complete removal of parts of the formation.

Using the technique finally developed, the shape and size of the aragonite spherulites in section correspond to their shape and size "in plan" on the specimens before preparation. It is therefore unlikely that the preparation has a significant effect on the form of the layer. However, the specimen is carefuly examined after each step of the preparation procedure, the condition of the layer rather than the bulk of the specimen being the important criterion.

The preparation procedure is as follows:-

(1) Large specimen, rinsed with distilled water, allowed to dry in laboratory air for at least 48 hours, then split in half and a small sample taken from near the centre of the exposed face using a miniature hammer and chisel.

(2) Sample encapsulated in polyester resin within a 25 mm diameter plastic ring. The edge of the sample to be studied being kept towards the centre of the ring; failure to do this often resulted in the "pull" from the ring, as the resin dried, damaging the layer.

(3) Specimen ground on fine diamond wheel, using minimal amount of water, to expose edges to be studied (maximum of 1 mm removed).

(4) Specimen lapped (on Vi-bro-lap), under light loading ($\triangleq$ 100-200 g), using 800 silicon carbide and water, for 24 hours.

(5) Specimen lapped on Hyprocel Pellon with rotating lap, under very light loading (50-150 g), using 3μm diamond and water, for 4 hours.

(6) Specimen polished on Metcloth with rotating lap, under minimal loading ($\triangleq$ 50 g), using $\frac{1}{2}\mu$m diamond and water, for 4 hours.

(7) Specimen washed in warm water with detergent, then washed in absolute alcohol.

Appendix 9 : Glossary of chemical terms

The ACTIVITY of a substance is the effective concentration that obeys thermodynamic laws. The activity of an ion, a, is related to the concentration of the ion, c, by an ACTIVITY COEFFICIENT, γ.

$$a = \gamma c$$

The activity coefficient is always less than 1 and approaches unity as the concentration of the solution decreases. The activity of a given ion depends upon the concentration of all ions present in the solution.

A COMPLEX ION or complex compound is formed as a result of strong interaction between a central metal cation and several surrounding anions and/or molecules. Complex ions are therefore generally treated as independent dissolved species with their own activities and activity coefficients. Occasionally it is useful to lump these effects of complexing with normal electrostatic attraction etc., into a TOTAL ACTIVITY COEFFICIENT, γ_T.

For any reversible reaction: $wW + xX + \ldots\ldots \quad yY + zZ\ldots.$

at equilibrium $$\frac{[Y]^y.[Z]^z....}{[W]^w.[X]^x....} = K$$

where square brackets denote activities and K is defined as the EQUILIBRIUM CONSTANT for the above reaction.

The ION ACTIVITY PRODUCT (IAP) of a salt, C_cD_d, in a particular solution is defined as $[C]^c.[D]^d$.

The SOLUBILITY PRODUCT (K_{sp}) of a salt is the IAP of the salt in a saturated solution in equilibrium with excess salt.

The DEGREE OF SATURATION (S) of a solution with respect to a solid is defined as

$$S = \frac{IAP}{K_{sp}},$$

S < 1 undersaturated;

S = 1 saturated;

S > 1 supersaturated.

The SALINITY of sea-water is defined as the total amount of solid material in grams contained in 1 kg of sea-water when all the bromide and iodide have been replaced by the equivalent amount of chloride, all the carbonate has been converted to oxide and all the organic matter has been completely oxidised.

Each ion that is in solution is surrounded by an *ion atmosphere* which contains an excess of oppositely charged ions. The ion atmosphere around a stationary ion is spherically symmetrical and the resultant force on the central ion is therefore zero. If, however, the ion is moving under the influence of a gradient of chemical or electrical potential, the ion atmosphere is deformed, with the opposite charge density in front of the moving ion being lower than that behind it. A retardation force therefore develops, producing decreased mobility; this is the RELAXATION EFFECT. The relaxation effect is appreciable only in the case where positive and negative ions move in opposite directions under the effect of an external potential gradient. In the case of diffusion, ions of opposite charge move in identical directions and the relaxation effect does not markedly influence ionic mobility (Erdey-Gruz 1974). This explains the observation that in diffusion the mobility of ions vary with electrolyte concentration to a far lesser degree than in the case of electrolytic conduction.

The other phenomenon arising from the interaction of ions is the ELECTROPHORETIC EFFECT. This effect is a consequence of the fact that water molecules in the vicinity of ions move with them. In diffusion the electrophoretic effect slows down the ions of higher mobility, while accelerating those of lower mobility. In electrolytic conduction the electrophoretic effect results in ions restricting the movement of ions of the opposite sign and hence reducing mobility.

ADSORPTION is a process in which molecules adhere to the surface of a solid. In PHYSICAL ADSORPTION the molecules are held to the surface of the adsorbent by van der Waal's forces. In CHEMICAL ADSORPTION the molecules adhere as a result of the formation of chemical bonds.